Mr. R.J. Templin

L.O. NAE-348-4 FILE BM49-10R-1 PREPARED BY JGL CHECKED BY JL	NATIONAL AERONAUTICAL ESTABLISHMENT OTTAWA, CANADA LABORATORY MEMORANDUM SECTION Aerodynamics	AE-46M NO HSAL-M-72 PAGE 1 OF 22 COPY NO 4 DATE 31 October 1956

SECURITY CLASSIFICATION ~~SECRET~~

SUBJECT Six-Component Supersonic Wind Tunnel Tests of a 1/80 Scale Model of the C-105 Aircraft

PREPARED BY J. G. LaBerge

ISSUED TO
Mr. J. H. Parkin
Dr. D. C. MacPhail
Mr. J. R. Templin (2)
Mr. J. Lukasiewicz (2)
Author
Aero Library (2)

Summary

Six-component supersonic wind tunnel tests were carried out on a 1/80 scale model of the C-105 aircraft at four Mach numbers. In all, 27 model configurations were investigated over a period of three months requiring a total of 1991 tunnel runs. This memorandum contains the results of these tests in the form of basic plots, cross-plots and final aerodynamic derivatives.

In order to expedite the publication of the data, the results are presented without detailed analysis.

Contents

List of Illustrations — Figure

Record of Plots

Variables	Parameter	Constants	Figure Number, M = 1.35	M = 1.57	M = 1.78	M = 2.03
Basic Plots						
C_L vs α	δ_e	$\delta_a = \delta_r = 0°$; $\beta = 0.1°$	5	25	48	71
"	"	" $\beta = 5.8°$	6	26	49	72
C_L vs C_D	"	" $\beta = 0.1°$	7	27	50	73
C_L^2 vs C_D	—	$\delta_e = \delta_a = \delta_r = 0°$; "	8			
C_L vs C_m	δ_e	$\delta_a = \delta_r = 0°$; "	9	29	52	75
"	"	" $\beta = 5.8°$	10	30	53	76
α vs C_m	"	" $\beta = 0.1°$	11	31	54	77
"	"	" $\beta = 5.8°$	12	32	55	78
α vs C_n	β	$\delta_e = \delta_a = \delta_r = 0°$	13	33	56	79
"	"	$\delta_e = \delta_a = 0°$; FIN OFF	14	34	57	80
"	δ_r	" $\beta = 0.1°$	15	35	58	81
"	δ_a	$\delta_e = \delta_r = 0°$; "	16	36	59	82
α vs C_Y	β	$\delta_e = \delta_a = \delta_r = 0°$	17	37	60	83

Record of Plots (Continued)

Variables	Parameter	Constants	Figure Number M 1.35	1.57	1.78	2.03
Basic Plots						
α vs C_Y	β	$\delta_e=\delta_a=0°$; FIN OFF	18	38	61	84
"	δ_r	" $\beta=0.1°$	19	39	62	85
"	δ_a	$\delta_e=\delta_r=0°$; "	20	40	63	86
α vs C_l	β	$\delta_e=\delta_a=\delta_r=0°$	21	41	64	87
"	"	$\delta_e=\delta_a=0°$; FIN OFF	22	42	65	88
"	δ_r	" $\beta=0.1°$	23	43	66	89
"	δ_a	$\delta_e=\delta_r=0°$; "	24	44	67	90
C_L vs α	δ_{a_L}	" "	-	45	68	91
α vs C_m	"	" "	-	46	69	92
α vs C_l	"	" "	-	47	70	93
Cross Plots						
C_L vs δ_e	α	$\delta_a=\delta_r=0°$; $\beta=0.1°$	94	110	129	148
"	"	" $\beta=5.8°$	95	111	130	149
C_m vs δ_e	C_L	" $\beta=0.1°$	96	112	131	150
"	α	" "	97	113	132	151
C_n vs β	"	$\delta_e=\delta_a=\delta_r=0°$	98	114	133	152
"	"	$\delta_e=\delta_a=0°$; FIN OFF	99	115	134	153
C_n vs δ_r	"	" $\beta=0.1°$	100	116	135	154
C_n vs δ_a	"	$\delta_e=\delta_r=0°$; "	101	117	136	155

Record of Plots (Concluded)

Variables	Parameter	Constants	Figure Number M			
			1.35	1.57	1.78	2.03
Derivatives, etc.						
$\eta_{ac}/\bar{c}$ vs M	—	$\delta_e=\delta_a=\delta_r=0°;\ \beta=0.1°$	174			
$(C_m)_{C_L=0}$ vs M	—	" "	175			
$(C_{m_{\delta e}})_{C_L}$ vs M	C_L	$\delta_a=\delta_r=0°$; "	176			
$(C_{m_{\delta e}})_\alpha$ vs M	α	" "	177			
$\eta_{cp}/\bar{c}$ vs M	—	" "	178			
C_{n_β} vs M	α	$\delta_e=\delta_a=\delta_r=0°$	179			
"	"	$\delta_e=\delta_a=0°$; FIN OFF	180			
$C_{n_{\delta r}}$ vs M	"	" $\beta=0.1°$	181			
$C_{n_{\delta a}}$ vs M	"	$\delta_e=\delta_r=0°$; "	182			
C_{Y_β} vs M	"	$\delta_e=\delta_a=\delta_r=0°$	183			
"	"	$\delta_e=\delta_a=0°$; FIN OFF	184			
$C_{Y_{\delta r}}$ vs M	"	" $\beta=0.1°$	185			
$C_{Y_{\delta a}}$ vs M	"	$\delta_e=\delta_r=0°$; "	186			
C_{l_β} vs M	"	$\delta_e=\delta_a=\delta_r=0°$	187			
"	"	$\delta_e=\delta_a=0°$; FIN OFF	188			
$C_{l_{\delta r}}$ vs M	"	" $\beta=0.1°$	189			
$C_{l_{\delta a}}$ vs M	"	$\delta_e=\delta_r=0°$; "	190			
$C_{L_{\delta a_L}}$ vs M	"	" "	191			
$\eta_{cp_a}/\bar{c}$ vs M	"	" "	192			
$y_{cp_a}/b_{/2}$ vs M	"	" "	193			

List of Symbols (Continued)

$(C_m)_{C_L = 0}$ Pitching moment coefficient for zero lift

C_{L_α} Lift-curve slope parameter at zero lift, per deg.

$C_{L_{\delta e}}$ Static stick fixed longitudinal stability parameter measured at $\delta e = 0°$, per deg.

$C_{m_{C_L}}$ Longitudinal static stability parameter, measured at zero lift

$\left(\frac{C_m}{\delta e}\right)_{C_L}$ Elevator power at constant lift measured at $\delta e = 0°$, per deg.

$\left(\frac{C_m}{\delta e}\right)_{\alpha}$ Elevator power at constant angle of attack measured at $\delta e = 0°$, per deg.

C_{n_β} Directional stability parameter measured at $\beta = 0°$, per deg.

$C_{n_{\delta r}}$ Rudder power measured at $\delta r = 0°$, per deg.

$C_{n_{\delta a}}$ $\frac{\partial C_n}{\partial \delta a}$ measured at $\delta a = 0°$, per deg.

C_{Y_β} Side force derivative measured at $\beta = 0°$, per deg.

$C_{Y_{\delta r}}$ $\frac{\partial C_Y}{\partial \delta r}$ measured at $\delta r = 0°$, per deg.

C_{l_β} Dihedral effect measured at $\beta = 0°$, per deg.

$C_{l_{\delta r}}$ $\frac{\partial C_l}{\partial \delta r}$ measured at $\delta r = 0°$, per deg.

$C_{l_{\delta a}}$ $\frac{\partial C_l}{\partial \delta a}$ measured at $\delta a = 0°$, per deg.

$C_{m_{\delta a_L}}$ $\frac{\partial C_m}{\partial \delta a_L}$ measured at $\delta a_L = 0°$, per deg.

$C_{l_{\delta a_L}}$ $\frac{\partial C_l}{\partial \delta a_L}$ measured at $\delta a_L = 0°$, per deg.

$C_{L_{\delta a_L}}$ $\frac{\partial C_L}{\partial \delta a_L}$ measured at $\delta a_L = 0°$, per deg.

D Drag along X_S axis, lbs.

List of Symbols (Continued)

e	Span efficiency factor = $\frac{1}{\pi AR} \frac{dC_L^2}{dC_D}$
h	Distance between balance resolving center and model CG in the pitch plane, 3.290 in.
k	Distance between balance resolving center and model CG in the yaw plane, 3.965 in.
L	Lift, lbs.
l	Rolling moment about X_S axis, in. lb.
l_l	Rolling moment response to rolling moment, in. lb.
M	Mach number
m	Pitching moment about model CG, in. lbs.
m_m	Pitching moment response to pitching moment, in.lb.
N	Normal force, lbs.
N_N	Normal force response to normal force, lb.
N_m	Normal force response to pitching moment, lb.
n	Yawing moment about model CG, in. lbs.
n_n	Yawing moment response to yawing moment, in.lb.
P_o	Stagnation pressure, psia
p	Free-stream static pressure, psia
p_S	Shield pressure, psia
R	Reynold number based on wing mean aerodynamic chord
S	WING GROSS AREA, 27.562 $IN.^2$
T_o	Stagnation temperature, °F
X_B	Body longitudinal axis
X_S	Stability longitudinal axis
X_W	Wind longitudinal axis
x_{ac}	Distance of the aerodynamic center from the leading edge of $\bar{C}$, in.

List of Symbols (Concluded)

x_{cp} Distance of the center of pressure from the leading edge of $\bar{C}$, due to elevator deflection, in.

x_{cp_a} Distance of the center of pressure from the leading edge of $\bar{C}$, due to single aileron deflection, in.

y_{cp_a} Lateral distance of the center of pressure from model plane of symmetry, due to single aileron deflection, in.

α Angle of attack, deg.

β Angle of side slip, deg.

δ_a Aileron deflection angle, positive for starboard aileron down, deg.

δ_{a_L} Aileron deflection angle when port aileron (i.e. Left) only is deflected while starboard aileron remains at 0°. Positive down, deg.

δ_e Elevator deflection angle, positive down, deg.

δ_r Rudder deflection angle, positive to port, deg.

$(\alpha)_{C_L = 0}$ Zero lift angle of attack, deg.

1. Introduction

Six-component force and moment measurements were made on a 1/80 scale model of the C-105 aircraft in the 30 inch tunnel. Tests were carried out at Mach numbers of 1.35, 1.57, 1.78 and 2.03, corresponding to a Reynolds number range of 1.35×10^6 to 1.70×10^6 based on the wing mean aerodynamic chord, see Fig. 4. Control angle deflection was represented by interchangeable fixed-angle controls while the model itself could be rotated in the pitch and yaw planes.

2. Test Model

The model was manufactured by Avro Aircraft Ltd., arranged for sting mounting from the rear. The model configuration was that having the ~~50~~ 30° nose, enlarged vertical tail, 3.5% thick wing, 5% notch, 10% extension outboard of the notch and drooped leading edge. The air intake ducts were left open at all times. The CG position of the model was located at 0.28 $\bar{C}$.

The table below lists the nominal as well as the measured deflection angles of the interchangeable elevators and ailerons used. The rudder angles were not measured.

The above angles were measured to an accuracy of about ± 0.1°. While the elevators and the rudders were fastened to the model by means of screws, the small size of the model necessitated soldering of the ailerons. When one of these blew off during a tunnel run it was replaced by another having a slightly different deflection. This difference was taken into account in the remainder of the tests.

A photograph of the model mounted on the balance is shown in Fig. 1, a diagram of the model showing leading dimensions is reproduced in Fig. 2.

3. Wind Tunnel

Tests were carried out in the 30 inch wind tunnel in which the Mach number was varied by changing nozzle blocks. The Mach number distributions were uniform to within ± 1% except at M = 2.03 where the variation was ± 1.5%. It was found to be more expeditious to test all model configurations at a given Mach number, rather than to change nozzles for a given configuration, inasmuch as most of the model changes could be accommodated between tunnel runs. Furthermore this procedure left the balance and balance support undisturbed for a series of model configurations.

The model experienced some wave interference at Mach number 1.35 for the highest negative angles of incidence. The results at these conditions were simply discarded.

The tunnel intake air was dried to a specific humidity of less than 0.0005, the stagnation pressure and temperature being approximately atmospheric. Runs of about 5 seconds duration were taken.

4. Model Mounting and Balance

The balance used in the present tests was of the external six-component electrical strain gage type supported on a movable sector. The latter entered the top of the tunnel, its radius being such that the CG of the model remained fixed in the working section when the model was pitched. Drive for the sector was provided externally by a geared-down electric motor with which the incidence could be set to an accuracy of about ± 0.02°.

The total incidence range that could be obtained was -16° to +20° but as it was desirable to reduce the tunnel blockage area at high incidences (and particularly at low Mach numbers) the model and balance were inverted. Thus at the highest incidence the sector contributed minimum blockage. The incidence range used for the tests was from -4° to +16° in steps of 2°.

A recessed channel in the sector was available for leading the balance electrical wires and the shield prossure tubing outside the tunnel.

The entire sector and drive assembly were mounted on a circular turntable fitting into the top of the tunnel. The turntable then could be rotated by means of a crank enabling the model to be set at yaw angles of up to ± 8°. Here the model could be positioned to an accuracy of about ± 0.05°.

Keyways in the downstream shank of the balance allowed it to be placed at various angles of roll in the lower sector boss. However, all tests were done with the balance (and model) at a nominal roll angle of 0°*.

A hardened steel adaptor was used to secure the model to the balance, the actual connection between model and adaptor being a two-dimensional taper fit. In order to simplify the data reduction, the center line of the balance was made to pass through the model CG by suitably cranking the adaptor. The forward portion of the adaptor was necessarily narrow so that it could slip between the two engine ducts. All changes in model configuration could be effected between tunnel runs with the model in place on the adaptor.

The balance was designed at the NAE and calibrated prior to the test program. A check calibration was carried out at the conclusion of the tests. The forces measured by the balance

* Although the model was tested at a nominal angle of roll of 0°, model and balance misalignments as well as deflections due to air loads resulted in an actual angle of roll varying between -0.5° to 0.4° depending on Mach number.

were the normal, axial and side forces acting on the model while the moments were the pitching, yawing and rolling moments about the CG position on the model. All components, with the exception of axial force, incorporated bonded strain gages whereas the axial force was obtained by means of a displacement-type strain gauge transducer. In addition, shield pressure was measured and for purposes of data reduction the axial force was corrected for free-stream pressure acting on an area equal to the cross-sectional area of the adaptor at the model base. Balance as well as shield pressure transducer outputs were carried to 7 high-speed potentiometer recorders.

5. Reduction of Data

Balance calibration yielded the following expressions for the body forces and moments together with component interactions:

$$N = N_N - N_m$$

$$Y = Y_Y - Y_n$$

$$A = A_A - A_T \alpha + (p_S - p) A_b - A_N - A_m - A_Y$$

$$m = m_m - hN = m_m - h (N_N - N_m)$$

$$n = n_n - kY = n_n - k (Y_Y - Y_n)$$

$$l = l_l$$

In the stability system of axes depicted in Fig. 3, these expressions become, in coefficient form:

$$C_L = \frac{1}{qS}\left[(N_N - N_m)\cos\alpha - \left\{A_A - A_T\alpha + (p_S - p)A_b - A_N - A_m - A_Y\right\}\sin\alpha\right]$$

$$C_Y = \frac{1}{qS}(Y_Y - Y_n)$$

$$C_D = \frac{1}{qS}\left[(N_N - N_m)\sin\alpha + \left\{A_A - A_T\alpha + (p_S - p)A_b - A_N - A_m - A_Y\right\}\cos\alpha\right]$$

$$C_m = \frac{1}{qS\bar{C}}\left[m_m - h(N_N - N_m)\right]$$

$$C_n = \frac{1}{qSb}\left[\left\{n_n - k(Y_Y - Y_n)\right\}\cos\alpha - l_1\sin\alpha\right]$$

$$C_l = \frac{1}{qSb}\left[l_1\cos\alpha + \left\{n_n - k(Y_Y - Y_n)\right\}\sin\alpha\right]$$

Corrections to the nominal angles of attack, yaw and roll determined by calibration, were applied to take into account balance and adaptor deflections due to model loads. Also the usual corrections due to model and balance misalignments in the tunnel were made.

The calibration check at the completion of the tests gave the following changes in the component and interaction calibration factors:

Component and Interaction	% Change in Calibration Factors
N_N	2
Y_Y	0
A_A	1
m_m	4
n_n	3
l_l	3
A_N	-125
A_Y	4
A_m	-10
N_m	-36
Y_n	-6

The effect of these changes in the balance calibration factors on the final aerodynamic coefficients is indicated in the table below:

Coefficient	Maximum % Change
C_L	1.1
C_Y	-0.1
C_D	2.7
C_m	-0.7
C_n	10.9
C_l	7.8

The data reduction was contracted out to the IBM company and was effected concurrently with the tunnel tests, the computer programming being necessarily frozen prior to the initiation of the tests and based on the initial balance calibration.

The aerodynamic center and various centers of pressure positions were calculated as follows:

$$\frac{x_{ac}}{\bar{c}} = 0.28 - \left(\frac{C_m}{C_L}\right)_{\delta_e = 0°}$$

$$\frac{x_{cp}}{\bar{c}} = 0.28 - \frac{\left(C_m \delta_e\right)\alpha = 0°}{\left(C_L \delta_e\right)\alpha = 0°} = \frac{x_{ac}}{\bar{c}} - \frac{\left(C_m \delta_e\right)C_L = 0}{\left(C_L \delta_e\right)\alpha = 0°}$$

$$\frac{x_{cp_a}}{\bar{c}} = 0.28 - \frac{\left(C_m \delta a_L\right)\alpha = 0°}{\left(C_L \delta a_L\right)\alpha = 0°}$$

$$\frac{y_{cp_a}}{b/2} = \frac{\left(C_l \delta a_L\right)\alpha = 0°}{\left(C_L \delta a_L\right)\alpha = 0°}$$

6. Test Procedure

As mentioned above, all model configurations were completely tested at one Mach number before changing nozzle blocks. For each model configuration the model was pitched through an angle of incidence range of -4° to 16° in steps of 2°, isolated tunnel runs being taken at each incidence setting.

The 27 model configurations as well as the sideslip angles at which they were tested are indicated by an 'x' in the table below. All angles are nominal.

Model Configurations Tested

β	$\delta_e = \delta_a = 0°$		$\delta_a = \delta_r = 0°$					
			δ_e (deg)					
Deg	$\delta_r = 0°$	Fin Off	10	5	-5	-10	-20	-30
-4	x	x						
-2	x	x						
0	x	x	x	x	x	x	x	x
2	x	x						
4	x	x						
6	x	x	x	x	x	x	x	x
8	x	x						

$\delta_e = \delta_a = \beta = 0°$								
δ_r (deg)								
4	2	-2	-4	-6	-8	-10	-15	-20
x	x	x	x	x	x	x	x	x

$\delta_e = \delta_r = \beta = 0°$				
δ_a (deg)				
-5	5	10	15	20
x	x	x	x	x

$\delta_e = \delta_r = \beta = 0°$				
δ_{a_L} (deg)*				
5	-5	-10	-15	-20
x	x	x	x	x

* It was not required to test this configuration at M = 1.35

As the model was inverted the maximum tunnel blockage occurred at an incidence of -4°. When choking effects were experienced at a Mach number of 1.35, the negative incidence was reduced in steps of 1° until wave interference appeared to be removed. Nevertheless, results at this Mach number were not considered reliable at negative incidences.

It had been determined from calibration that balance and model tare weights were significant only insofar as the axial force was concerned. Consequently a tare weight correction to axial force only (i.e. component of tare weight in direction of axial force due to incidence) was incorporated in the data reduction equations. Inasmuch as this correction was quite linear, in actual practice the axial force recorder was zeroed with the model at zero incidence, following which the required incidence was given the model and a tunnel run taken. The chart reading was then simply based on the original zero.

FIG. 1 PHOTOGRAPH OF MODEL AND BALANCE MOUNTED ON SECTOR.

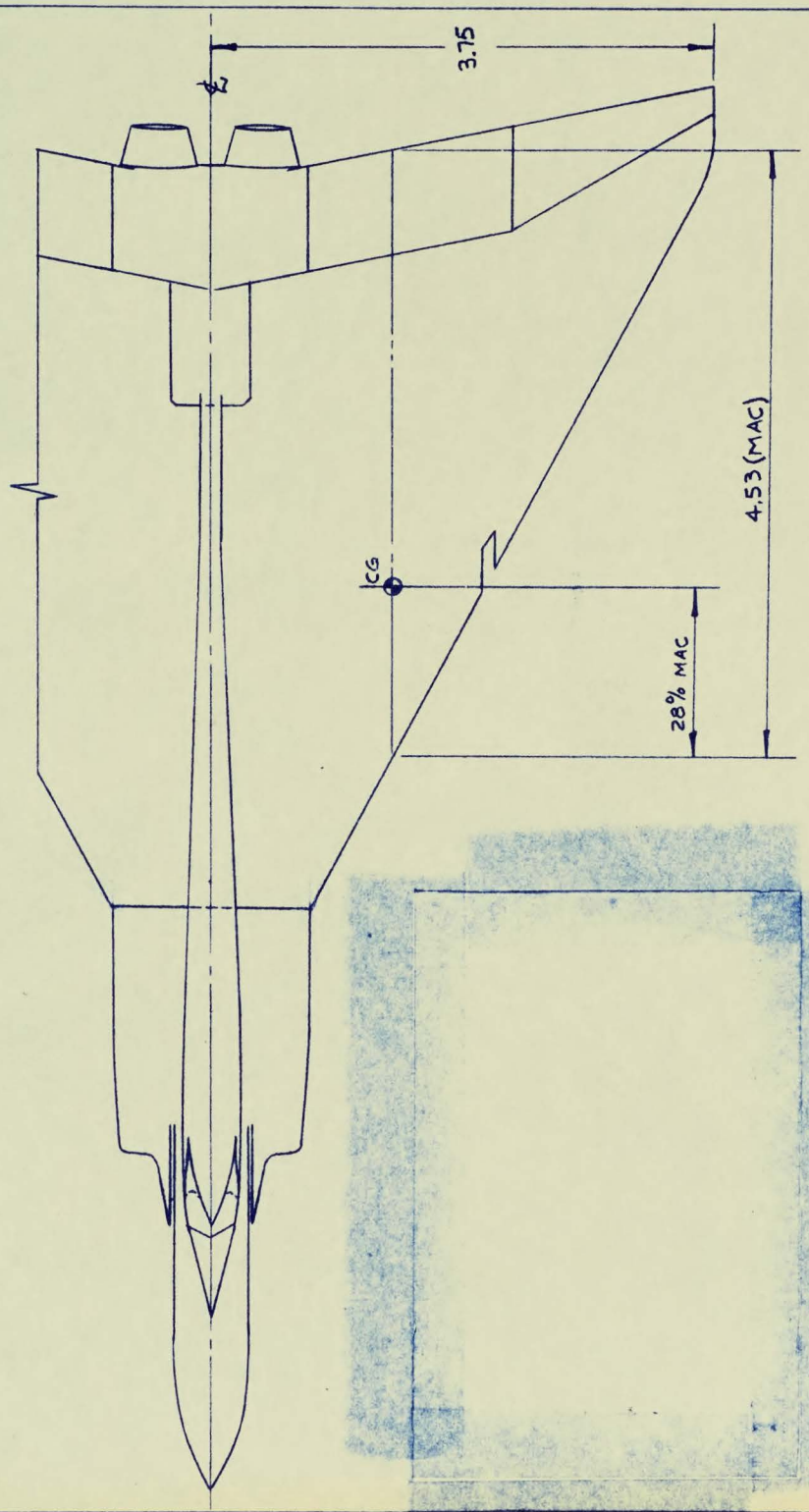

ALL DIMENSIONS IN INCHES

FIG. 2 DIAGRAM OF 60 SCALE MODEL

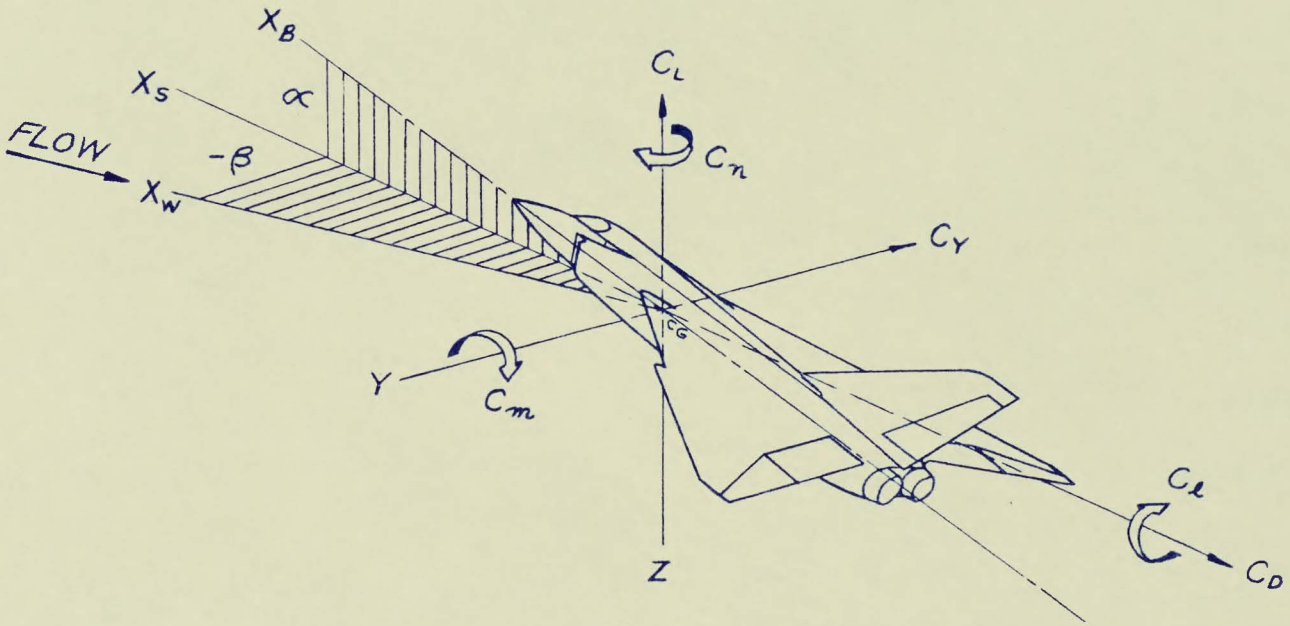

NOTE - ARROWHEADS POINT IN POSITIVE SENSE

FIG. 3 STABILITY SYSTEM OF AXES USED

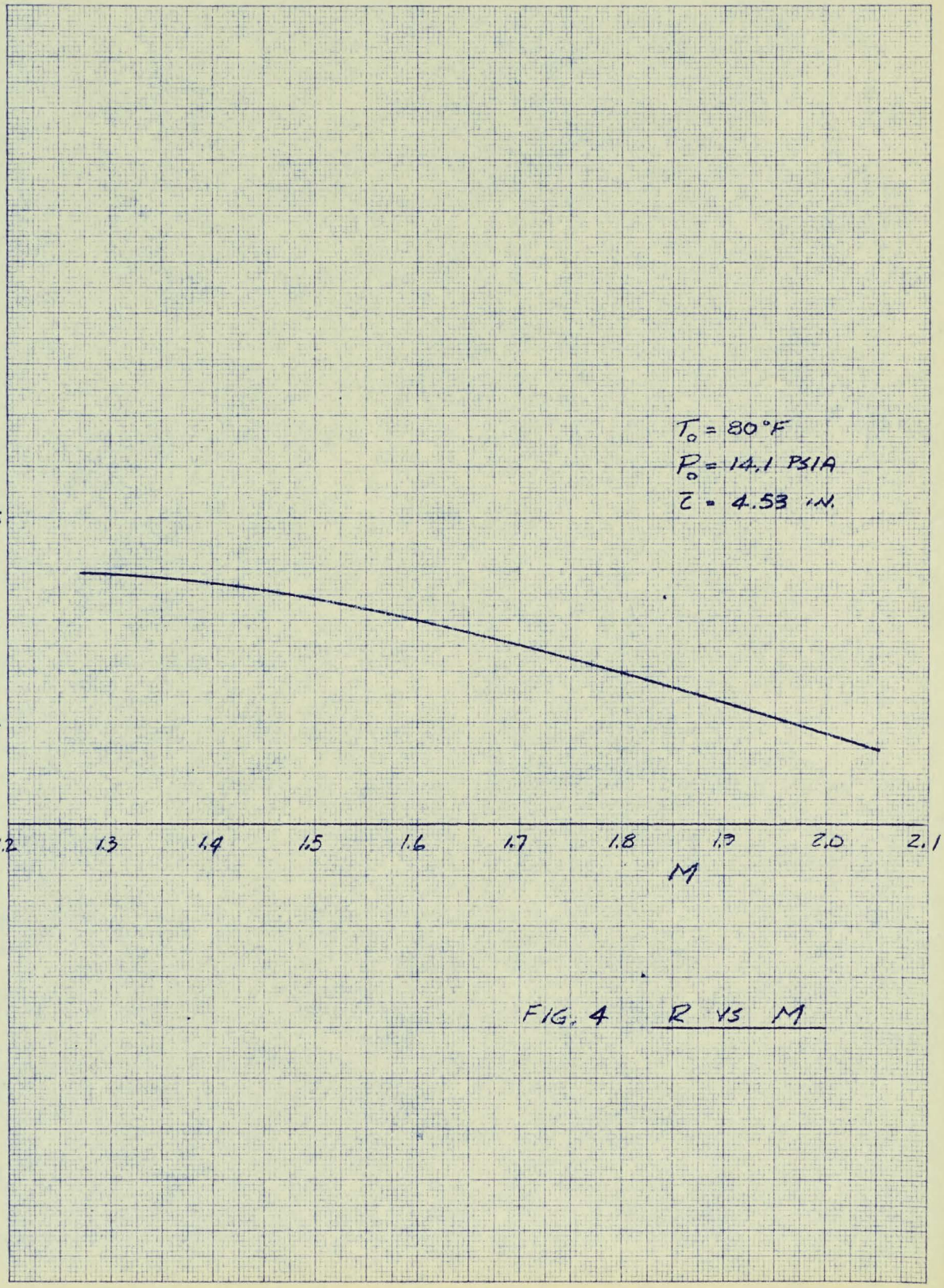

FIG. 4 R VS M

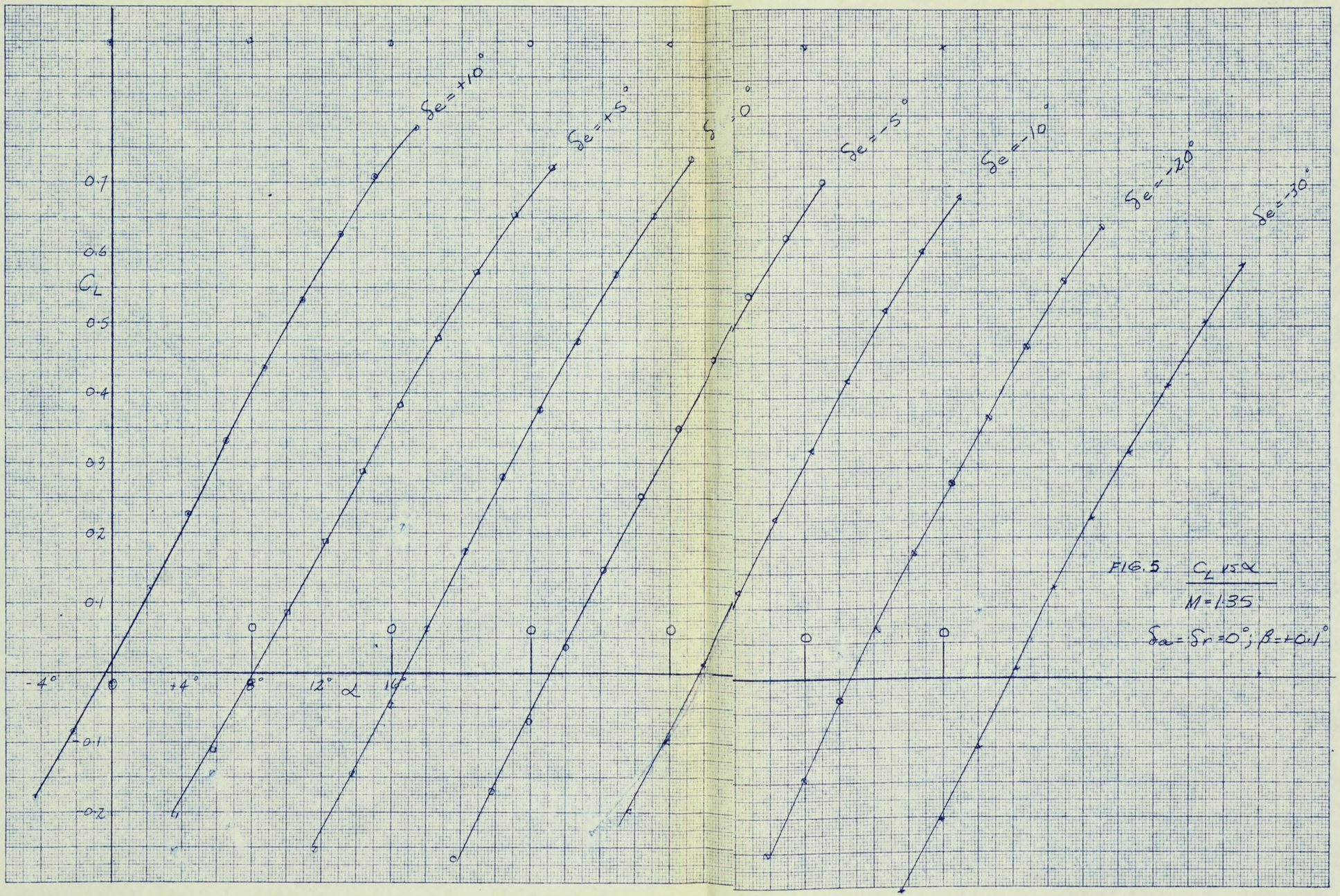

FIG. 5 C_L vs α

$M = 1.35$

$\delta_a = \delta_r = 0°$; $\beta = +0.1°$

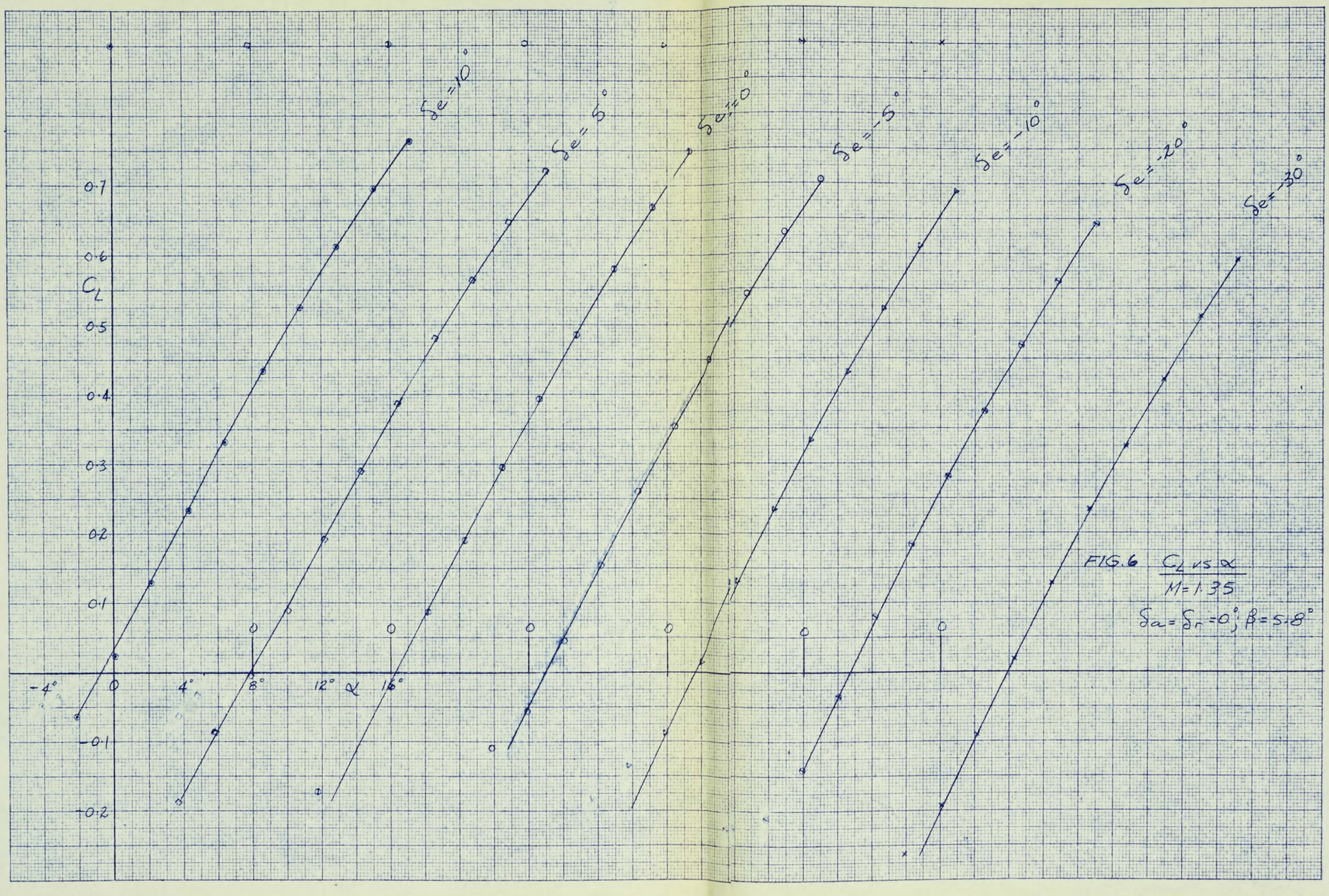

FIG.6 C_L vs α
M=1.35
$\delta_a=\delta_r=0°$; $\beta=5.8°$

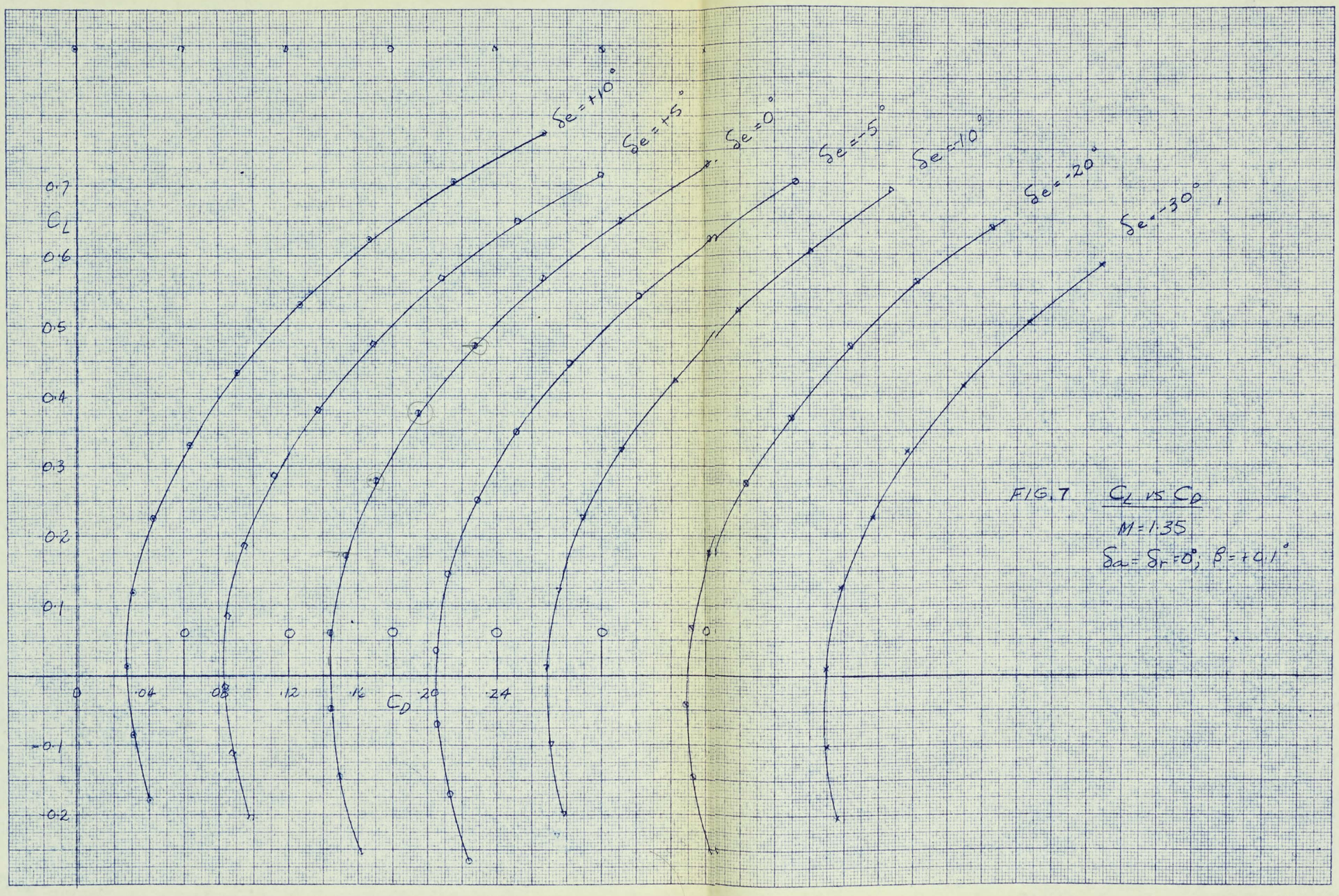

FIG. 7 C_L vs C_D

$M = 1.35$

$\delta_a = \delta_r = 0°$; $\beta = +0.1°$

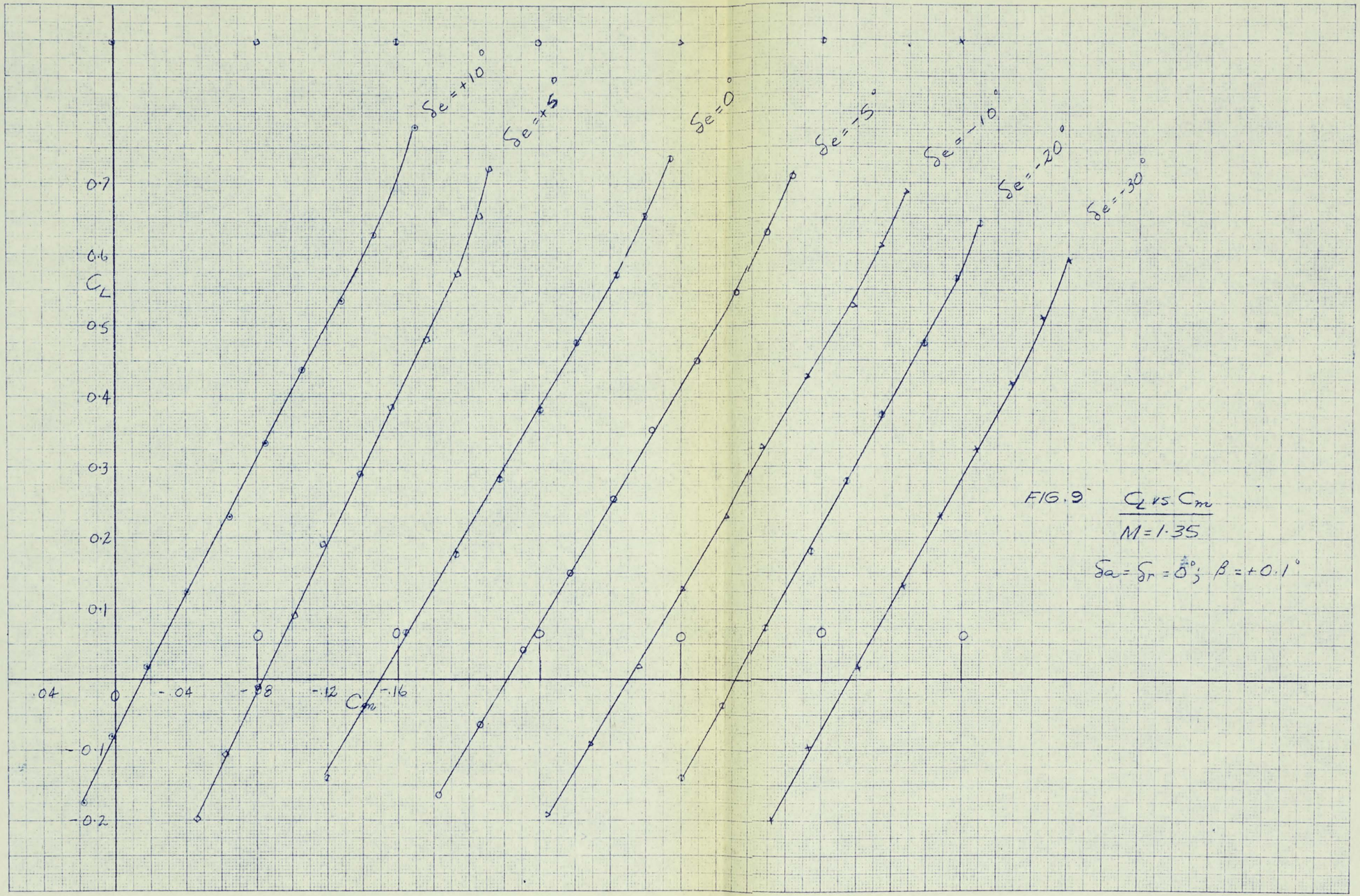

FIG. 9 C_L vs C_m

$M = 1.35$

$\delta_a = \delta_r = 0°$; $\beta = +0.1°$

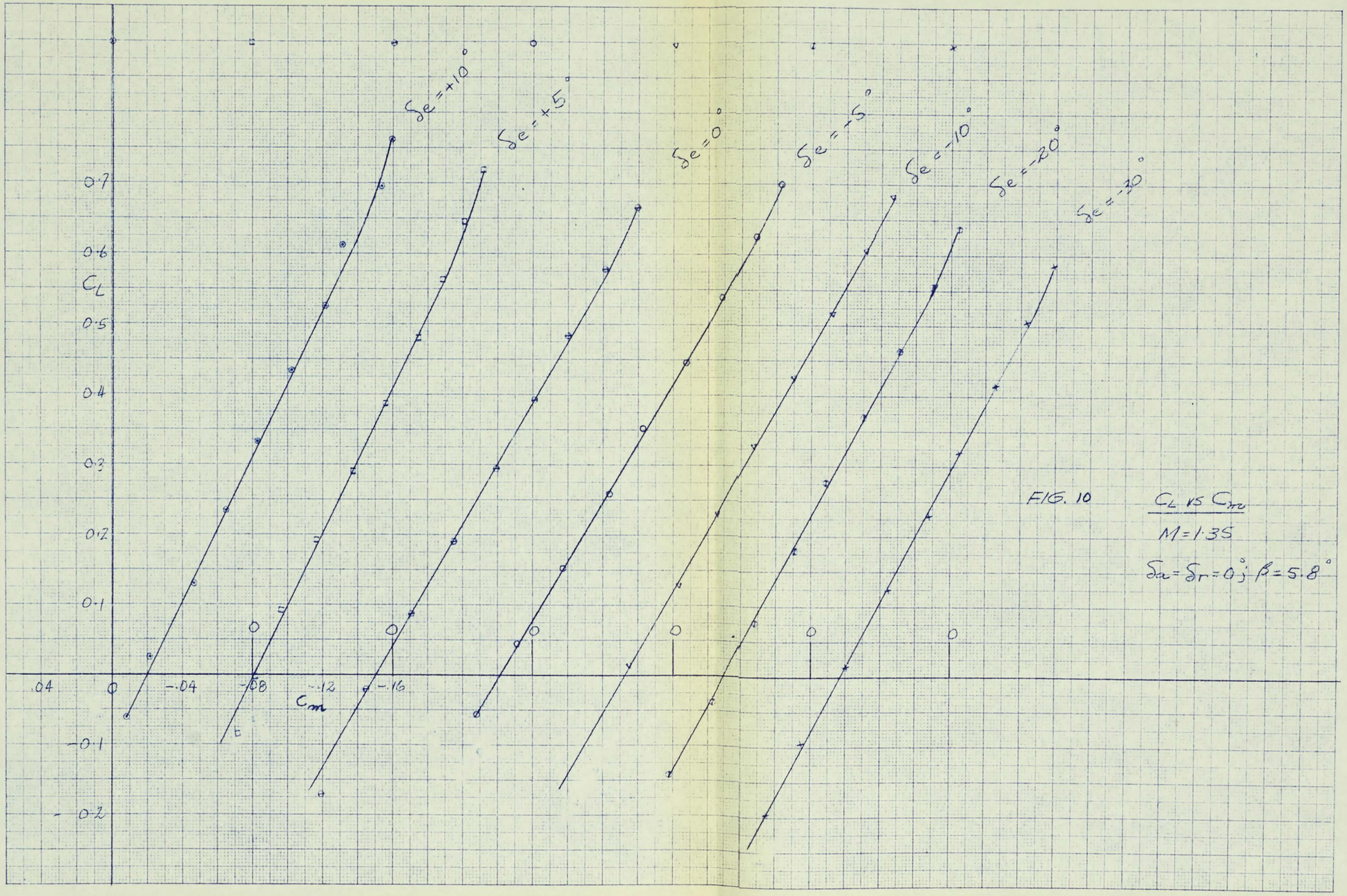

FIG. 10 C_L vs C_m

$M = 1.35$

$\delta_a = \delta_r = 0°$; $\beta = 5.8°$

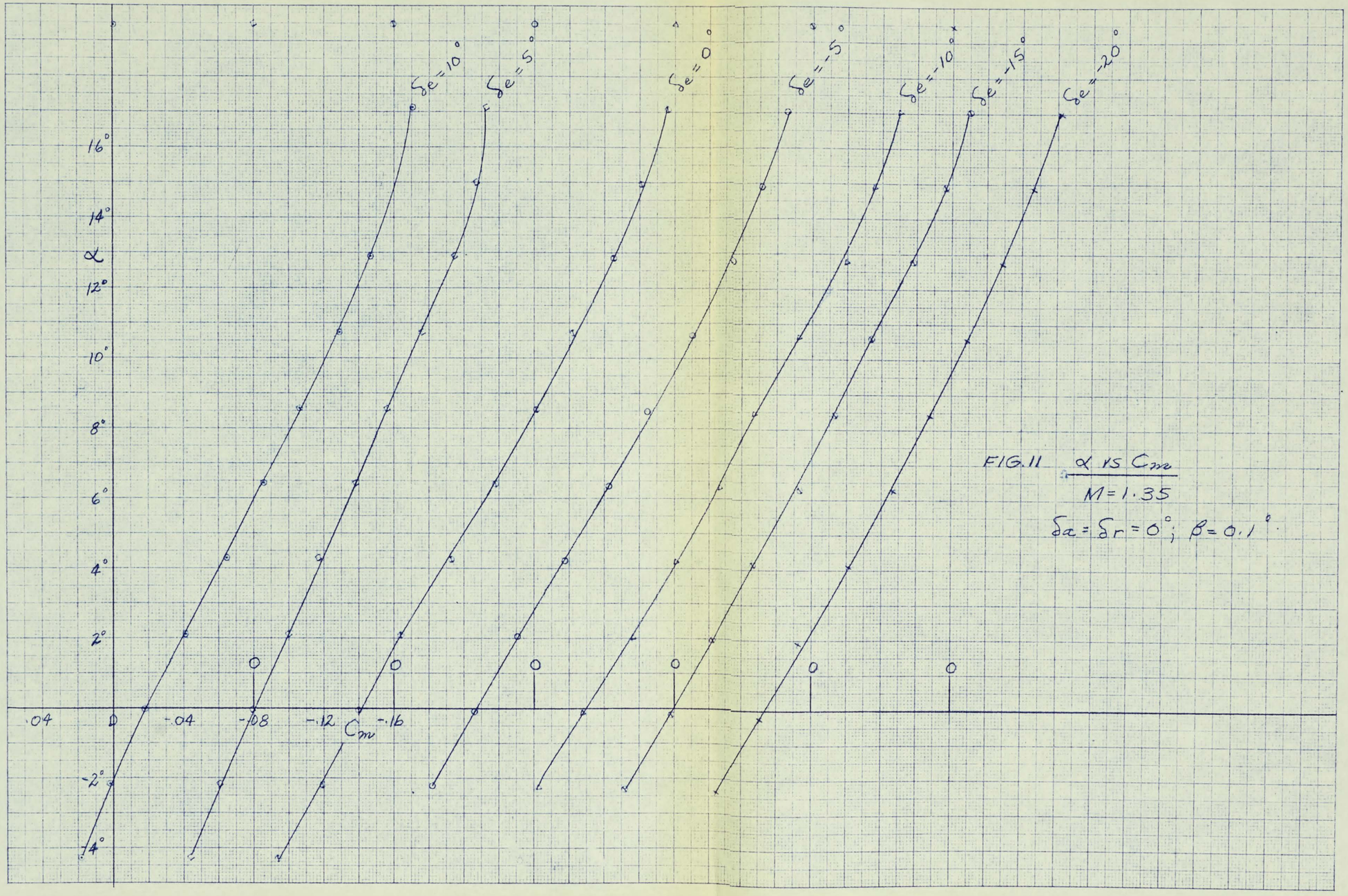

FIG. 11 α vs C_m

$M = 1.35$

$\delta_a = \delta_r = 0°$; $\beta = 0.1°$

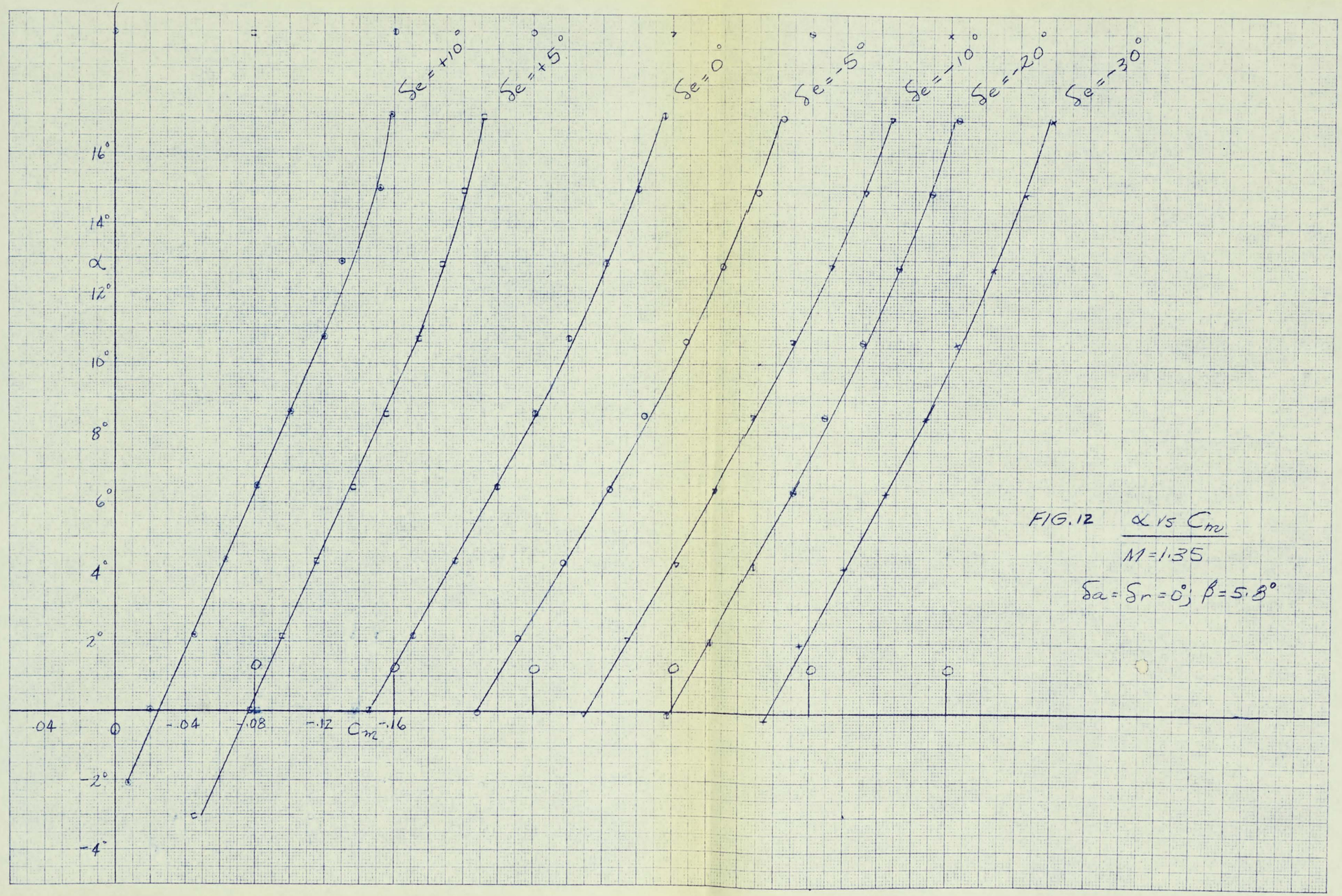

FIG. 12 α vs C_m

M=1.35

$\delta_a = \delta_r = 0°$; $\beta = 5.8°$

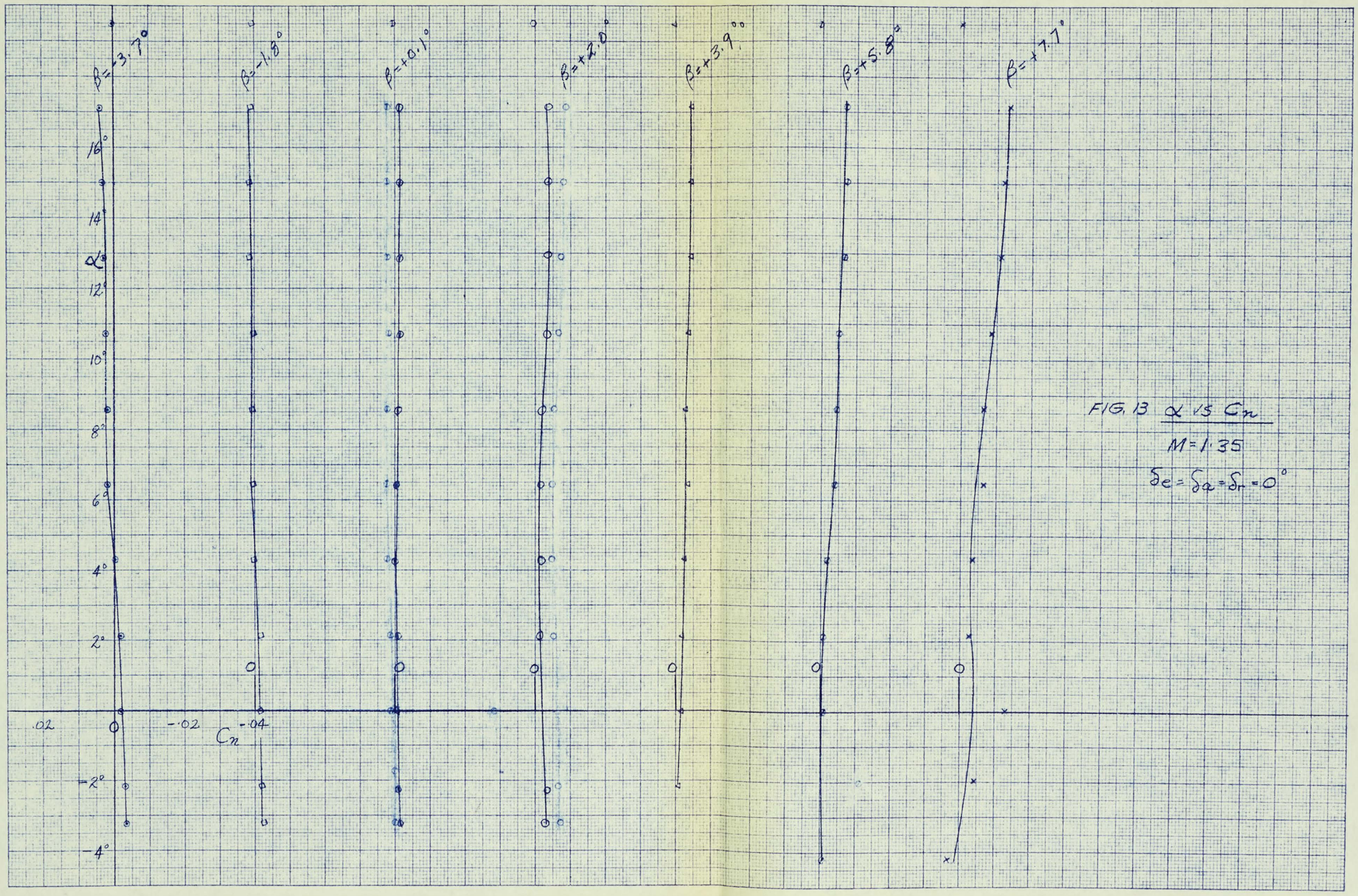

FIG. 13 α vs C_n

M = 1.35

$\delta_e = \delta_a = \delta_r = 0°$

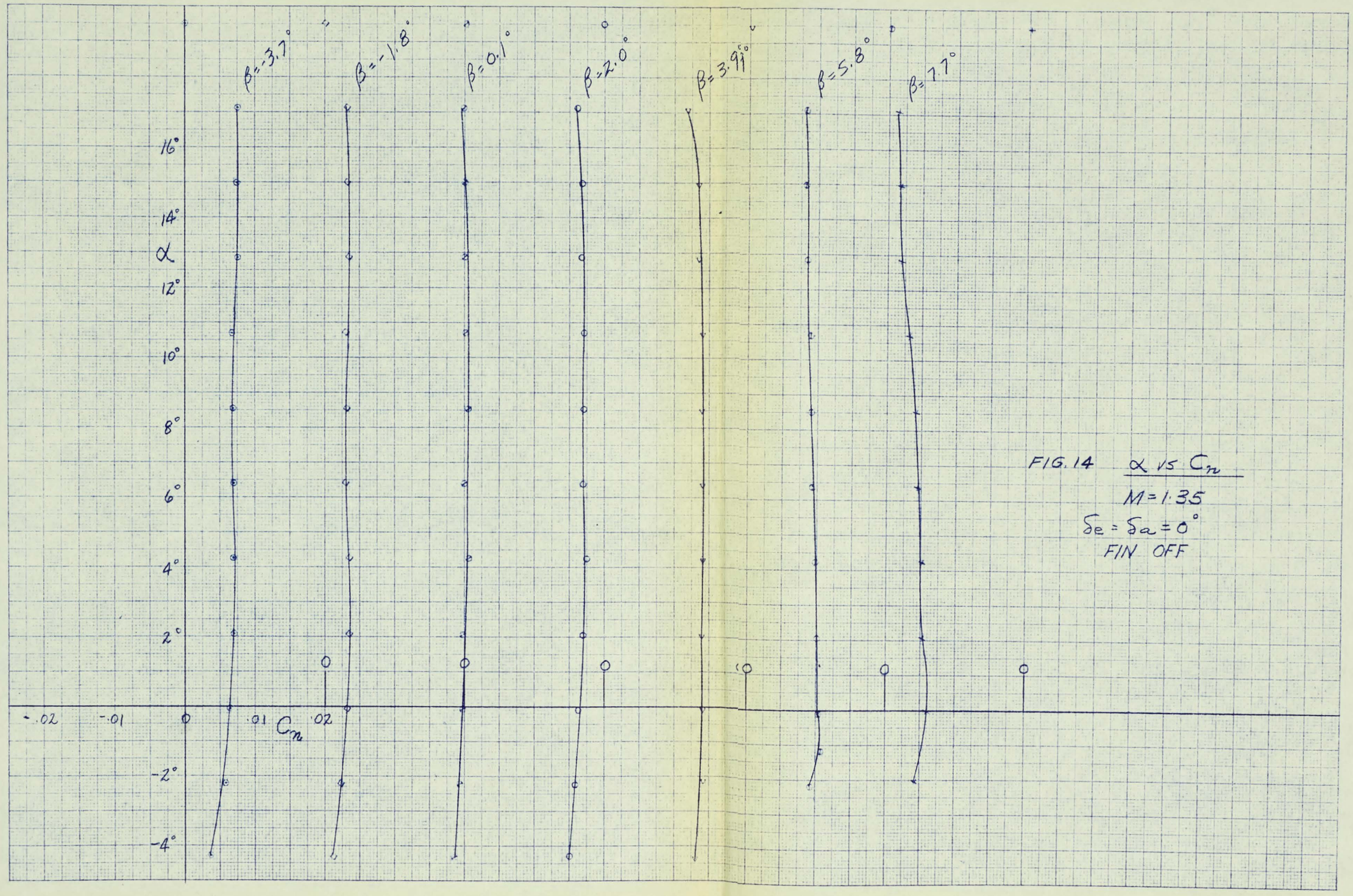

FIG. 14 α vs C_n

$M = 1.35$

$\delta_e = \delta_a = 0°$

FIN OFF

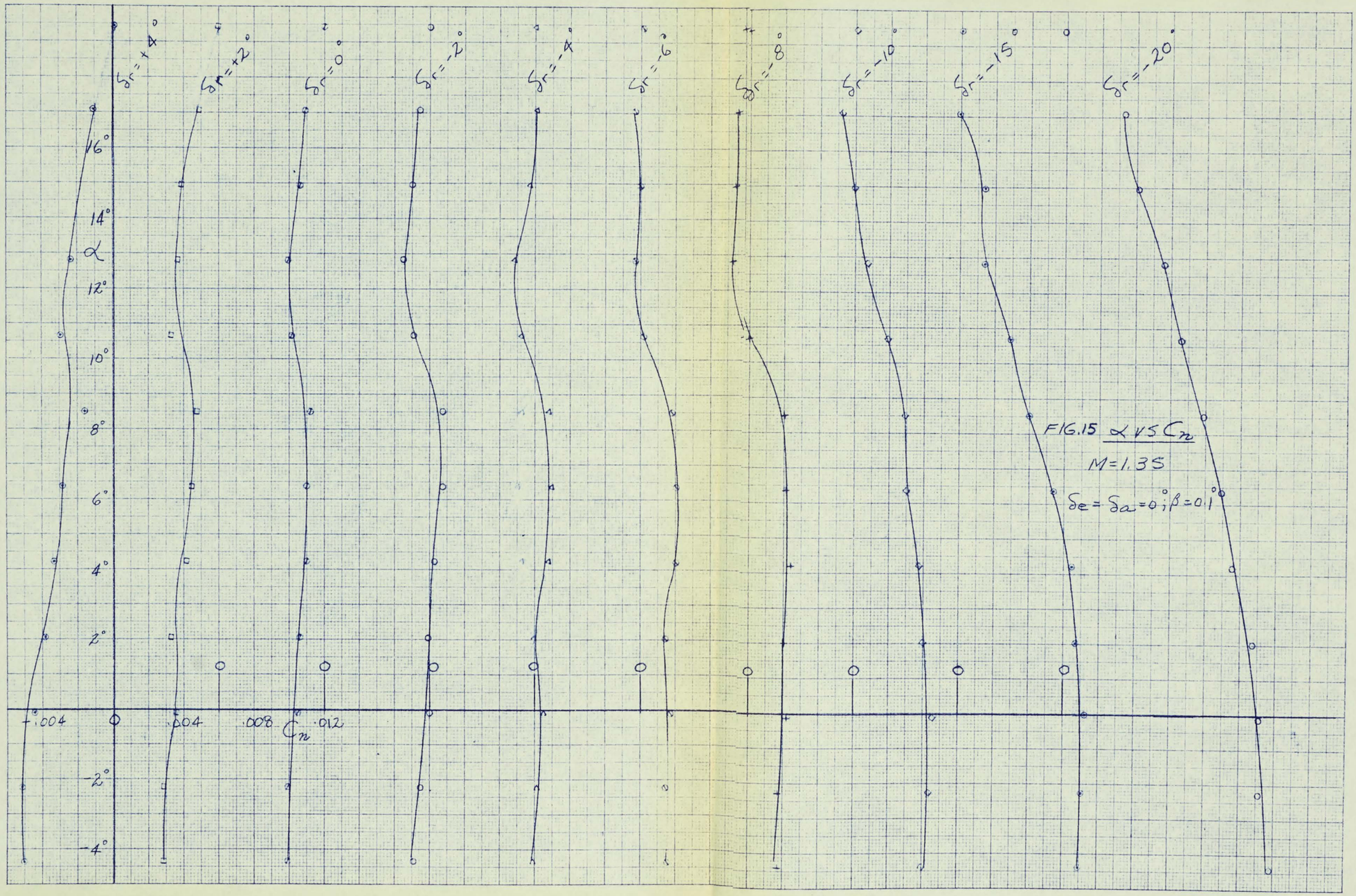

FIG.15 α VS C_n

M=1.35

$\delta_e = \delta_a = 0°; \beta = 0.1°$

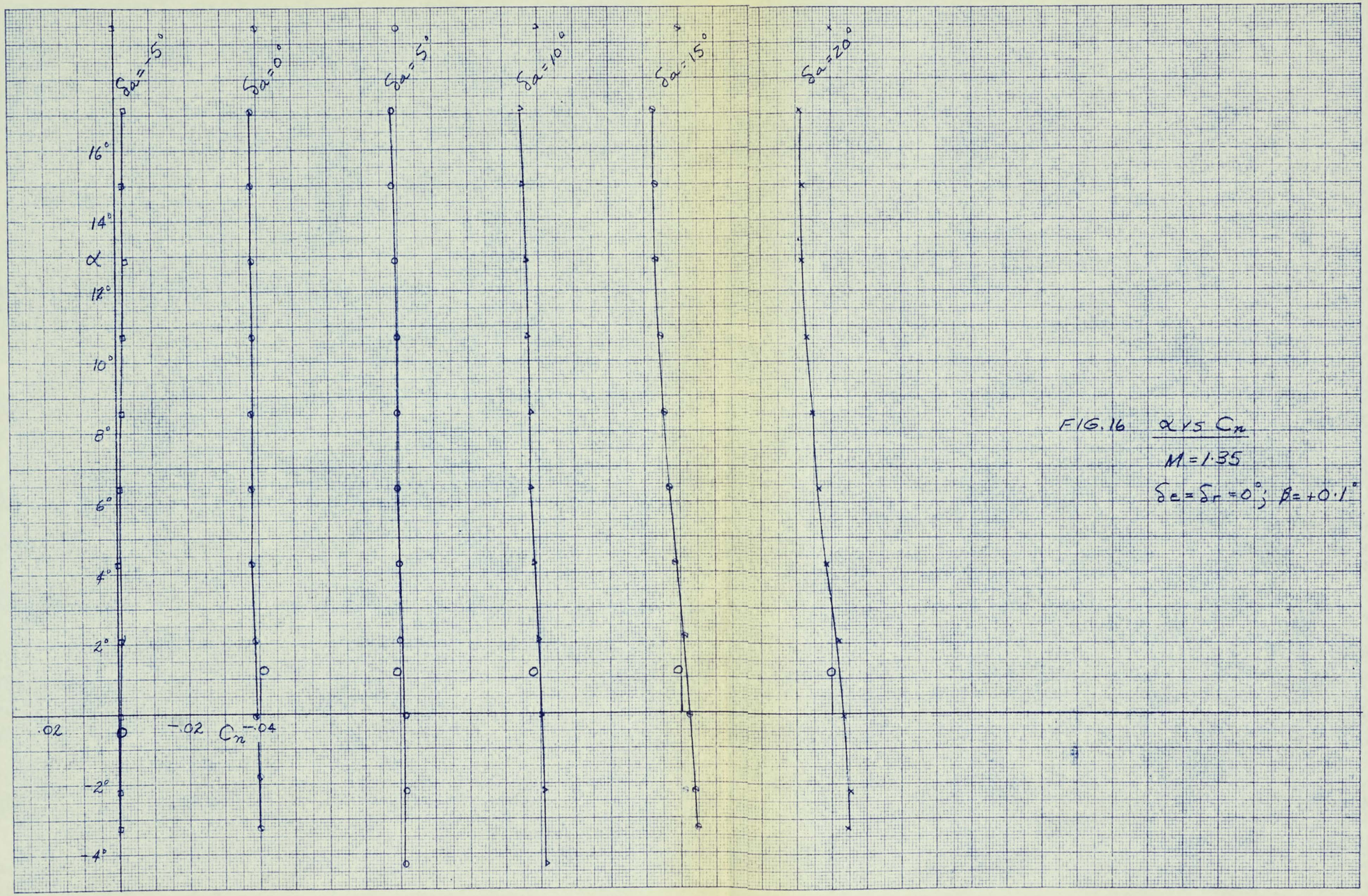

FIG. 16 α vs C_n

$M = 1.35$

$\delta_e = \delta_r = 0°$; $\beta = +0.1°$

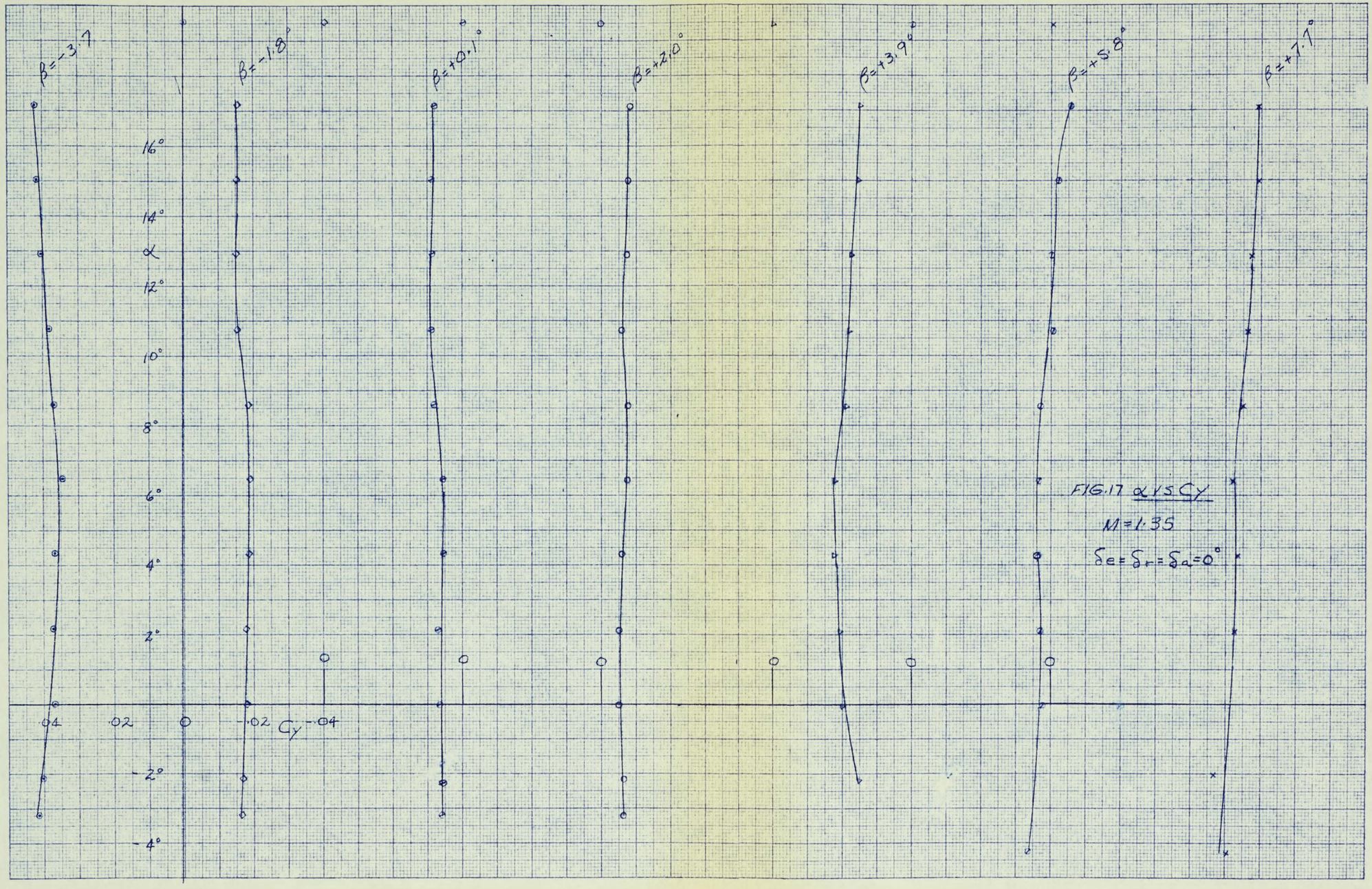

FIG. 17 α VS Cy

M=1.35

$\delta_e = \delta_r = \delta_a = 0°$

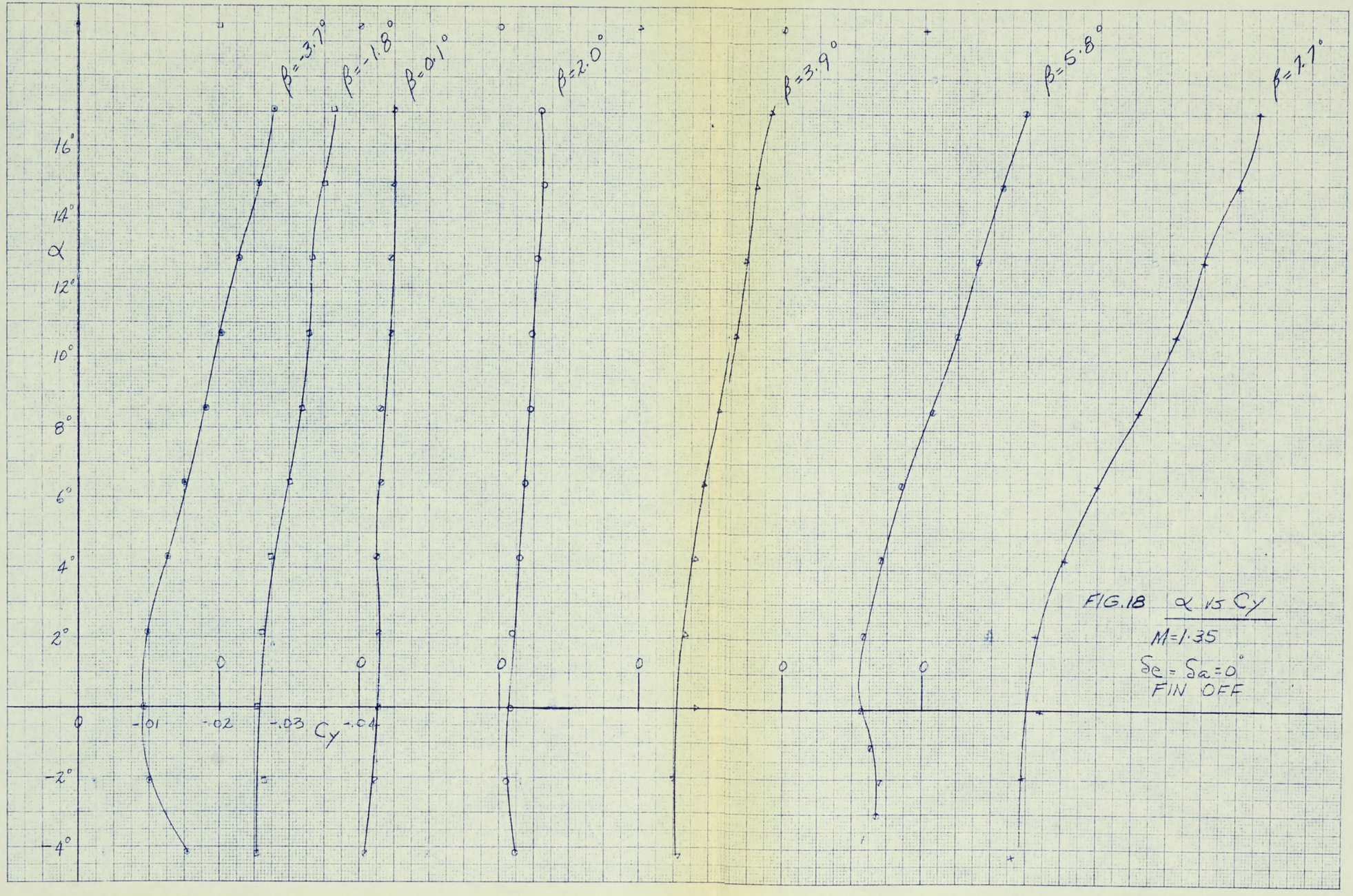

FIG.18 α VS Cy

M=1.35

δe = δa = 0°

FIN OFF

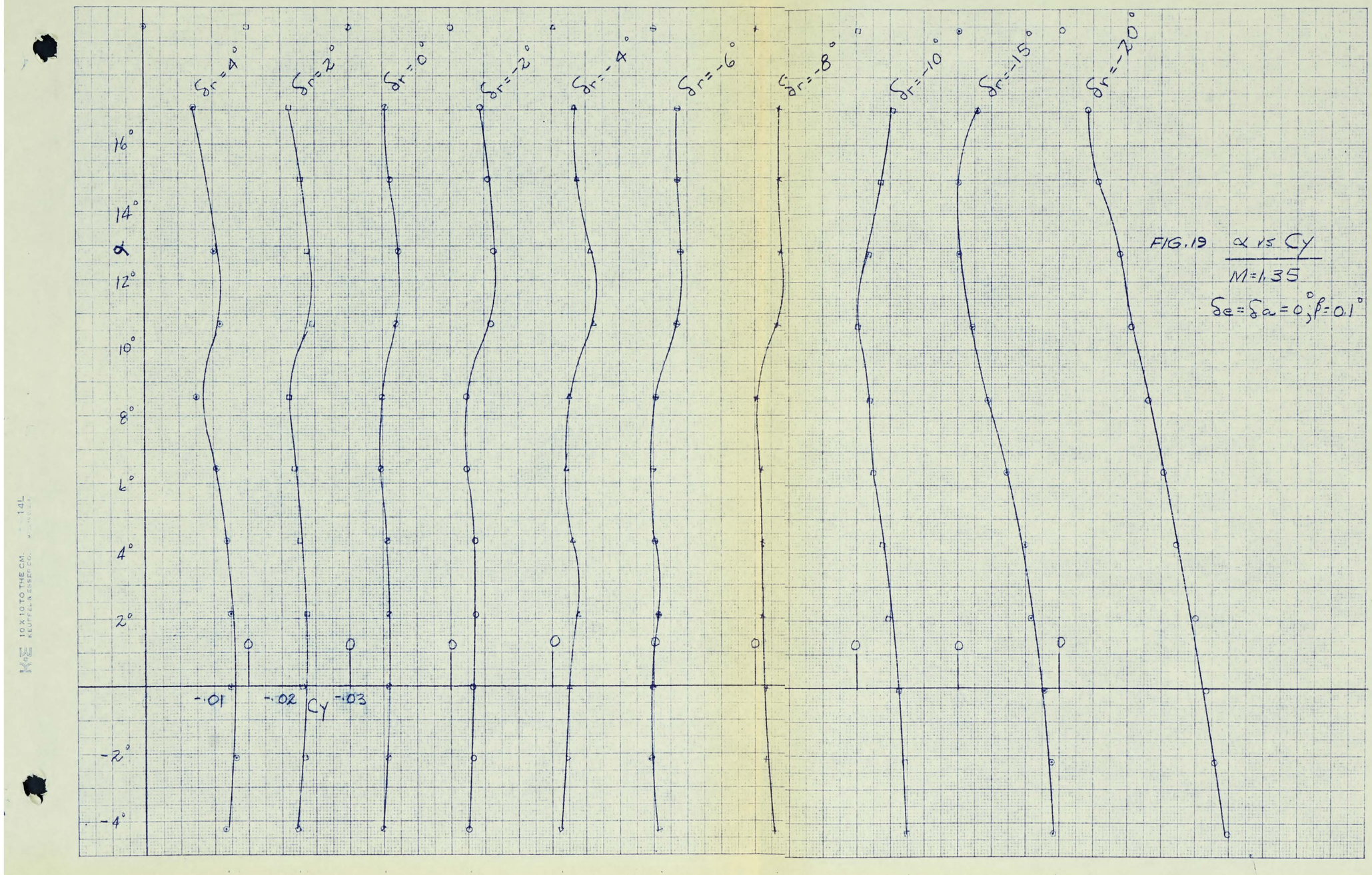

FIG. 19 α vs Cy

M=1.35

$\delta_e = \delta_a = 0°, \beta = 0.1°$

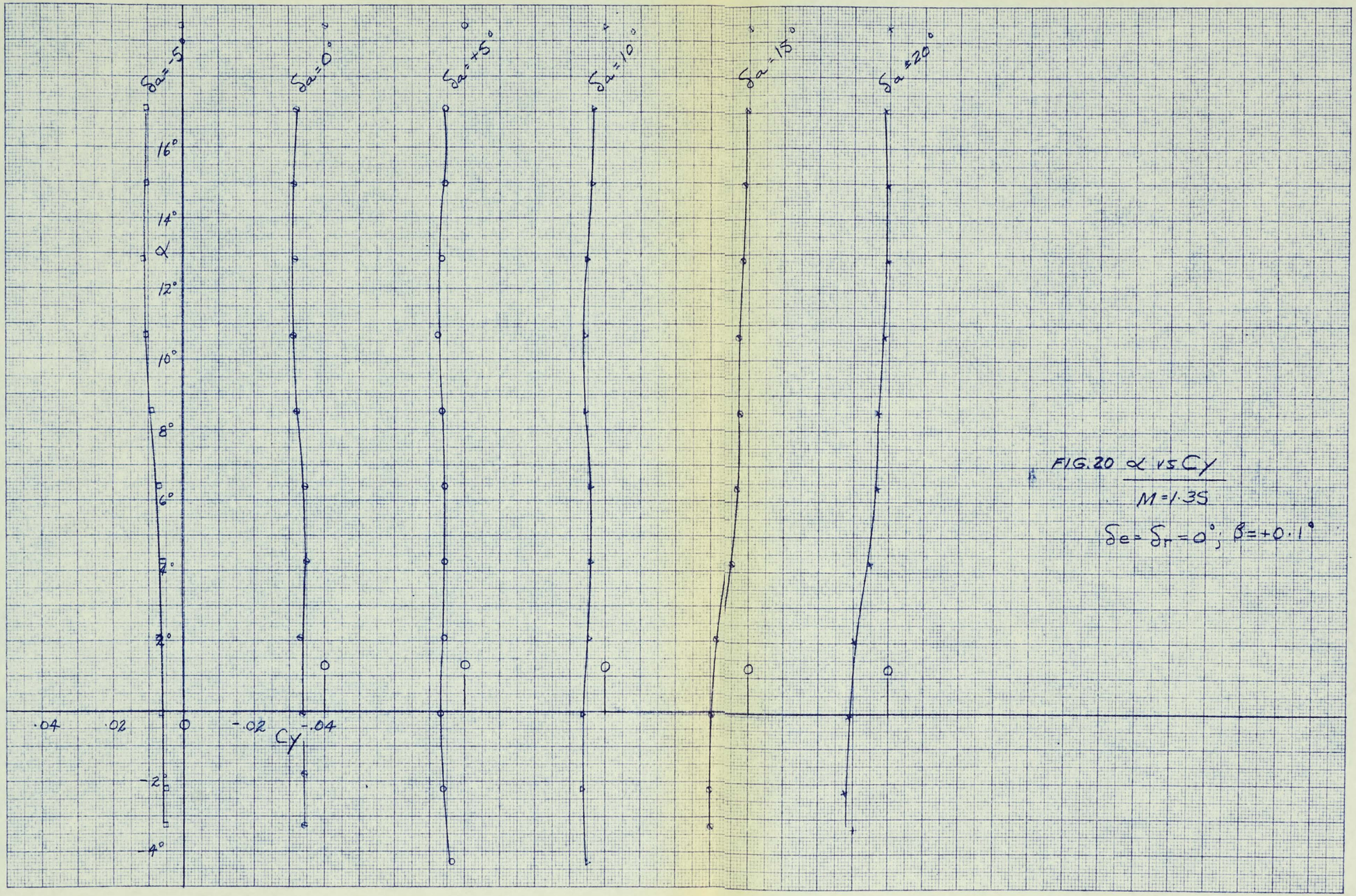

FIG. 20 α vs Cy

M = 1.35

$\delta_e = \delta_r = 0°$; $\beta = +0.1°$

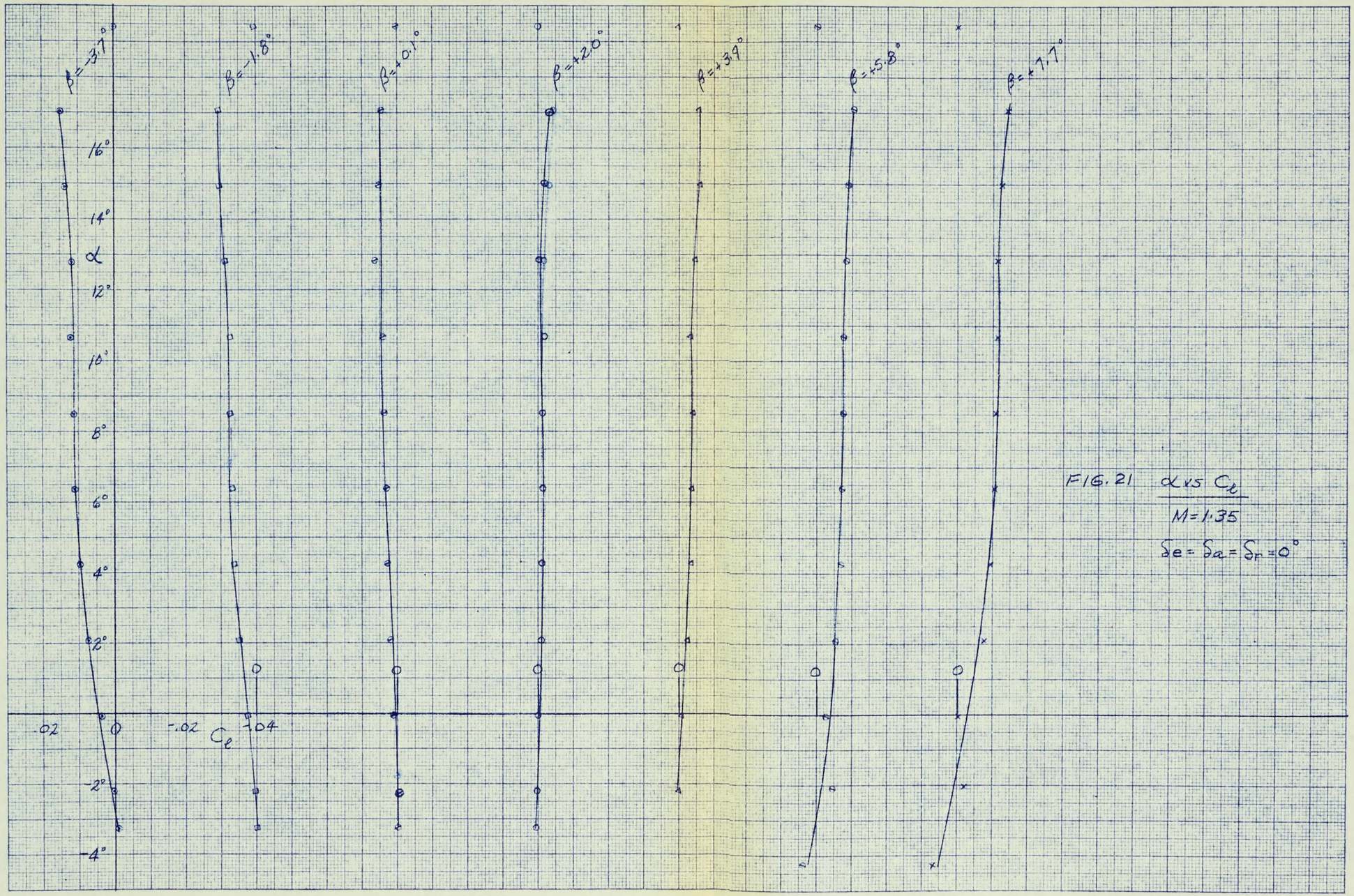

FIG. 21 α vs C_ℓ

$M = 1.35$

$\delta_e = \delta_a = \delta_r = 0°$

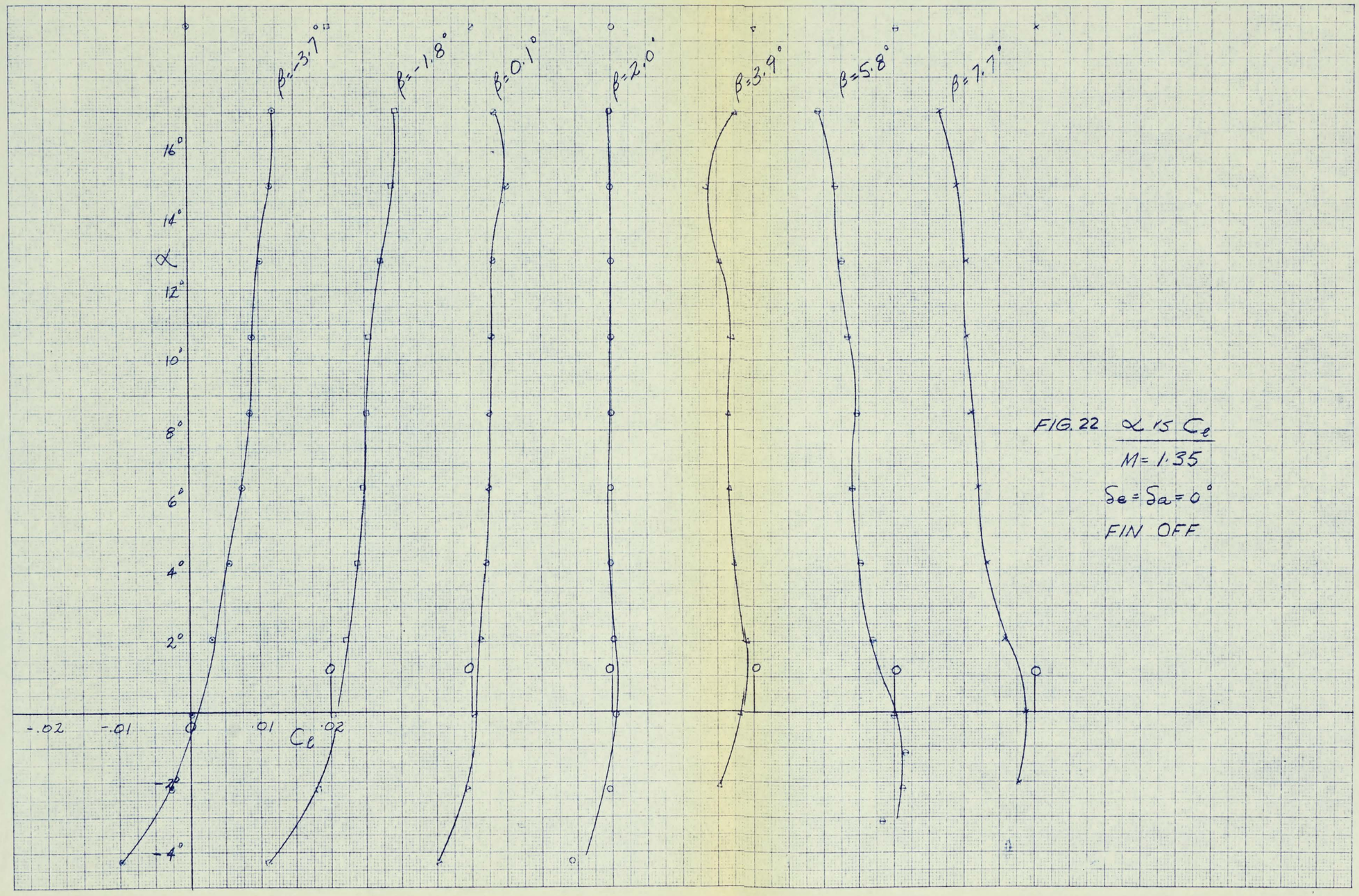

FIG. 22 α vs C_ℓ

$M = 1.35$

$\delta_e = \delta_a = 0°$

FIN OFF

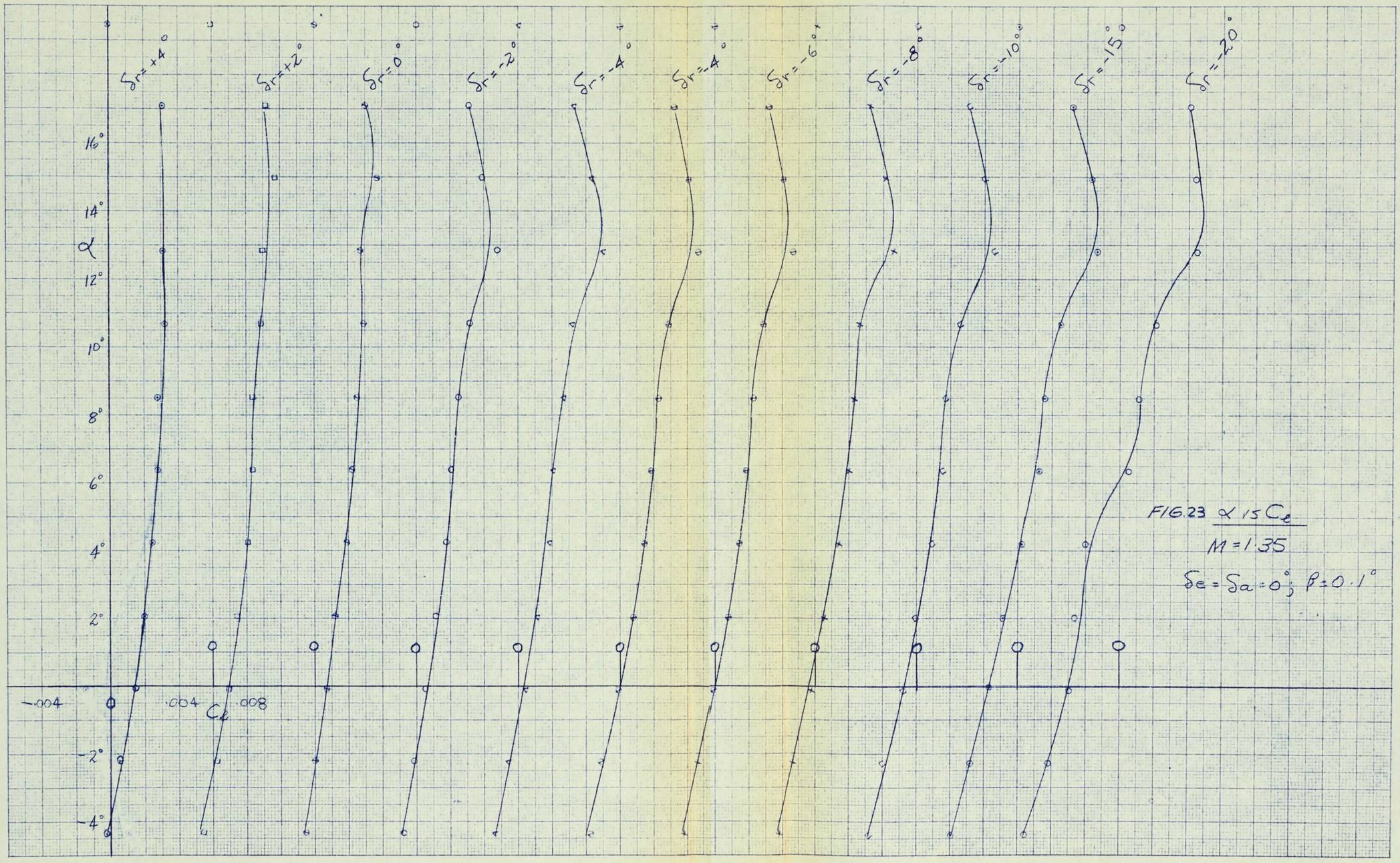

FIG. 23 α vs C_l

$M = 1.35$

$\delta e = \delta a = 0°$; $\beta = 0.1°$

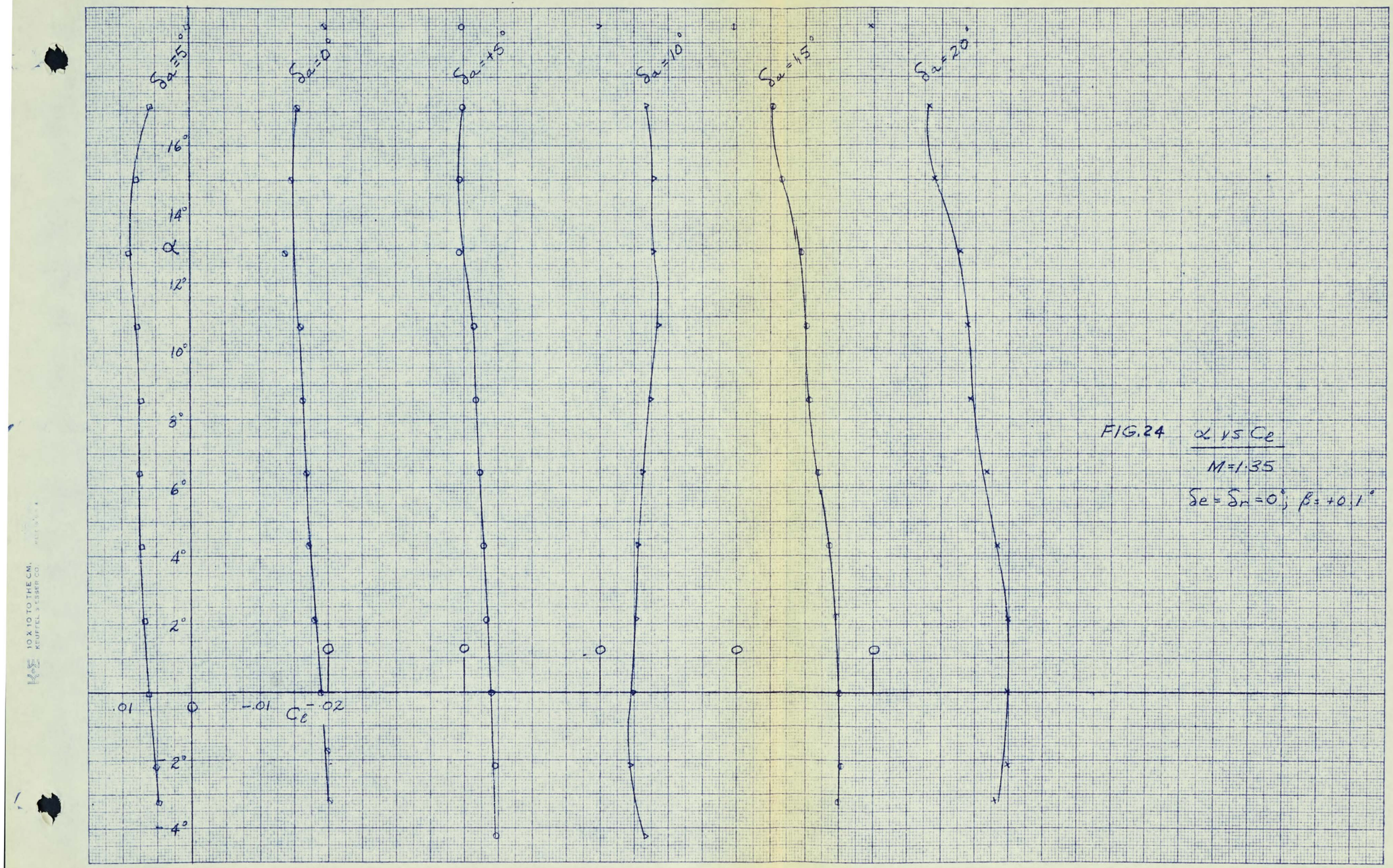

FIG.24 α vs C_ℓ

M=1.35

$\delta_e=\delta_r=0°$; $\beta=+0.1°$

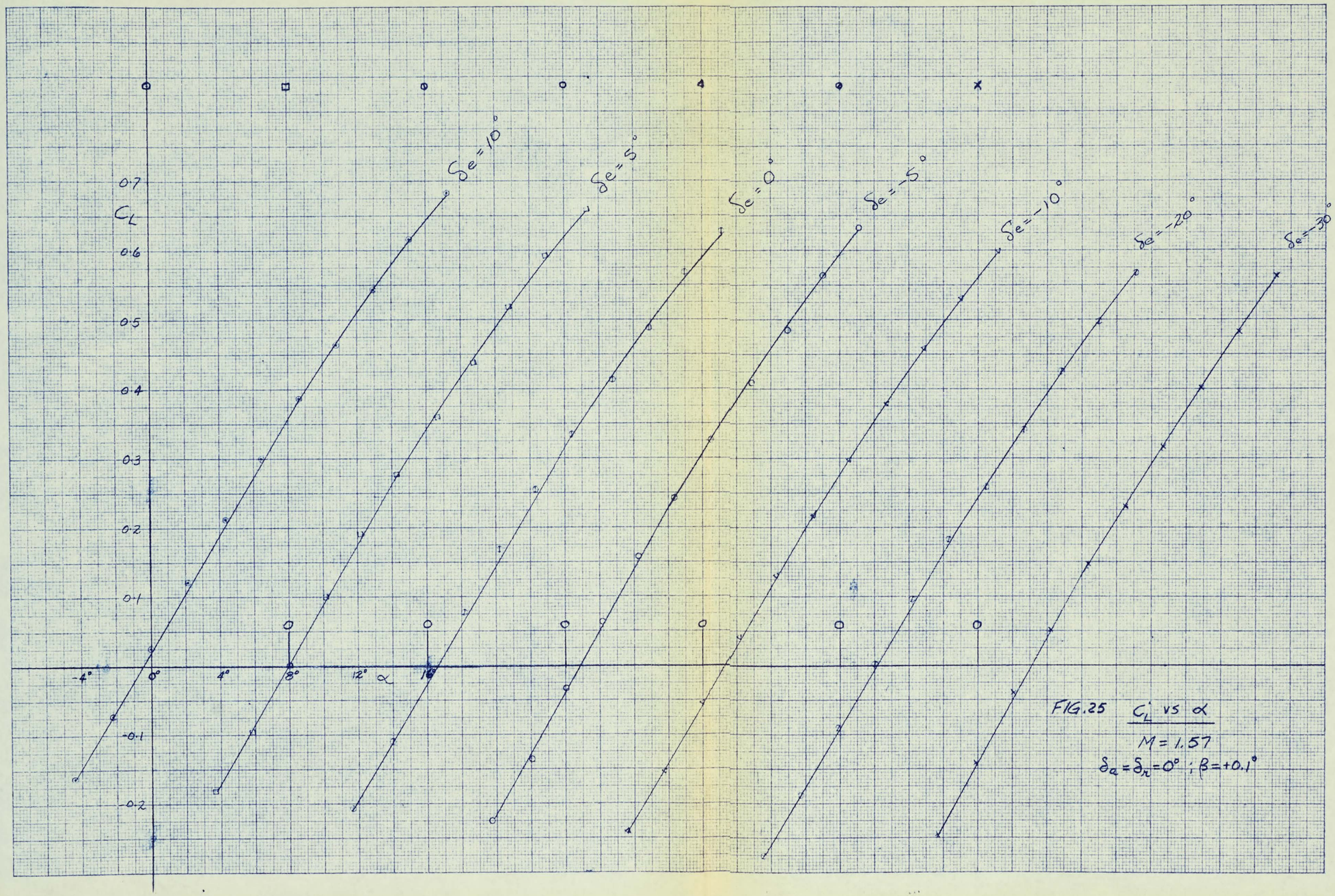

FIG. 25 C_L vs α

$M = 1.57$

$\delta_a = \delta_r = 0°$; $\beta = +0.1°$

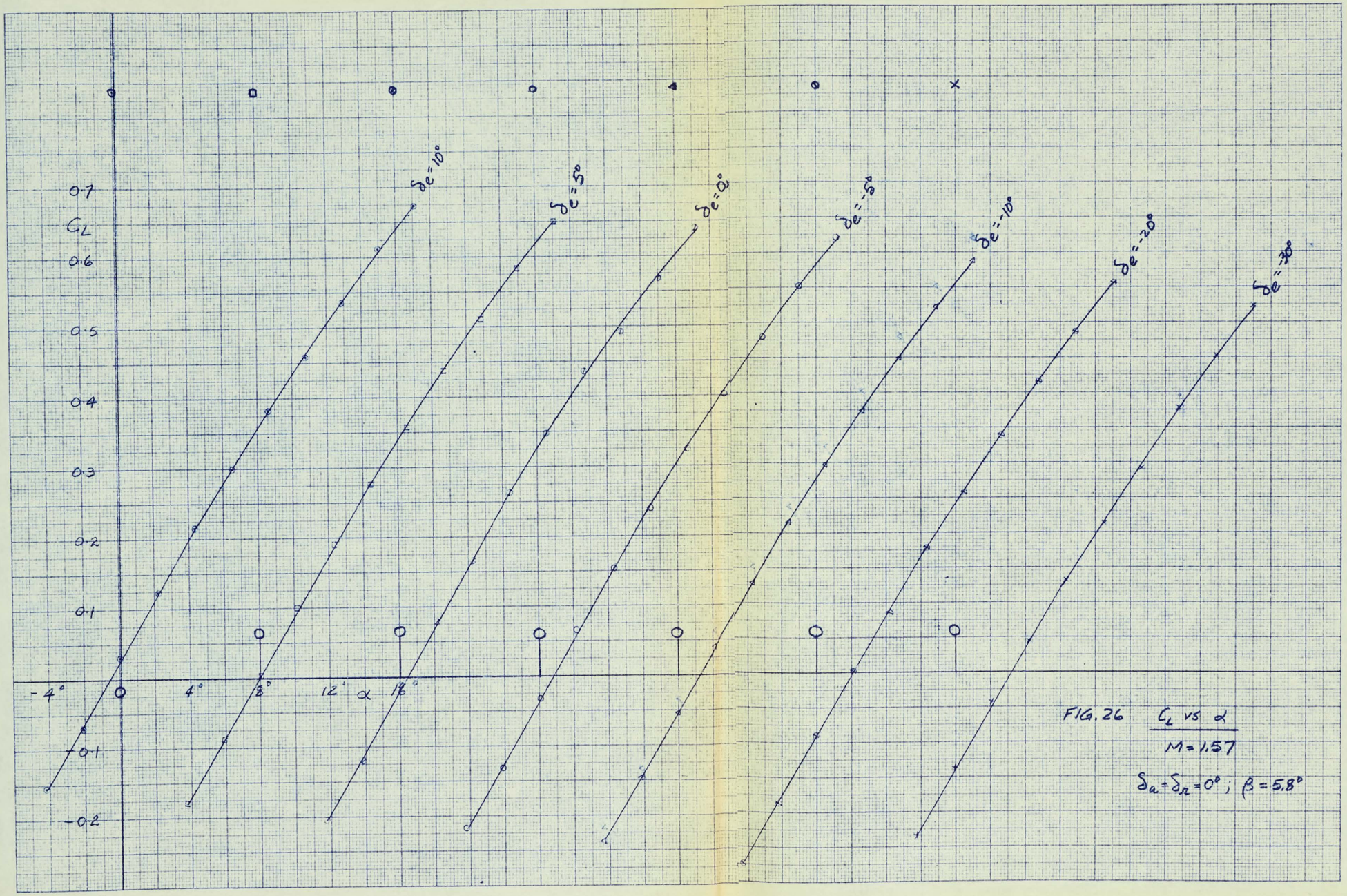

FIG. 26 C_L vs α

$M = 1.57$

$\delta_a = \delta_R = 0°$; $\beta = 5.8°$

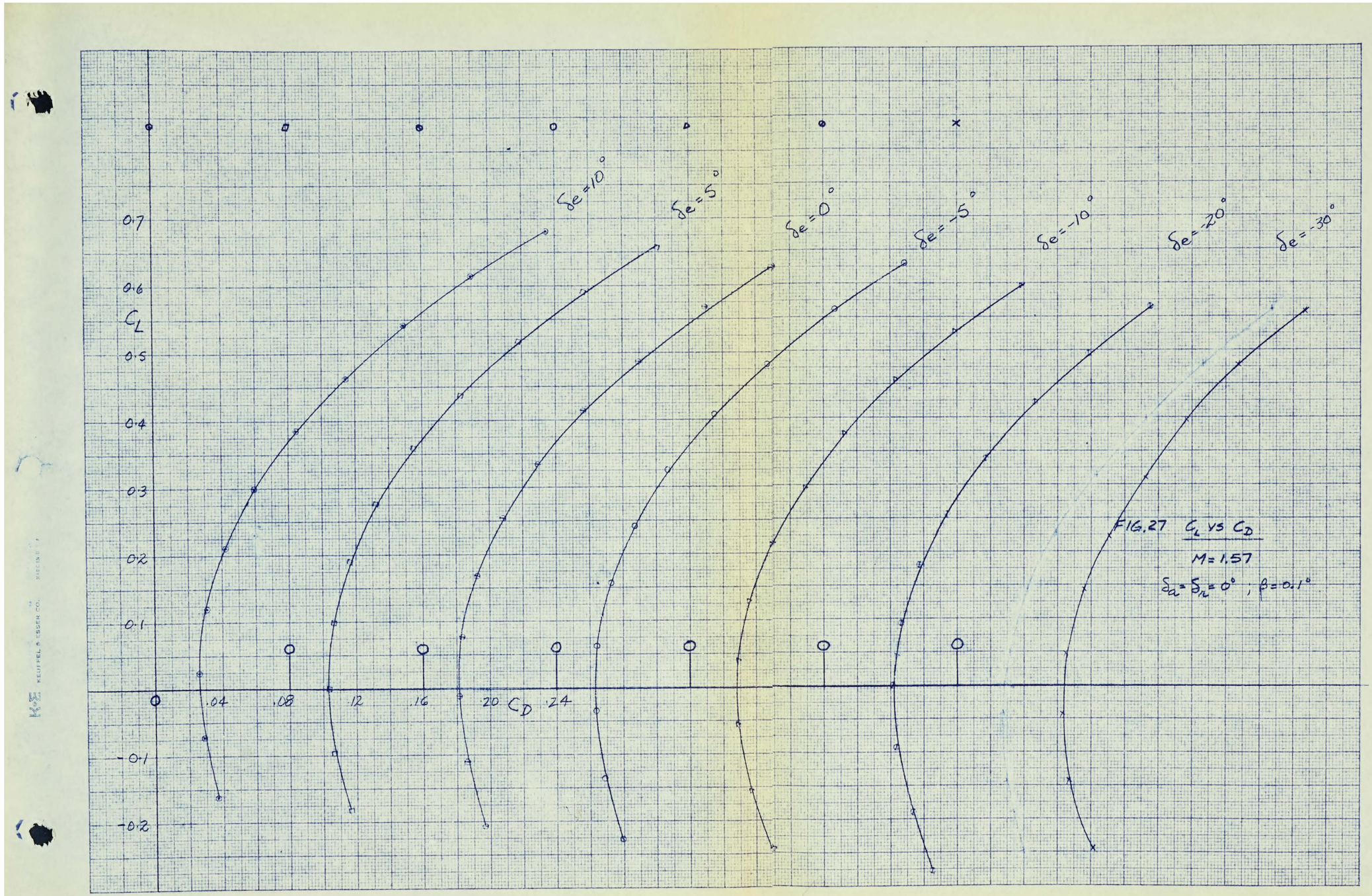

FIG. 27 C_L vs C_D

$M = 1.57$

$\delta_a = \delta_r = 0°$; $\beta = 0.1°$

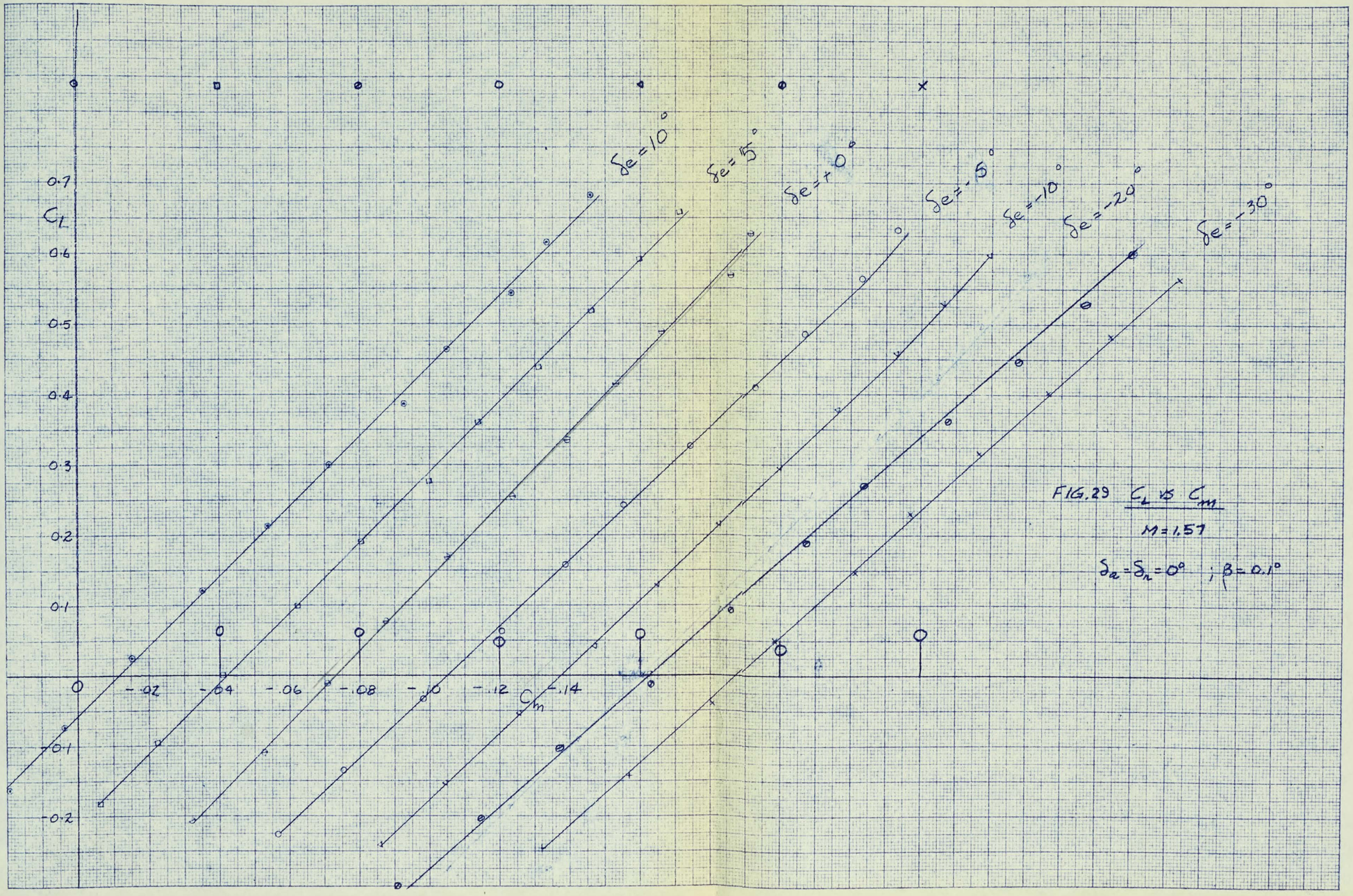

FIG. 29 C_L vs C_M

$M = 1.57$

$\delta_a = \delta_r = 0°$; $\beta = 0.1°$

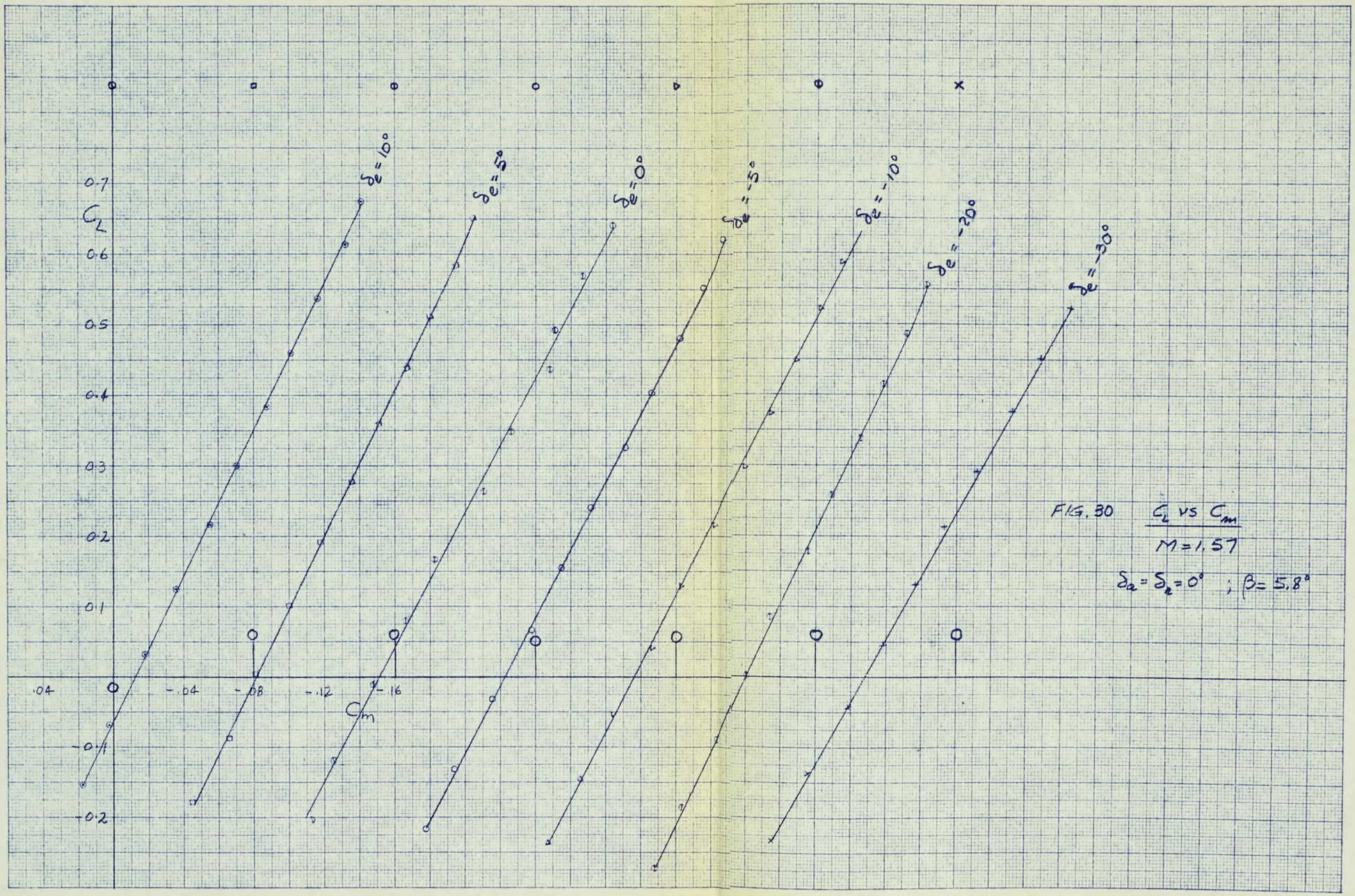

FIG. 30 C_L vs C_m

$M = 1.57$

$\delta_a = \delta_r = 0°$; $\beta = 5.8°$

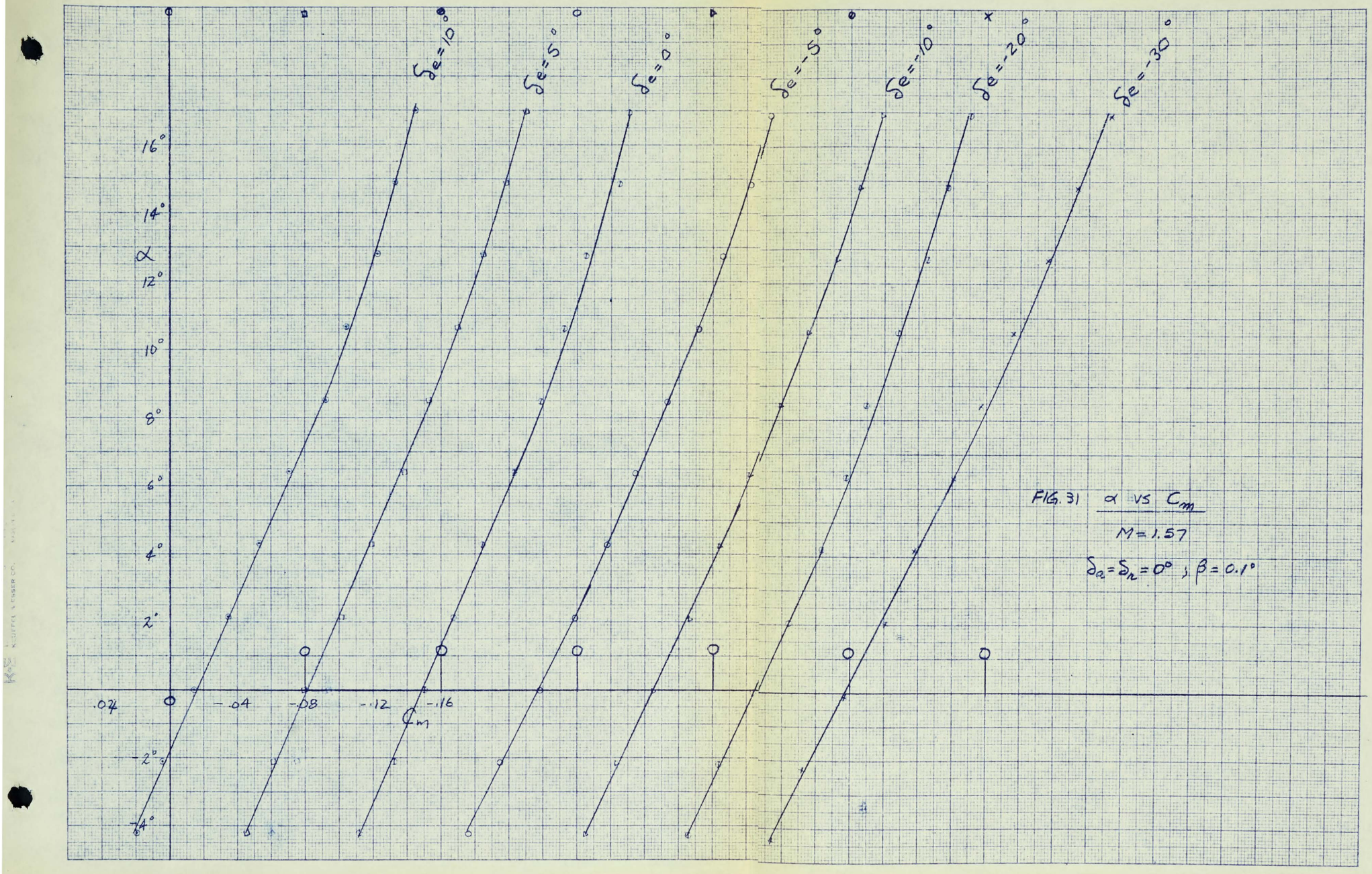

FIG. 31 α vs C_m

$M = 1.57$

$\delta_a = \delta_r = 0°$; $\beta = 0.1°$

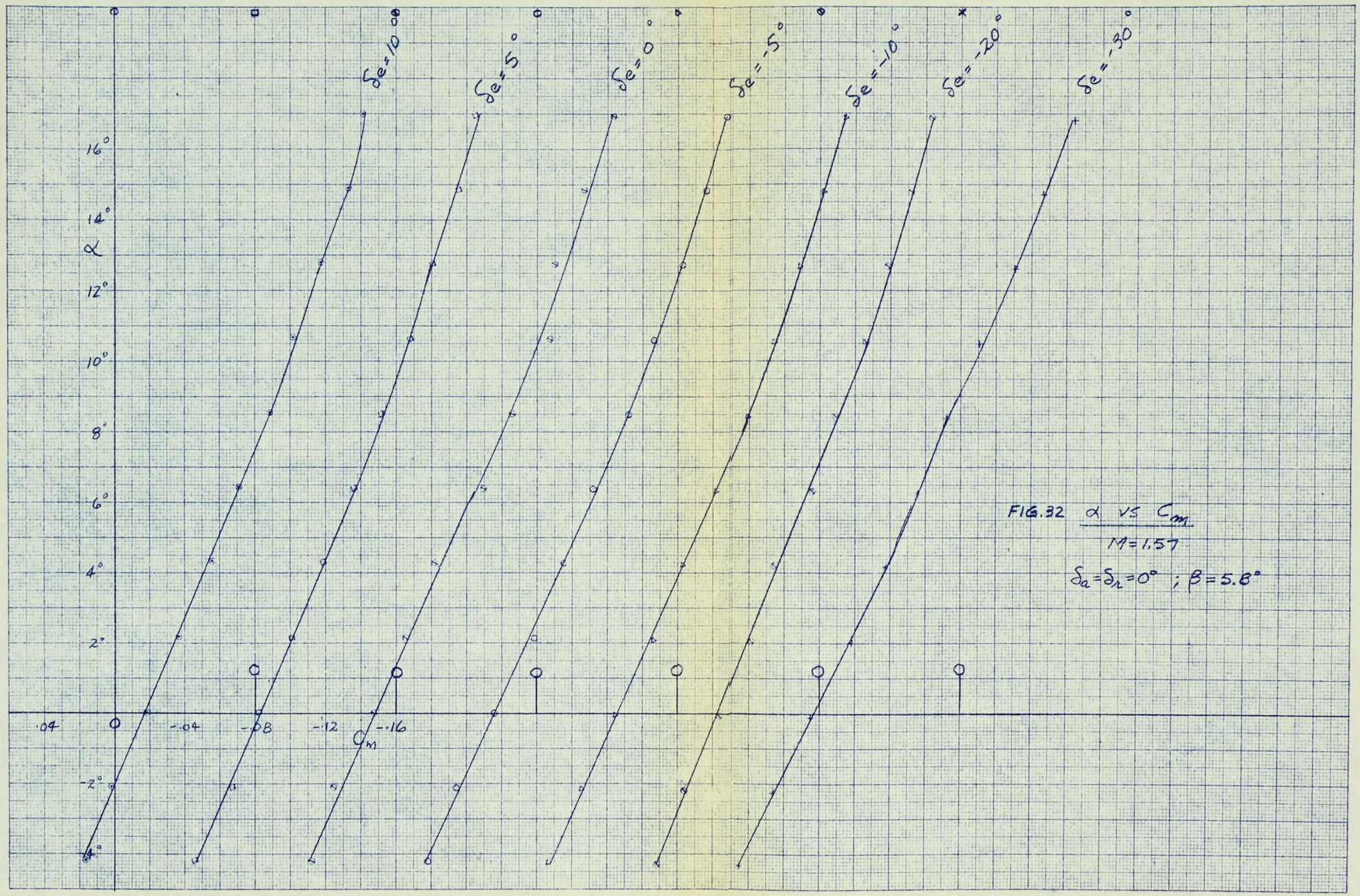

FIG. 32 α vs C_m

$M = 1.57$

$\delta_a = \delta_r = 0°$; $\beta = 5.8°$

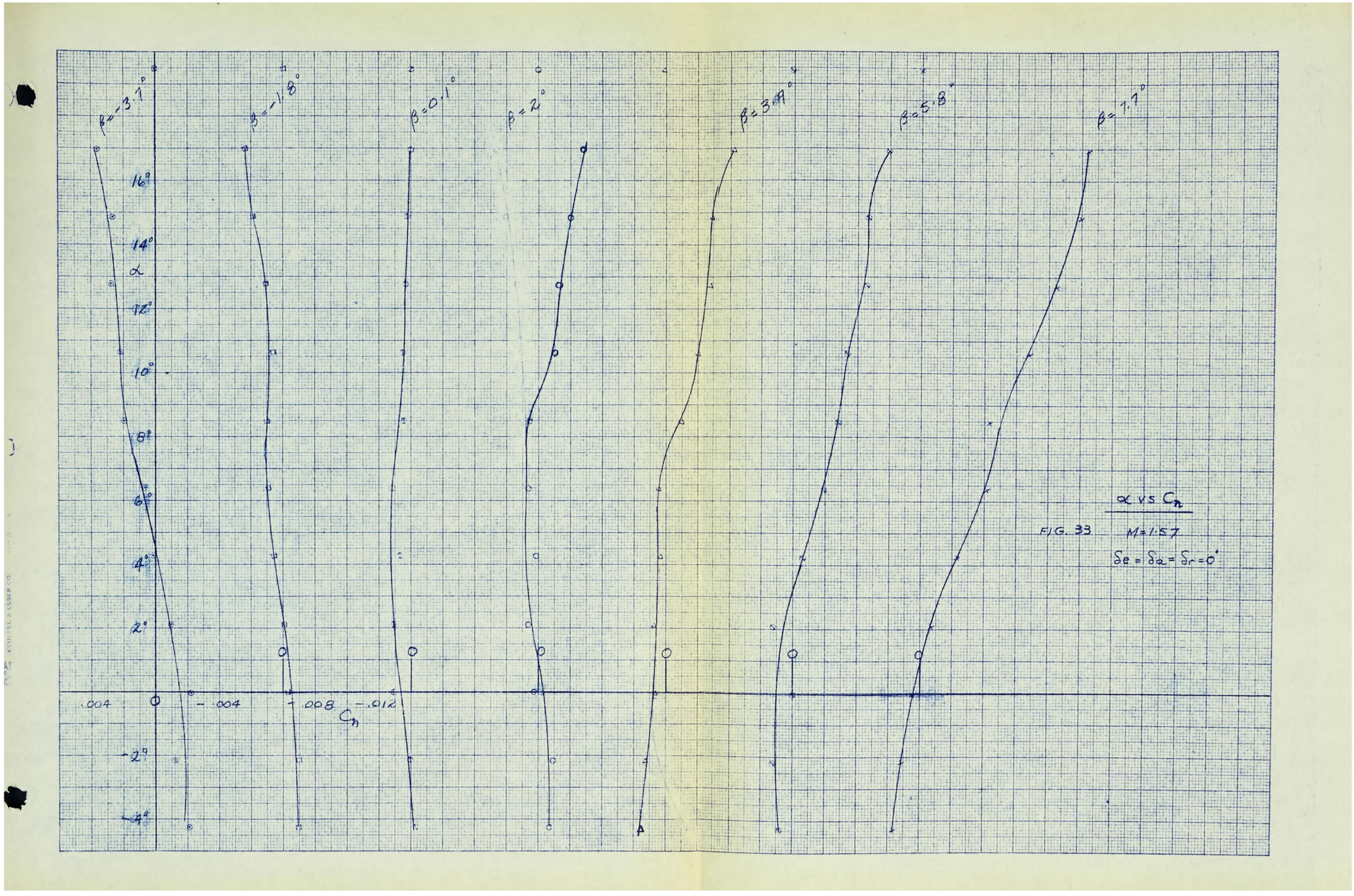

α vs C_n

FIG. 33 M=1.57

$\delta_e = \delta_{e_2} = \delta_r = 0°$

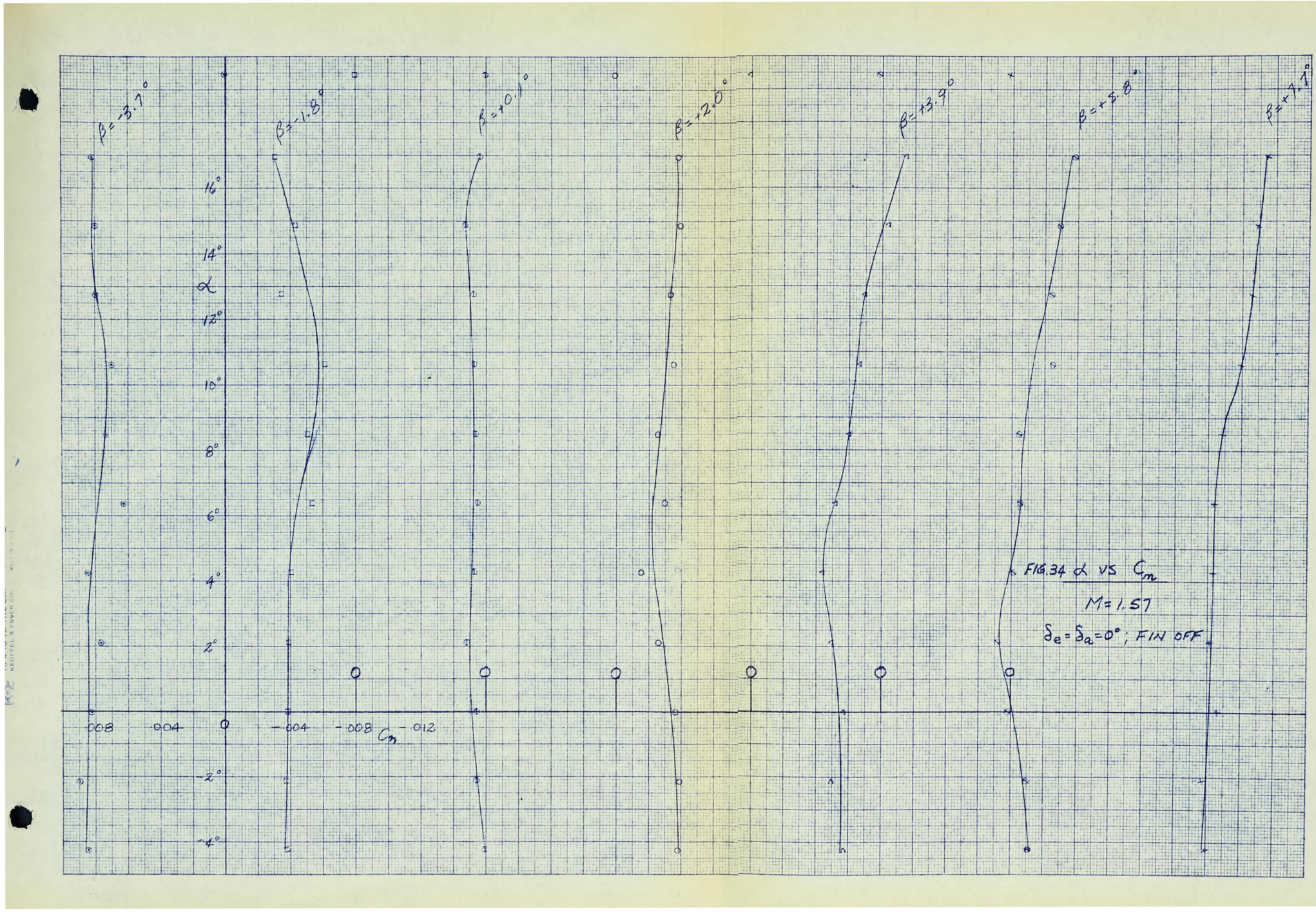

FIG. 34 α VS C_m

$M = 1.57$

$\delta_e = \delta_a = 0°$; FIN OFF

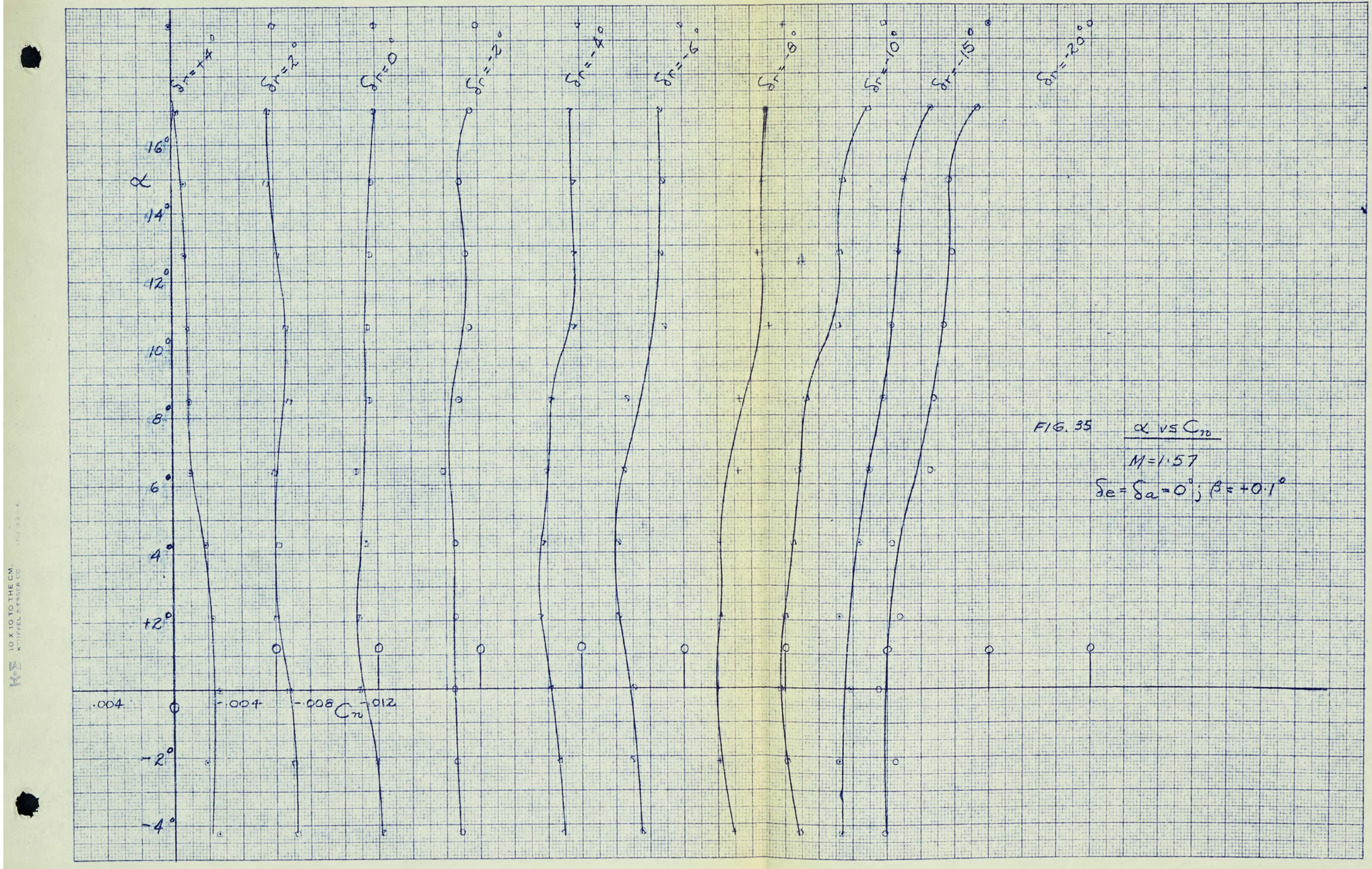

FIG. 35 α vs C_n

$M=1.57$

$\delta_e=\delta_a=0^\circ$; $\beta=+0.1^\circ$

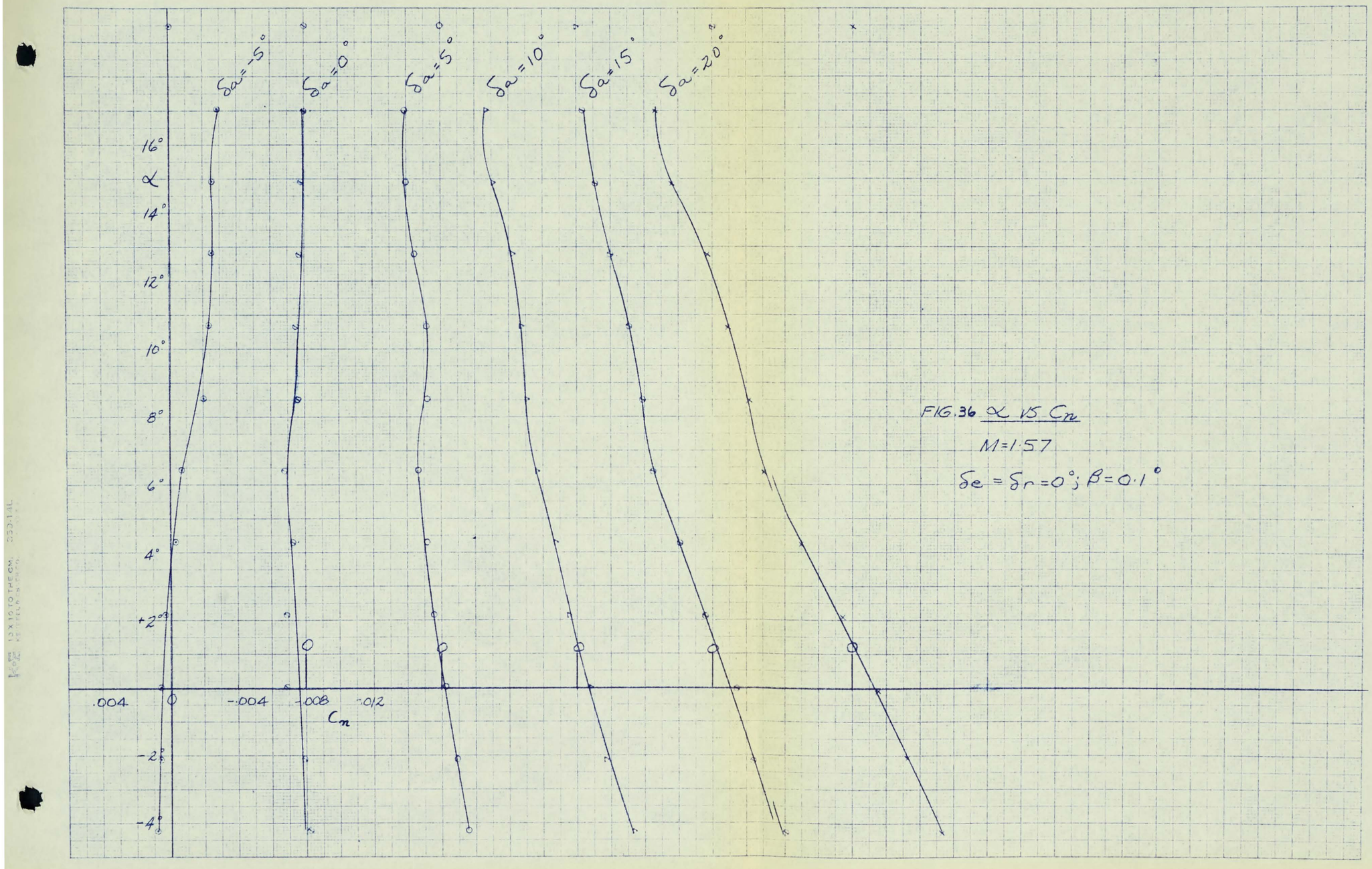

FIG. 36 α VS C_n

$M = 1.57$

$\delta_e = \delta_r = 0°$; $\beta = 0.1°$

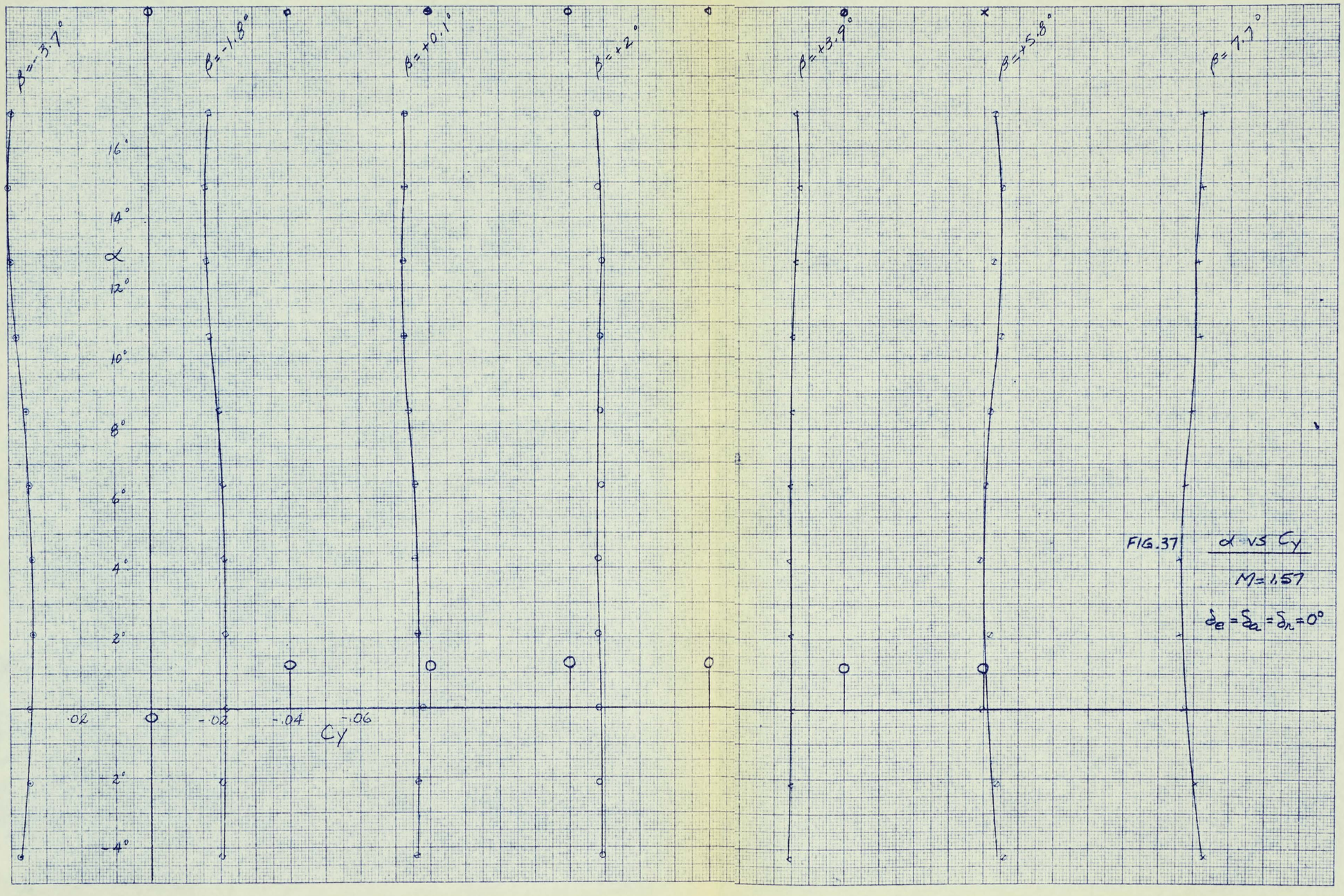

FIG. 37 α vs C_y

M = 1.57

$\delta_e = \delta_{a_L} = \delta_{a_R} = 0°$

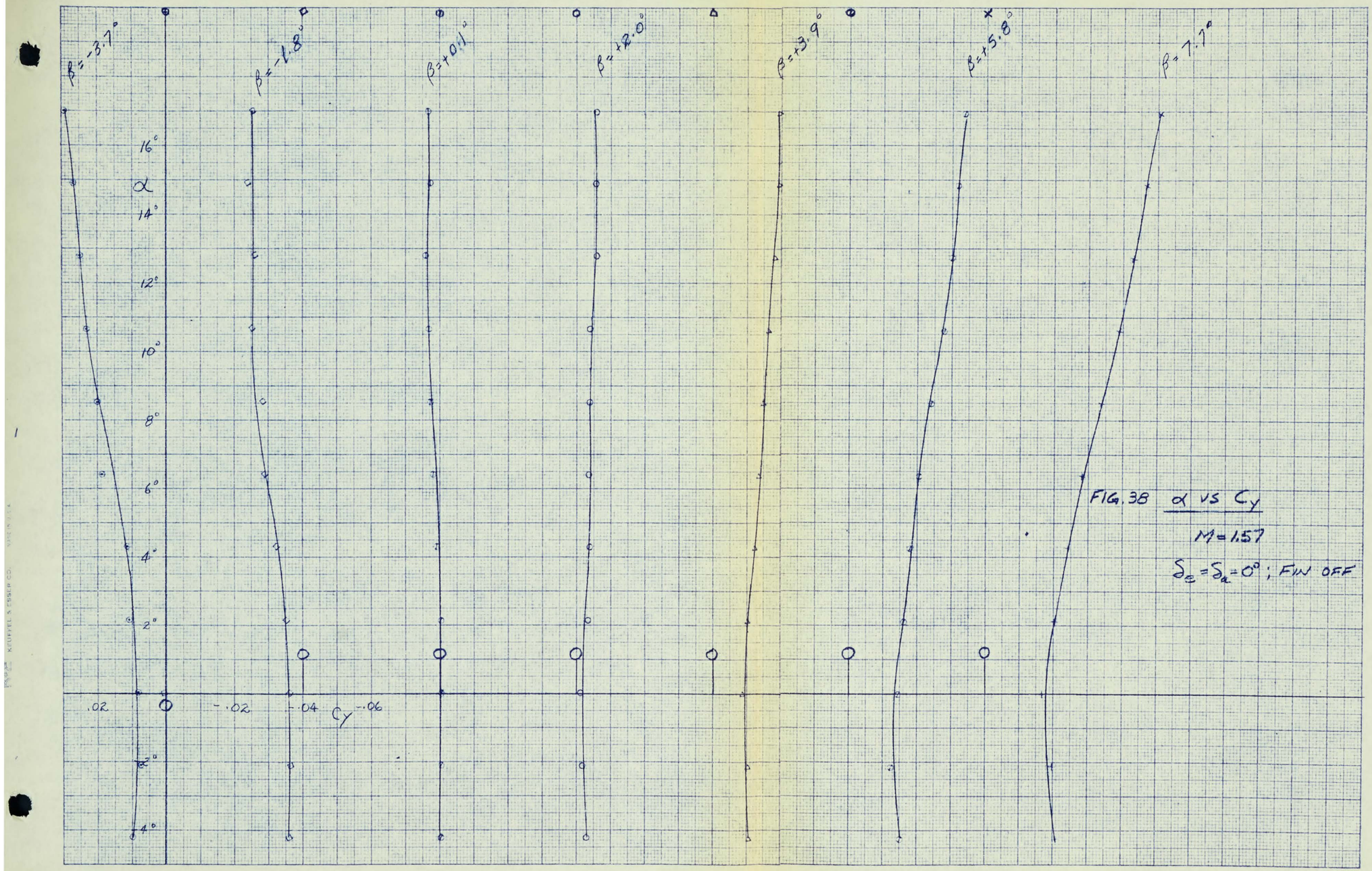

FIG. 38 α vs C_y

M = 1.57

$\delta_e = \delta_a = 0°$; FIN OFF

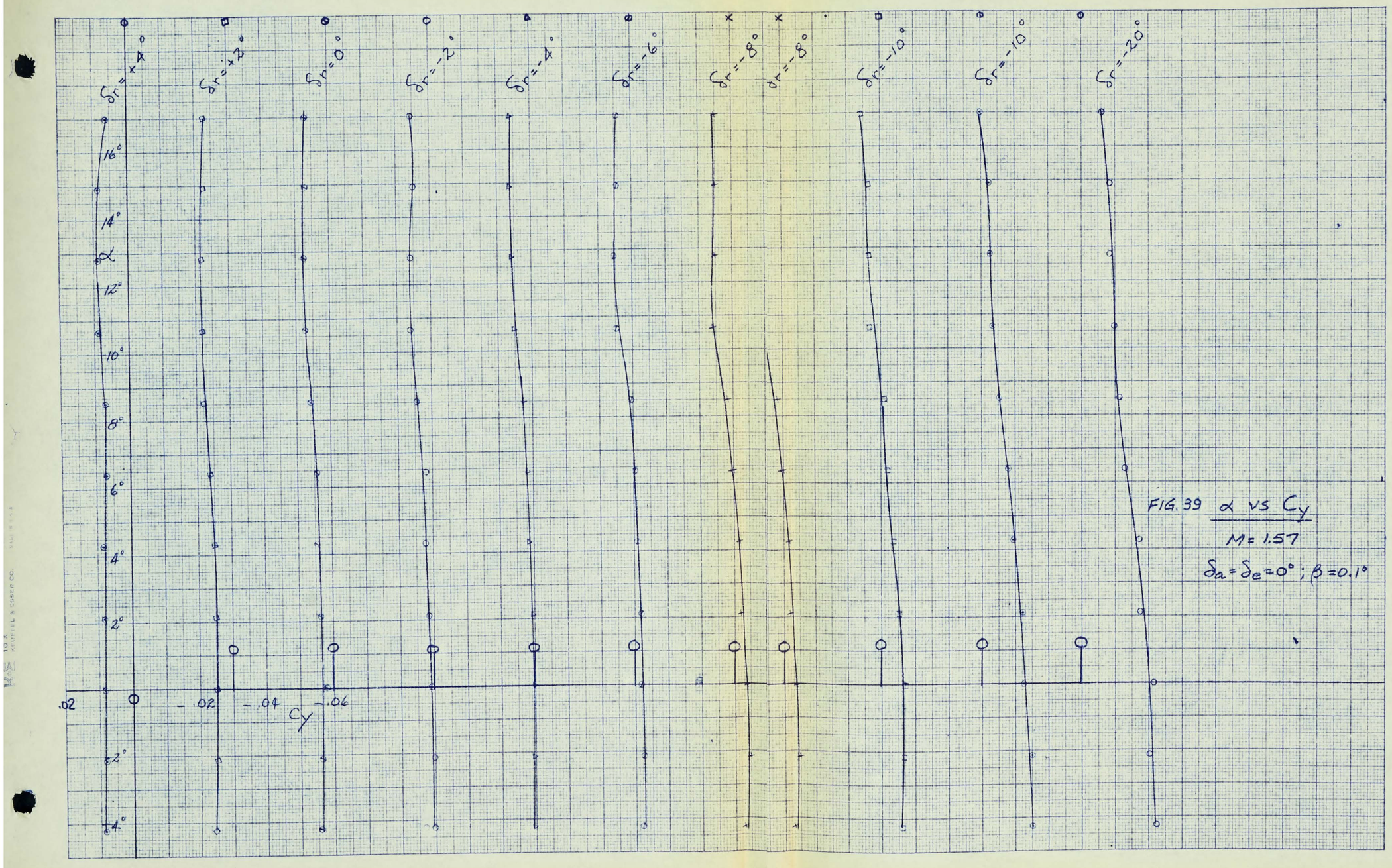

FIG. 39 α vs C_y

$M = 1.57$

$\delta_a = \delta_e = 0°$; $\beta = 0.1°$

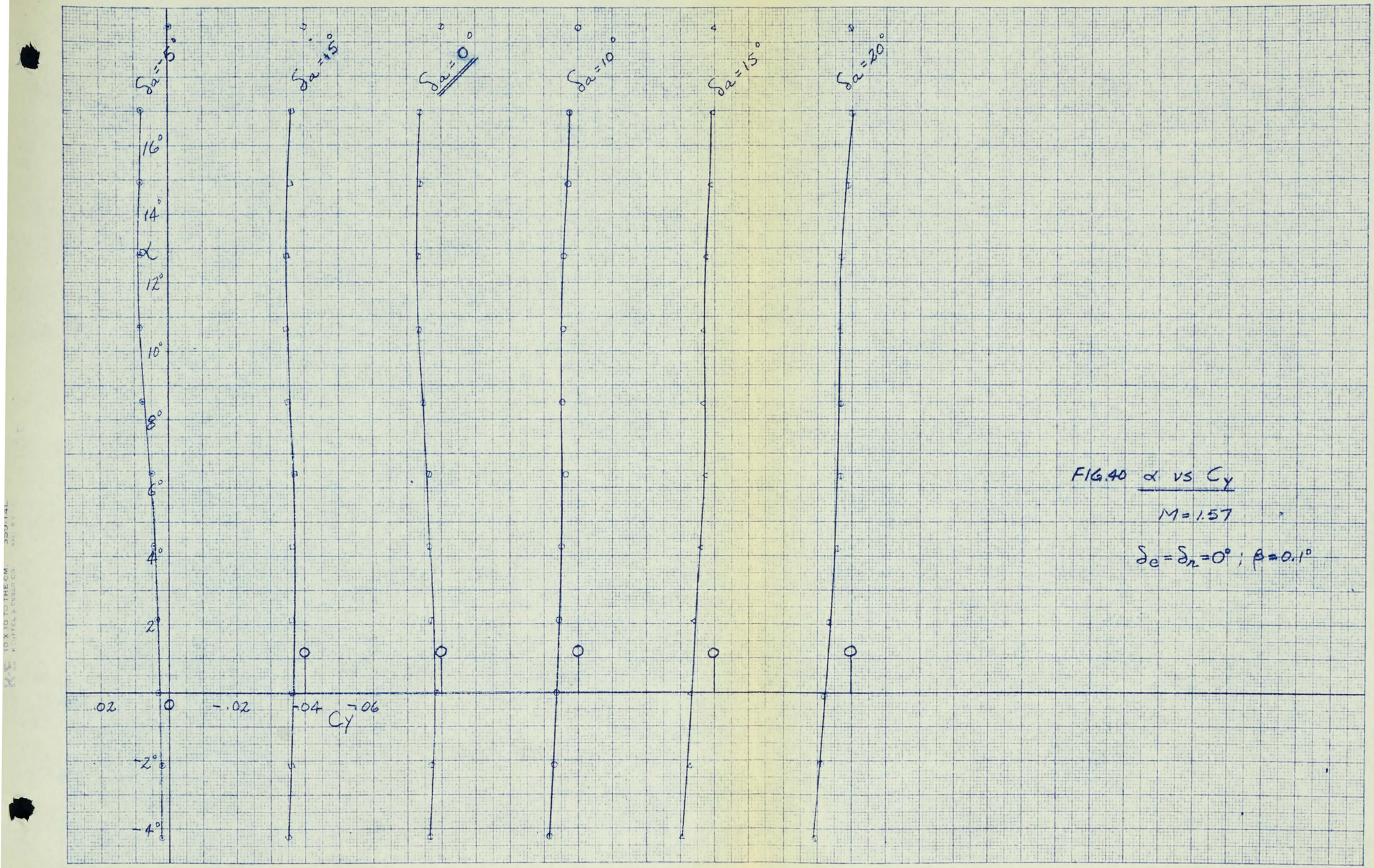

FIG.40 α vs C_Y

$M = 1.57$

$\delta_e = \delta_r = 0°$; $\beta = 0.1°$

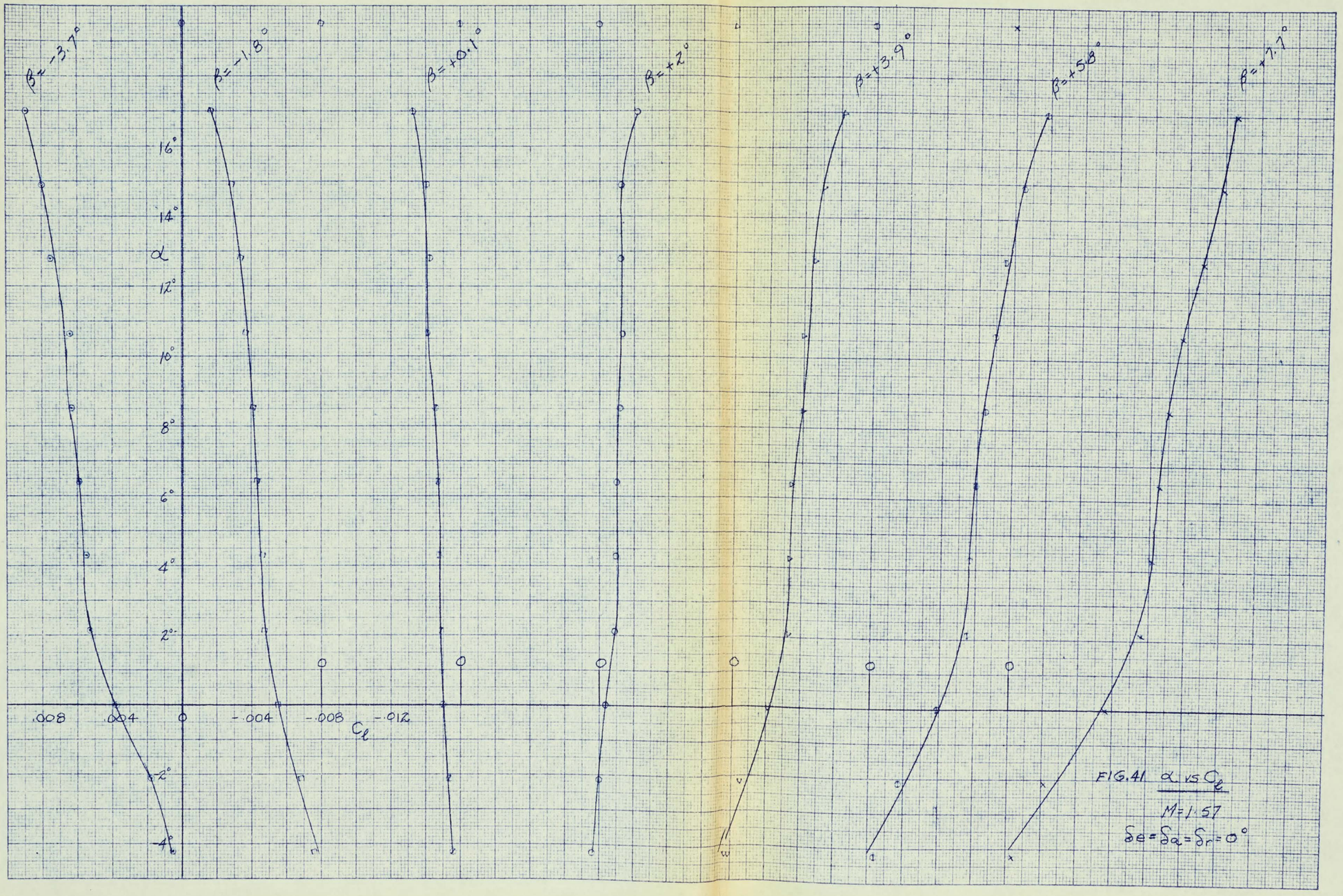

FIG. 41 α vs C_l

$M = 1.57$

$\delta_e = \delta_a = \delta_r = 0°$

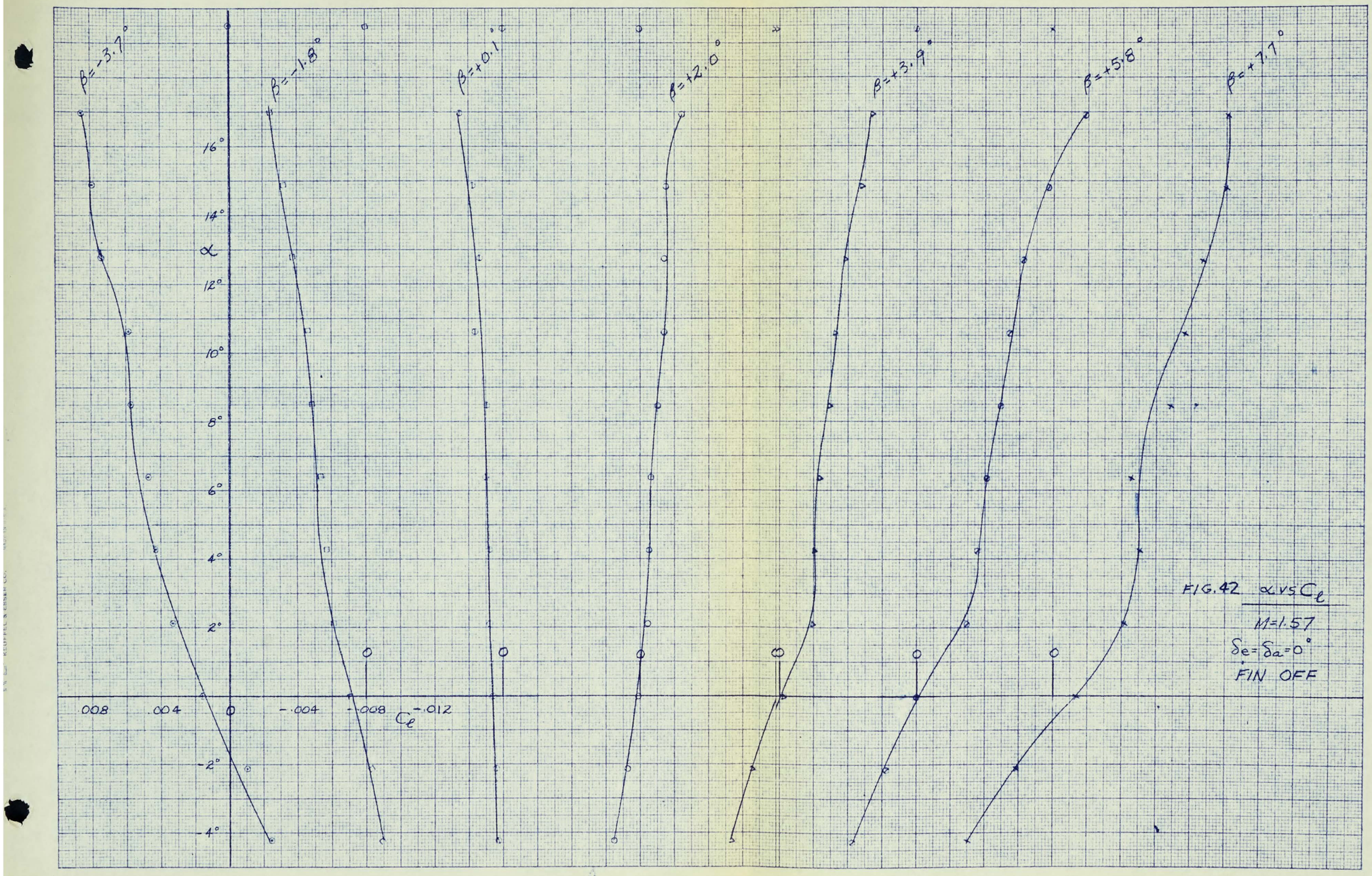

FIG. 42 α vs C_ℓ

$M = 1.57$

$\delta_e = \delta_a = 0°$

FIN OFF

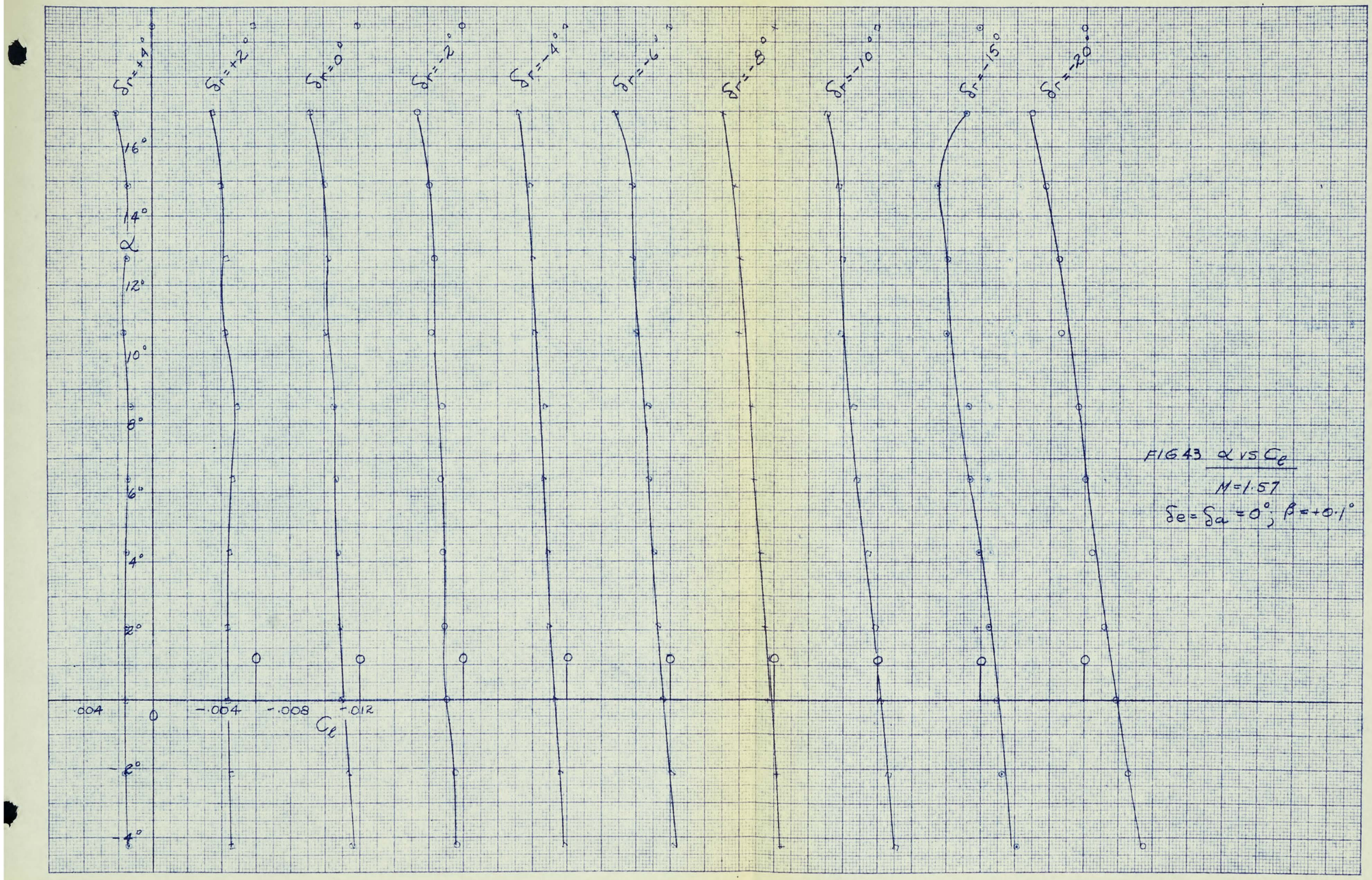

FIG 43 α vs C_ℓ

M=1.57

$\delta_e = \delta_a = 0°$; $\beta = +0.1°$

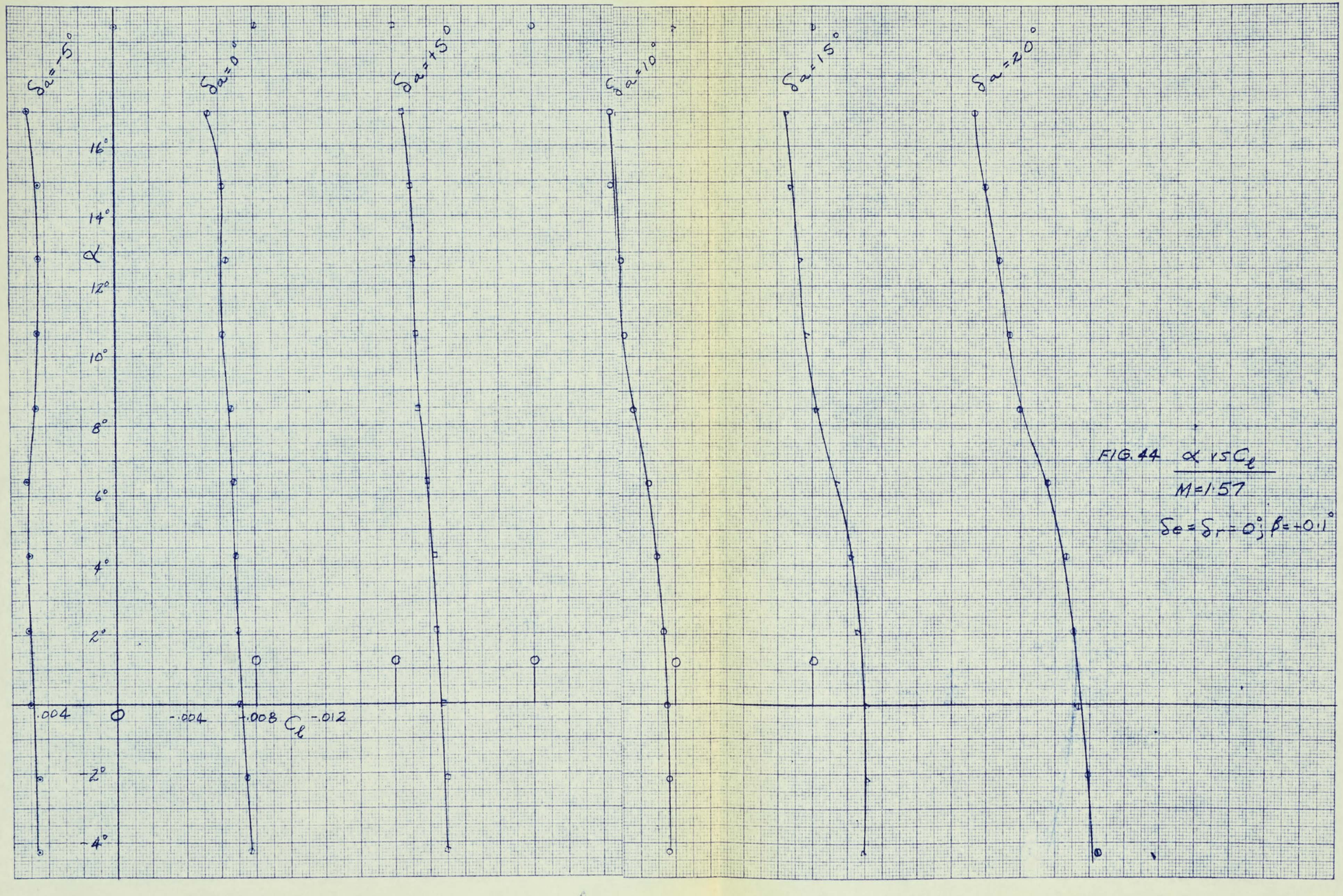

FIG. 44 α vs C_l

$M = 1.57$

$\delta_e = \delta_r = 0°$; $\beta = +0.1°$

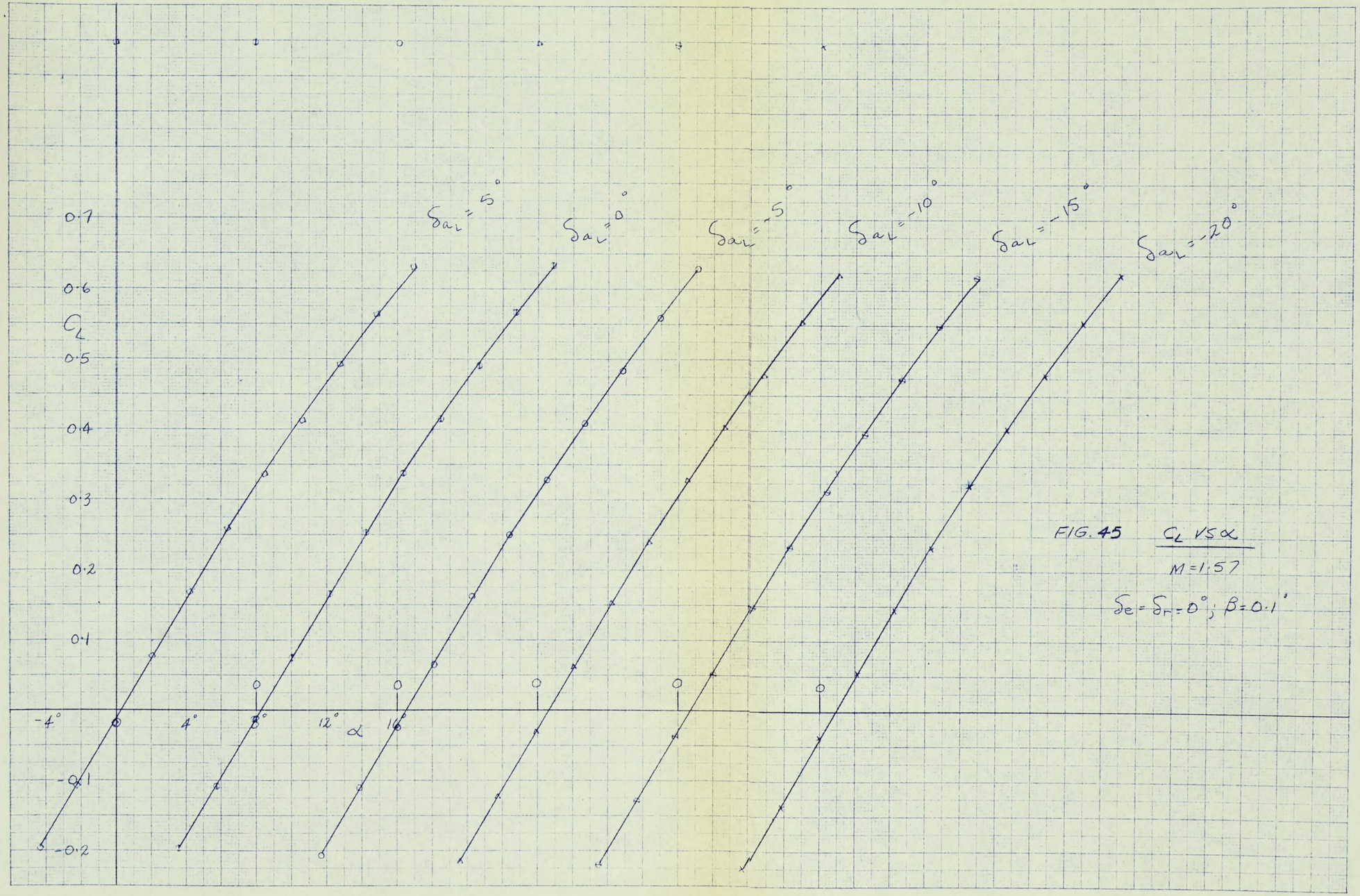

FIG. 45 C_L VS α

$M = 1.57$

$\delta_e = \delta_r = 0°$; $\beta = 0.1°$

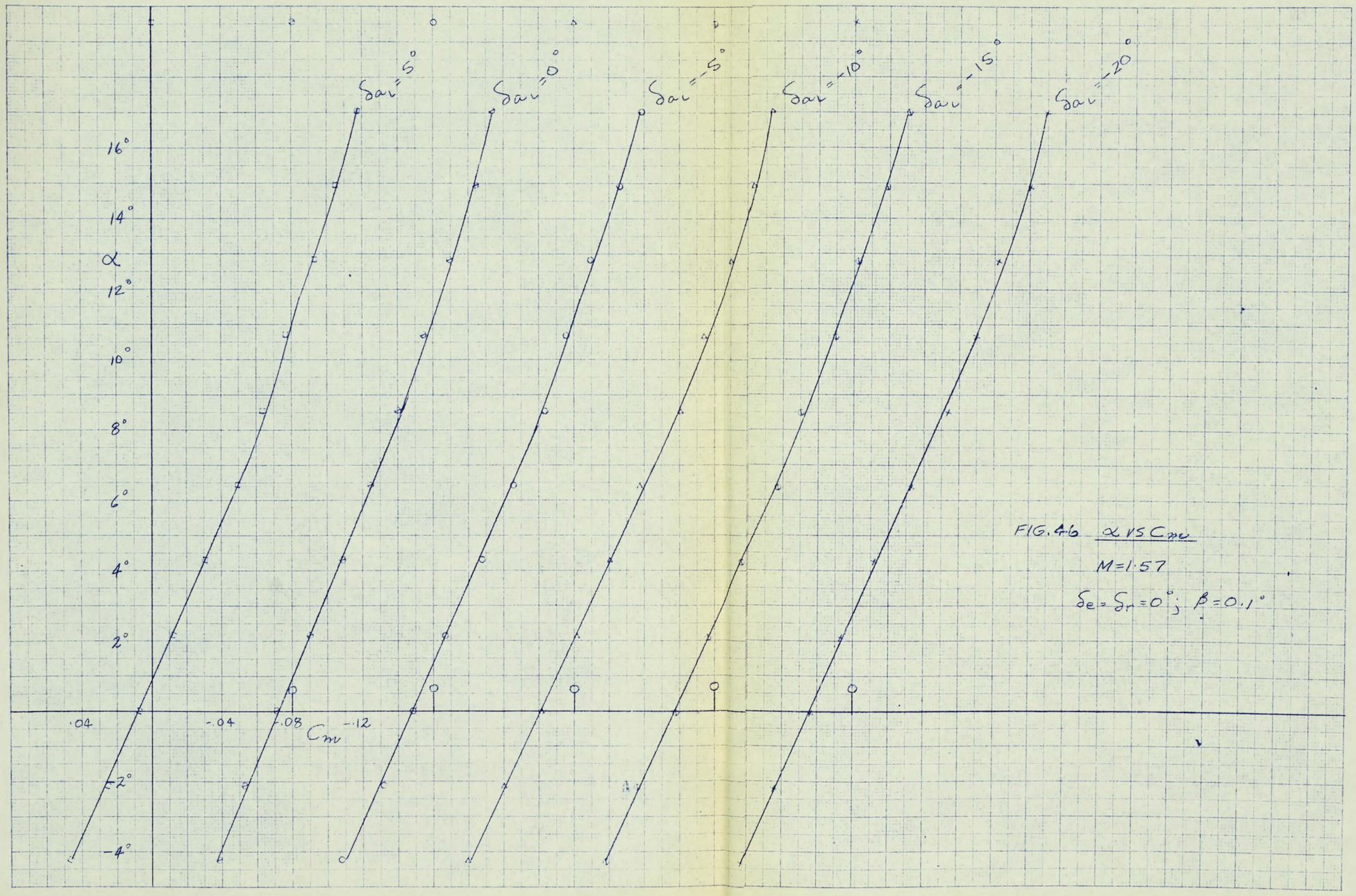

FIG. 46 α VS C_m

$M = 1.57$

$\delta_e = \delta_r = 0°$; $\beta = 0.1°$

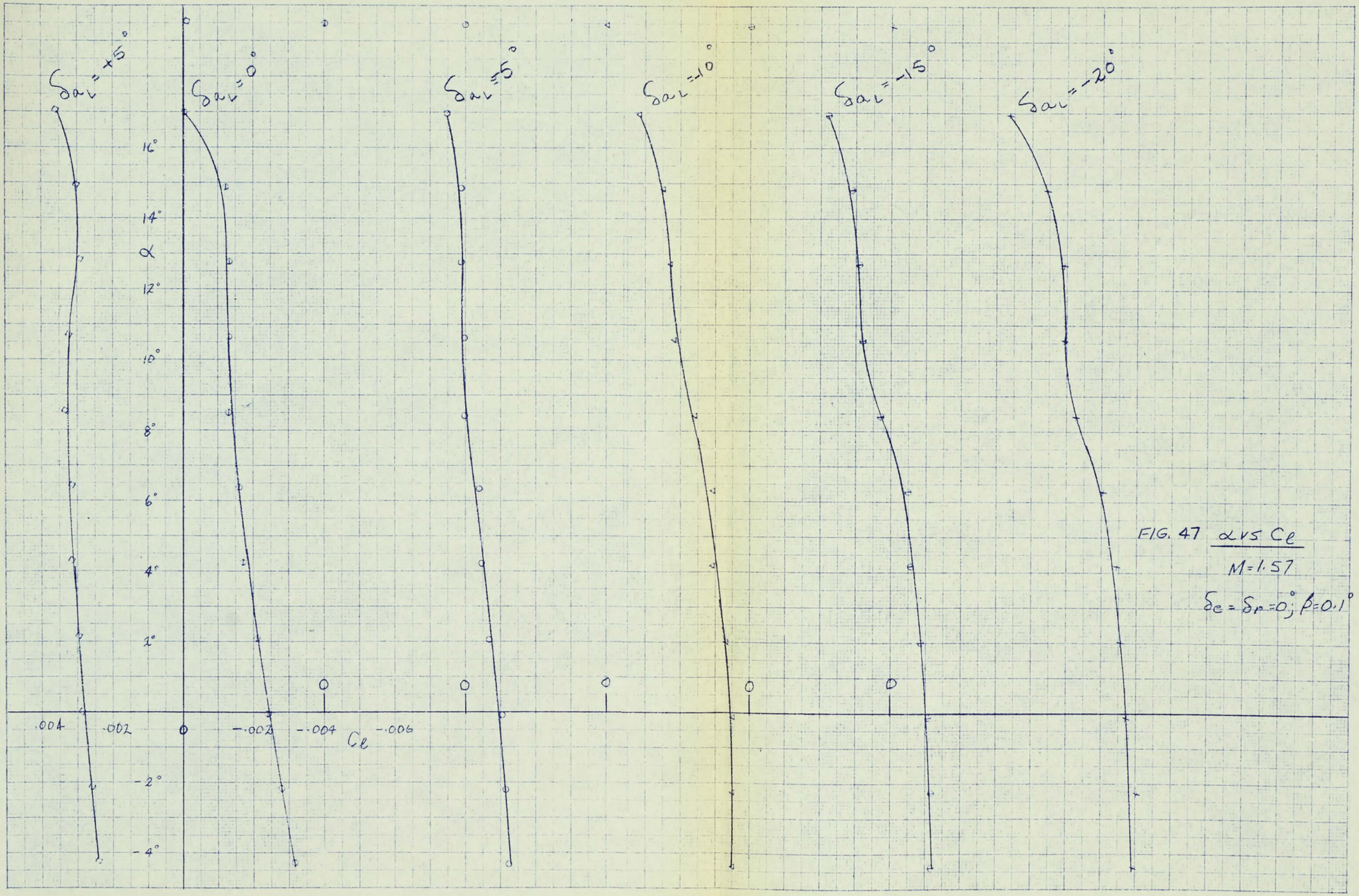

FIG. 47 α vs C_ℓ

$M = 1.57$

$\delta_e = \delta_p = 0°$; $\beta = 0.1°$

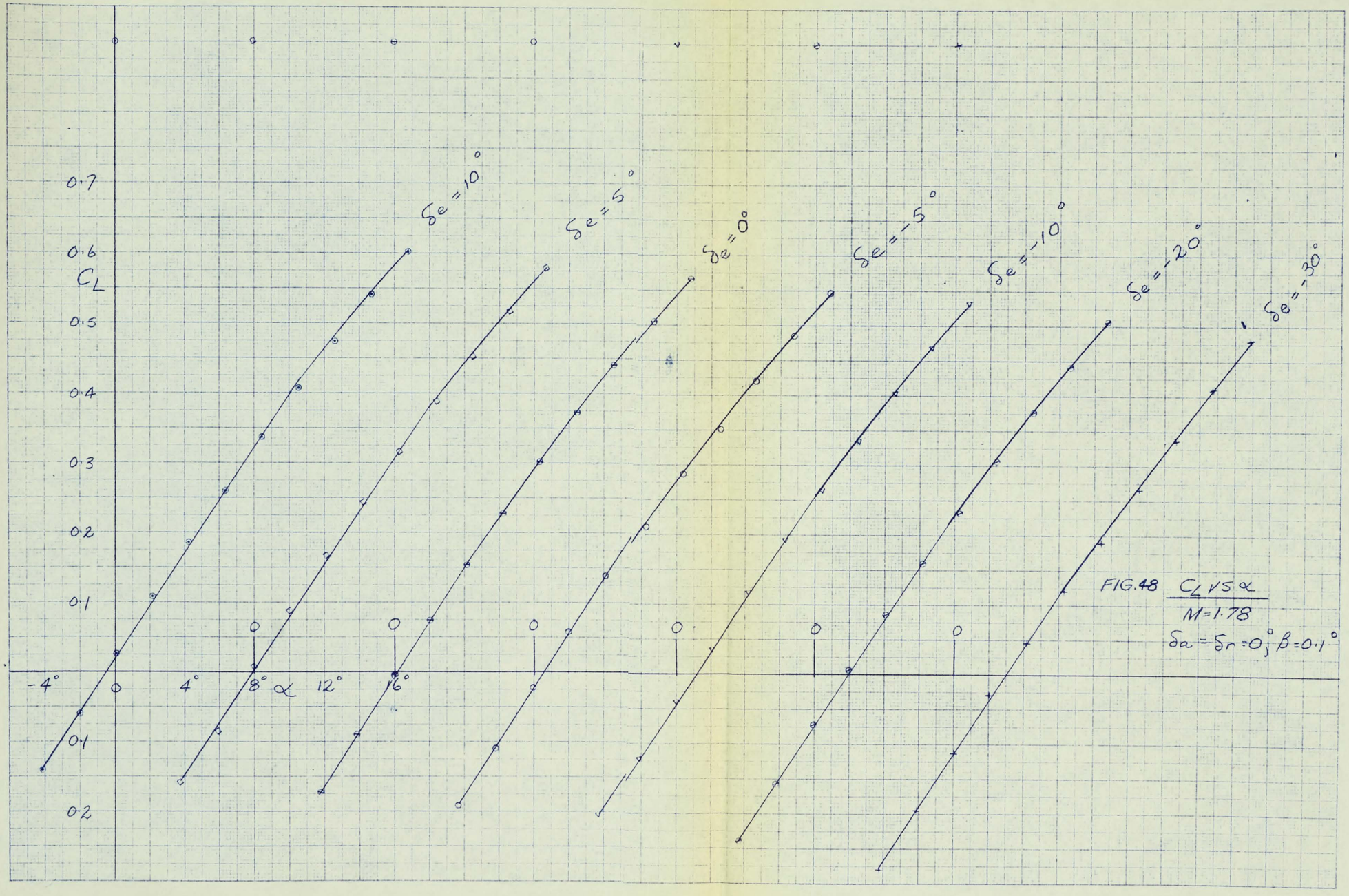

FIG. 48 C_L VS α

$M = 1.78$

$\delta a = \delta r = 0°$; $\beta = 0.1°$

FIG. 49 C_L vs α

$M = 1.78$

$\delta_a = \delta_r = 0°$ $\beta = 5.8°$

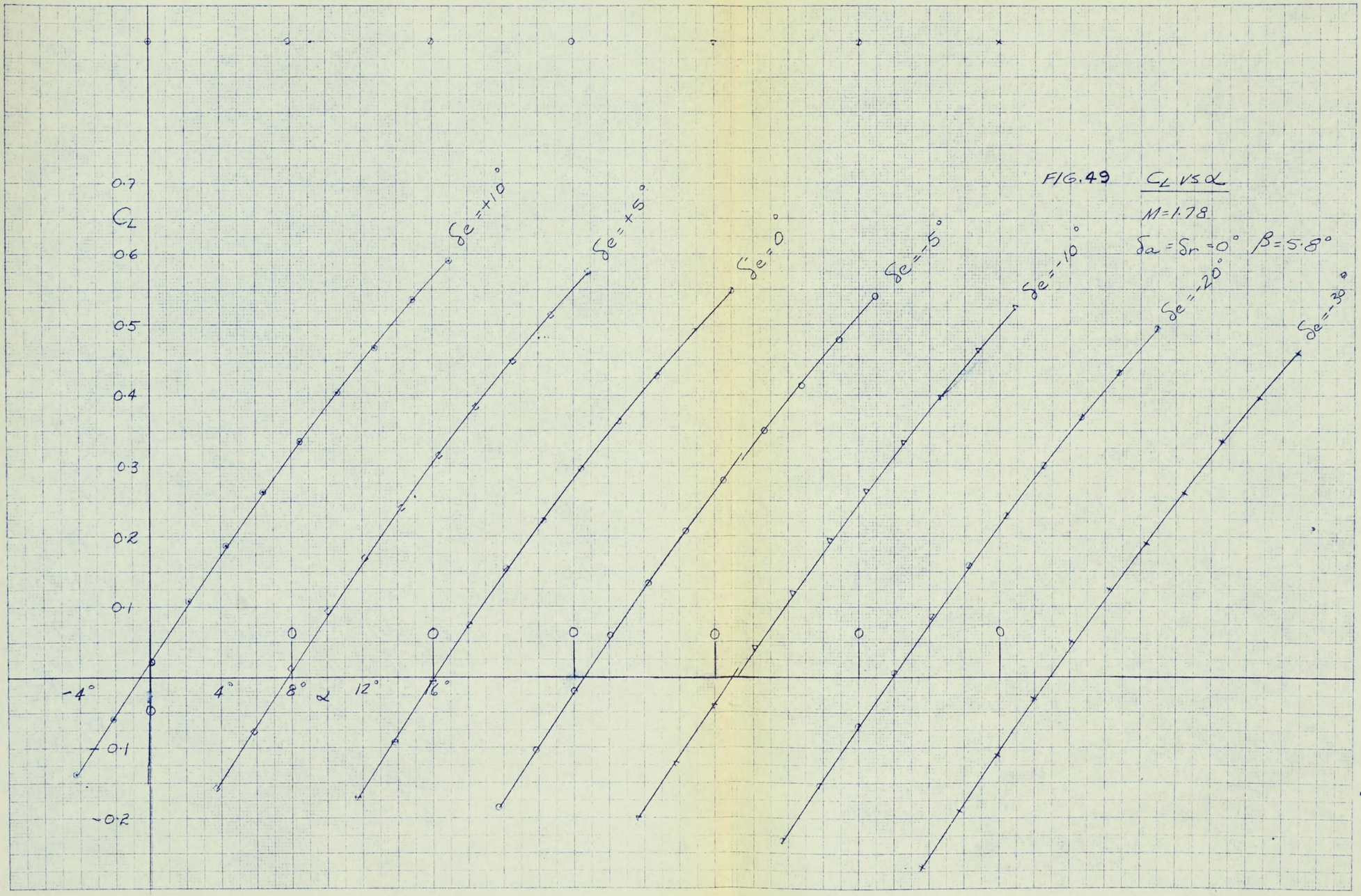

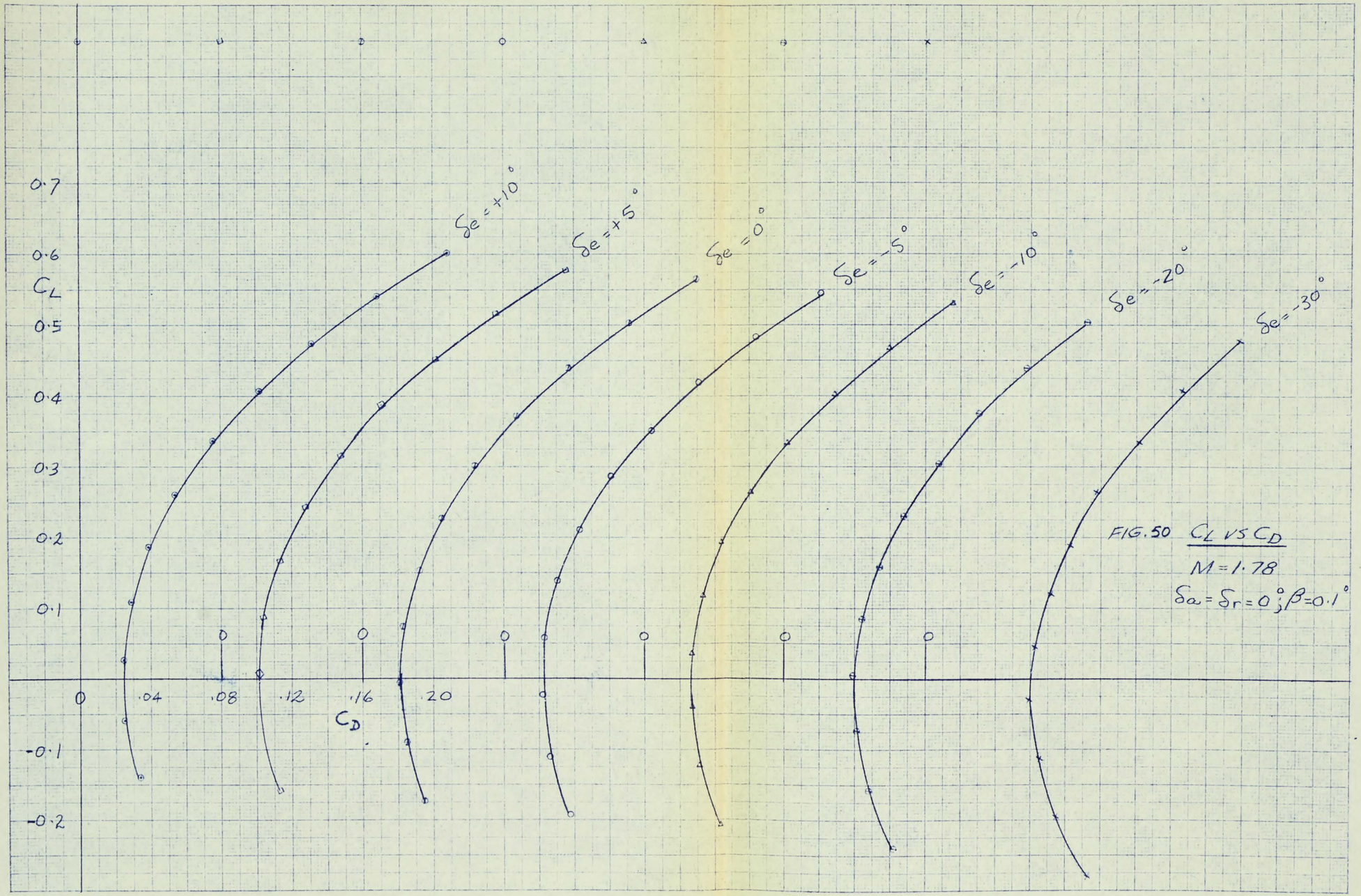

FIG. 50 C_L VS C_D

$M = 1.78$

$\delta_a = \delta_r = 0°; \beta = 0.1°$

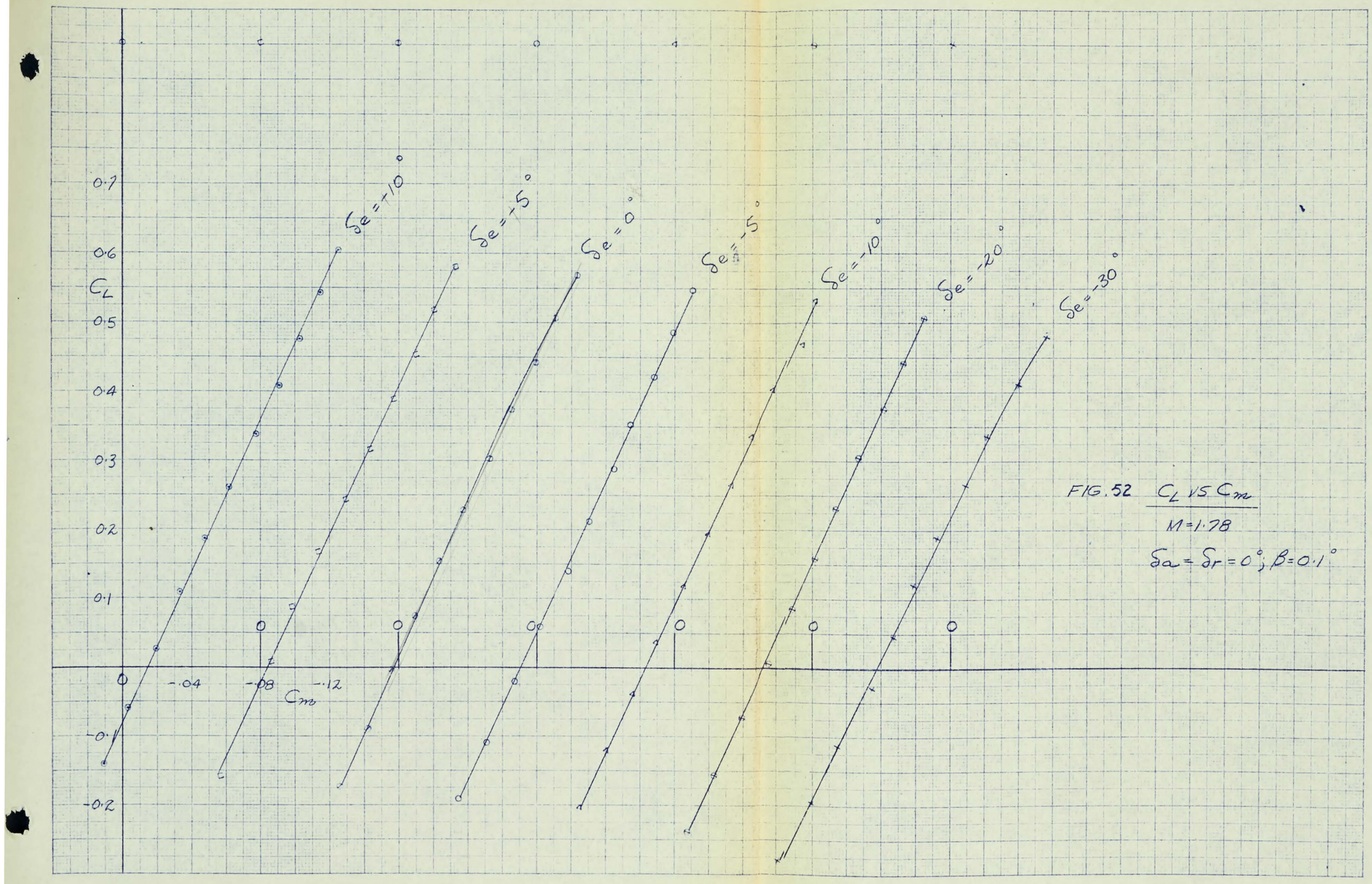

FIG. 52 C_L VS C_m

$M = 1.78$

$\delta_a = \delta_r = 0°$; $\beta = 0.1°$

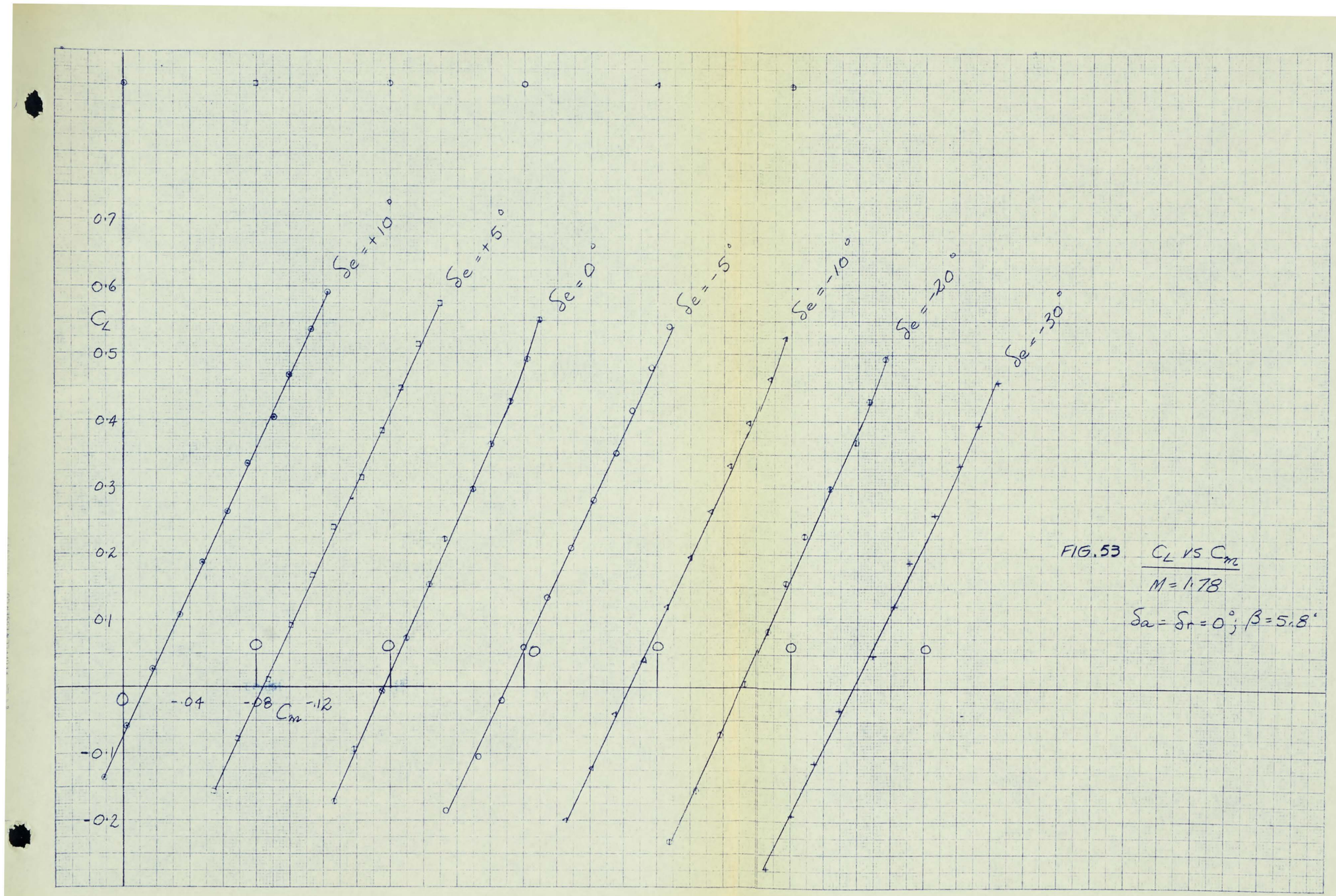

FIG. 53 C_L vs C_m

$M = 1.78$

$\delta_a = \delta_r = 0°$; $\beta = 5.8°$

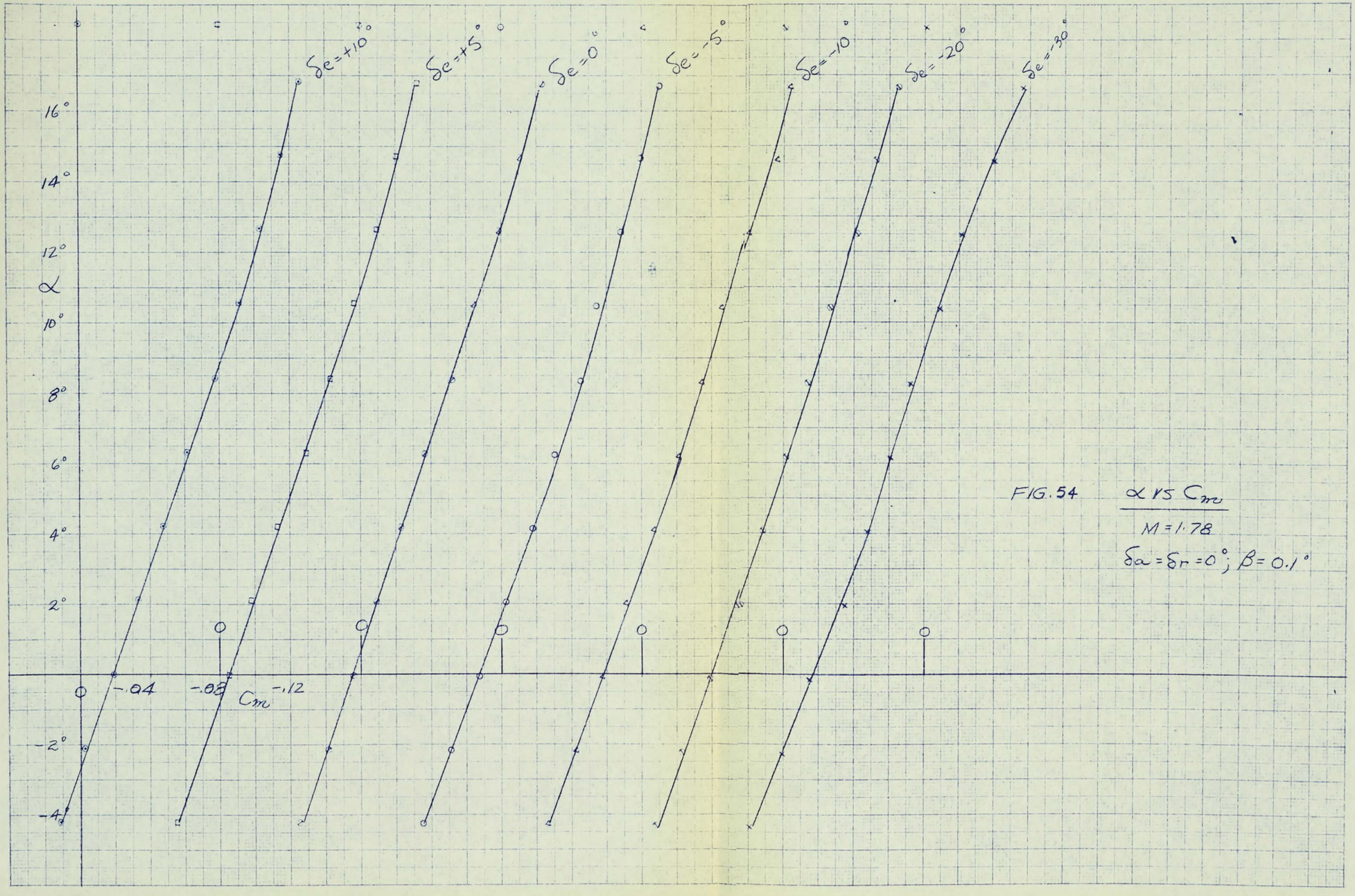

FIG. 54 α vs C_m

$M = 1.78$

$\delta_a = \delta_r = 0°$; $\beta = 0.1°$

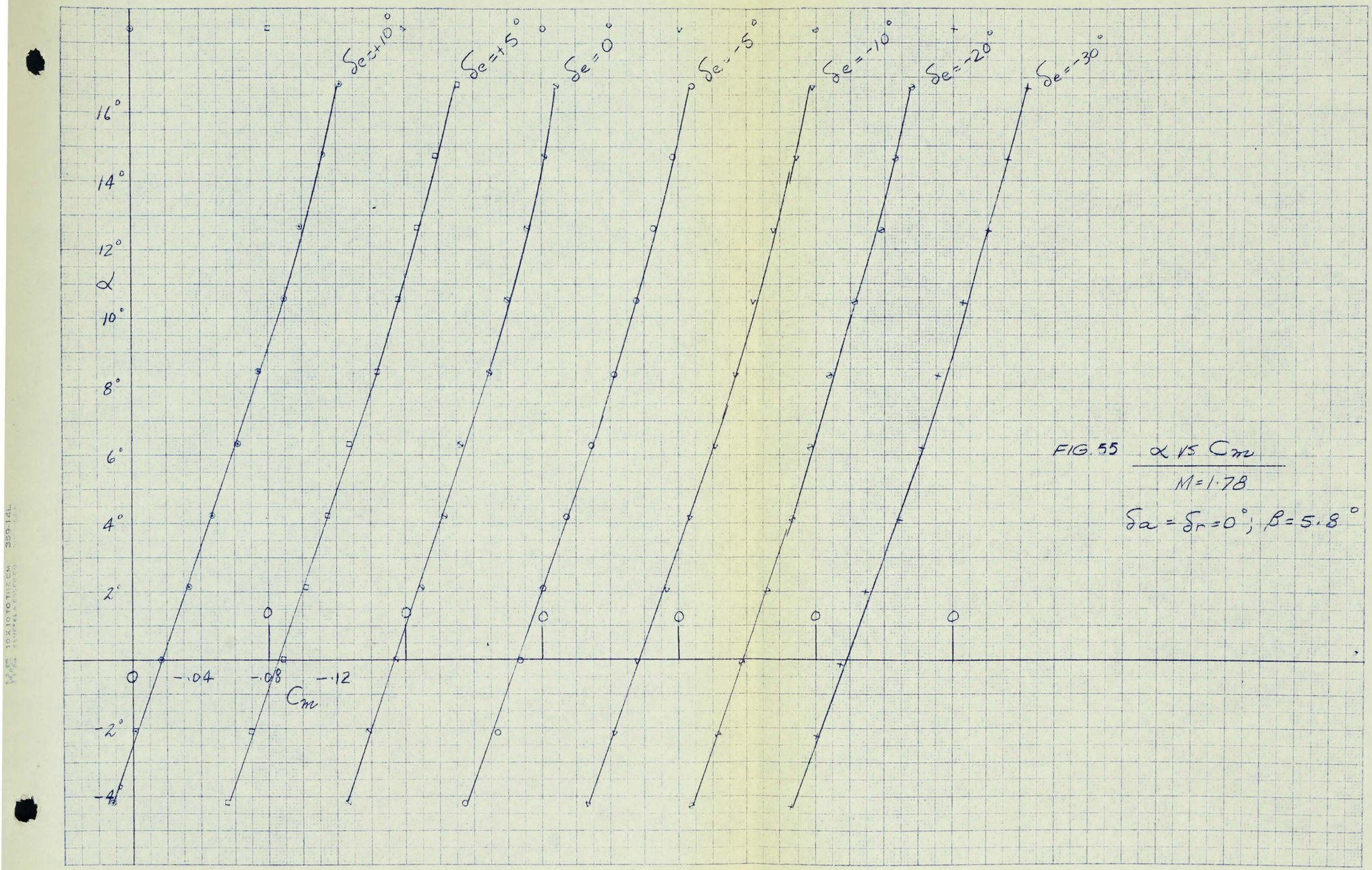

FIG. 55 α VS C_m

$M = 1.78$

$\delta_a = \delta_r = 0°$; $\beta = 5.8°$

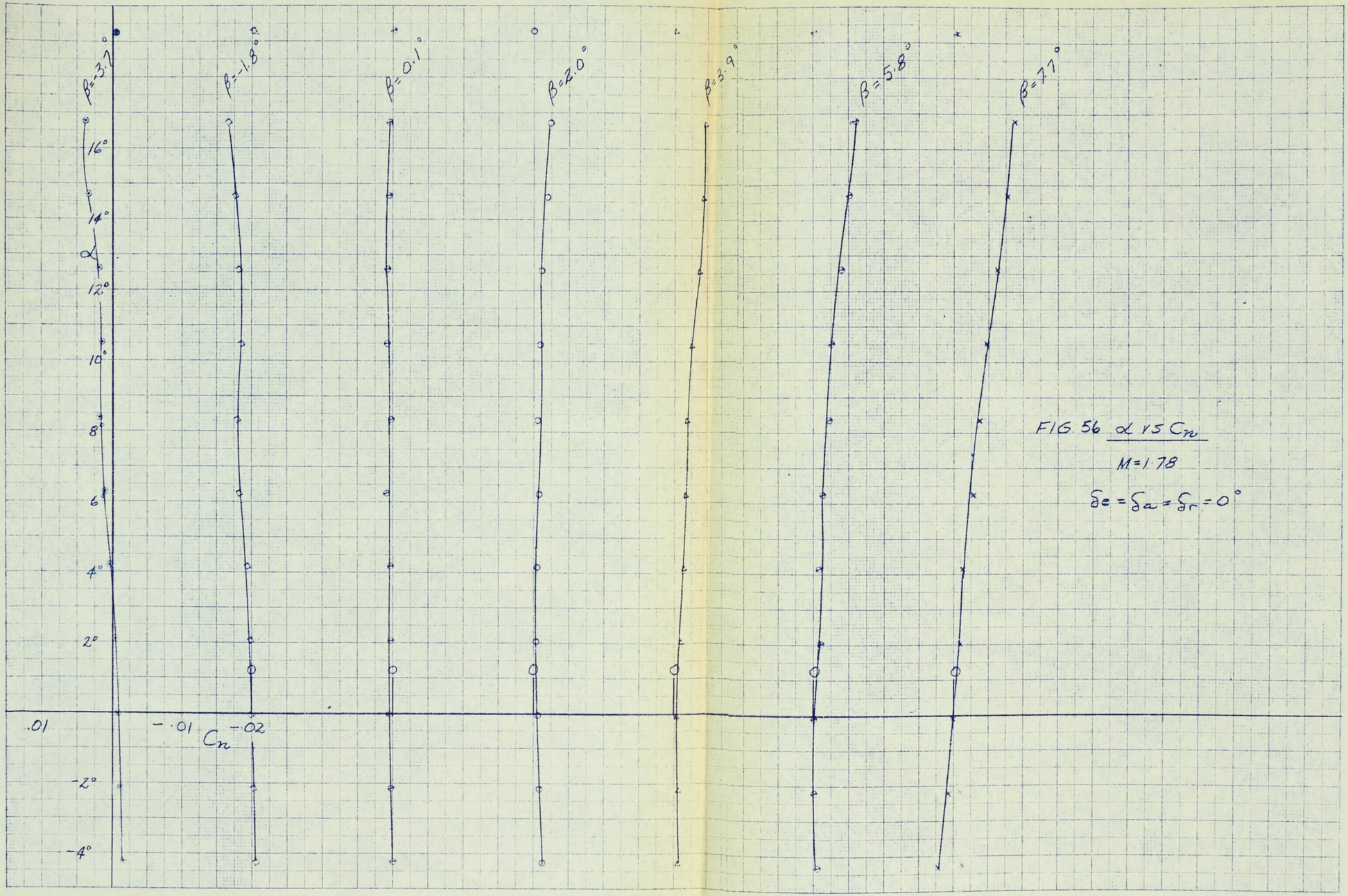

FIG. 56 α vs C_n

M = 1.78

$\delta_e = \delta_a = \delta_r = 0°$

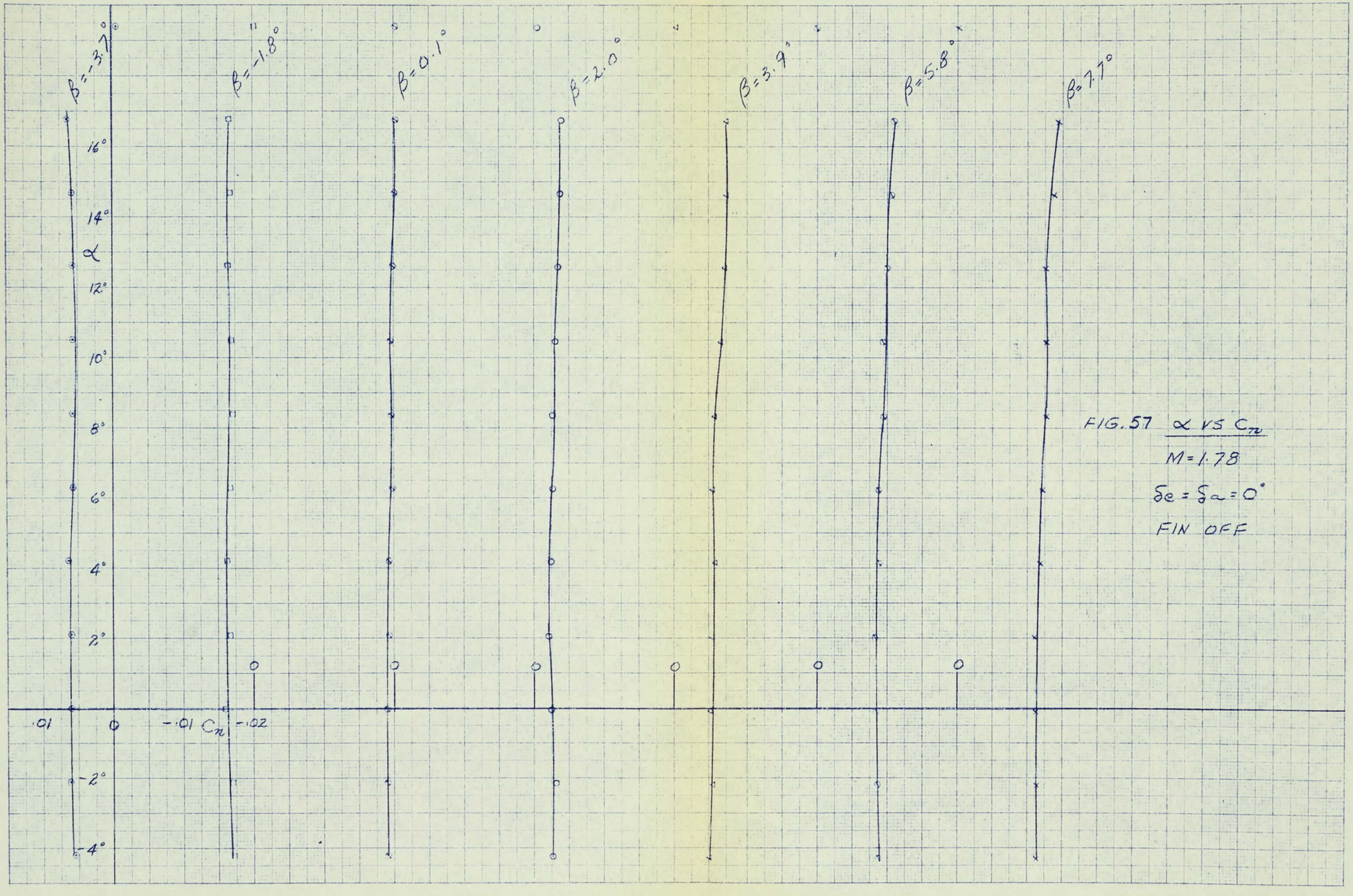

FIG. 57 α VS C_n

M = 1.78

$\delta e = \delta a = 0°$

FIN OFF

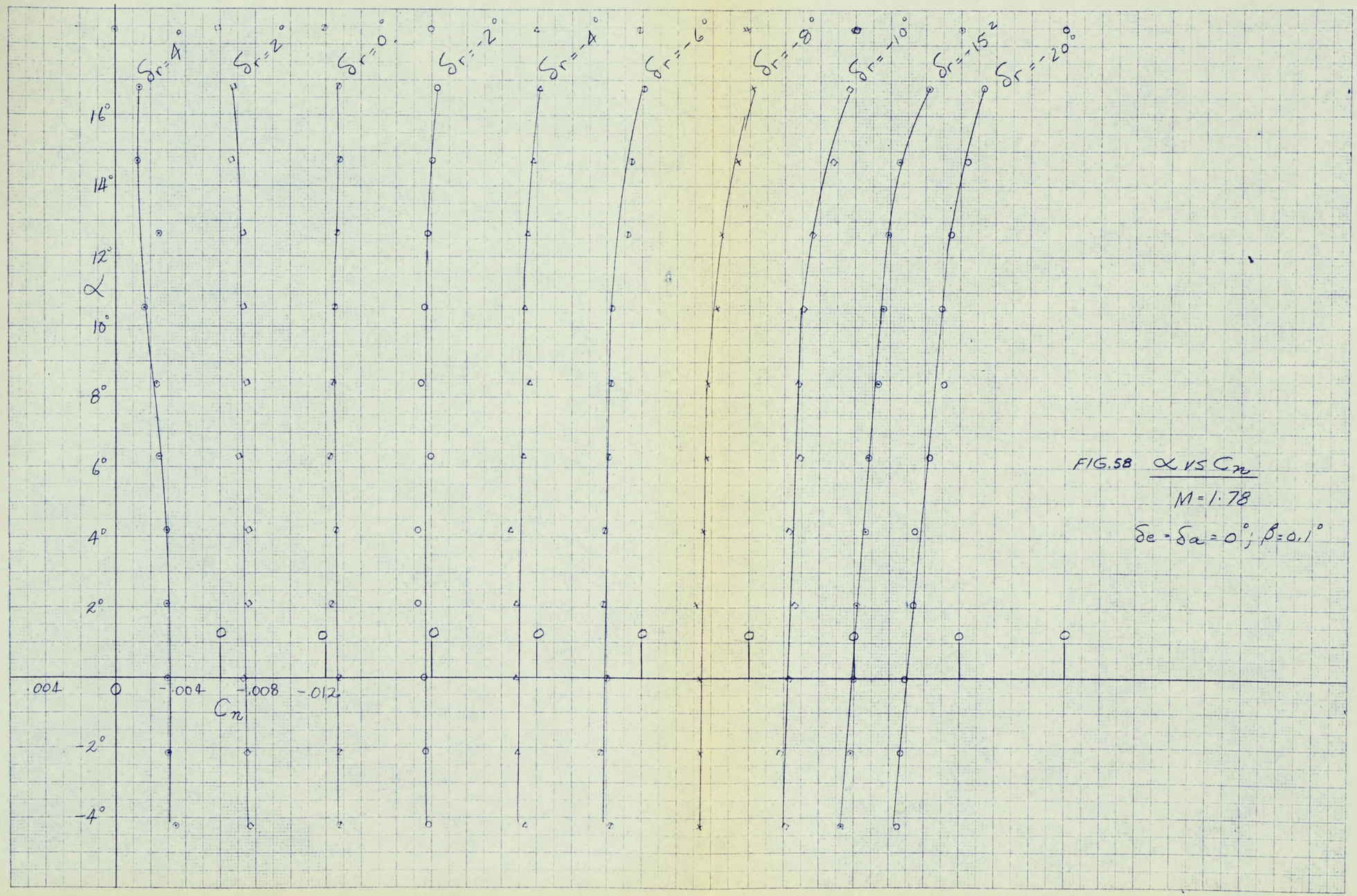

FIG. 58 α VS C_n

$M = 1.78$

$\delta_e = \delta_a = 0°$; $\beta = 0.1°$

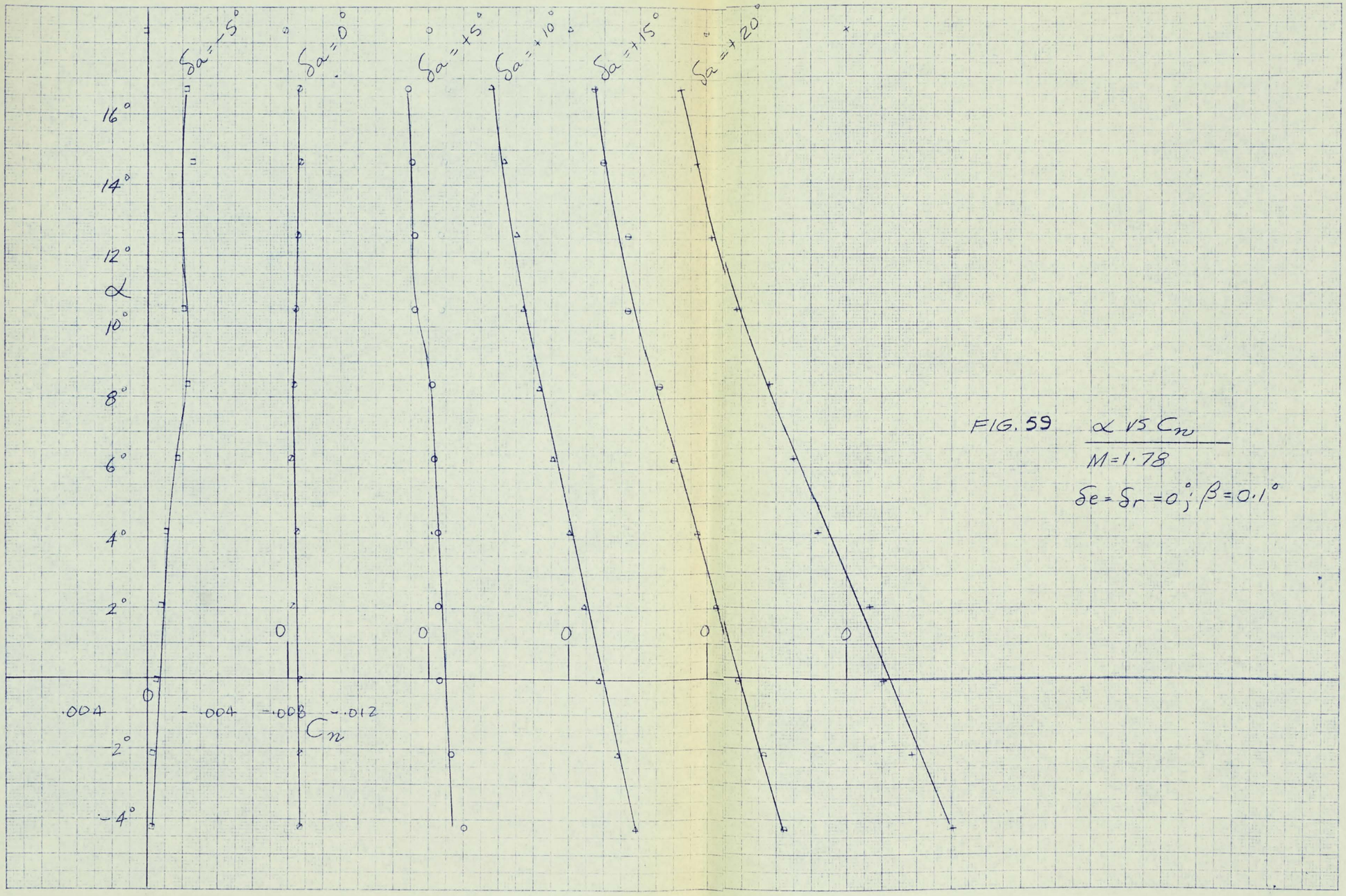

FIG. 59 α VS C_n

M=1.78

$\delta_e = \delta_r = 0°$; $\beta = 0.1°$

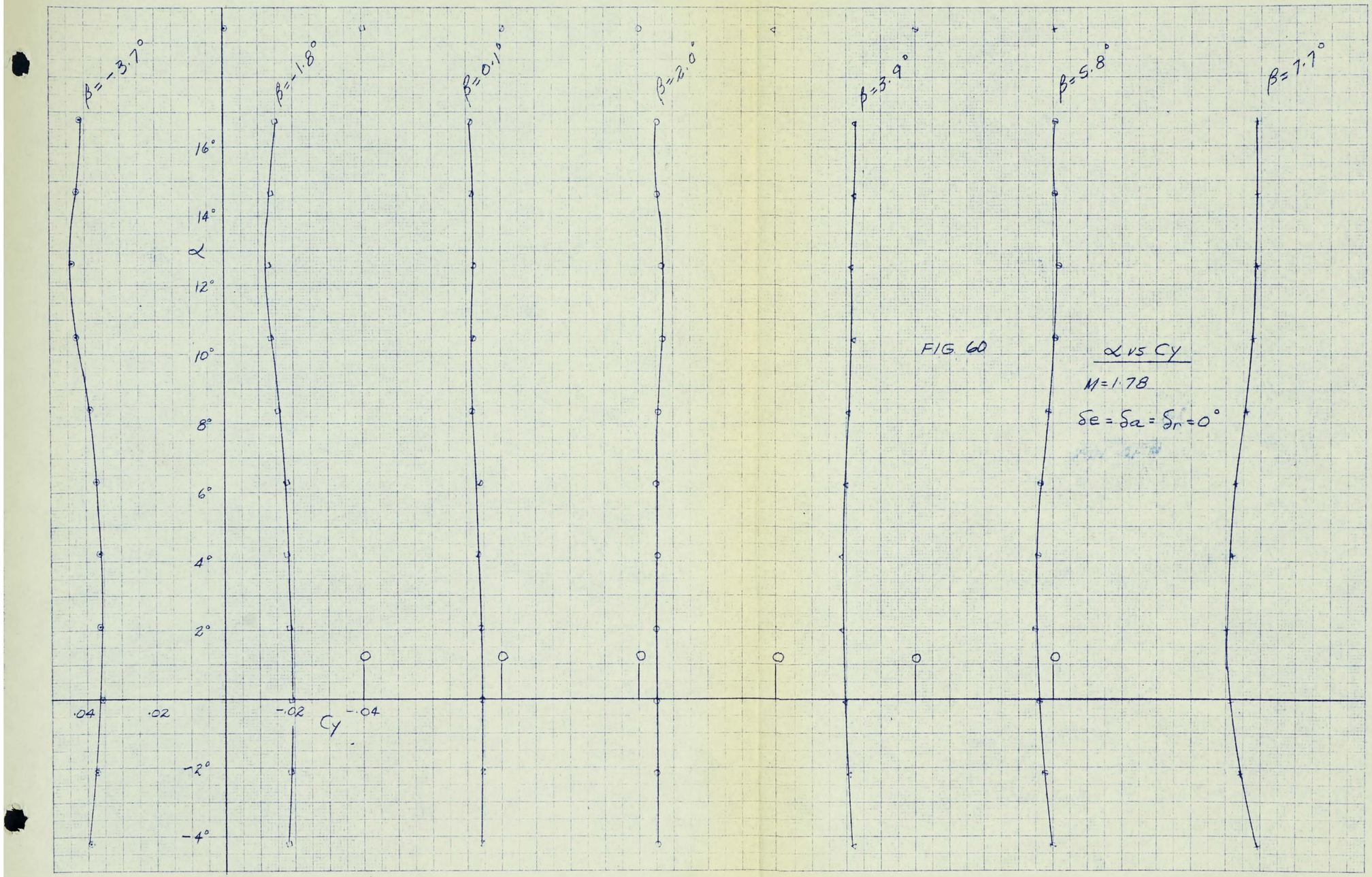

FIG 60

α vs Cy

M=1.78

$\delta_e = \delta_a = \delta_r = 0°$

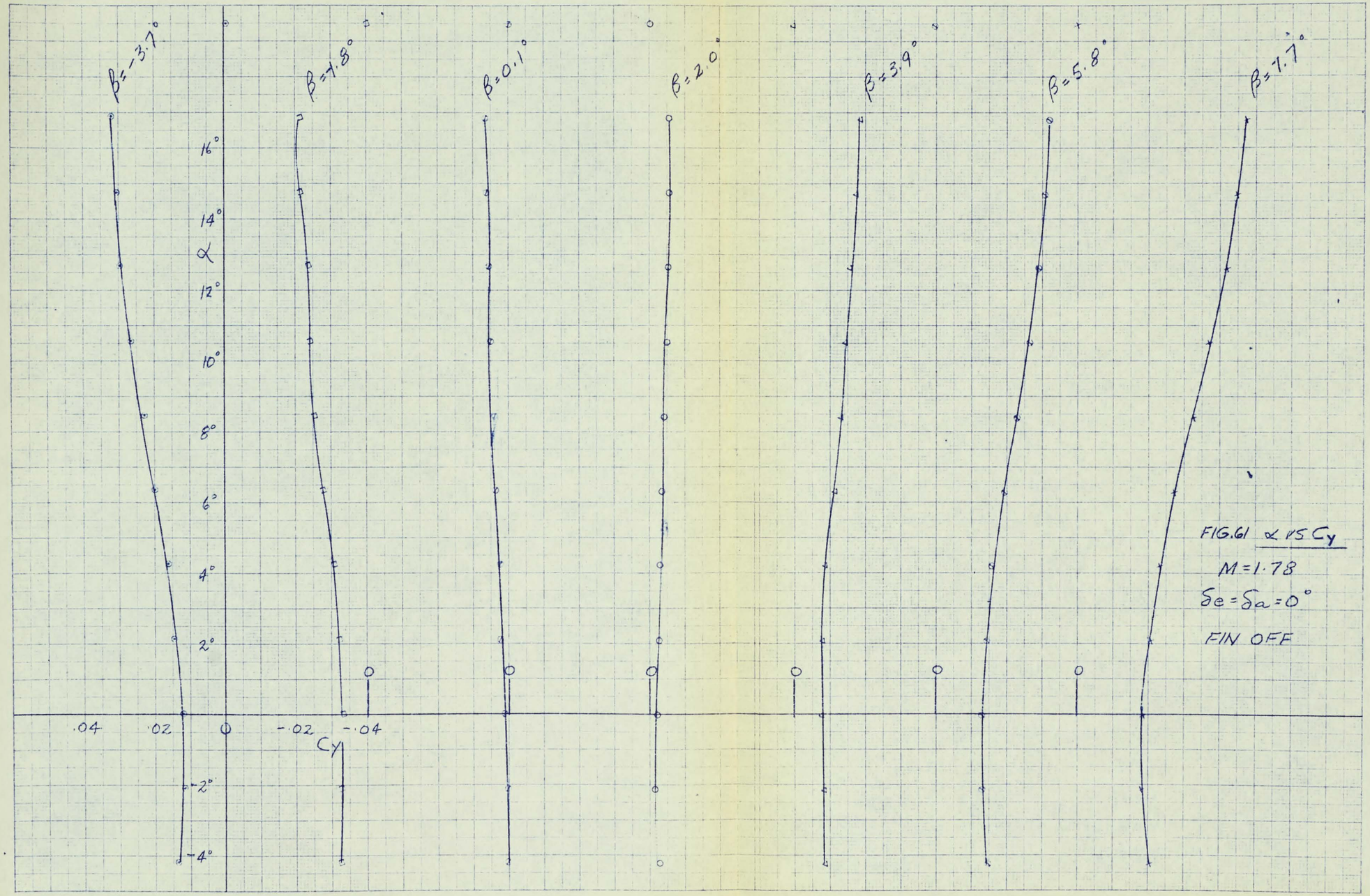

FIG.61 α VS C_y

$M = 1.78$

$\delta e = \delta a = 0°$

FIN OFF

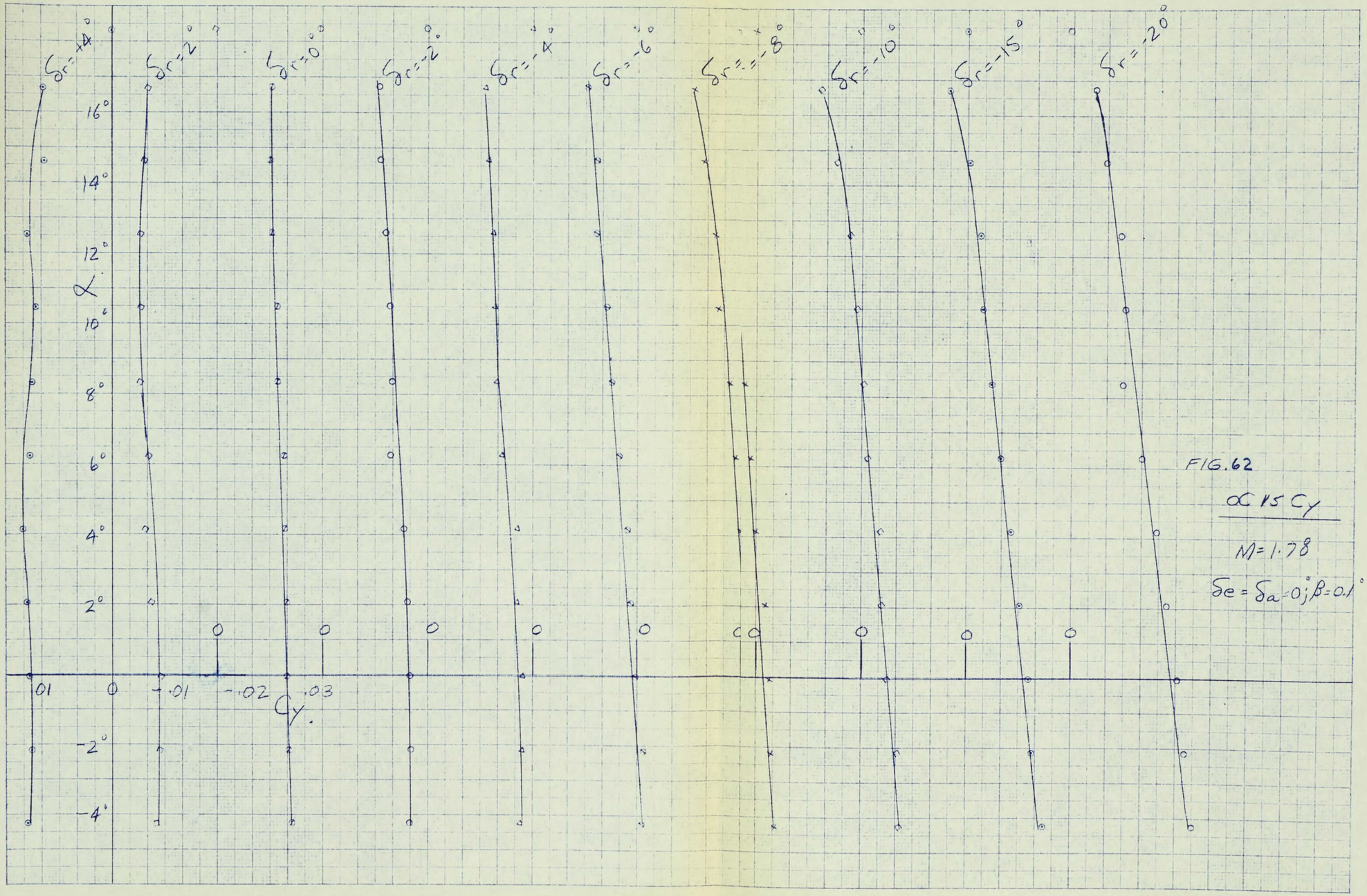

FIG. 62

α VS C_y

$M = 1.78$

$\delta e = \delta a = 0°; \beta = 0.1°$

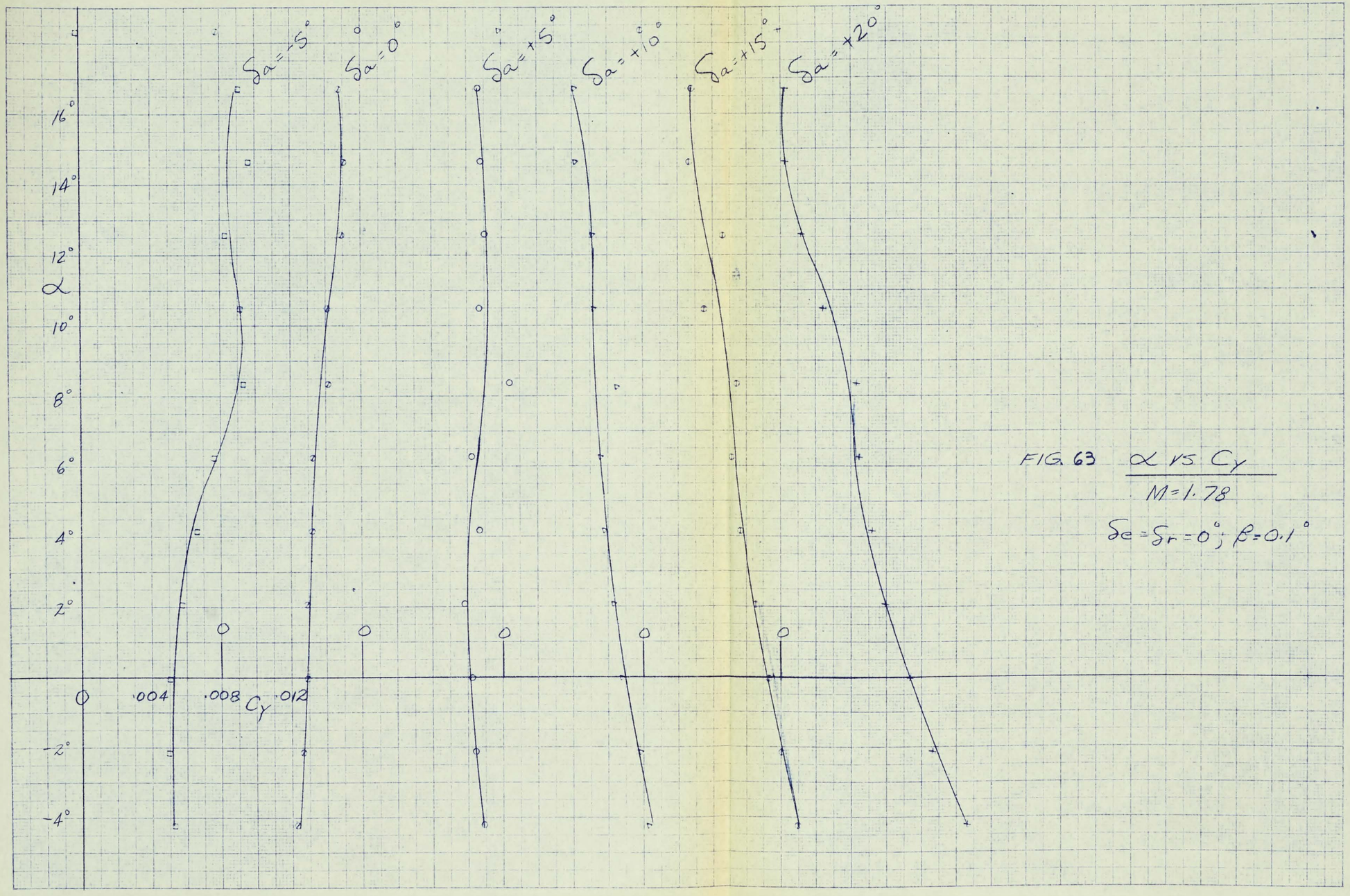

FIG. 63 α vs C_y

$M = 1.78$

$\delta e = \delta r = 0°$; $\beta = 0.1°$

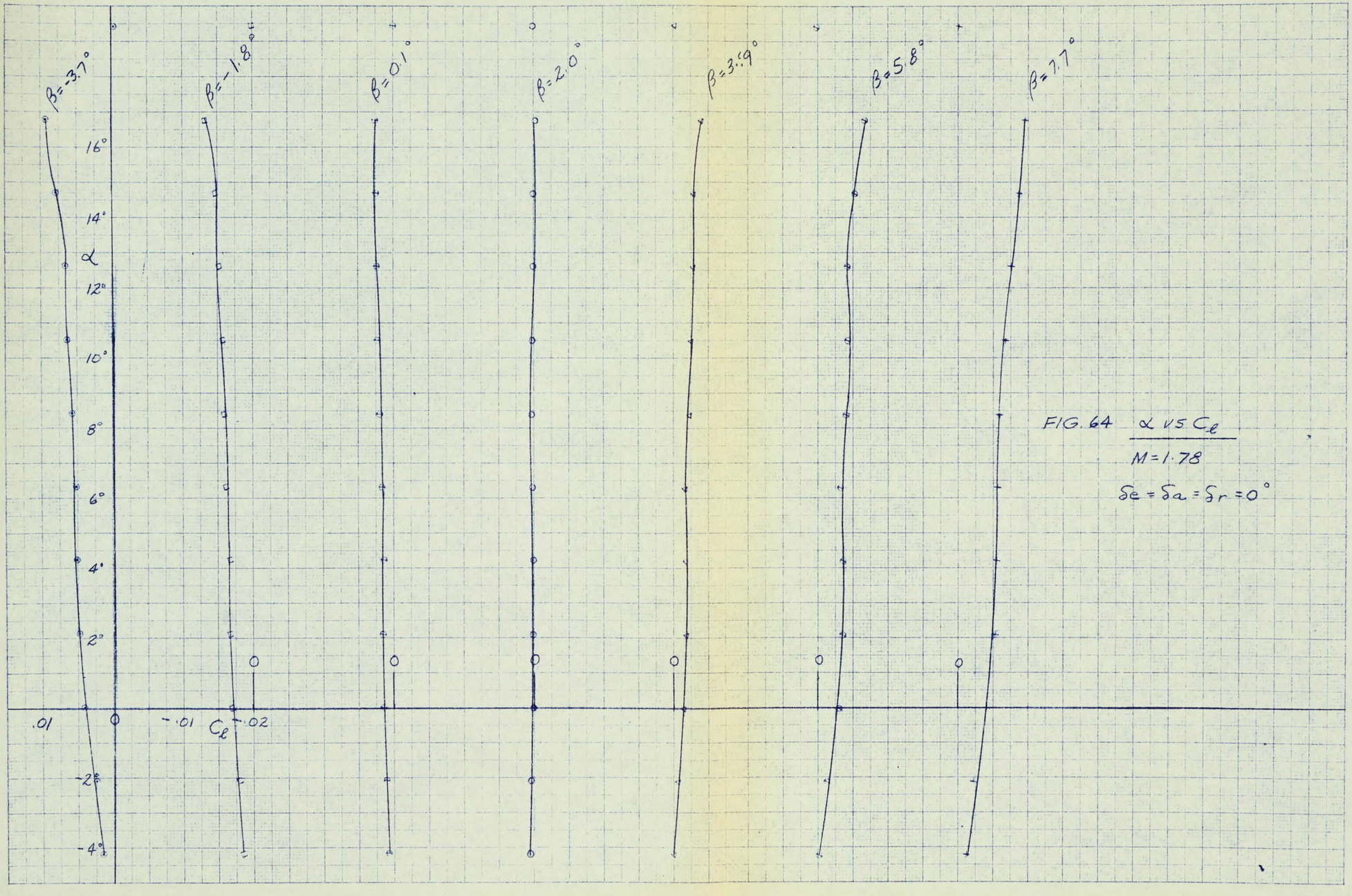

FIG. 64 α VS C_ℓ

$M = 1.78$

$\delta e = \delta a = \delta r = 0°$

β=-3.7°

β=-1.8°

β=0.1°

β=2.0°

β=3.9°

β=5.8°

β=7.7°

16°
α
14°
12°
10°
8°
6°
4°
2°
-2°
-4°

.01 0 -.01 C_ℓ -.02

FIG. 65 α VS C_ℓ

M=1.78
$\delta_e = \delta_a = 0°$
FIN OFF

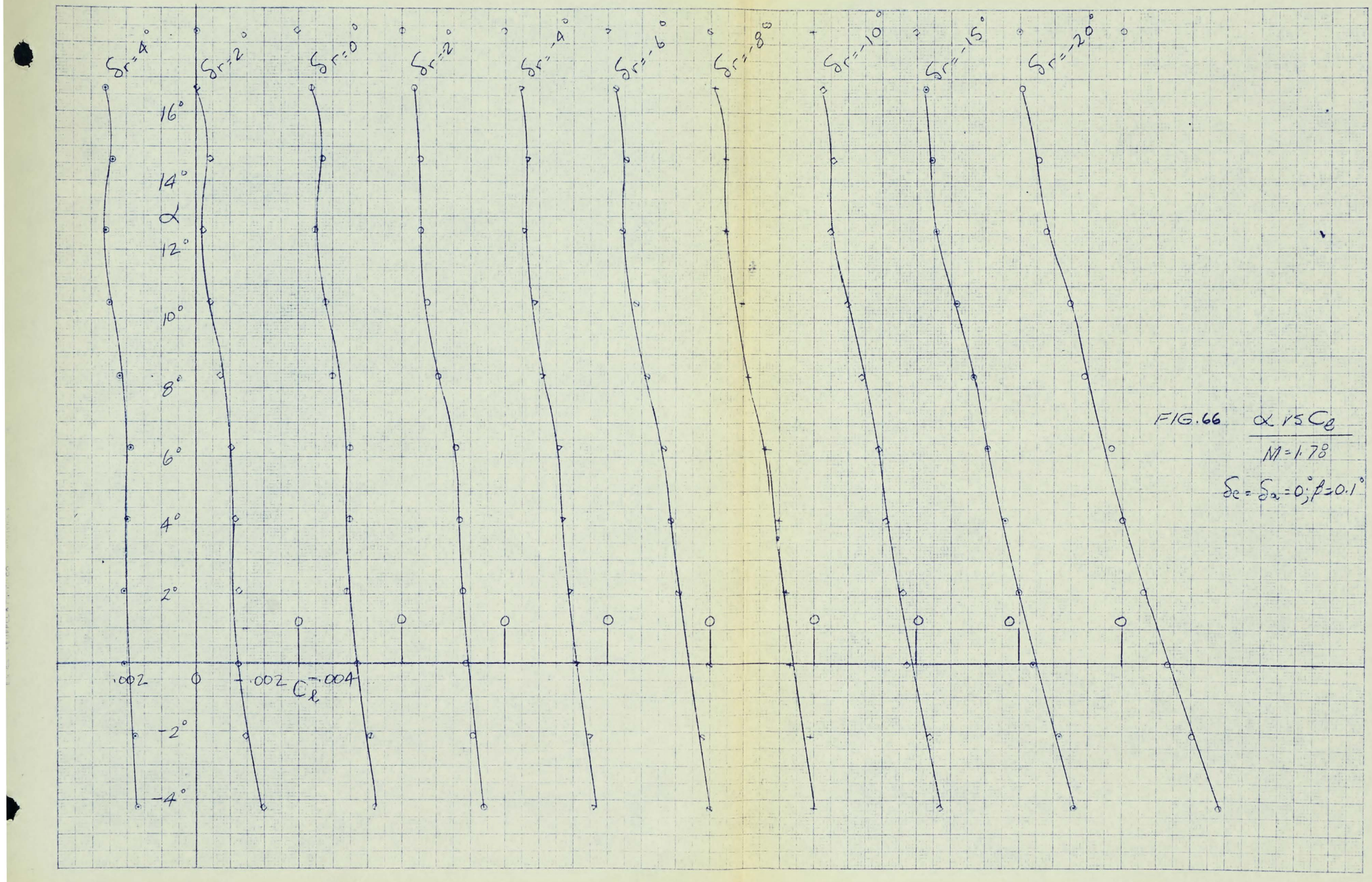

FIG. 66 α vs C_ℓ

$M = 1.78$

$\delta_e = \delta_a = 0°; \beta = 0.1°$

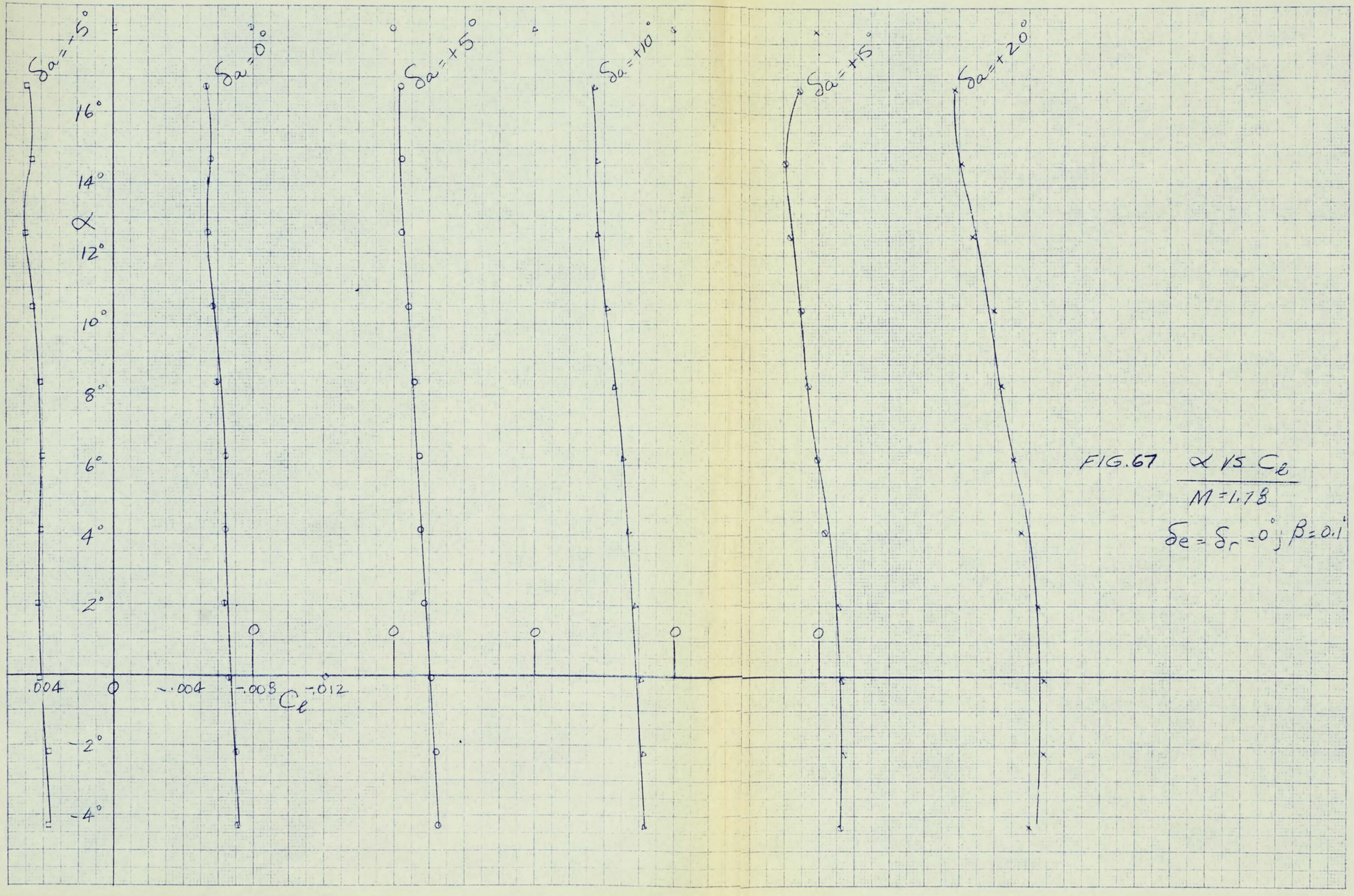

FIG. 67 α VS C_ℓ

M = 1.78

$\delta_e = \delta_r = 0°$; $\beta = 0.1°$

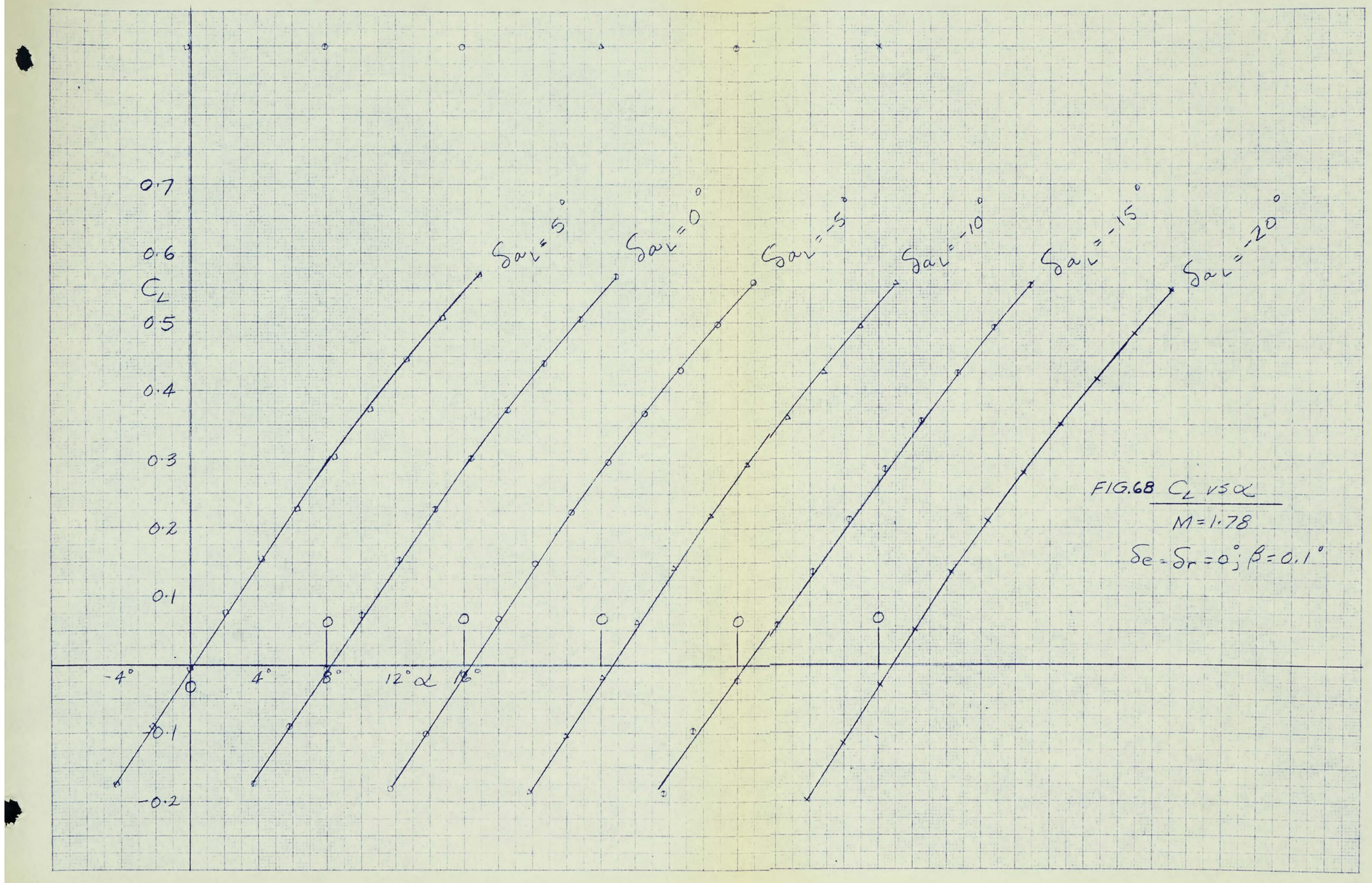

FIG.68 C_L vs α

$M=1.78$

$\delta_e=\delta_r=0°$; $\beta=0.1°$

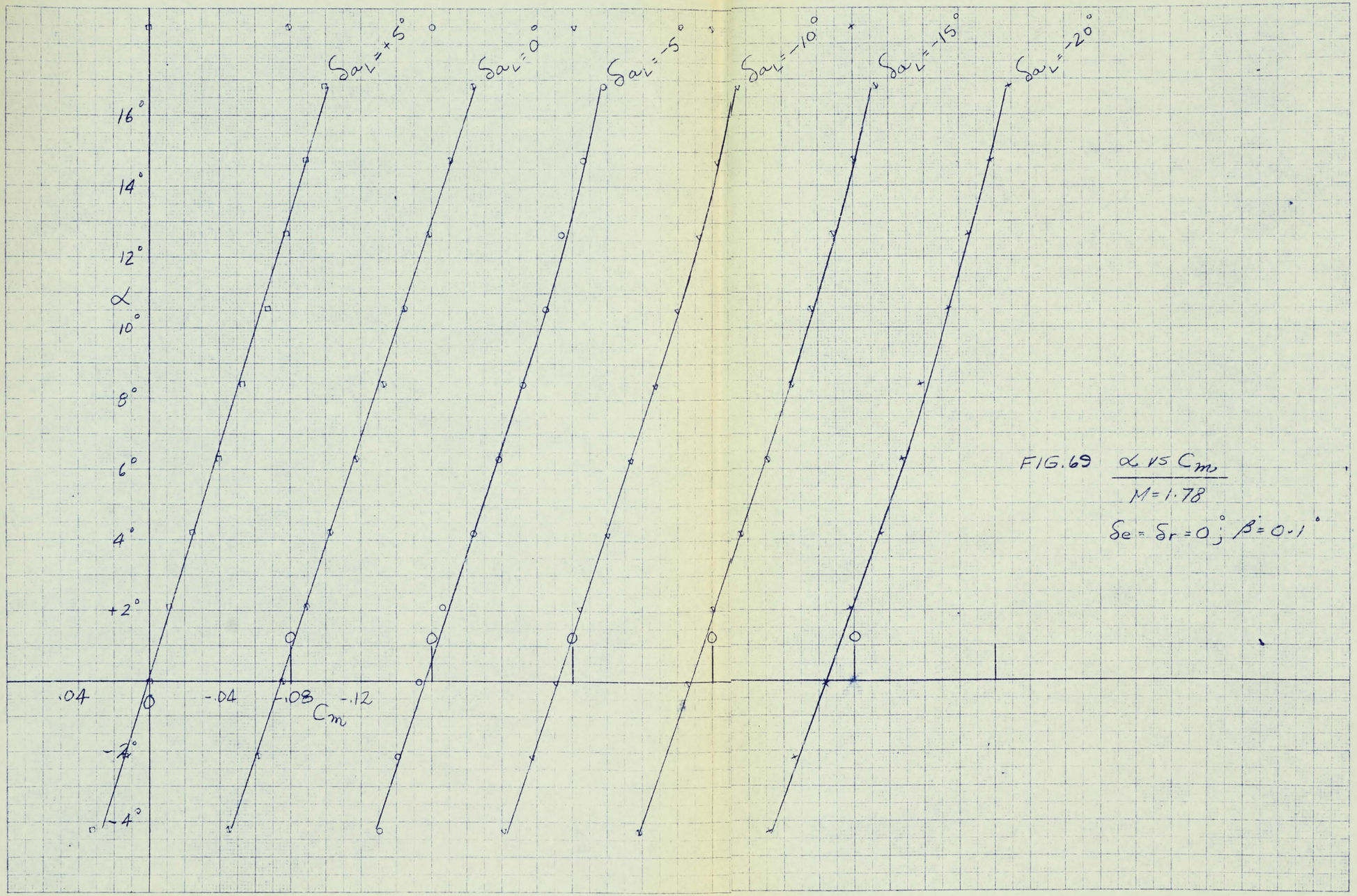

FIG. 69 α vs C_m

$M = 1.78$

$\delta_e = \delta_r = 0°$; $\beta = 0.1°$

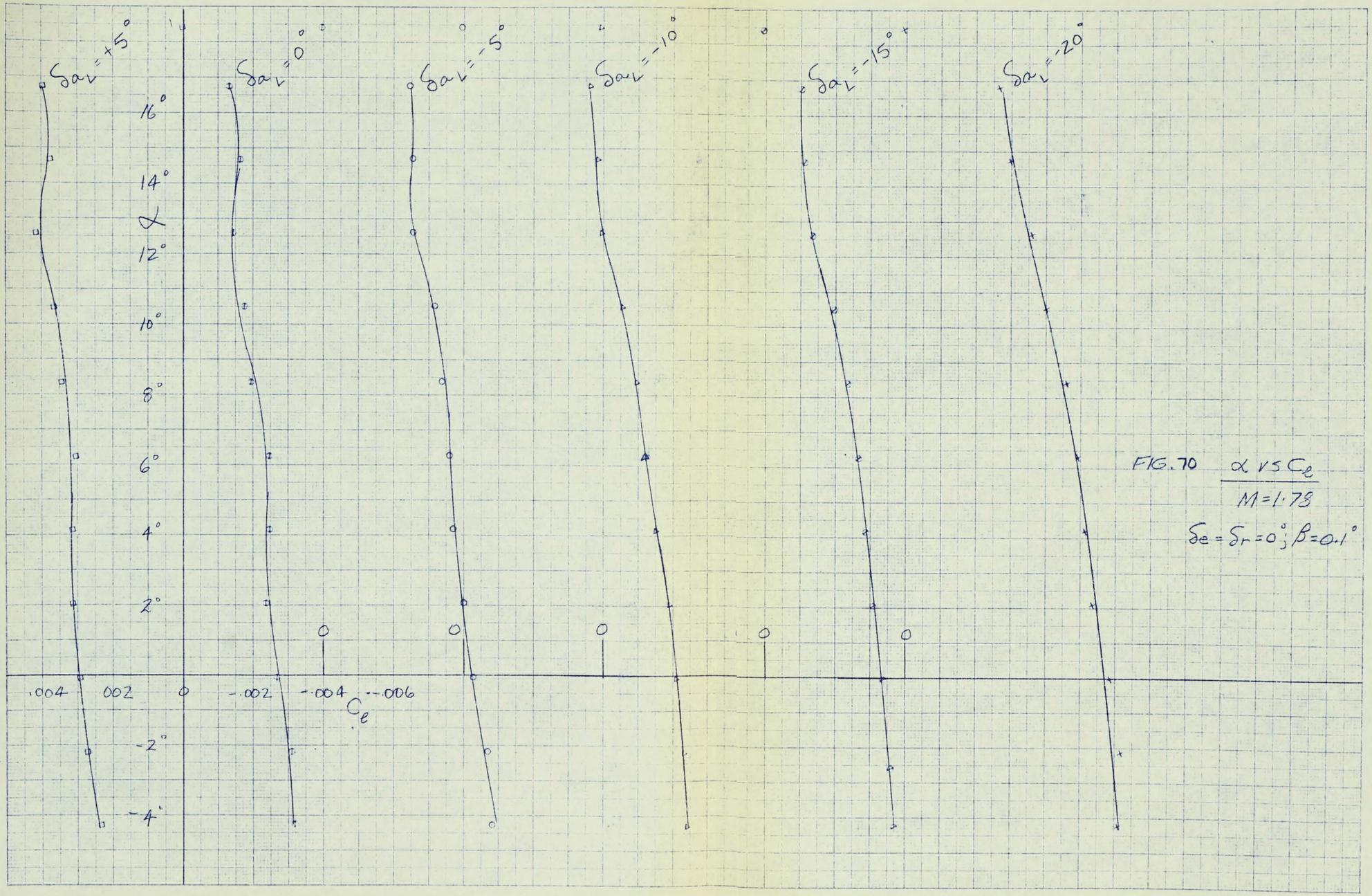

FIG. 70 α vs C_ℓ

$M = 1.78$

$\delta_e = \delta_r = 0°; \beta = 0.1°$

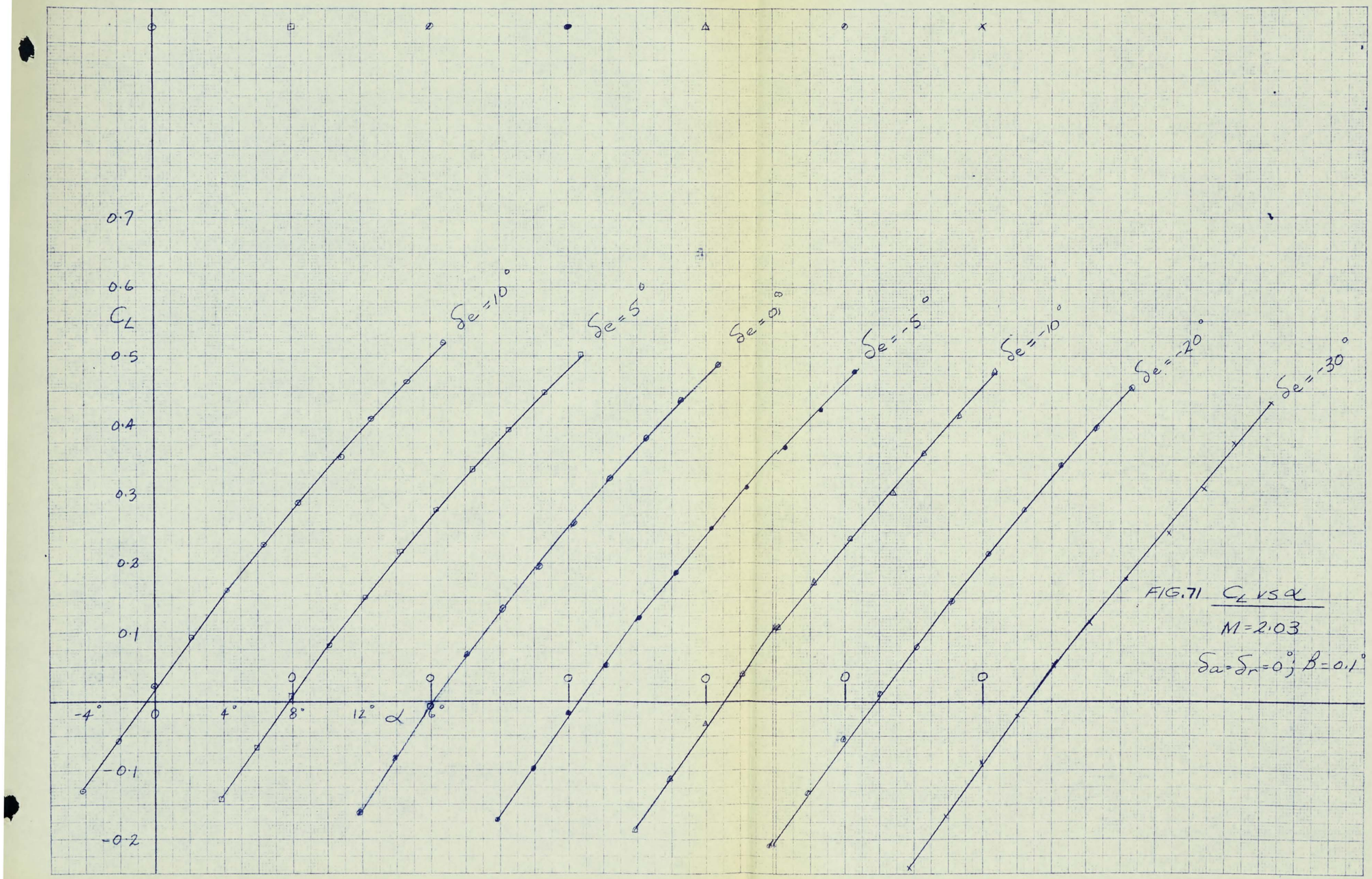

FIG.71 C_L vs α

M=2.03

$\delta_a=\delta_r=0°$; $\beta=0.1°$

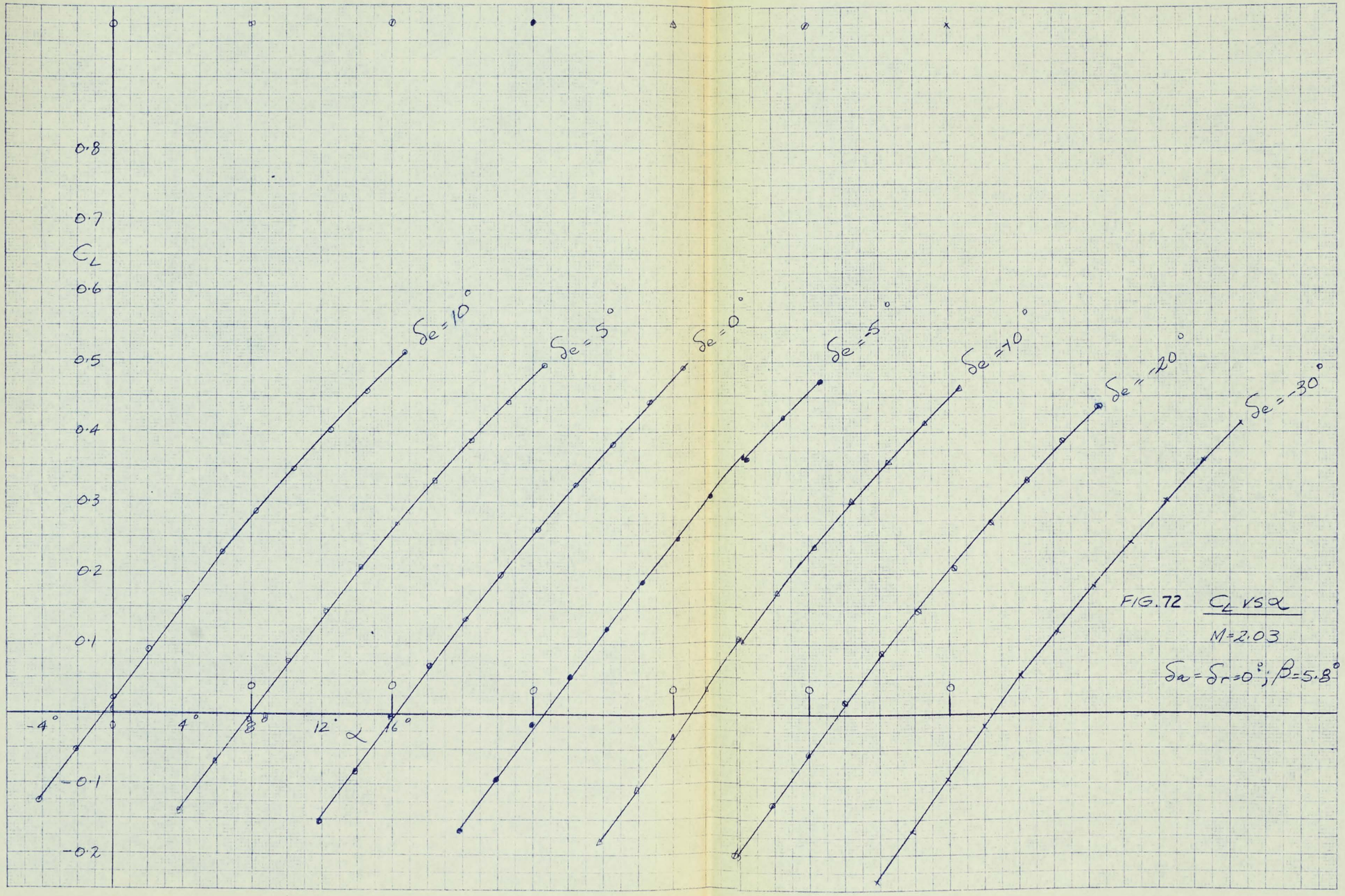

FIG. 72 C_L VS α

$M = 2.03$

$\delta_a = \delta_r = 0°$; $\beta = 5.8°$

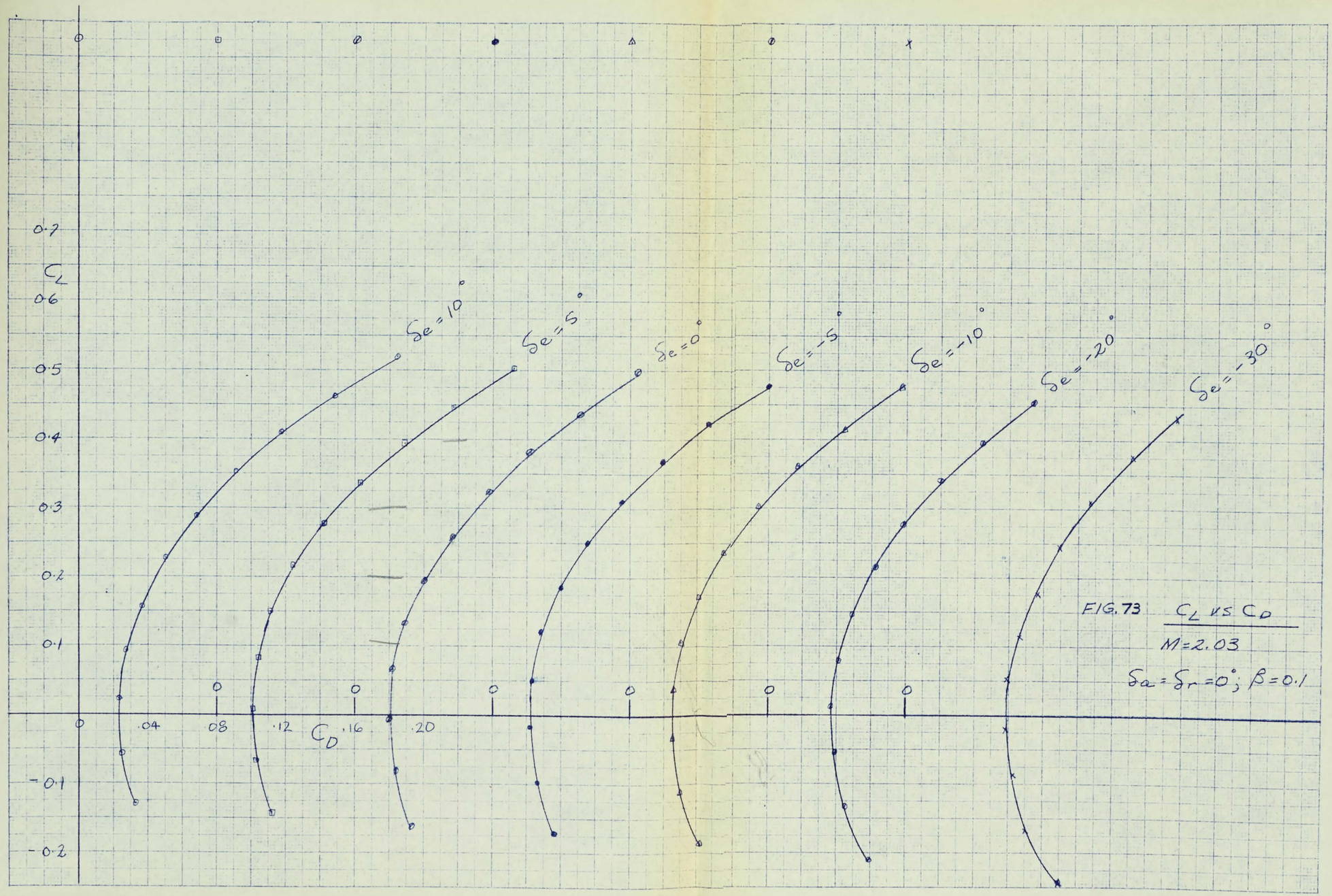

FIG. 73 C_L vs C_D

$M=2.03$

$\delta_a=\delta_r=0°$; $\beta=0.1$

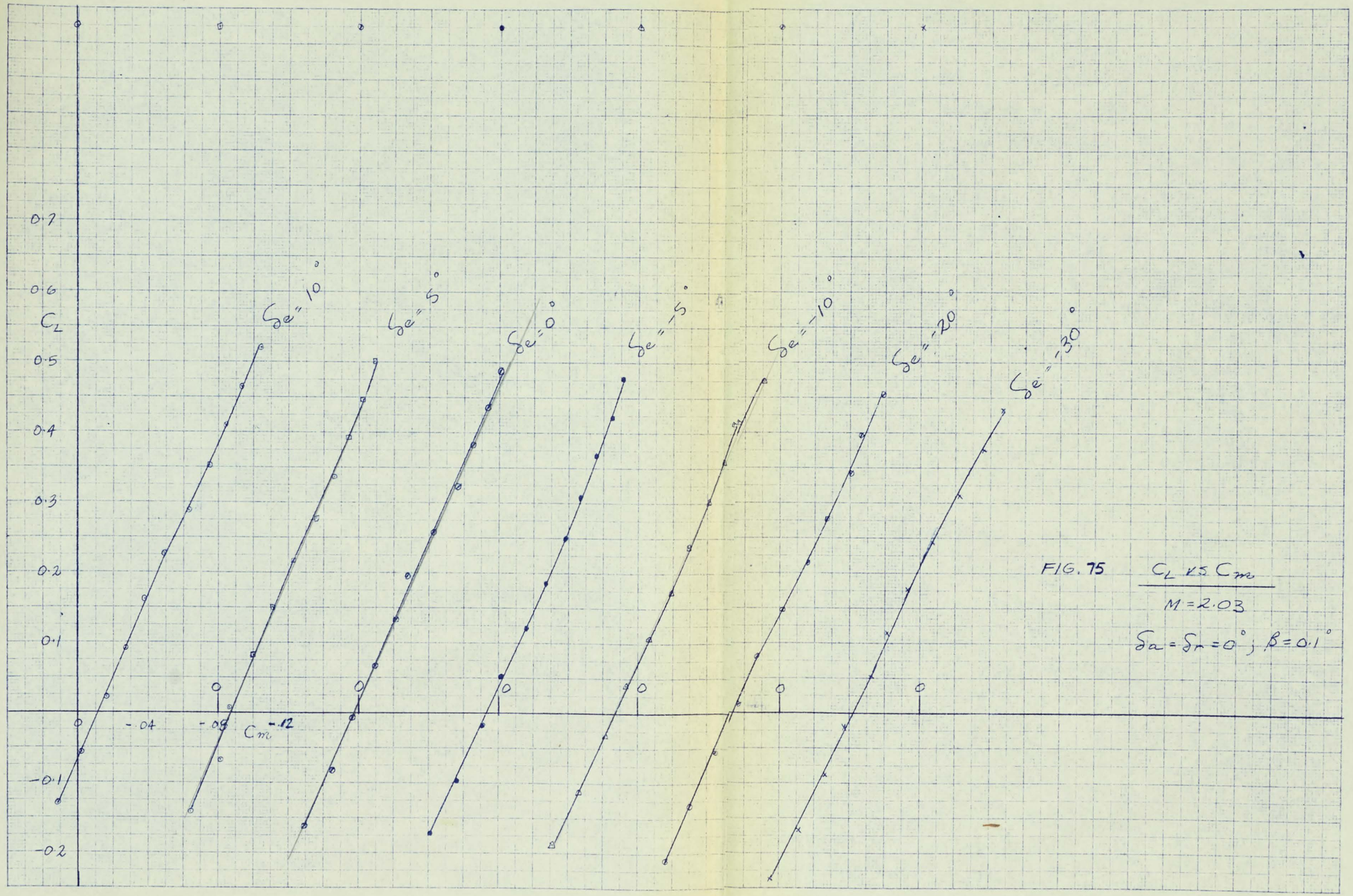

FIG. 75 C_L vs C_m

$M = 2.03$

$\delta_a = \delta_r = 0°$; $\beta = 0.1°$

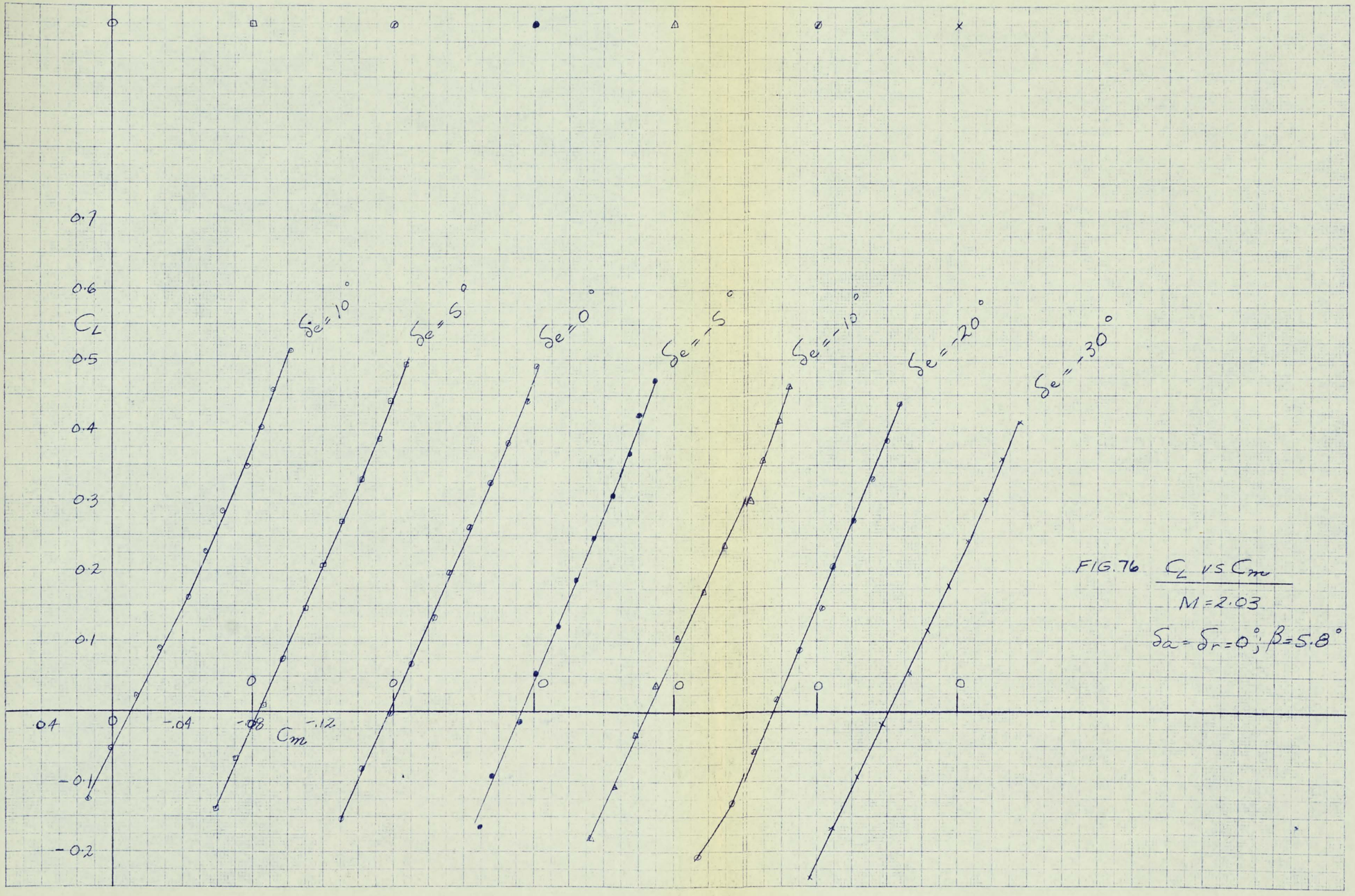

FIG. 76 C_L vs C_m

$M = 2.03$

$\delta_a = \delta_r = 0°$; $\beta = 5.8°$

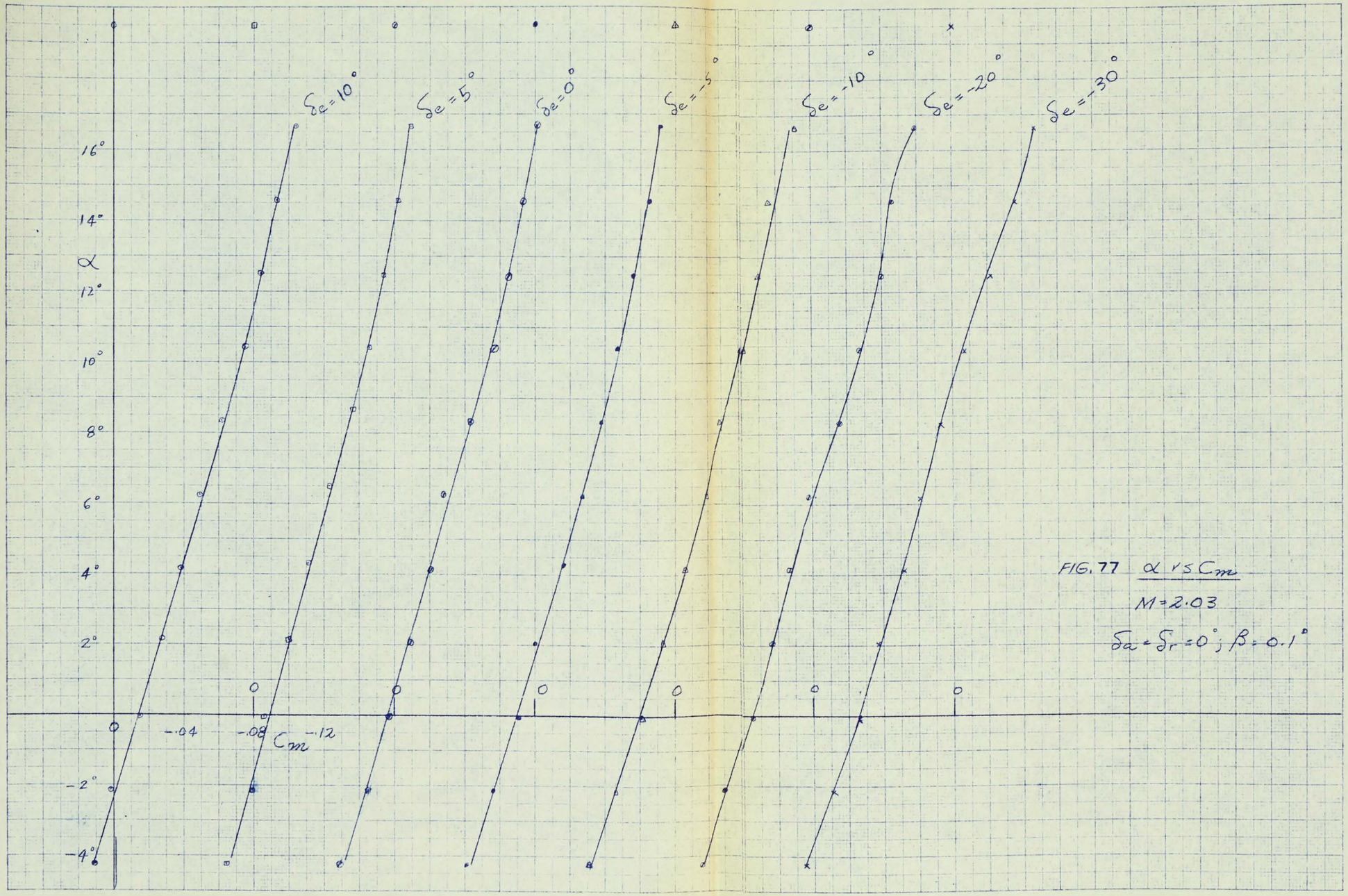

FIG. 77 α vs C_m

$M = 2.03$

$\delta_a = \delta_r = 0°$; $\beta = 0.1°$

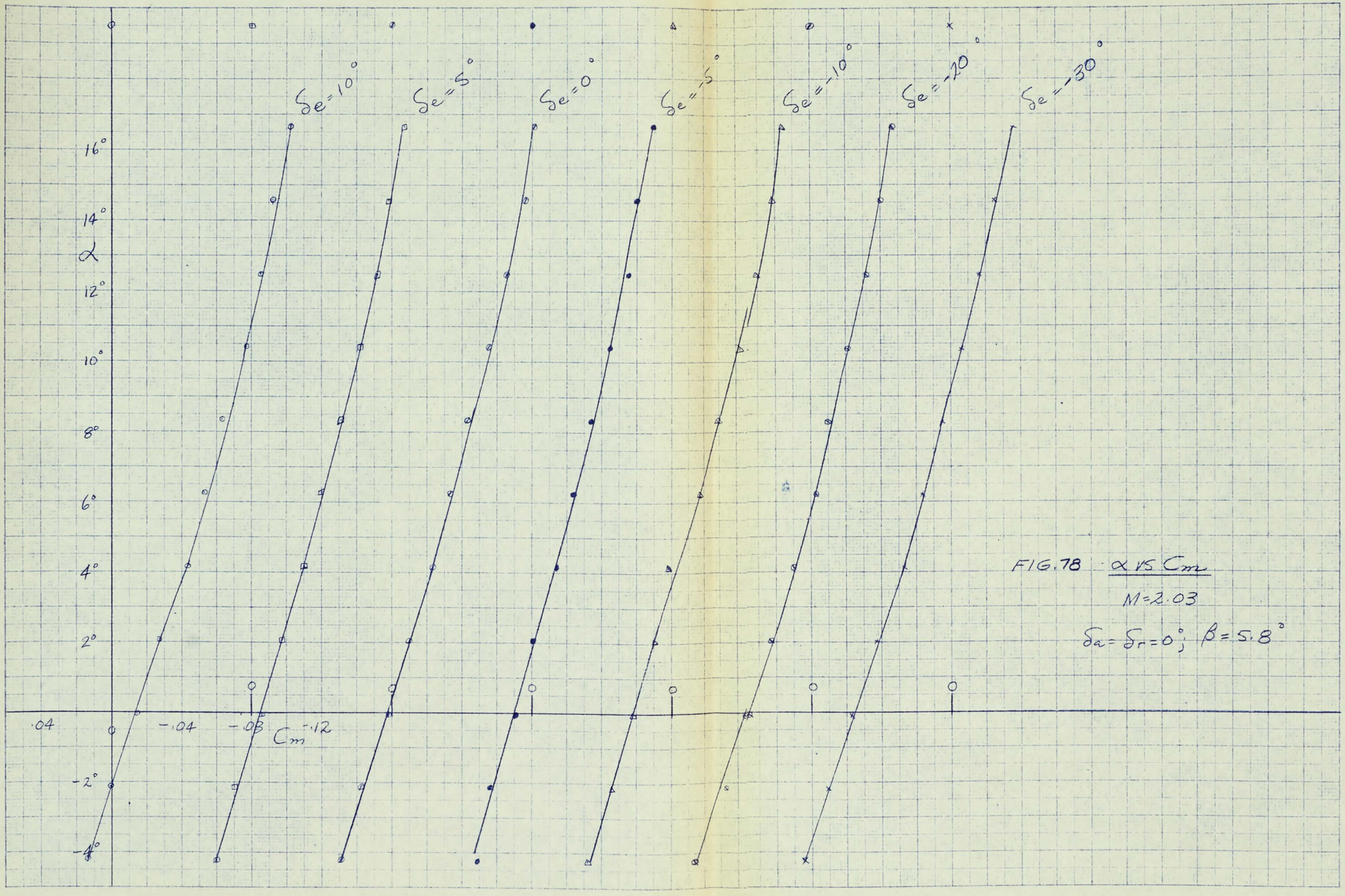

FIG. 78 α VS C_m

$M = 2.03$

$\delta_a = \delta_r = 0°$; $\beta = 5.8°$

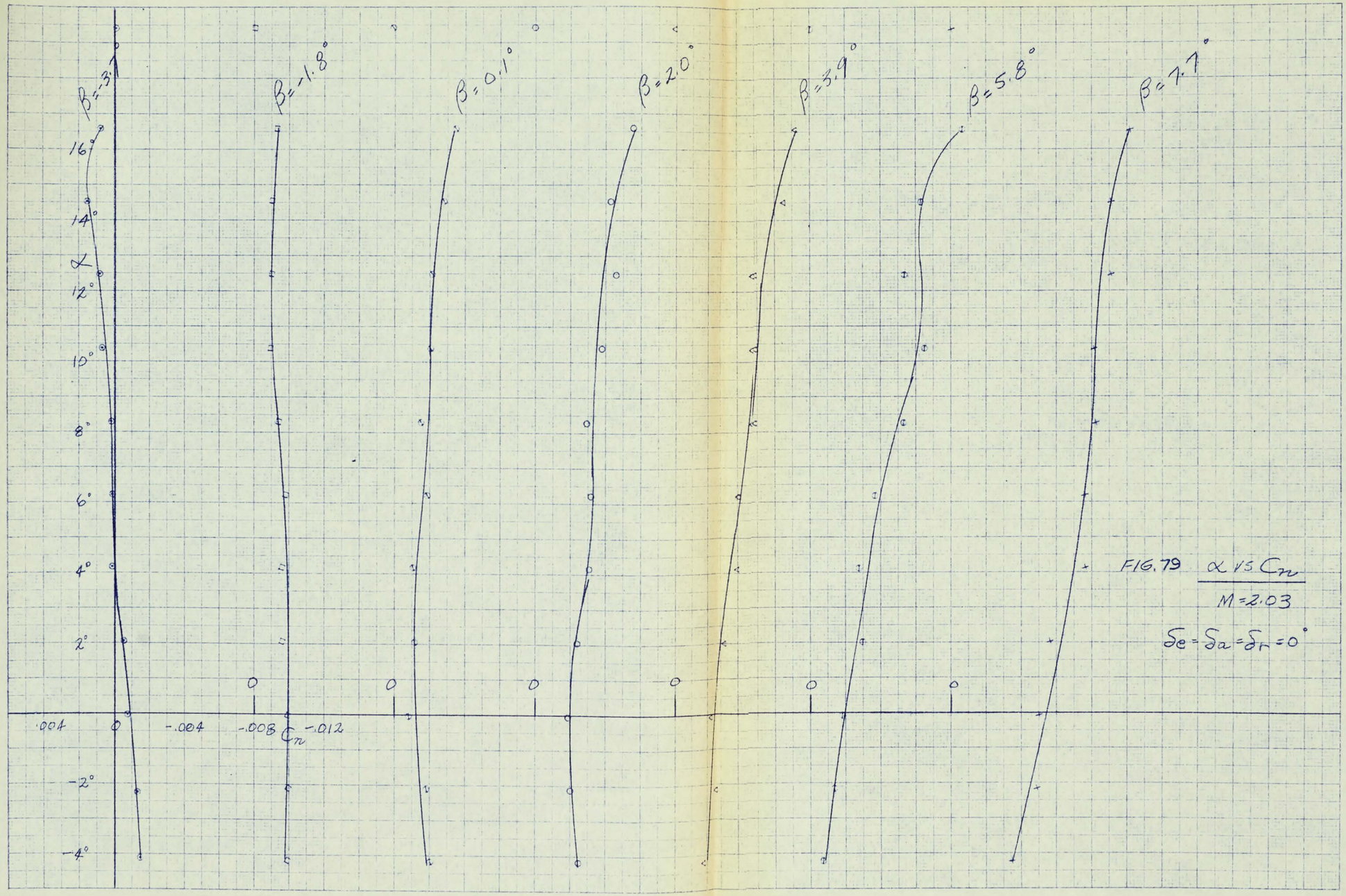

FIG. 79 α vs C_n

$M = 2.03$

$\delta_e = \delta_a = \delta_r = 0°$

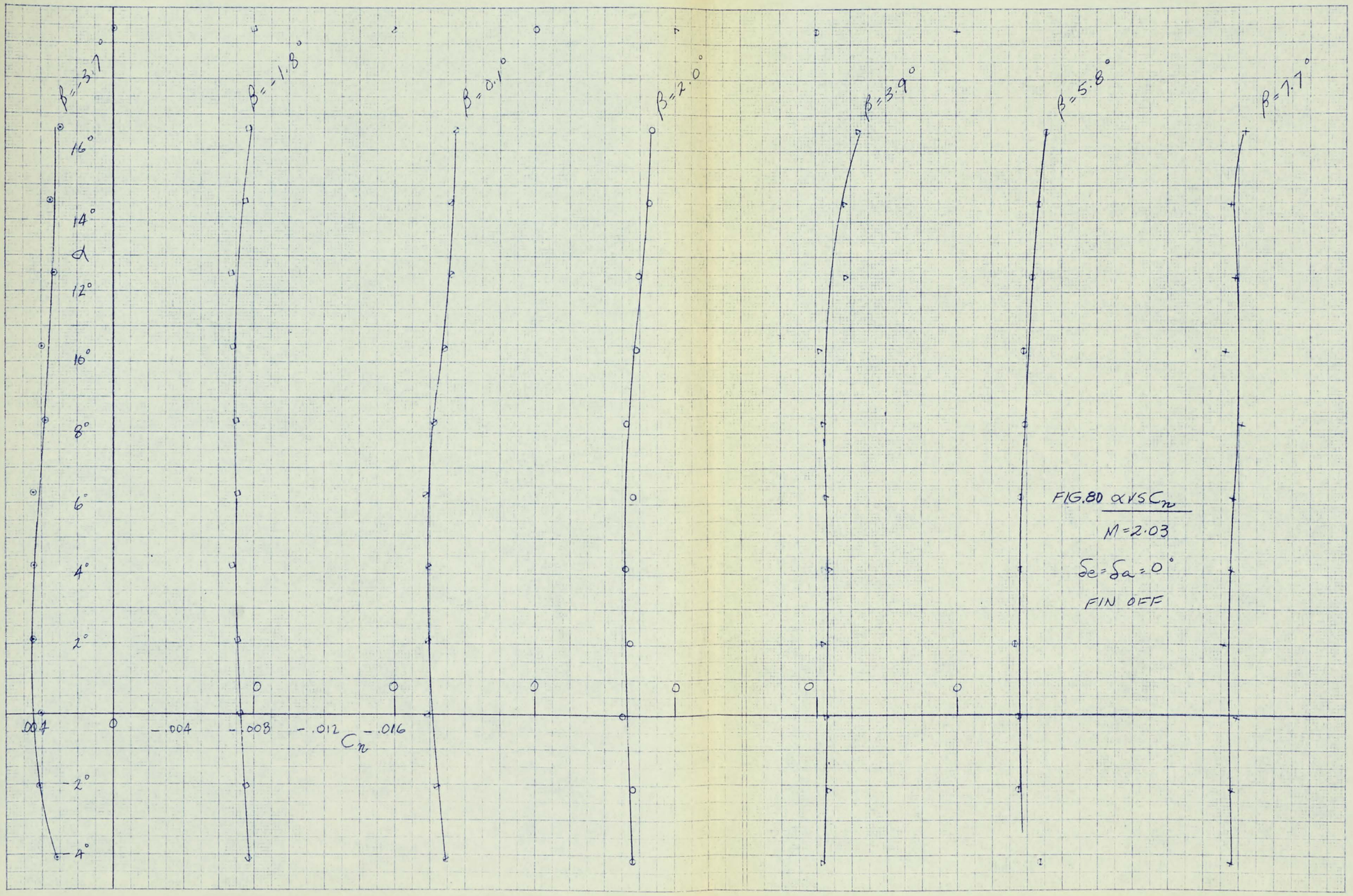

FIG. 80 α VS C_n

$M = 2.03$

$\delta_e = \delta_a = 0°$

FIN OFF

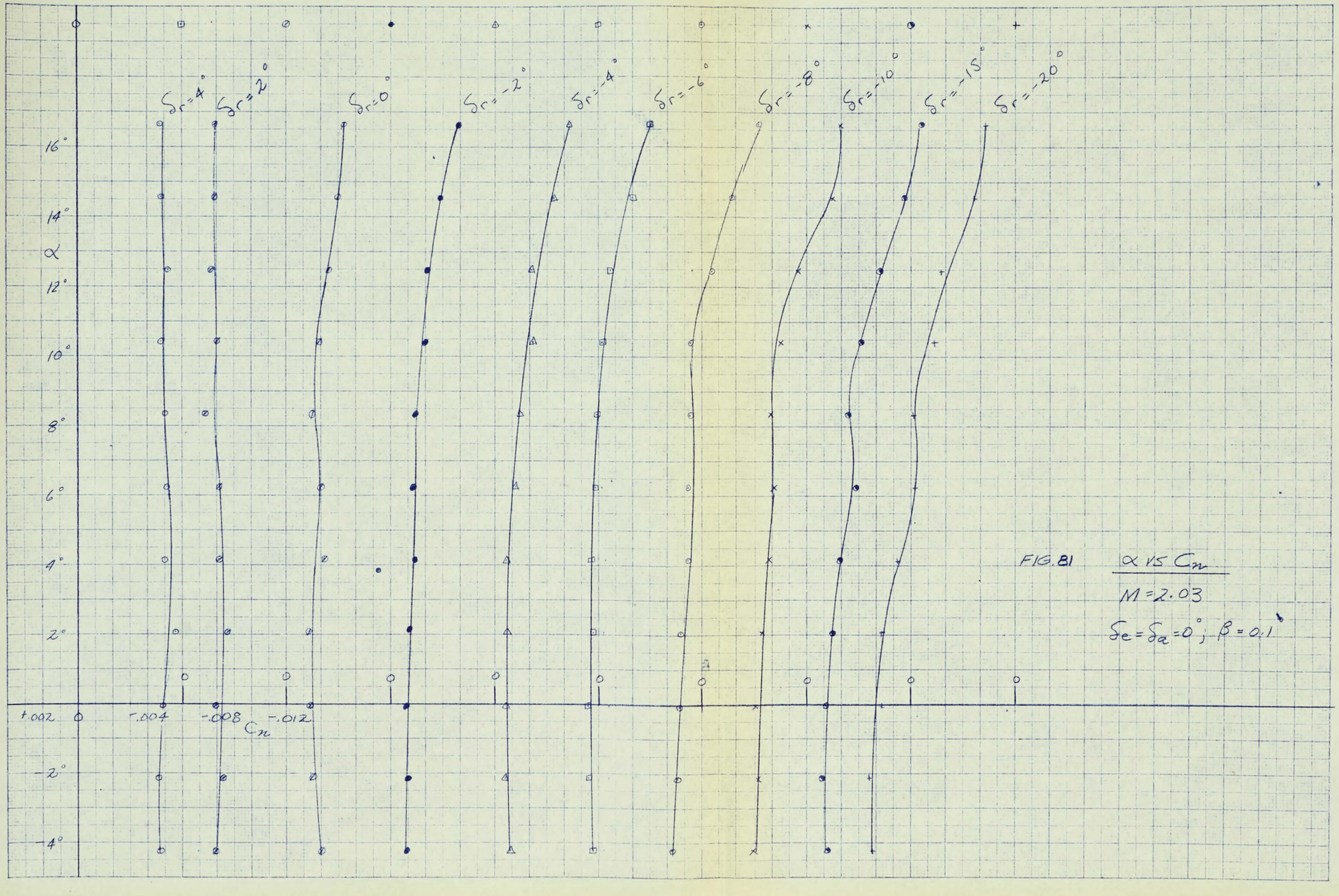

FIG. 81 α vs C_n

$M = 2.03$

$\delta_e = \delta_a = 0°$; $\beta = 0.1°$

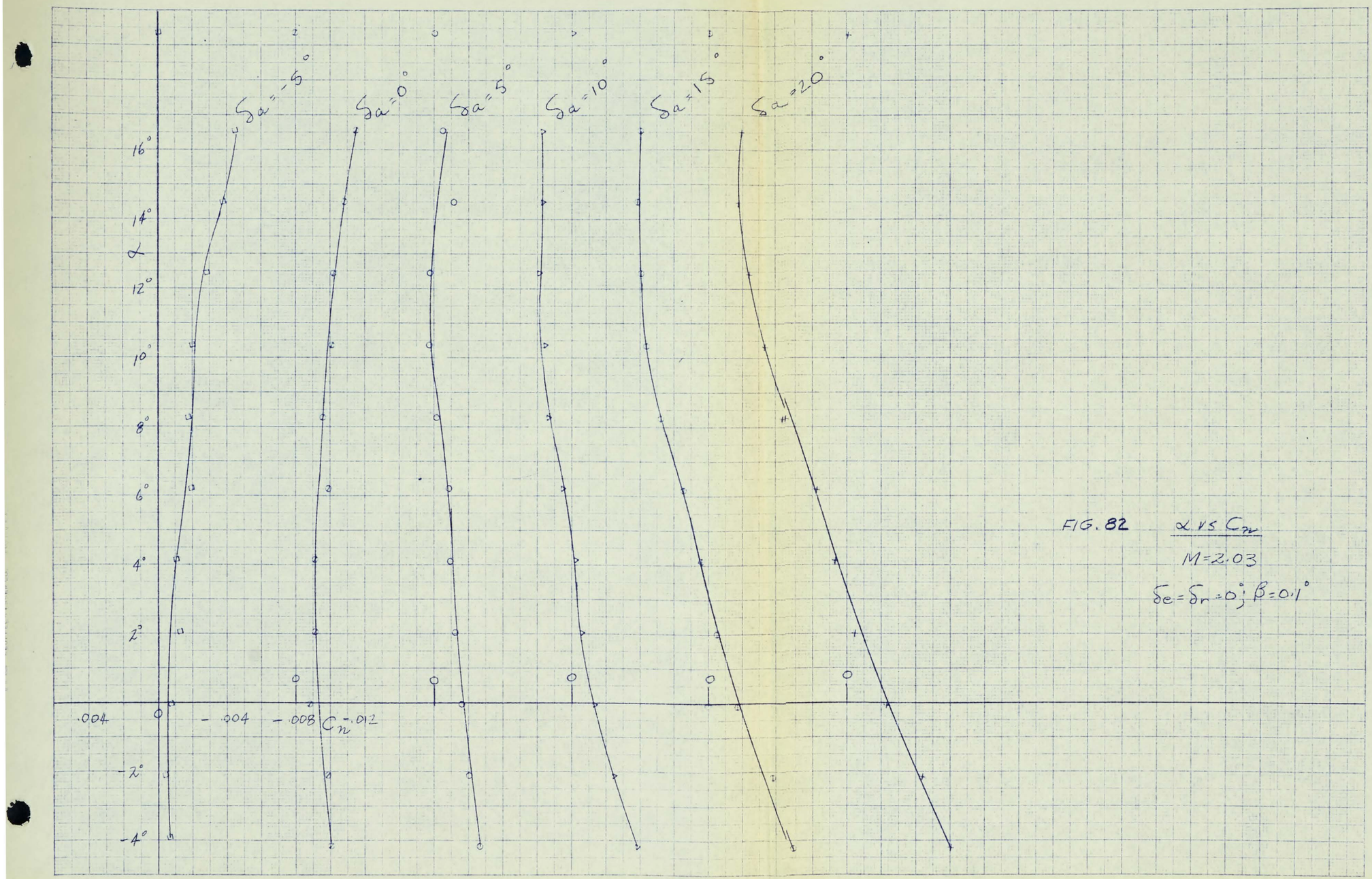

FIG. 82 α vs C_n

$M = 2.03$

$\delta_e = \delta_r = 0°$; $\beta = 0.1°$

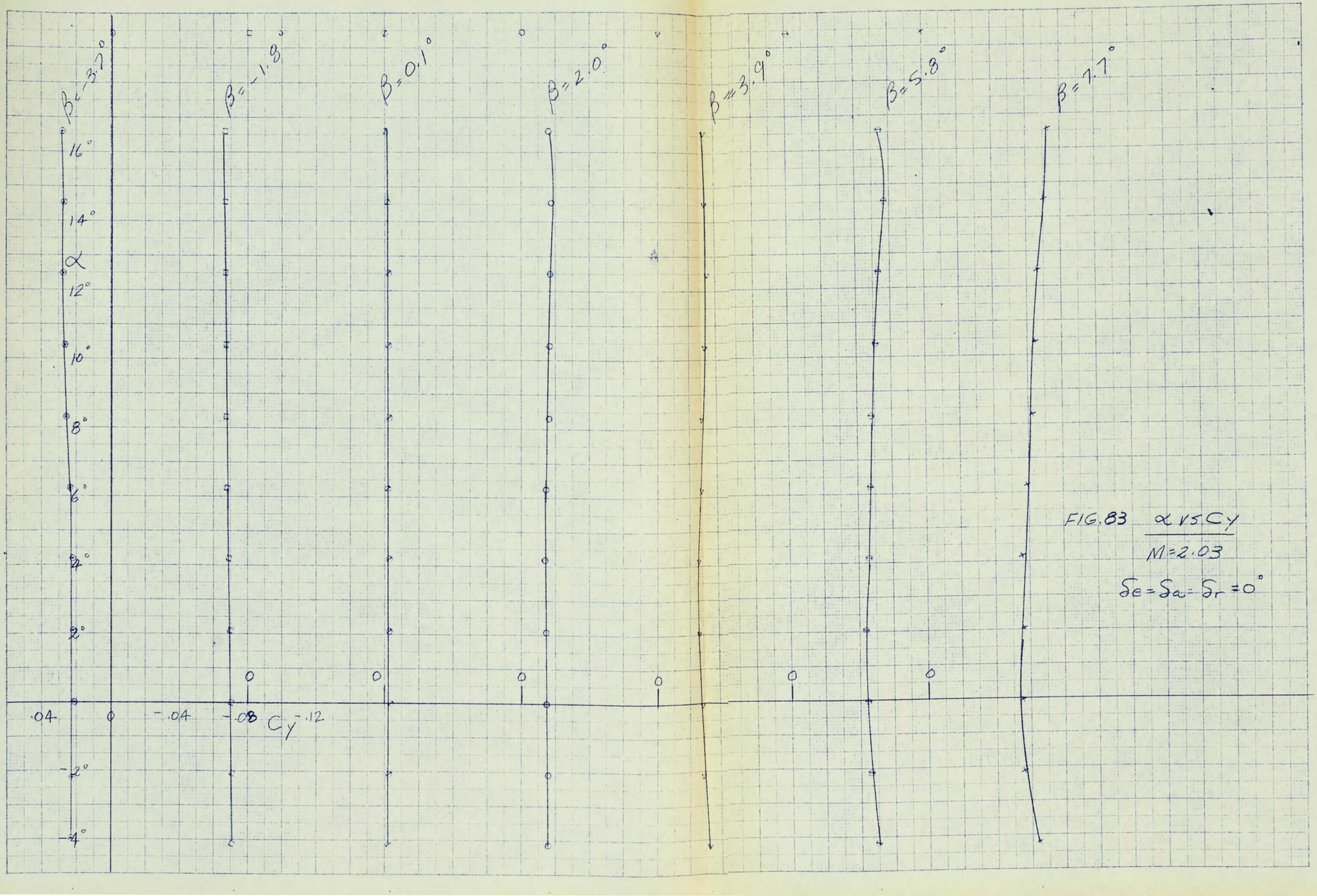

FIG. 83 α VS C_y

$M = 2.03$

$\delta_e = \delta_a = \delta_r = 0°$

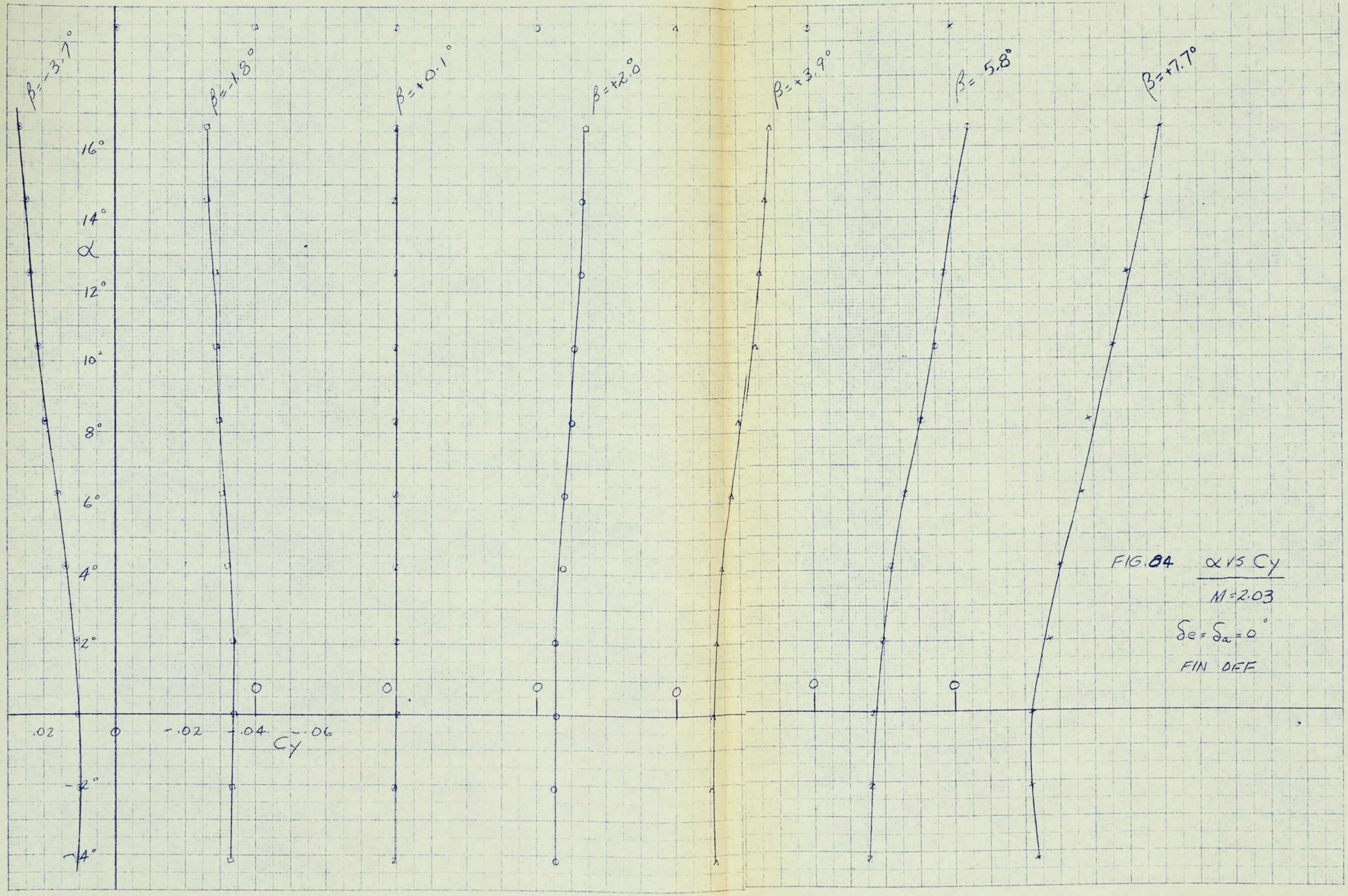

FIG. 84 α vs Cy

M=2.03

$\delta_e = \delta_a = 0°$

FIN OFF

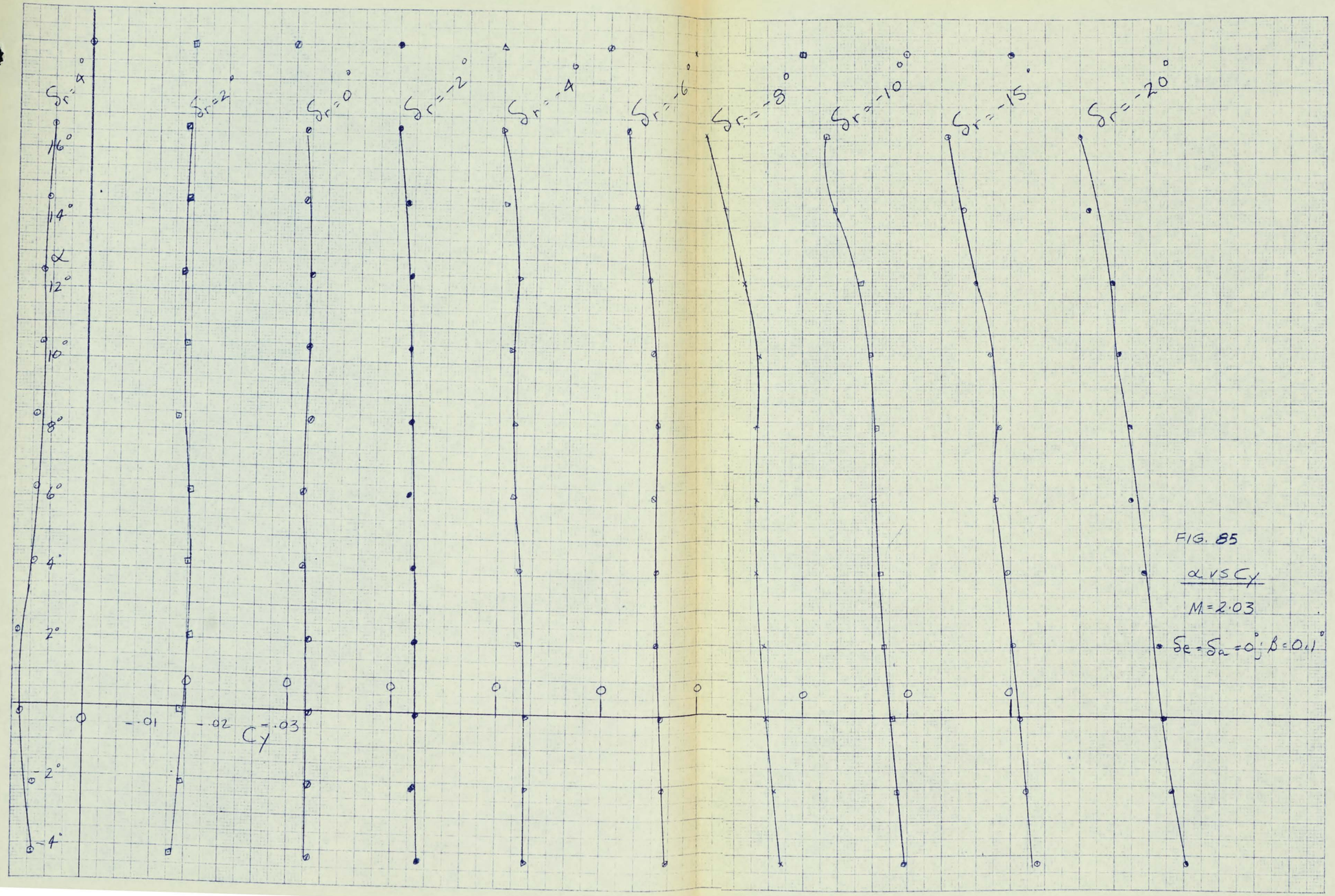

FIG. 85

α vs C_y

M = 2.03

$\delta_e = \delta_a = 0°$; $\beta = 0.1°$

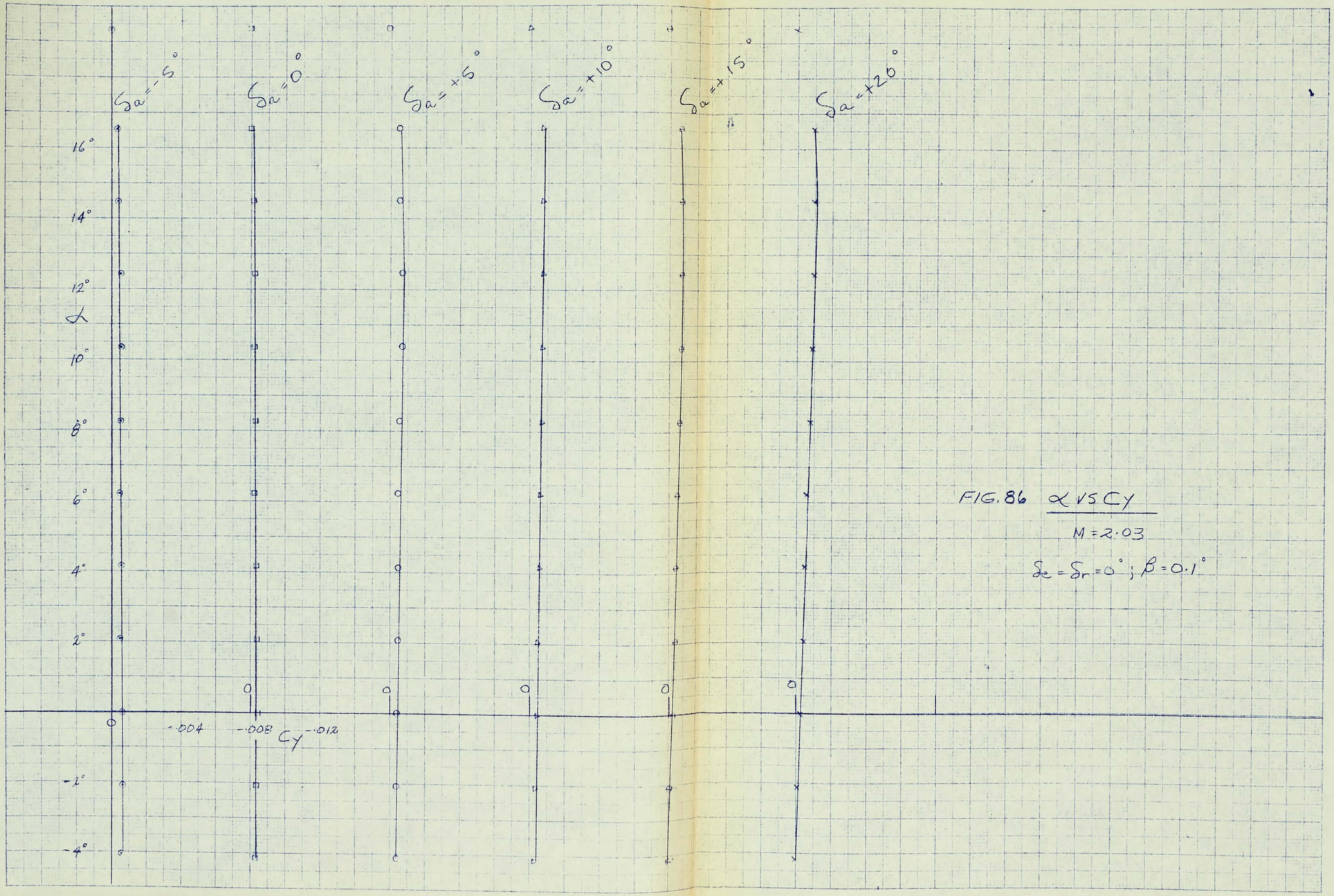

FIG. 86 α VS Cy

M = 2.03

$\delta_e = \delta_r = 0°$; $\beta = 0.1°$

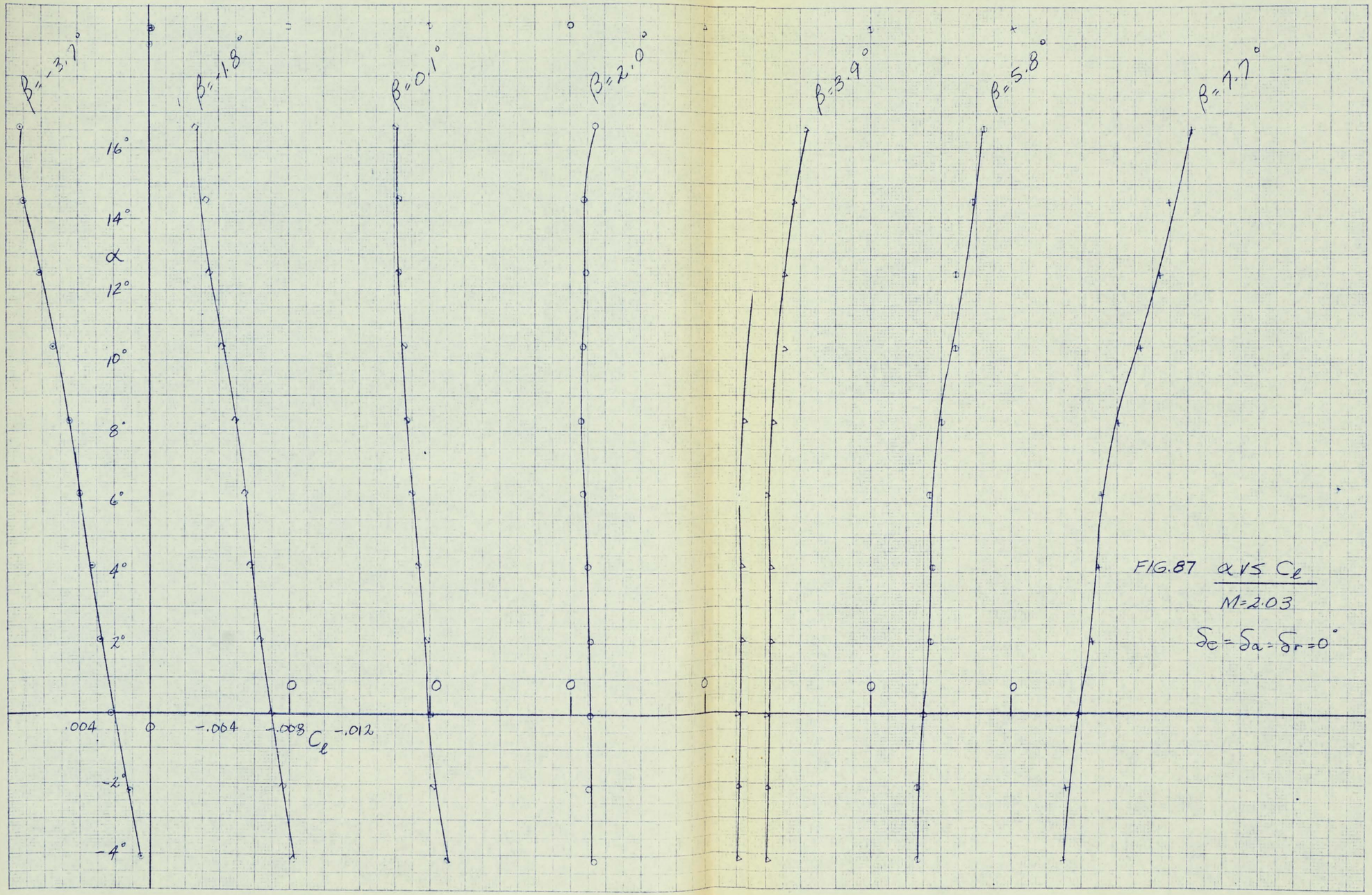

FIG. 87 α VS C_ℓ

$M = 2.03$

$\delta_e = \delta_a = \delta_r = 0°$

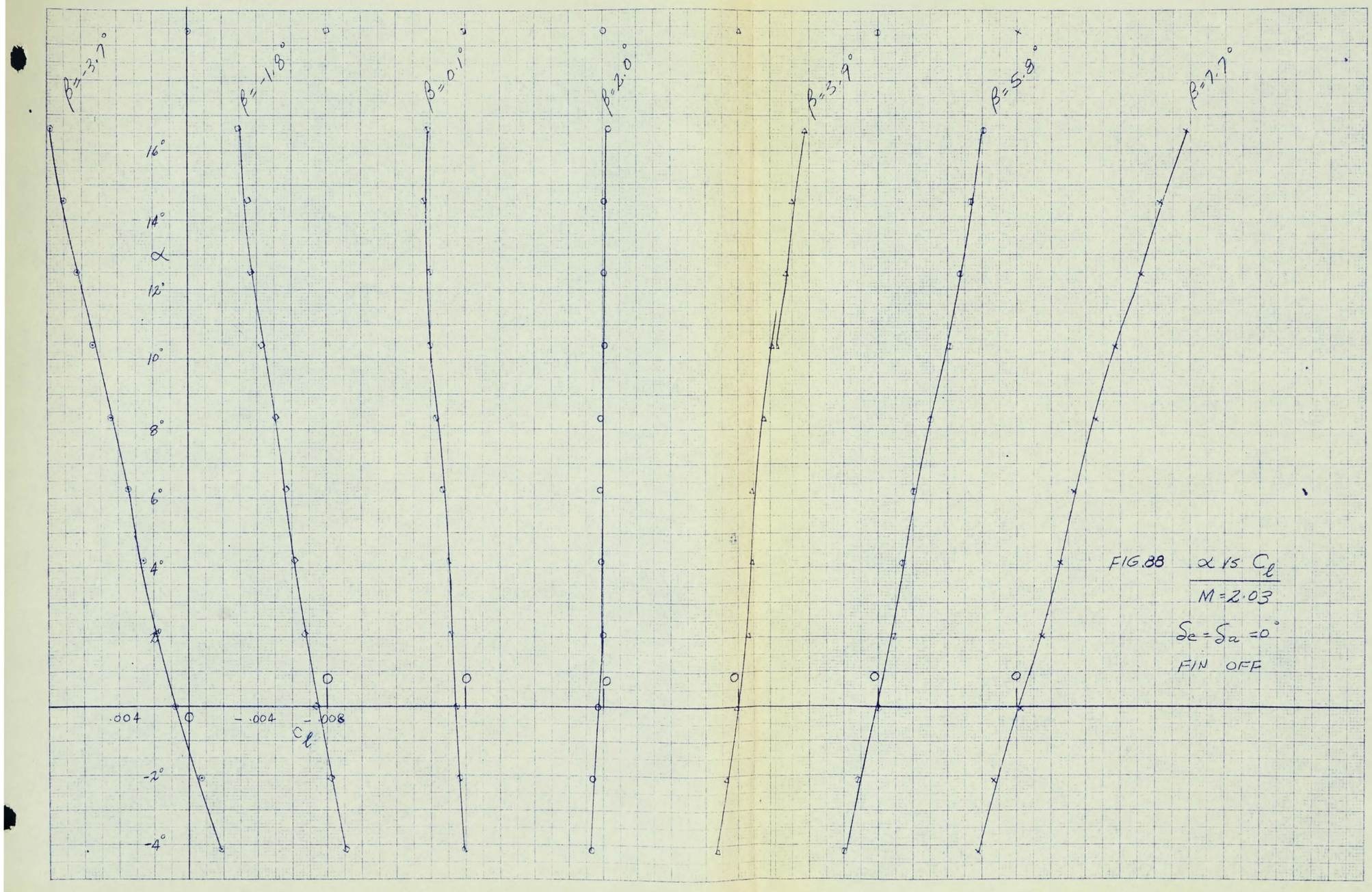

FIG.88 α vs C_l

$M = 2.03$

$\delta_e = \delta_a = 0°$

FIN OFF

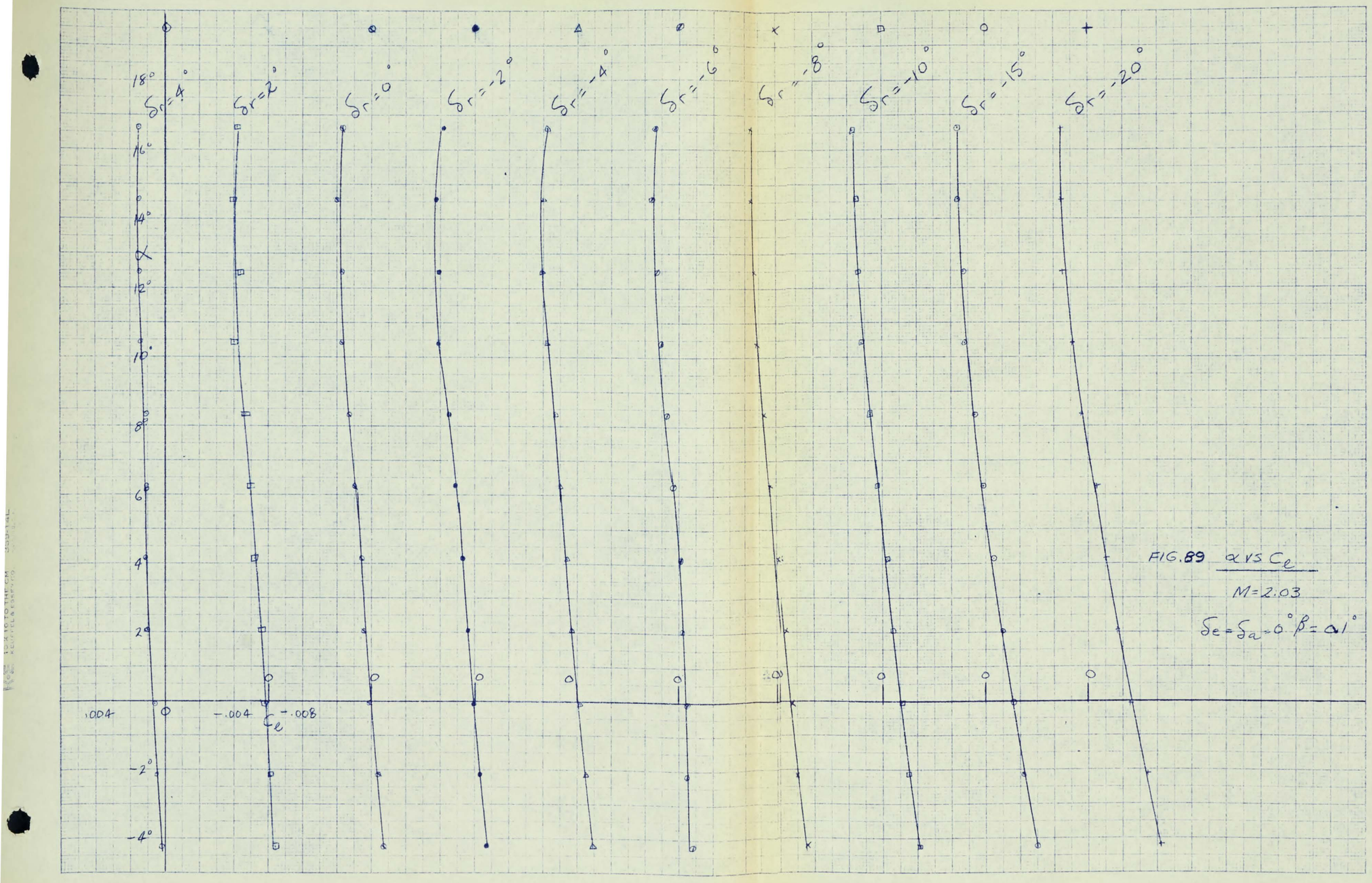

FIG. 89 α vs C_l

$M = 2.03$

$\delta_e = \delta_a = 0° \quad \beta = 0°$

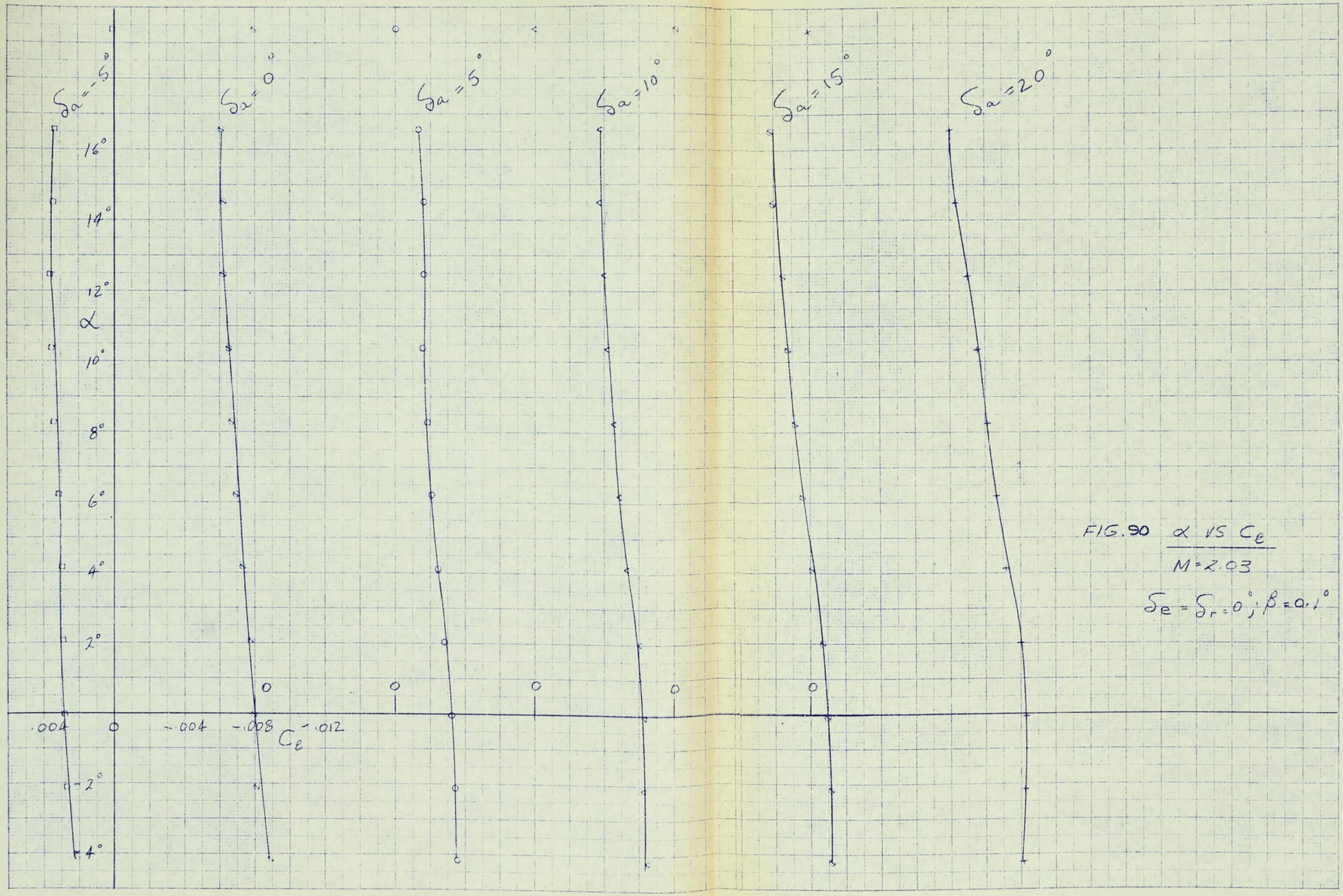

FIG. 90 α VS C_ℓ

$M = 2.03$

$\delta_e = \delta_r = 0°$; $\beta = 0.1°$

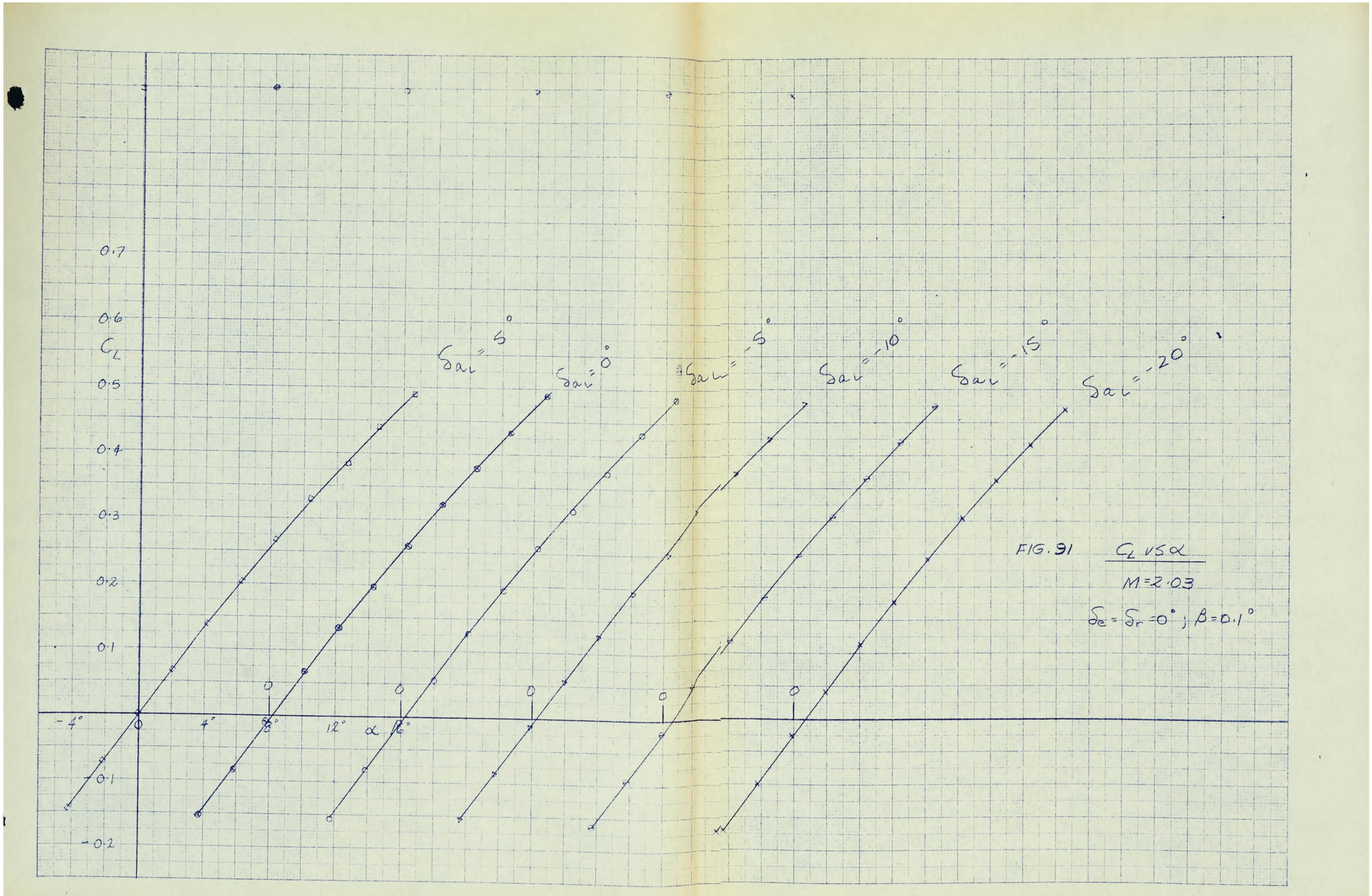

FIG. 91 C_L VS α

$M=2.03$

$\delta_e=\delta_r=0°$; $\beta=0.1°$

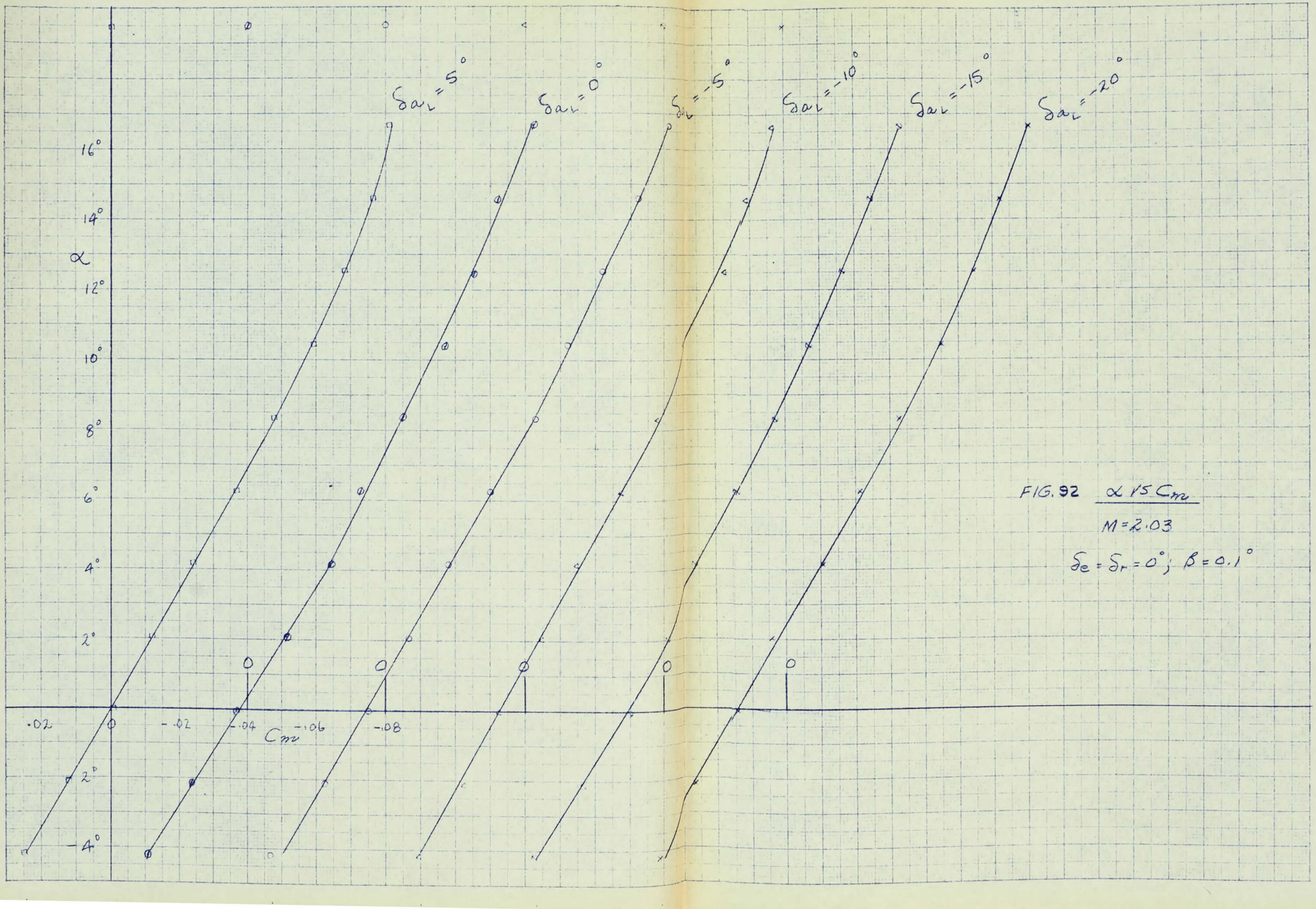

FIG. 92 α VS C_m

$M = 2.03$

$\delta_e = \delta_r = 0°$; $\beta = 0.1°$

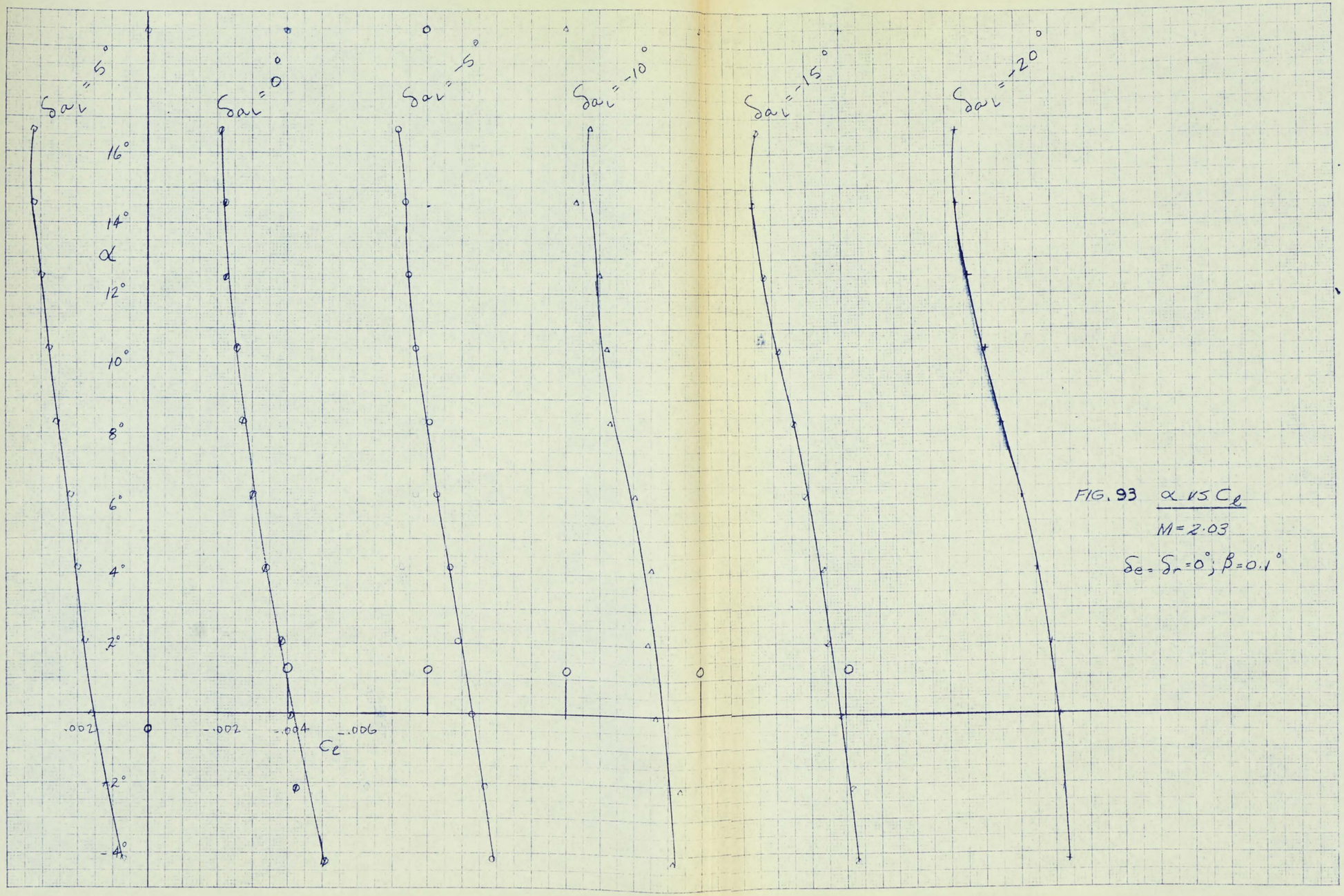

FIG. 93 α vs C_ℓ

$M = 2.03$

$\delta_e = \delta_r = 0°$; $\beta = 0.1°$

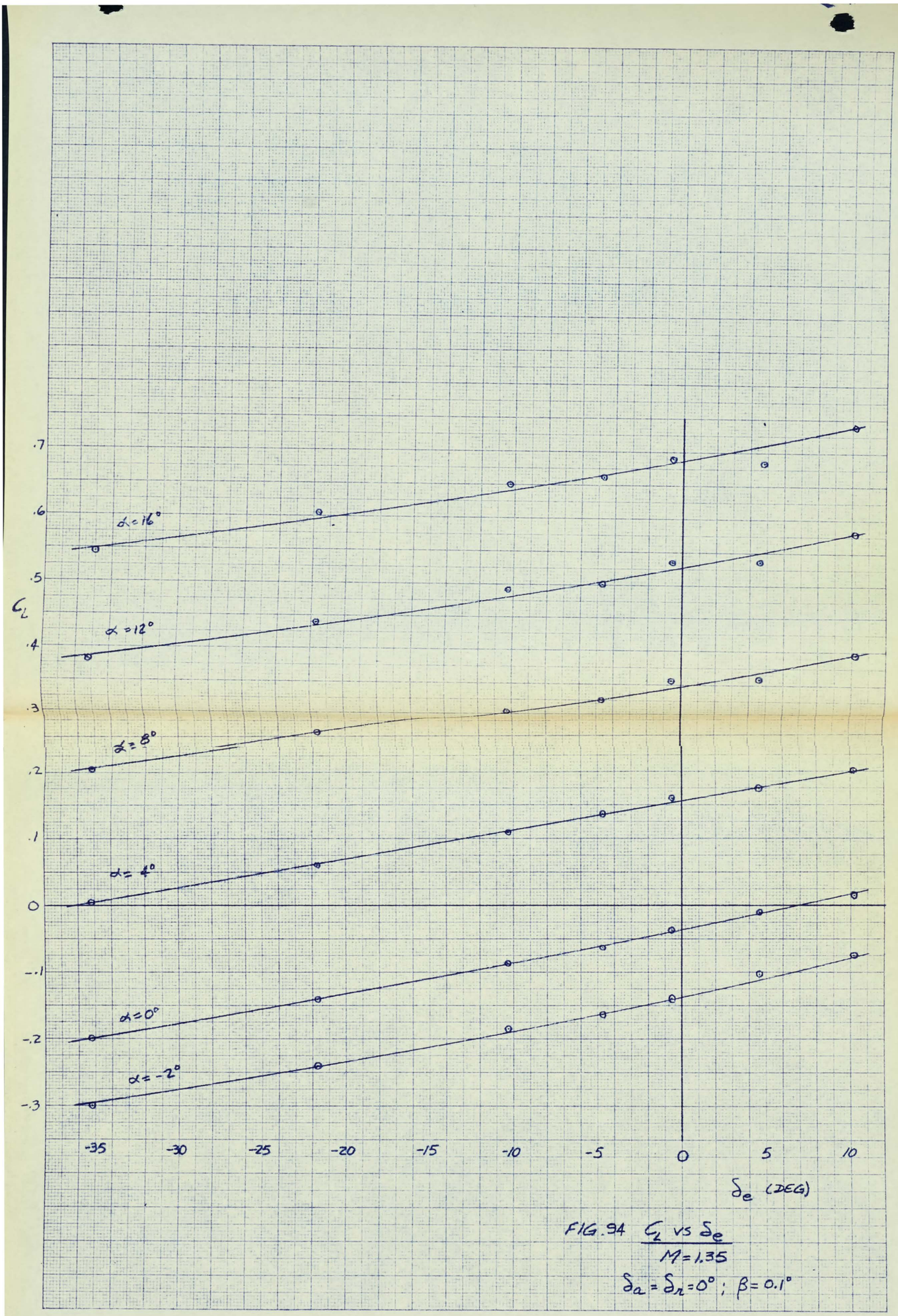

FIG. 94 C_L vs δ_e

$M = 1.35$

$\delta_a = \delta_r = 0°$; $\beta = 0.1°$

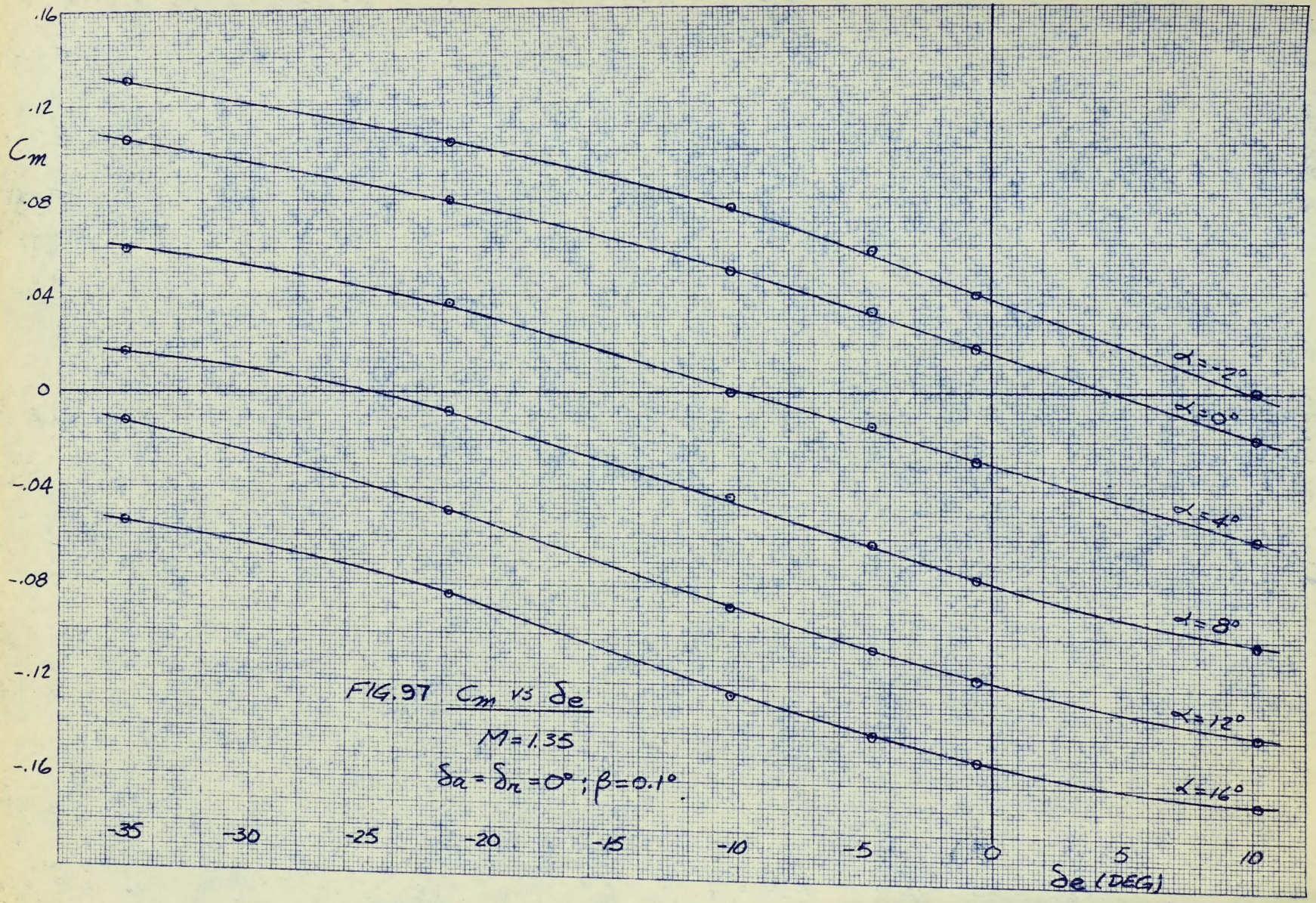

FIG. 97 C_m vs δ_e

$M = 1.35$

$\delta_a = \delta_r = 0°$; $\beta = 0.1°$

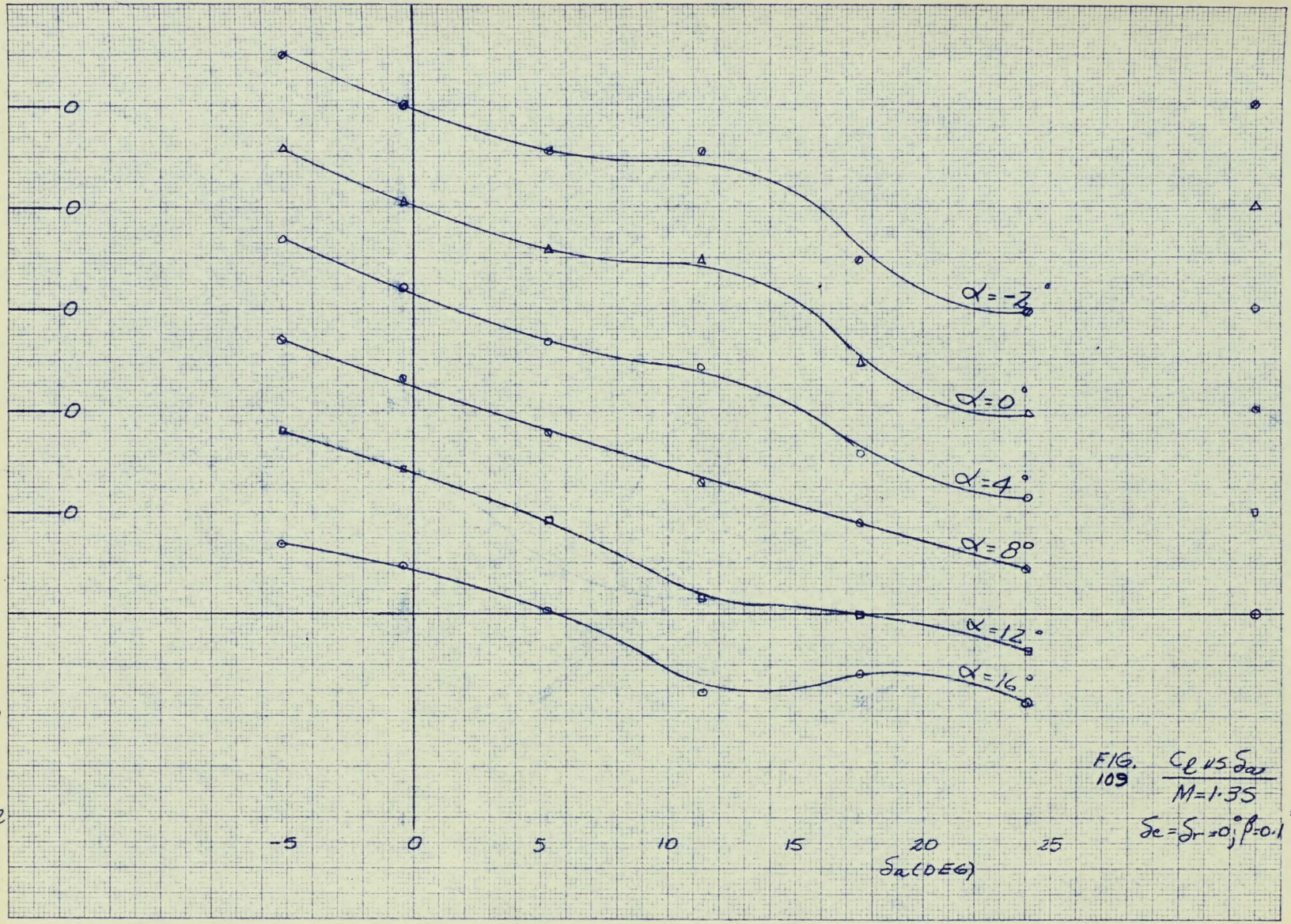

FIG. 109 C_ℓ VS. δ_a

$M = 1.35$

$\delta_e = \delta_r = 0°; \beta = 0.1°$

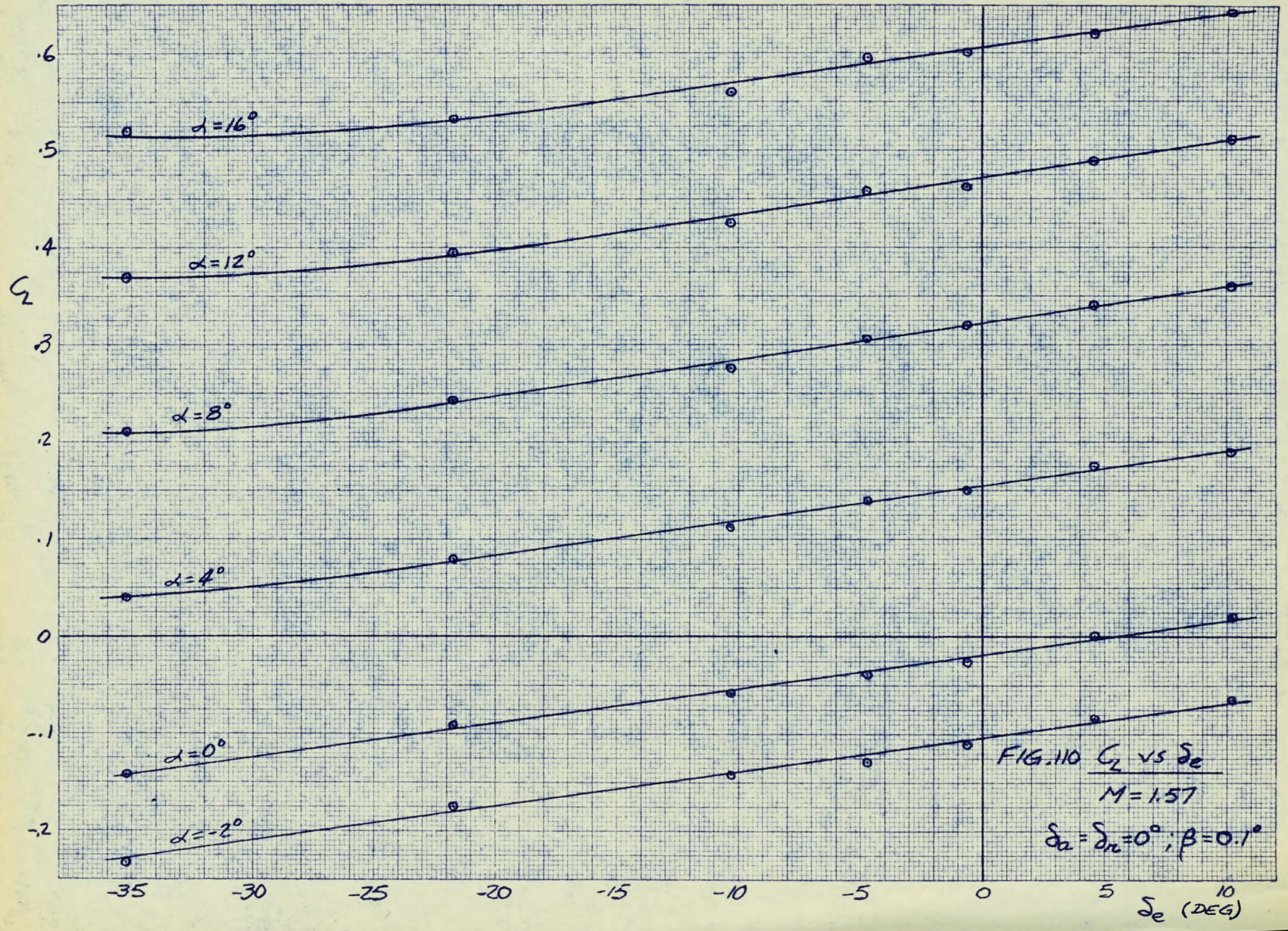

FIG. 110 C_L vs δ_e

$M = 1.57$

$\delta_a = \delta_r = 0°$; $\beta = 0.1°$

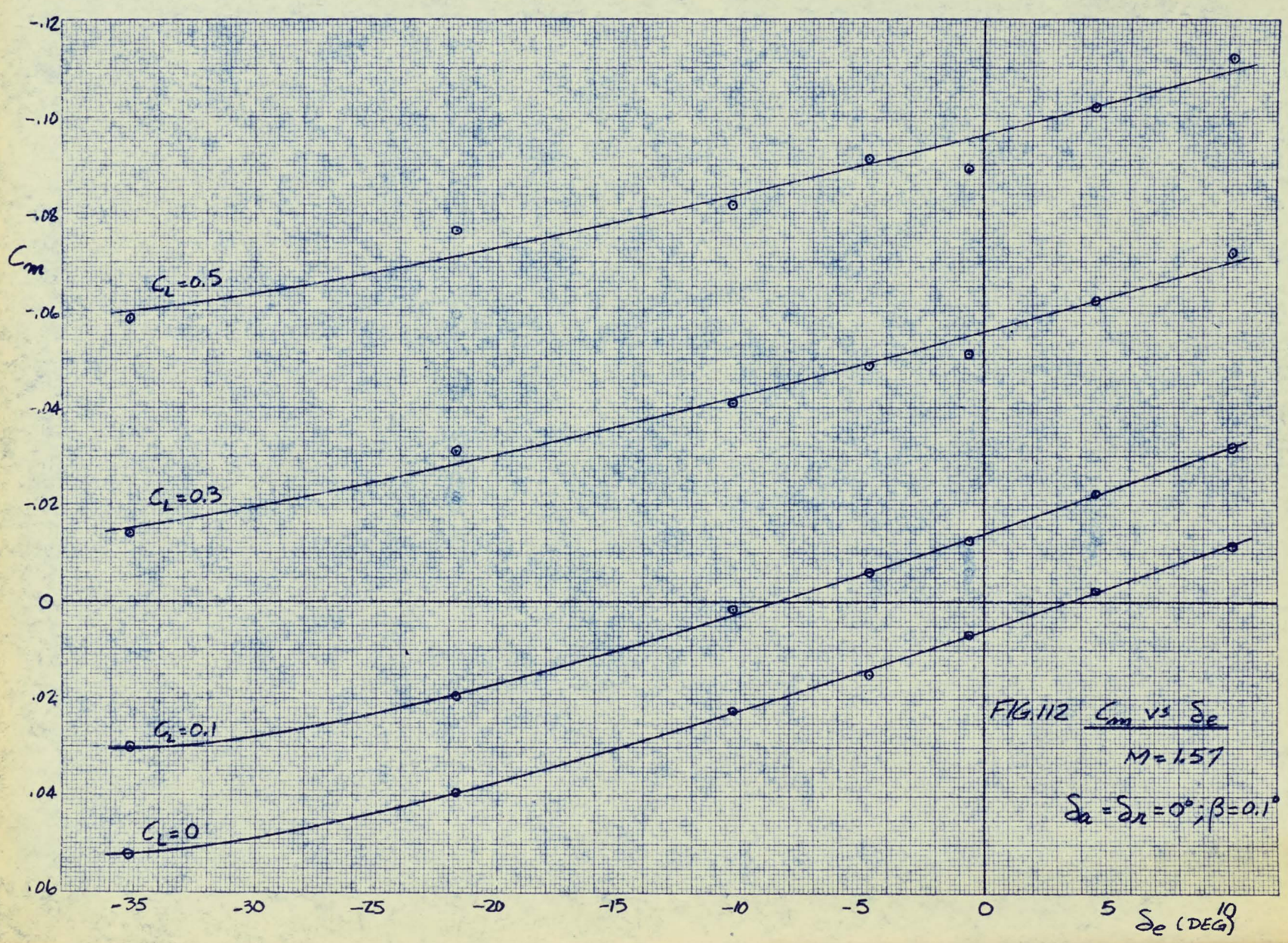

FIG. 112 C_m vs δ_e

$M = 1.57$

$\delta_a = \delta_r = 0°$; $\beta = 0.1°$

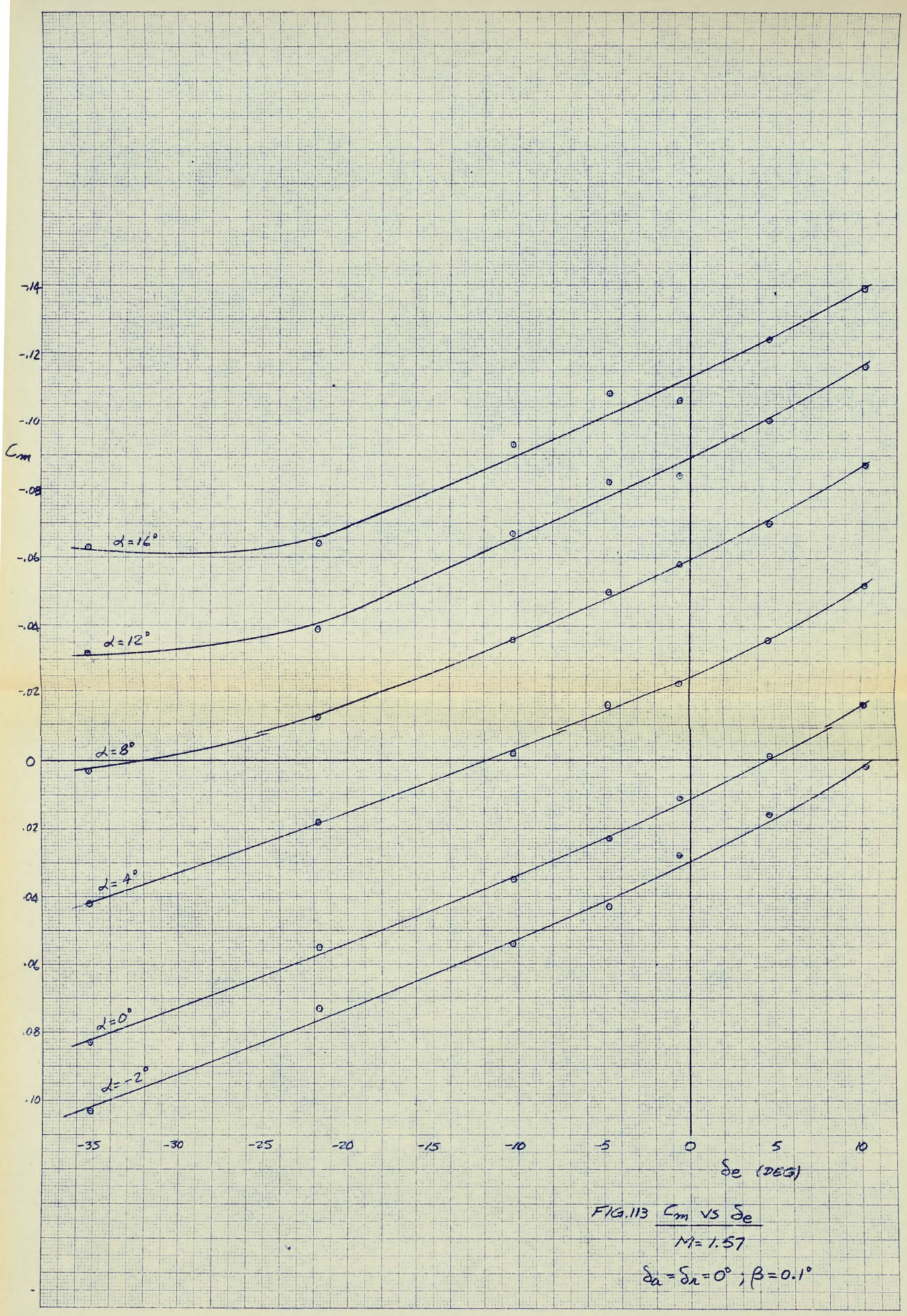

FIG. 113 C_m vs δ_e

$M = 1.57$

$\delta_a = \delta_r = 0° ; \beta = 0.1°$

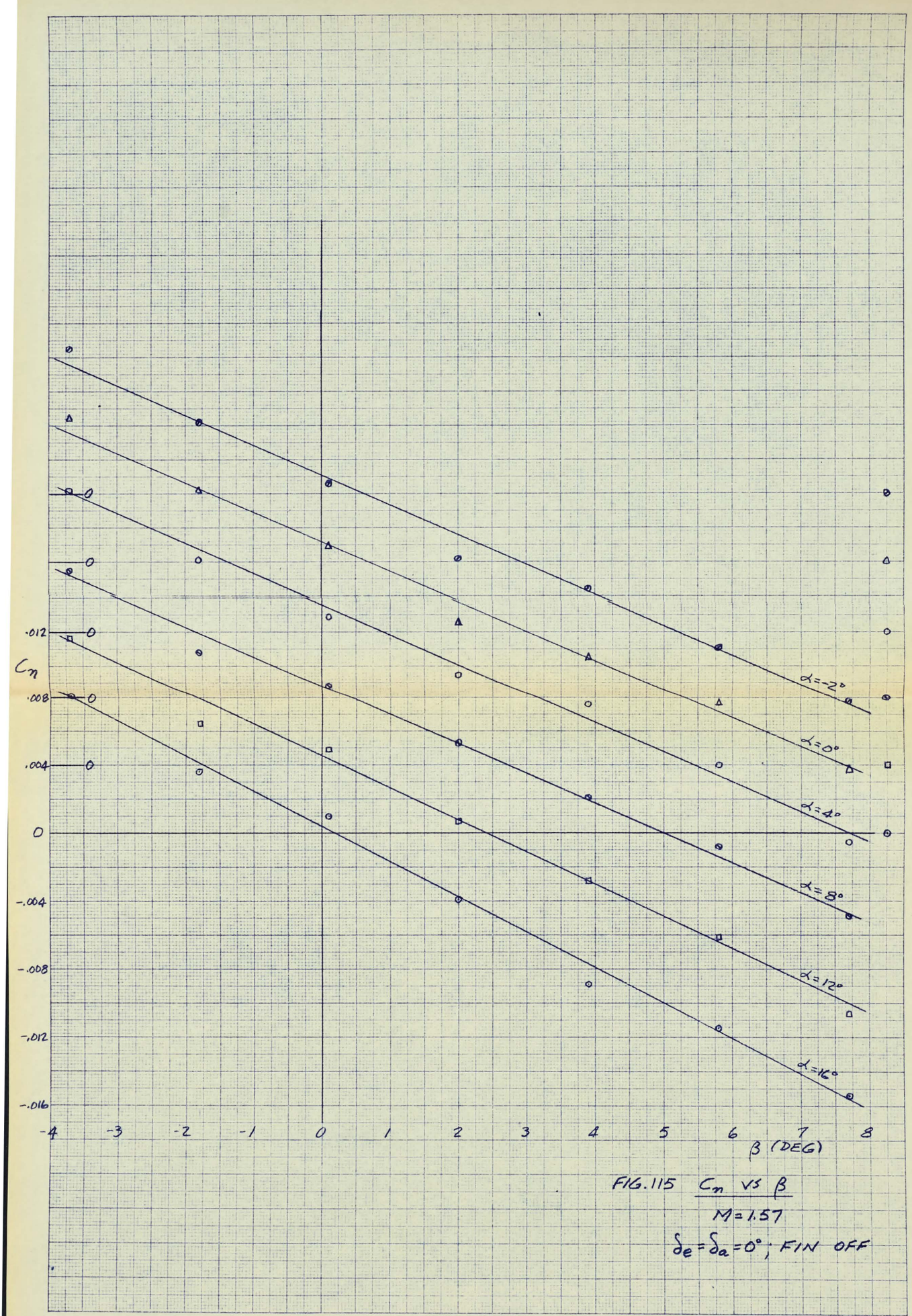

FIG. 115 C_n vs β

$M = 1.57$

$\delta_e = \delta_a = 0°$; FIN OFF

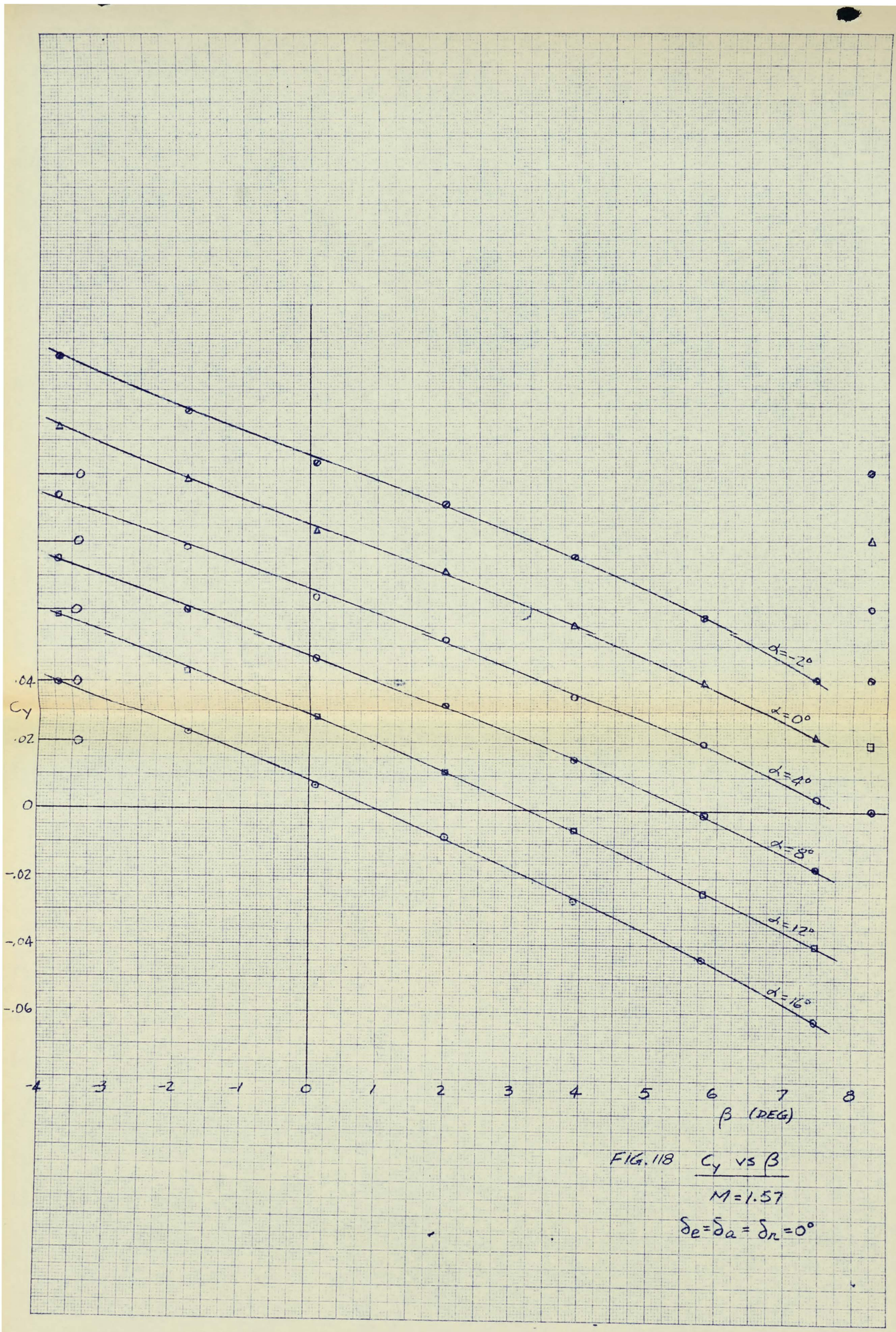

FIG. 118 C_Y vs β

$M = 1.57$

$\delta_e = \delta_a = \delta_r = 0°$

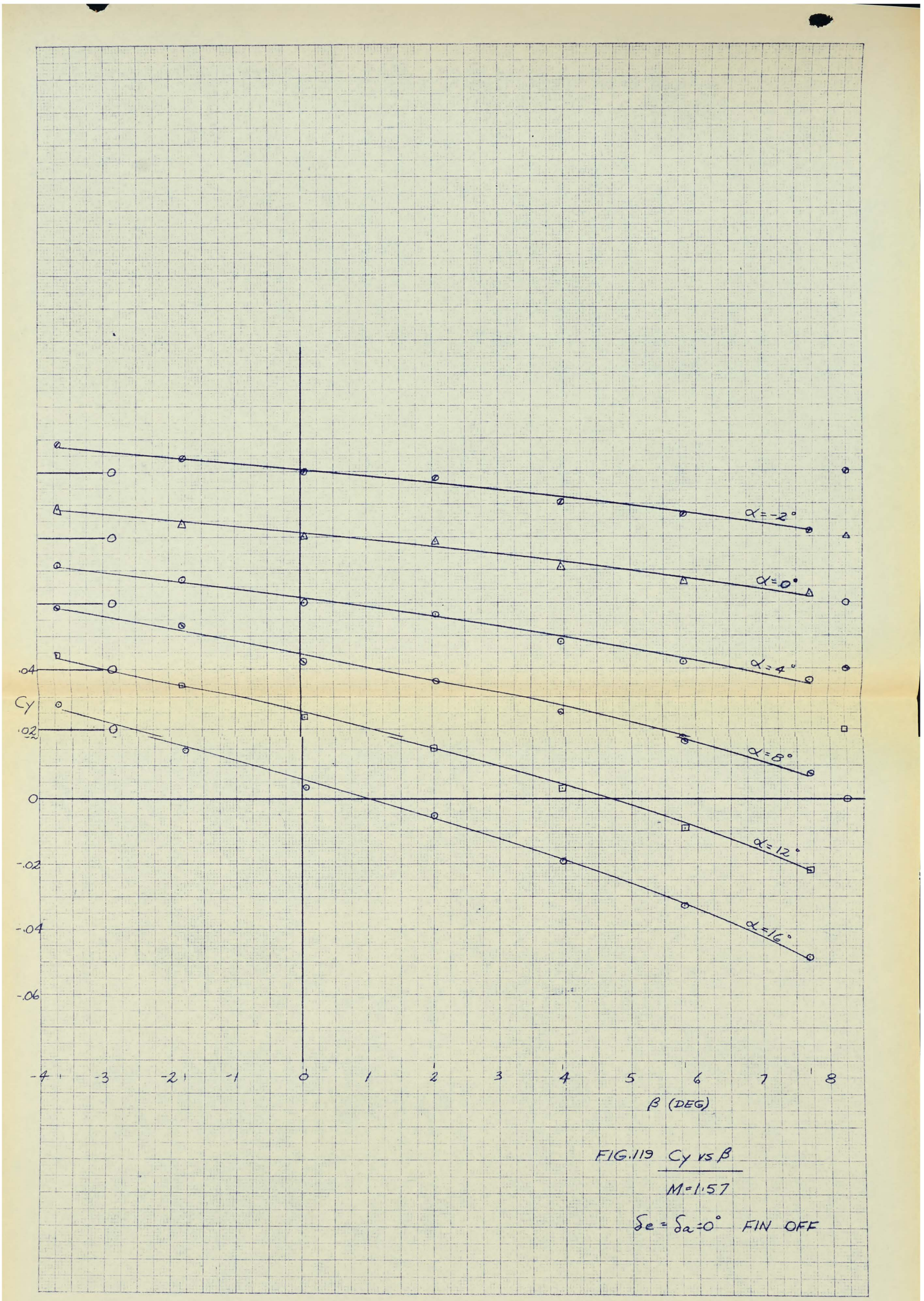

FIG.119 Cy vs β

M=1.57

δe = δa = 0° FIN OFF

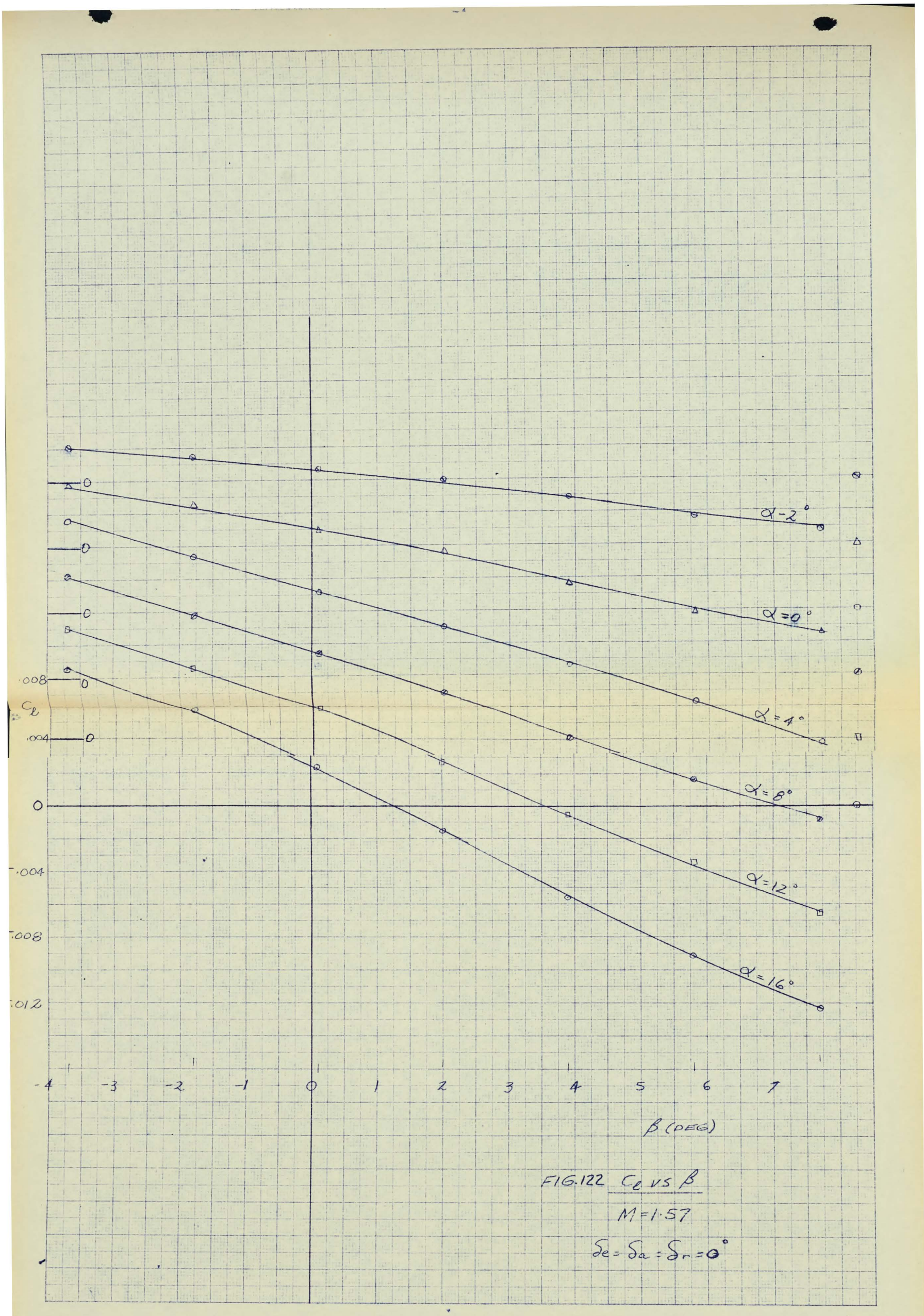

FIG. 122 C_ℓ vs β

$M = 1.57$

$\delta_e = \delta_a = \delta_r = 0°$

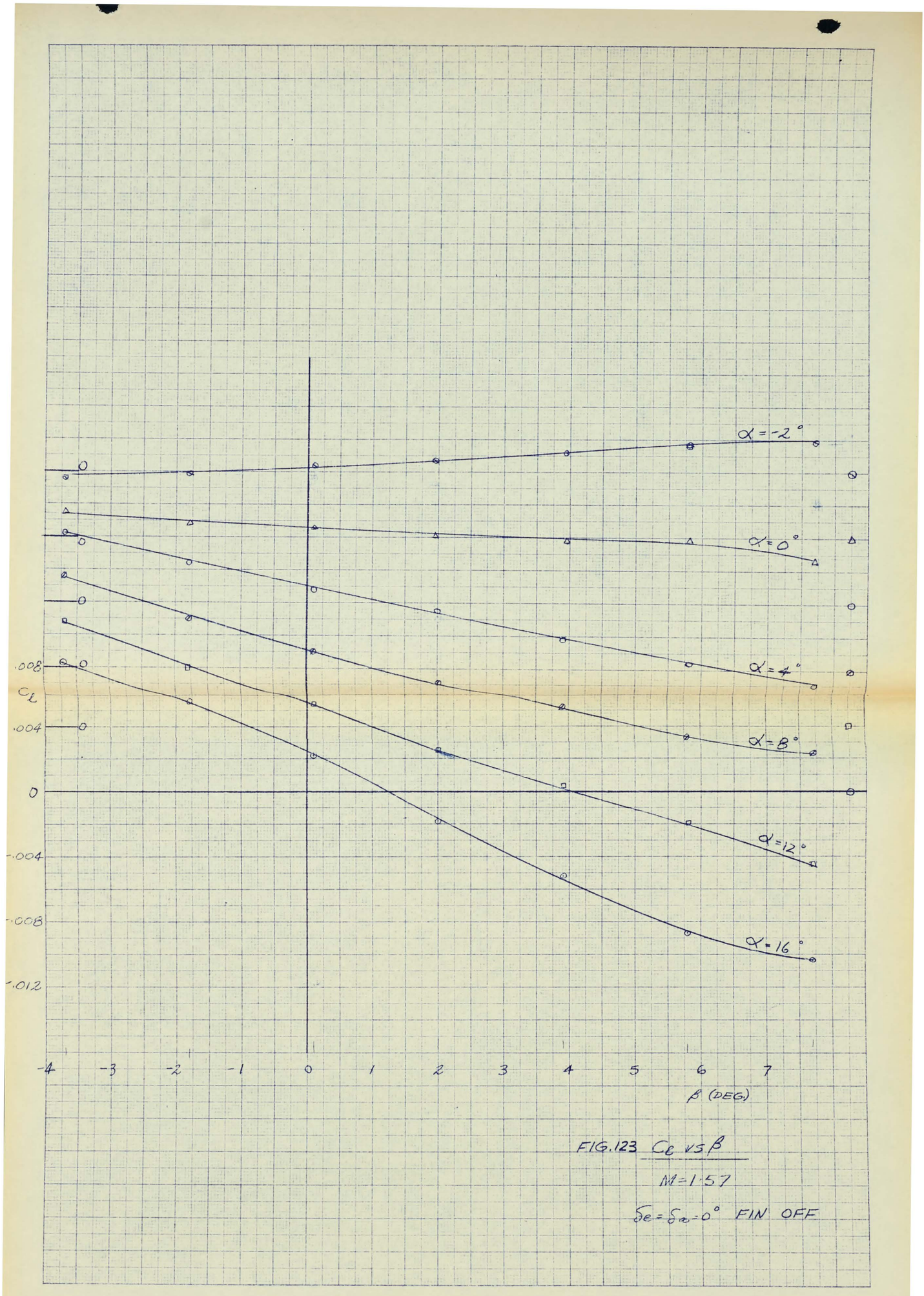

FIG. 123 C_ℓ VS β

$M = 1.57$

$\delta_e = \delta_a = 0°$ FIN OFF

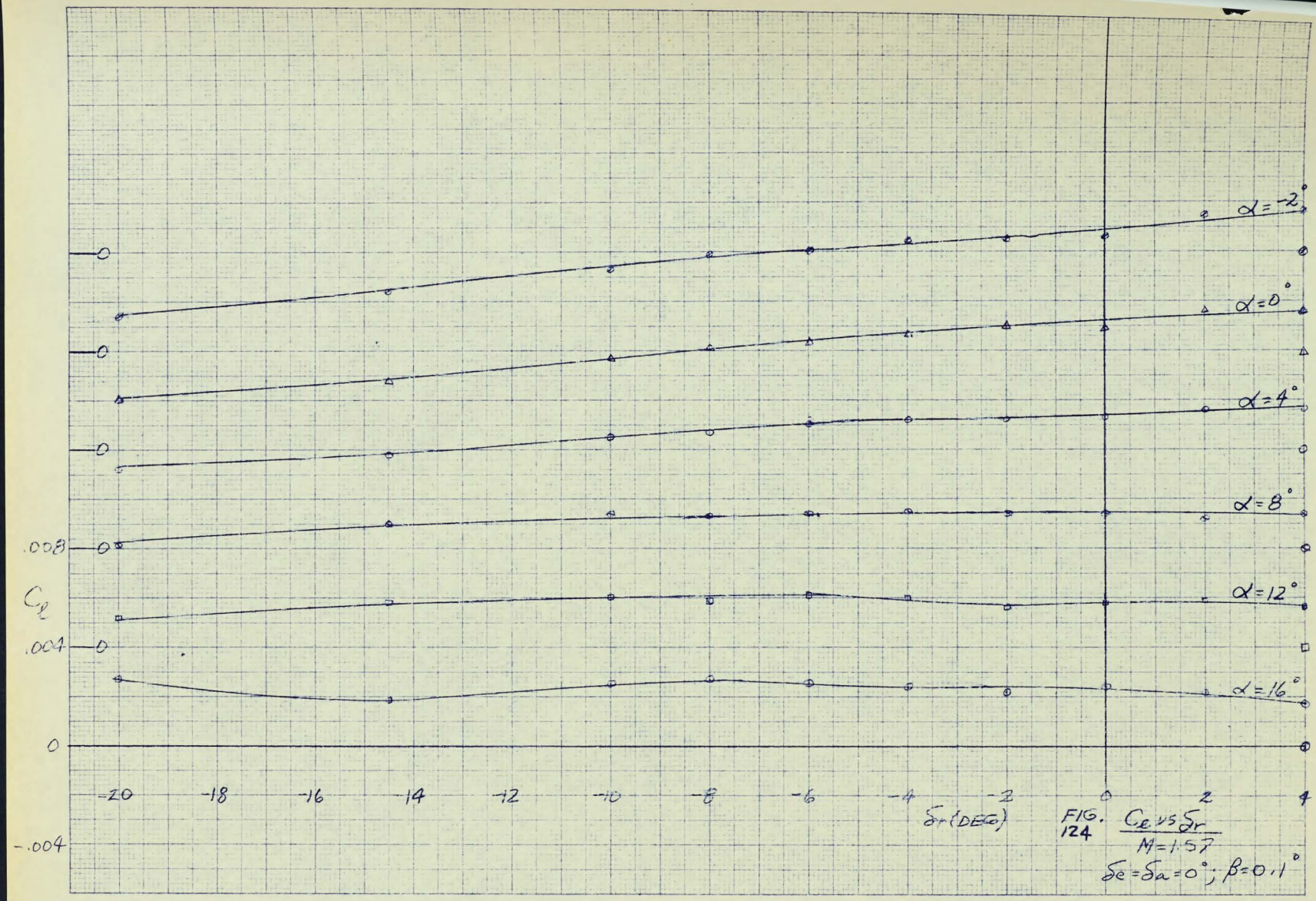

FIG. 124 C_ℓ vs δ_r
M = 1.57
$\delta_e = \delta_a = 0°$; $\beta = 0.1°$

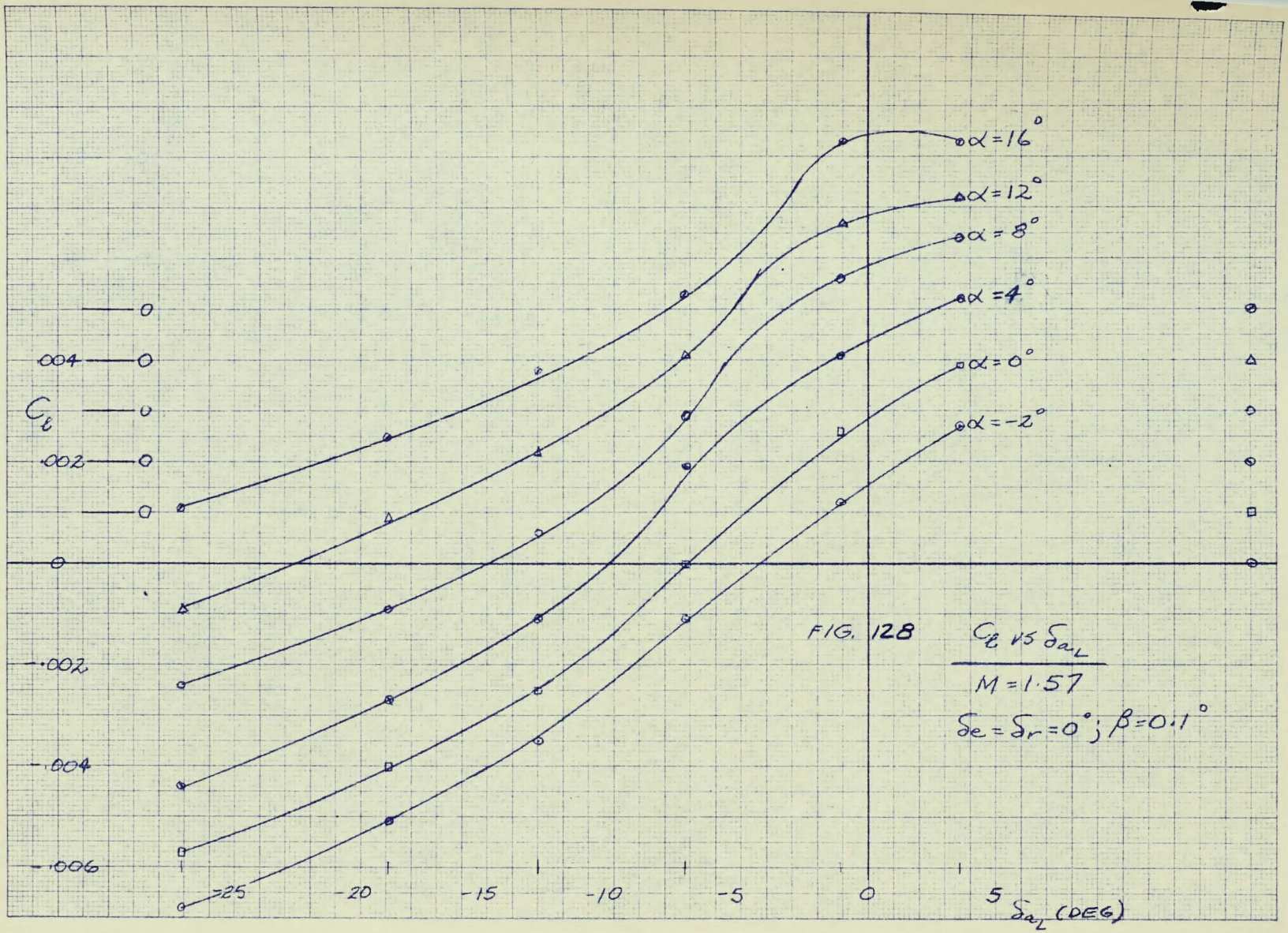

FIG. 128 C_ℓ vs δ_{a_L}

$M = 1.57$

$\delta_e = \delta_r = 0°$; $\beta = 0.1°$

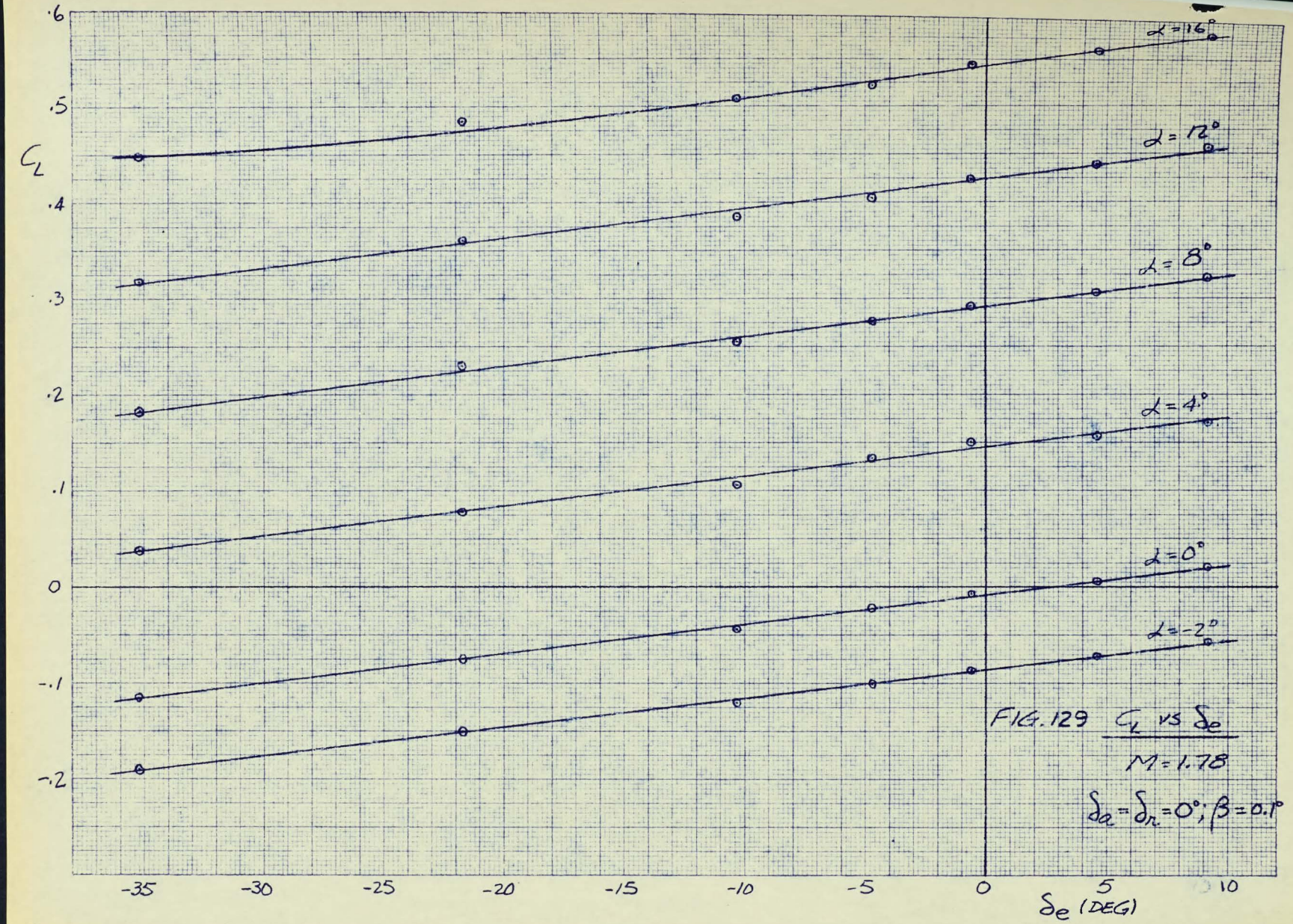

FIG. 129 C_L VS δ_e

$M = 1.78$

$\delta_a = \delta_r = 0°; \beta = 0.1°$

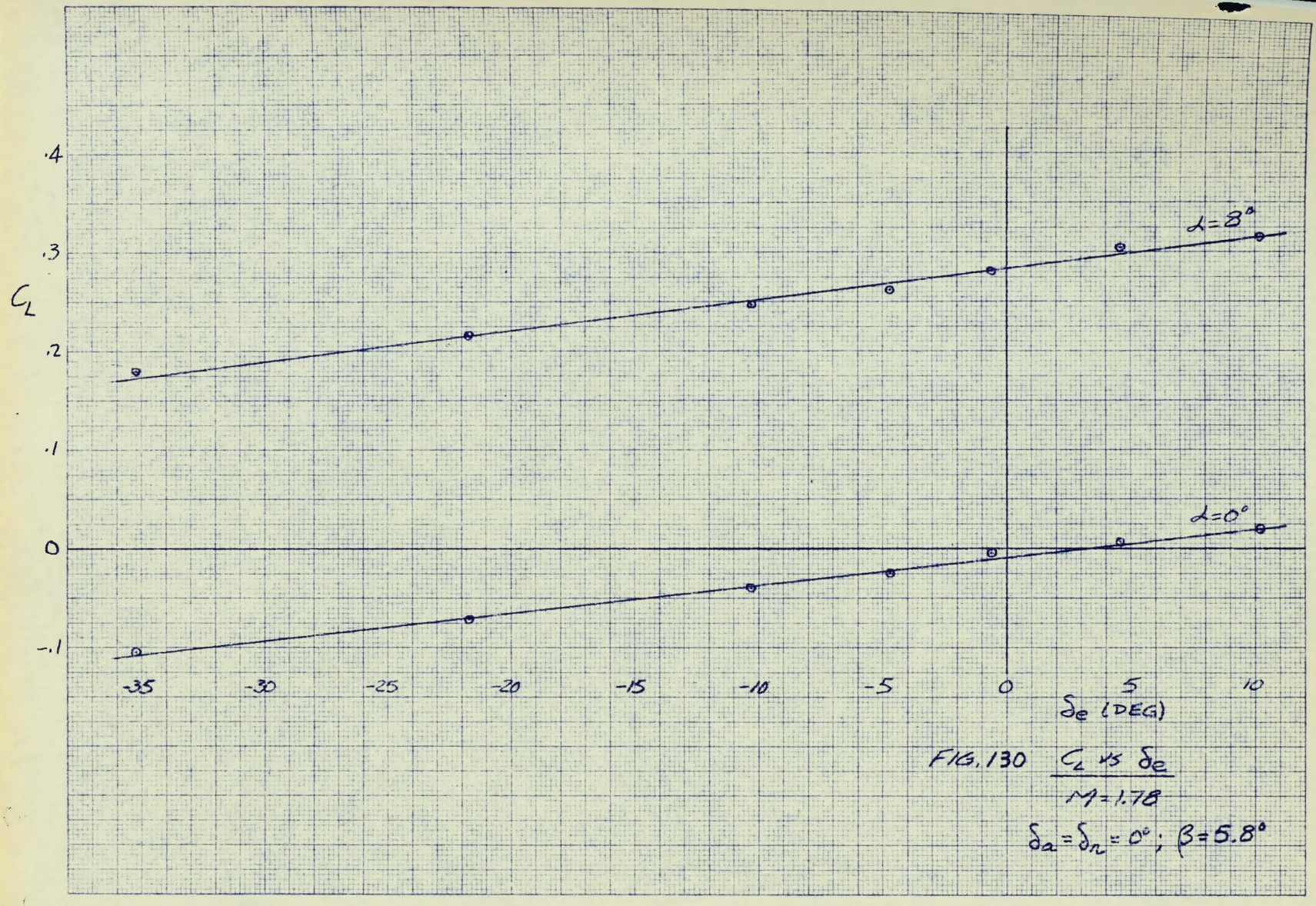

FIG. 130 C_L vs δ_e

$M = 1.78$

$\delta_a = \delta_r = 0°$; $\beta = 5.8°$

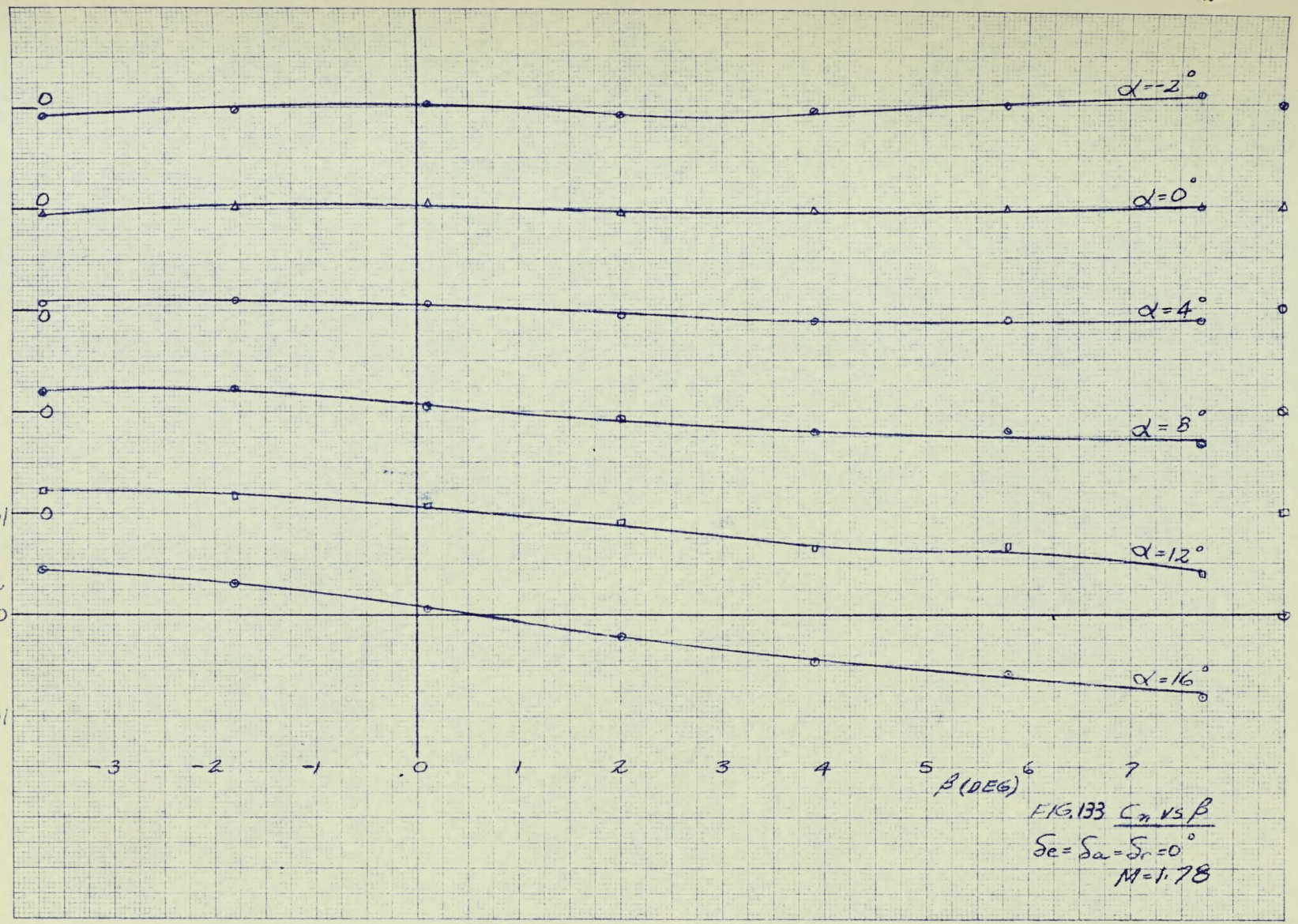

FIG. 133 C_m vs β

$\delta_e = \delta_a = \delta_r = 0°$

$M = 1.78$

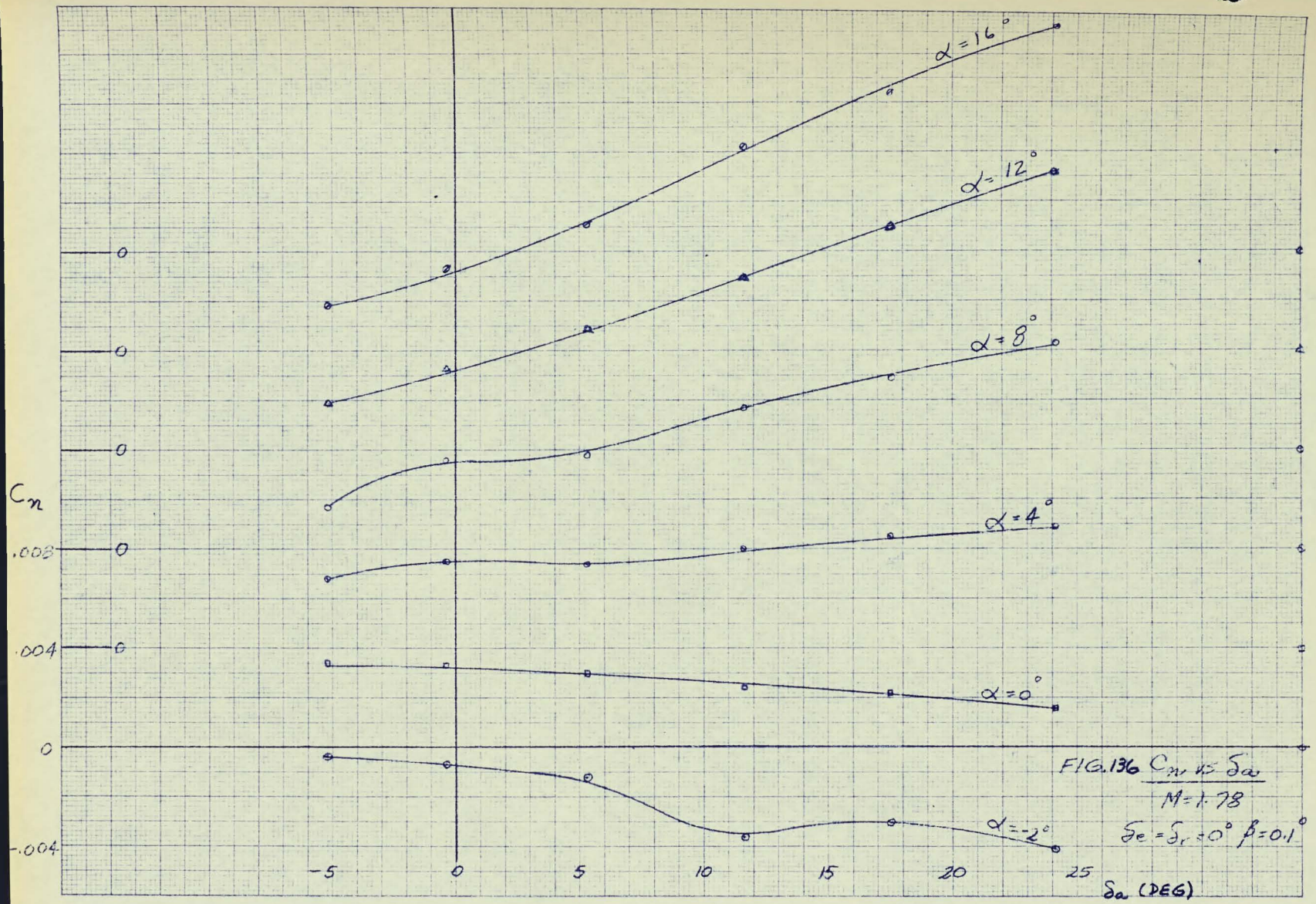

FIG. 136 C_n vs δ_a

M = 1.78

$\delta_e = \delta_r = 0°$ $\beta = 0.1°$

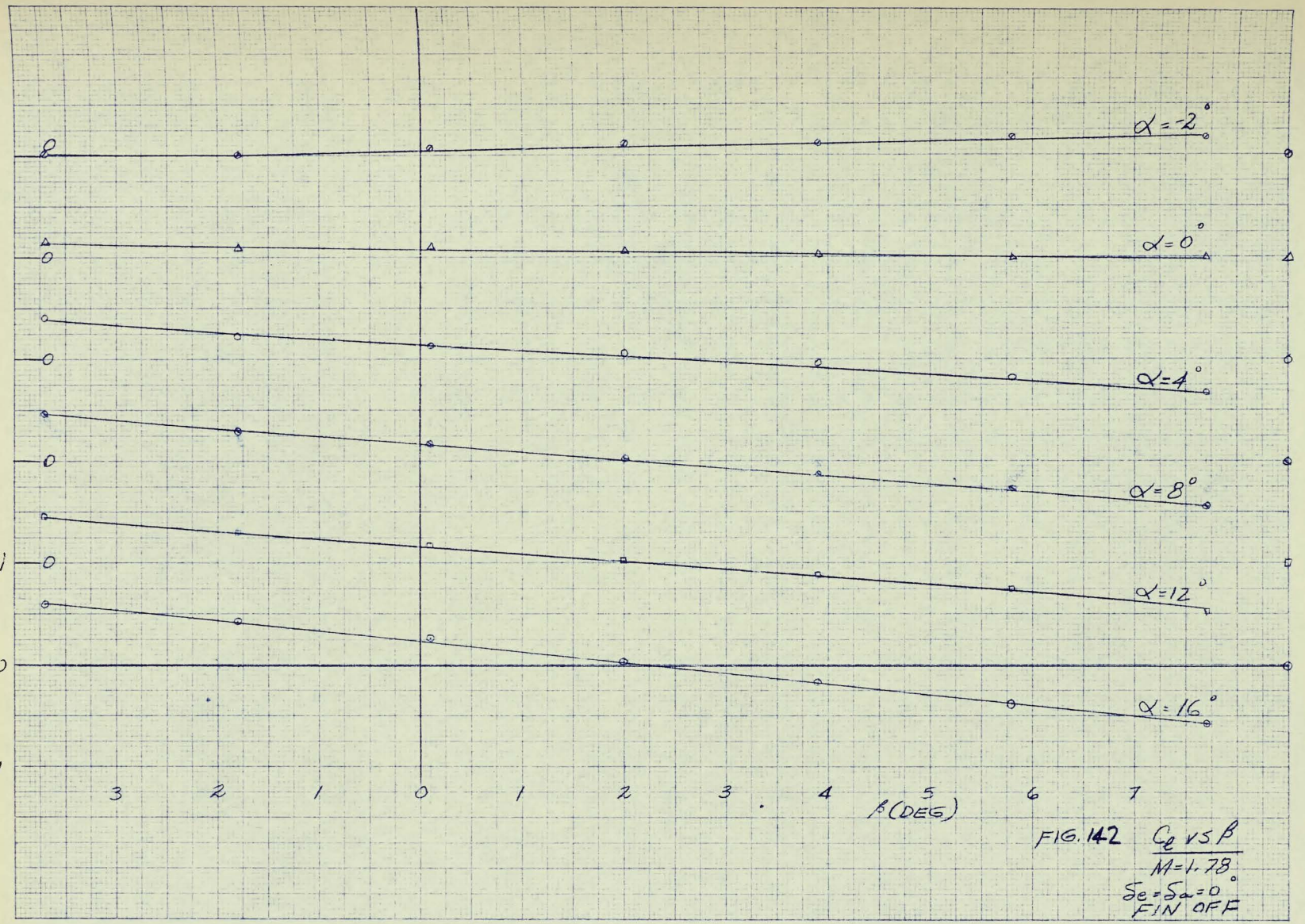

FIG. 142 C_ℓ vs β
M = 1.78°
$\delta_e = \delta_a = 0$
FIN OFF

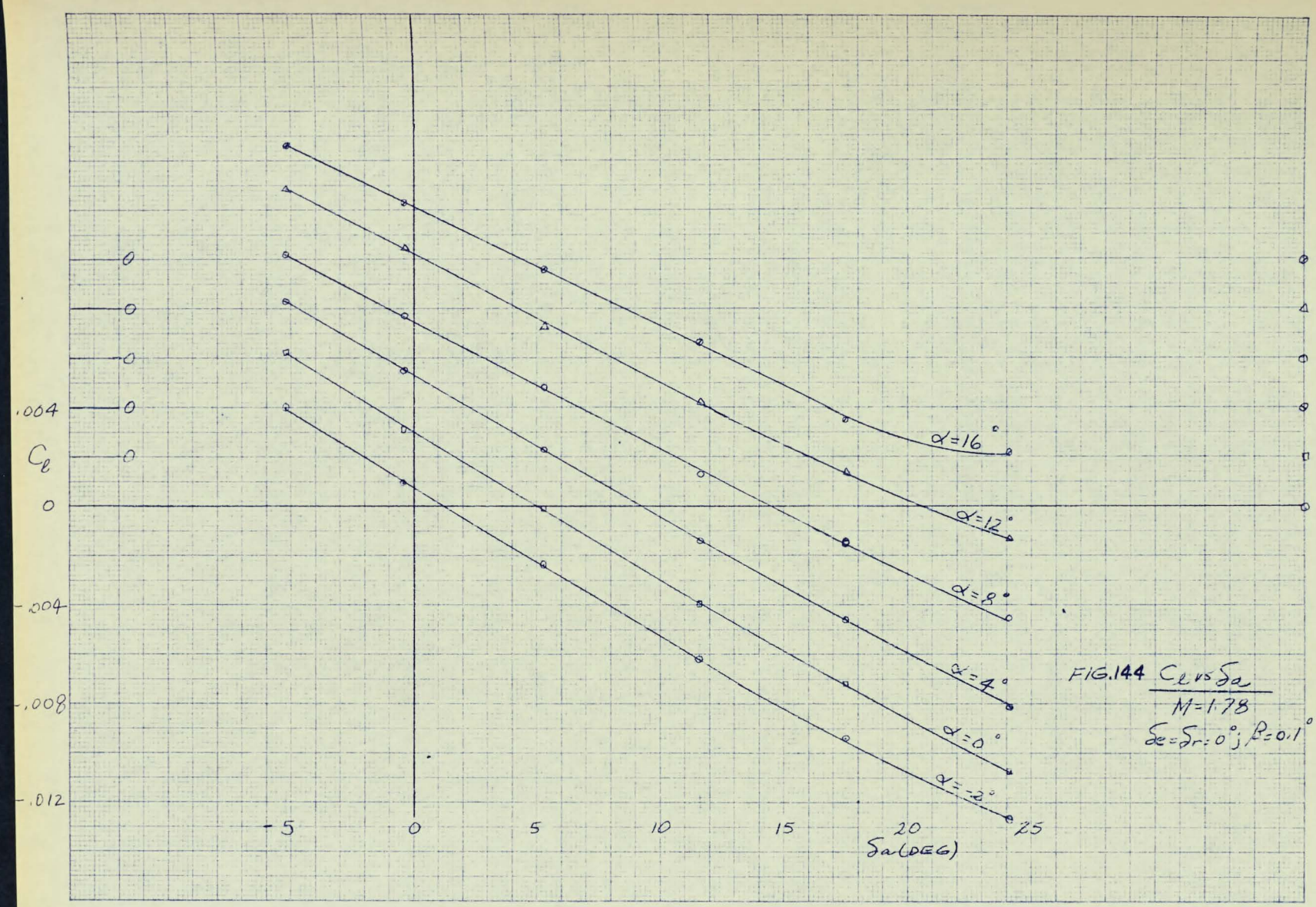

FIG.144 C_ℓ vs δ_a

M=1.78

$\delta_e=\delta_r=0°$; $\beta=0.1°$

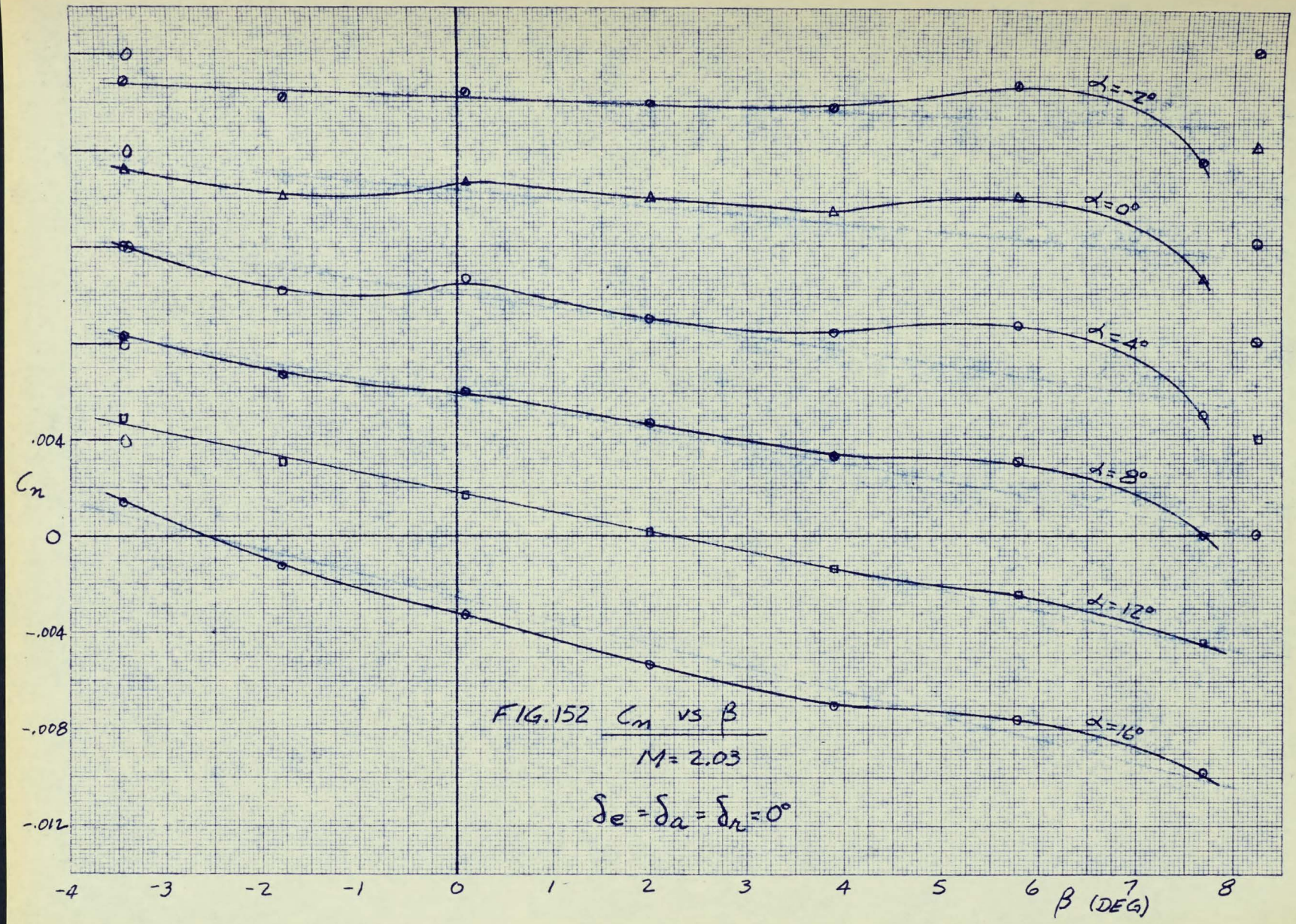

FIG. 152 C_n vs β

$M = 2.03$

$\delta_e = \delta_a = \delta_r = 0°$

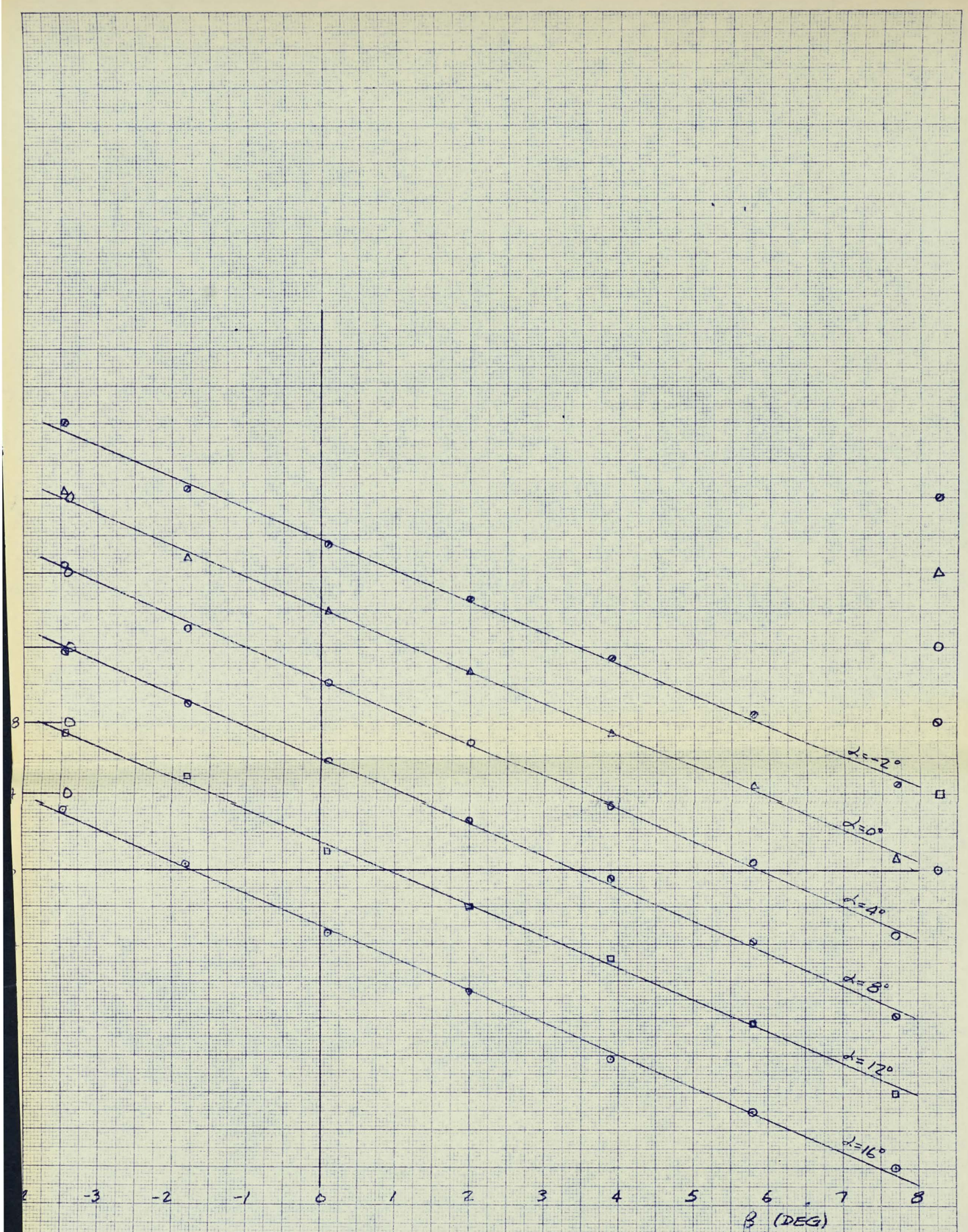

FIG. 153 C_m vs β

$M = 2.03$

$\delta_e = \delta_a = 0°$; FIN OFF

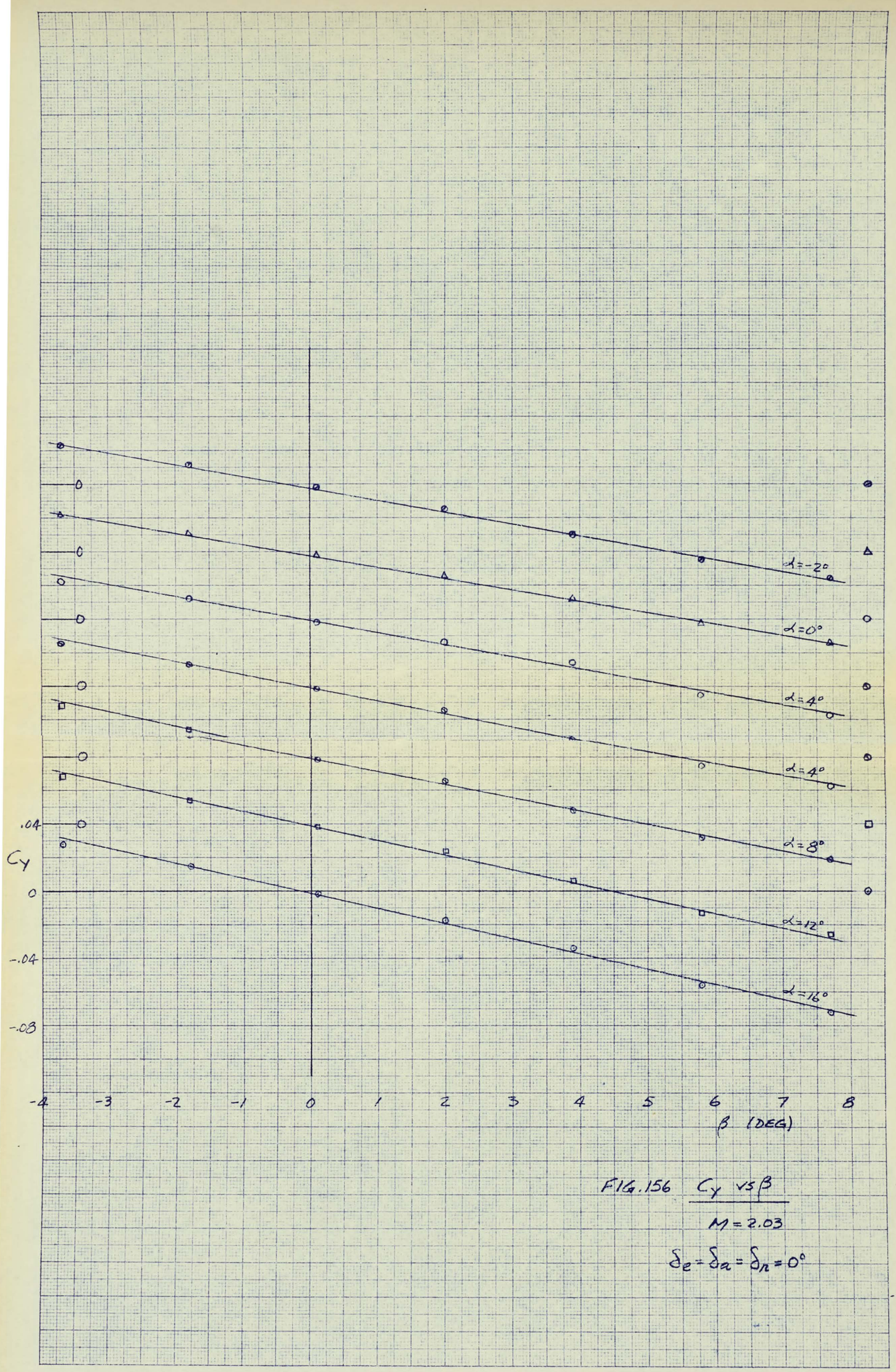

FIG. 156 C_y vs β

$M = 2.03$

$\delta_e = \delta_a = \delta_r = 0°$

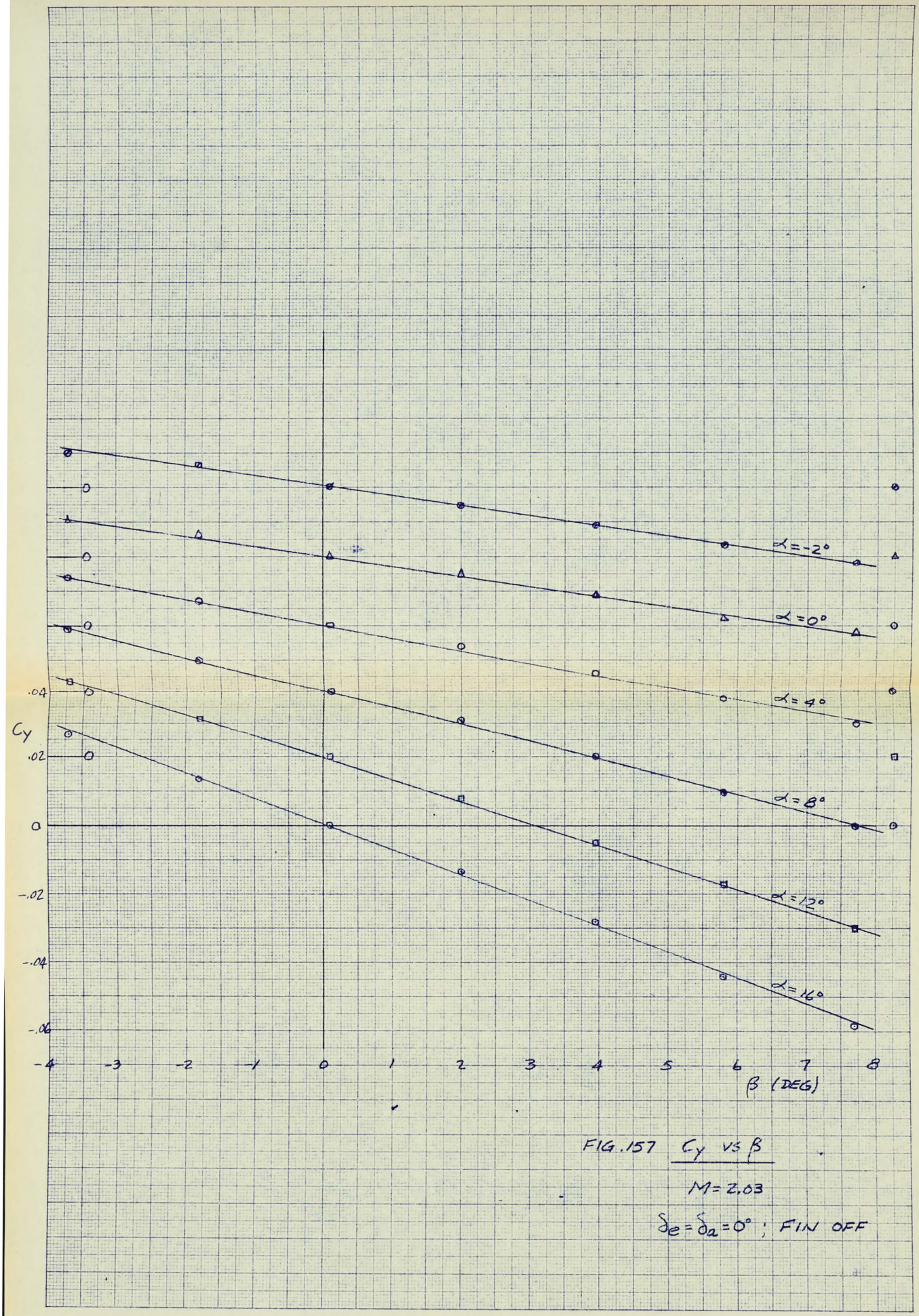

FIG. 157 C_y vs β

$M = 2.03$

$\delta_e = \delta_a = 0°$; FIN OFF

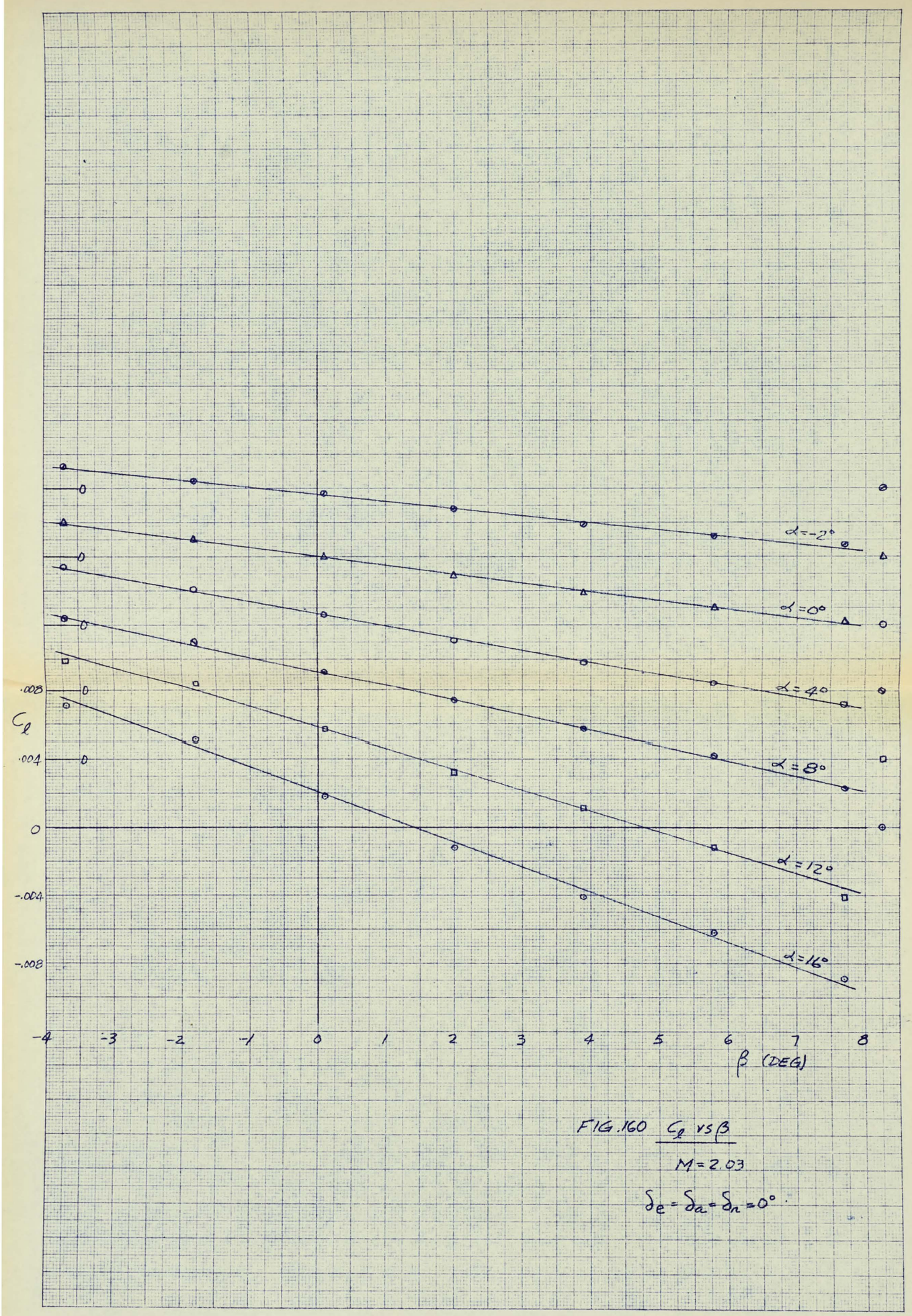

FIG. 160 C_l vs β

$M = 2.03$

$\delta_e = \delta_a = \delta_r = 0°$

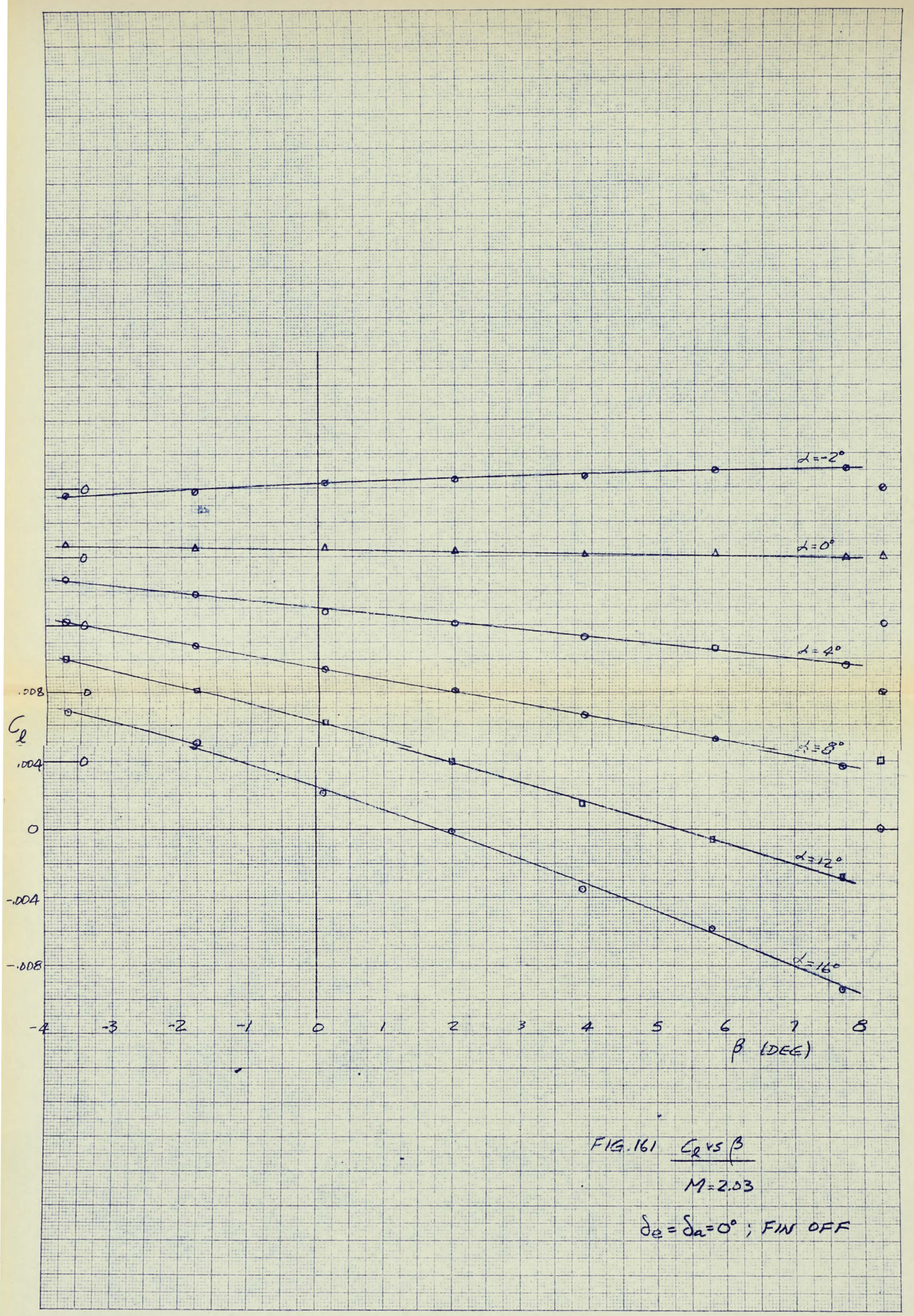

FIG. 161 C_l vs β

$M = 2.03$

$\delta_e = \delta_a = 0°$; FIN OFF

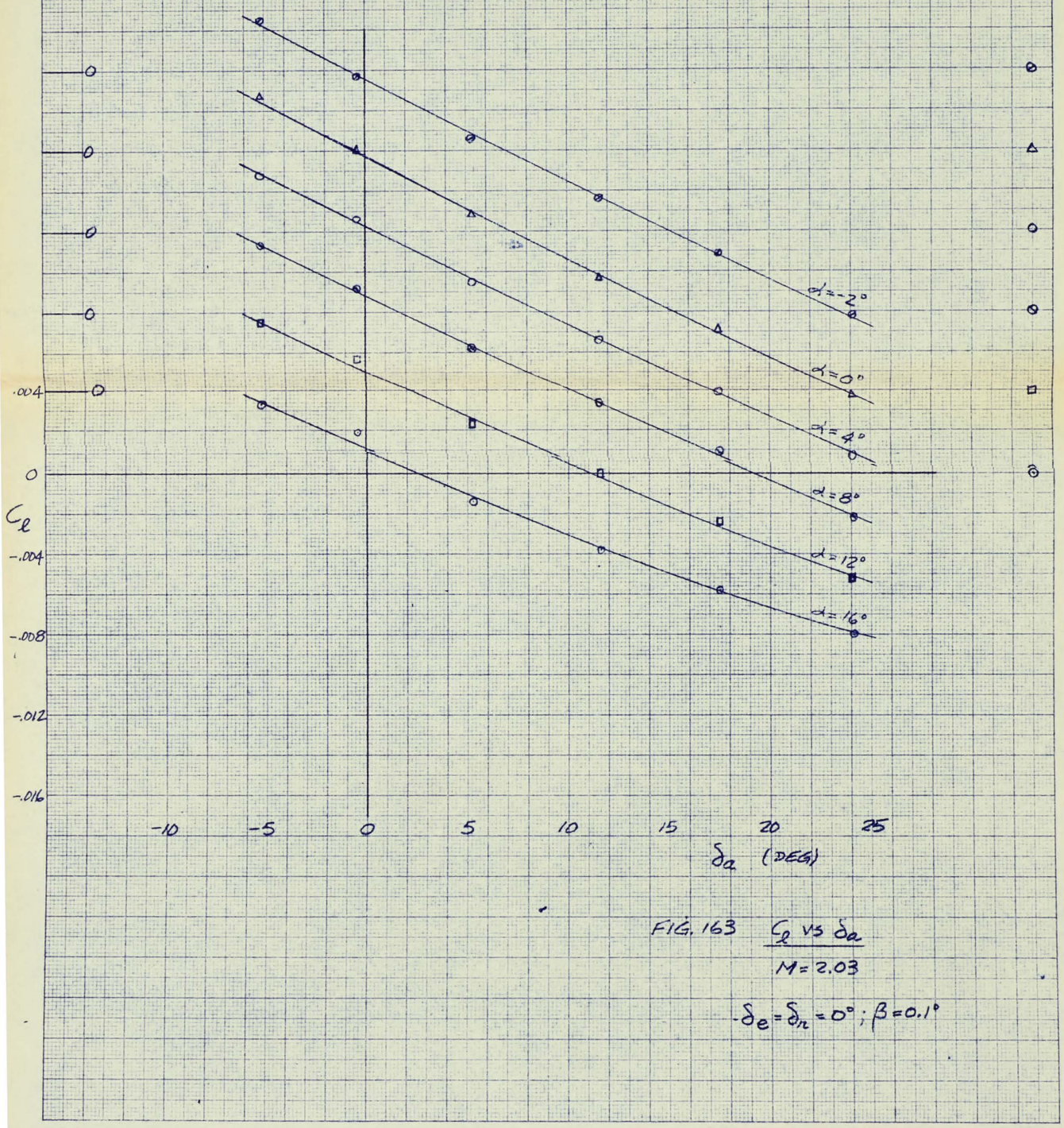

FIG. 163 C_ℓ VS δ_a

$M = 2.03$

$\delta_e = \delta_r = 0°$; $\beta = 0.1°$

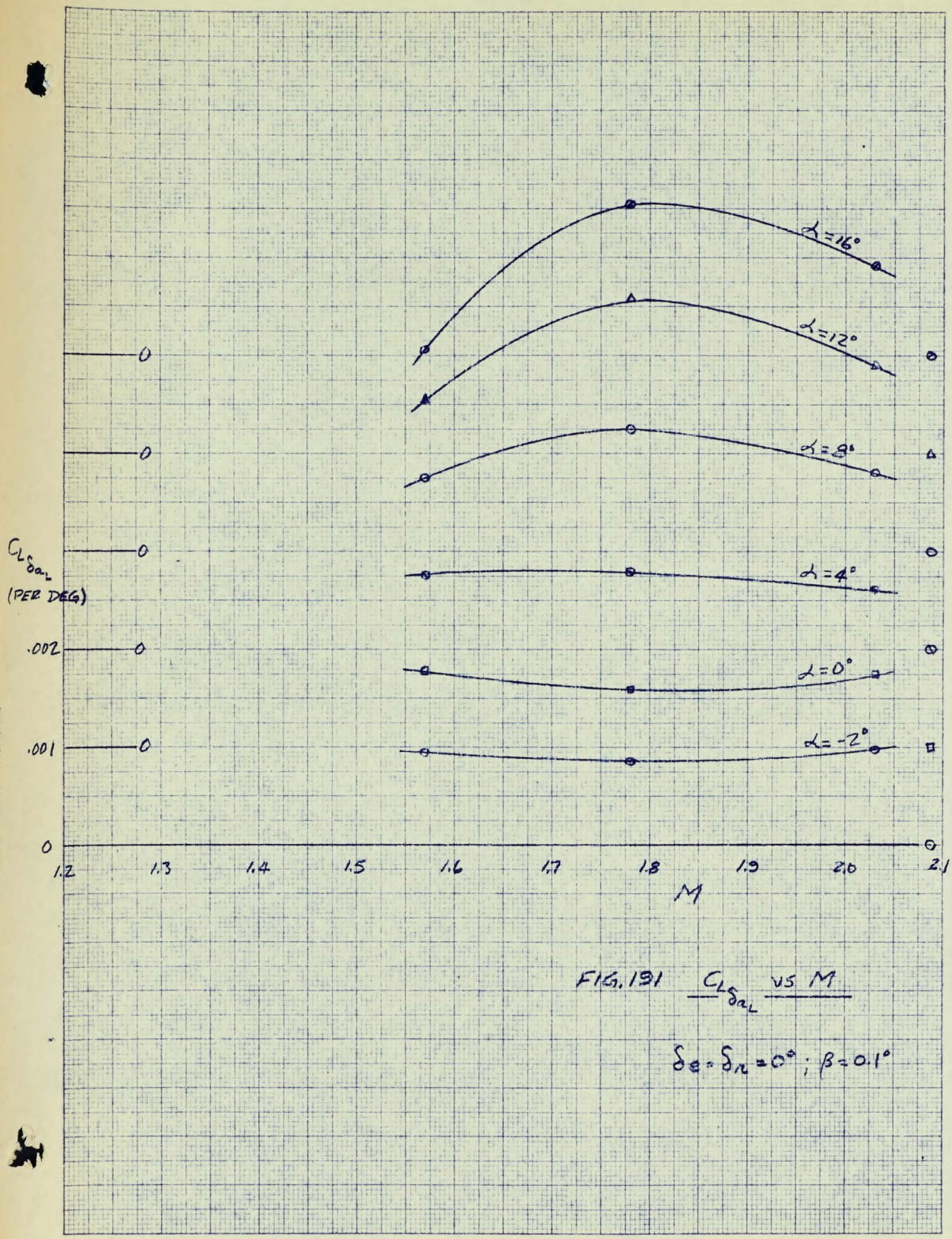

FIG. 131 $C_{L_{\delta a_L}}$ VS M

$\delta_e = \delta_r = 0°$; $\beta = 0.1°$